The Dissertation Committee for Michael Clinton Koetting certifies that this is the approved version of the following dissertation:

Stimulus-Responsive Delivery Systems for Enabling the Oral Delivery of Protein Therapeutics Exhibiting High Isoelectric Point

Committee:

Nicholas A. Peppas, Supervisor

Lydia Contreras

Christopher Ellison

Jeanne Stachowiak

Tom Truskett

Stimulus-Responsive Delivery Systems for Enabling the Oral Delivery of Protein Therapeutics Exhibiting High Isoelectric Point

by

Michael Clinton Koetting, B.S., M.S.E.

Dissertation

Presented to the Faculty of the Graduate School of

The University of Texas at Austin

in Partial Fulfillment

of the Requirements

for the Degree of

Doctor of Philosophy

The University of Texas at Austin

May 2015

Dedication

This work is dedicated to my family and friends who have supported me endlessly.

Acknowledgements

I owe thanks to many individuals who have assisted me throughout the course of the research presented herein. To begin, I thank my advisor, Dr. Nicholas Peppas, for providing me the opportunity and guidance needed to grow as a researcher.

Thank you also to all of my colleagues in the Peppas lab who have assisted me in my research and made my graduate experience enjoyable. I have benefitted greatly from the expertise and advice of my fellow labmates, namely: Mary Caldorera-Moore, Brenda Carrillo-Conde, Cody Schoener, Bill Liechty, Brandon Slaughter, Diane Forbes, Jennifer Knipe, Amey Puranik, Jonathan Peters, Stephanie Steichen, Heidi Culver, Lindsey Sharpe, Sarena Horava, David Spencer, John Clegg, and Angela Wagner. Thank you also to my undergraduate students Joseph Guido, Annie Zhang, Malvika Gupta, David Tai, and Christy Nguyen, who were all vital in the completion of this work.

I also thank my family for their untiring support and guidance throughout my life, as well as all of my friends, who have made the journey so wonderful along the way.

Finally, I would like to thank the National Institutes of Health and the Cockrell School of Engineering for their funding of my research and education.

Stimulus-Responsive Delivery Systems for Enabling the Oral Delivery of Protein Therapeutics Exhibiting High Isoelectric Point

Michael Clinton Koetting, Ph.D.

The University of Texas at Austin, 2015

Supervisor: Nicholas A. Peppas

Protein therapeutics offer numerous advantages over small molecule drugs and are rapidly becoming one of the most prominent classes of therapeutics. Unfortunately, they are delivered almost exclusively by injection due to biological obstacles preventing high bioavailability via the oral route. In this work, numerous approaches to overcoming these barriers are explored.

pH-Responsive poly(itaconic acid-co-N-vinylpyrrolidone) (P(IA-co-NVP)) hydrogels were synthesized, and the effects of monomer ratios, crosslinking density, microparticle size, protein size, and loading conditions were systematically evaluated using *in vitro* tests. P(IA-co-NVP) hydrogels demonstrated up to 69% greater equilibrium swelling at neutral conditions than previously-studied poly(methacrylic acid-co-N-vinylpyrrolidone) hydrogels and a 10-fold improvement in time-sensitive swelling experiments. Furthermore, P(IA-co-NVP) hydrogel microparticles demonstrated up to a 2.7-fold improvement in delivery of salmon calcitonin (sCT) compared to methacrylic acid-based systems, with a formulation comprised of a 1:2 ratio of itaconic acid to N-vinylpyrrolidone demonstrating the greatest delivery capability.

Vast improvement in delivery capability was achieved using reduced ionic strength conditions during drug loading. Use of a 1.50 mM PBS buffer during loading yielded an 83-fold improvement in delivery of sCT compared to a standard 150 mM buffer. With this improvement, a daily dose of sCT could be provided using P(IA-co-NVP) microparticles in one standard-sized gel capsule. P(IA-co-NVP) was also tested with larger proteins urokinase and Rituxan. Crosslinking density provided a facile method for tuning hydrogels to accommodate a wide range of protein sizes.

The effects of protein PEGylation were also explored. PEGylated sCT displayed lower release from P(IA-co-NVP) microparticles, but displayed increased apparent permeability across a Caco-2 monolayer by two orders of magnitude. Therefore, PEG-containing systems could yield high bioavailability of orally delivered proteins.

Finally, a modified SELEX protocol for cellular selection of transcellular transport-initiating aptamers was developed and used to identify aptamer sequences showing enhanced intestinal perfusion. Over three selection cycles, the selected aptamer library showed significant increases in absorption, and from an initial library of 1.1 trillion sequences, 5-10 sequences were selected that demonstrated up to 10-fold amplification compared to the naïve library. These sequences could provide a means of overcoming the significant final barrier of intestinal absorption.

Table of Contents

List of Tables

List of Figures

Chapter 1: Introduction

Protein therapy offers a number of advantages in disease treatment that cannot be matched by traditional therapy with small molecule drugs. The complex structure of proteins enables complex and effective therapeutic functions with unmatched specificity, equating to more effective medications with fewer side effects. As such, protein therapy is the most rapidly expanding area of modern medicine, already treating scores of diseases with the potential to treat thousands more.

Unfortunately, therapeutic proteins are almost universally administered via injections, which can be painful, inconvenient, and embarrassing. Protein therapeutics generally require repeated administration, so the cumulative frustration with a painful and inconvenient administration method often causes patients to intentionally skip injections, leading to dangerous lapses in treatment.

Oral delivery of therapeutics is generally considered the most desirable of drug administration routes. It is easy to self-administer, highly familiar to all patients, generally less expensive, and completely free of biohazard sharps waste, chronic irritation, and scarring. With the protein therapeutics market expanding rapidly to meet the needs of millions of patients, the time to develop improvements to the basic delivery strategy is now. Development of an oral delivery strategy for protein therapeutics would be a boon to both patients and the pharmaceutical industry by offering improved patient quality of life and reduced cost as this young class of therapeutics expands.

Unfortunately, despite significant interest, the oral route has not yet been adopted with protein-based drugs due to significant biological obstacles, including: the acidic, proteolytic environment of the stomach, which denatures proteins before reaching the bloodstream; proteolytic enzymes in the small intestine; the mucosal and epithelial cell linings of the small intestine, which have evolved to keep large macromolecules and organisms from entering the bloodstream; and longevity in the body once present in the bloodstream. All of these issues lead to negligible bioavailability of protein therapeutics via the oral route without a well-designed delivery system that overcomes these obstacles.

Numerous such delivery systems have been proposed and studied, although none have reached use on the market as a result of insufficient bioavailability to make the final product financially feasible. One promising delivery strategy has been to use the large and rapid shift in pH from the stomach to the small intestine to trigger the release of protein therapeutics from pH-responsive hydrogels. Much work has been performed with such systems for insulin, but charge interactions have limited the use of these systems with proteins exhibiting a high isoelectric point.

In this thesis, multiple strategies for overcoming the numerous barriers blocking the path to oral delivery of high isoelectric point therapeutic proteins are explored. pH-Responsive and enzymatically-degradable hydrogel microparticles are evaluated as protein delivery vehicles. The effects of numerous hydrogel design variables on oral protein delivery capability are evaluated. Bioconjugation strategies to improve protein bioavailability are also explored, and the effects of bioconjugation on drug delivery and

intestinal transport are assessed. Finally, an aptamer-based strategy for enhancing the intestinal absorption of macromolecules is proposed, and the results of the aptamer discovery process are presented.

Chapter 2: Background

2.1 PROTEIN THERAPEUTICS

Protein therapeutics has become the cornerstone of modern medicine, and now represents the most rapidly expanding class of new therapeutics. Protein-based drugs have remained one of the most common classes of newly FDA-approved drugs for the past few years, accounting for 23% of new drugs in 2012[1] and 20% of new drugs in 2011.[2] Since the first recombinant protein therapeutic, insulin, was approved three decades ago in 1982, over 150 different protein-based drugs have received FDA approval to treat an impressive array of diseases. Protein therapeutics have accordingly grown into a large global market, with sales of over $108 billion in 2010, and projected sales of $165 billion by 2018.[3–5] As of the end of 2013, 9 of the 20 best-selling drug products in the world are protein therapeutics, as listed in Table 2-1.[6]

Protein therapy has enjoyed such rapid expansion because it offers several distinct advantages over traditional small molecule-based pharmaceutics. The advantages primarily stem from the additional complexity offered by a large molecule made of many individual units, allowing function to be determined by both structure and functional groups, not solely the functional groups as with small molecule drugs. As a result, proteins have significantly fewer systemic side effects because their complex structure enables them to act with high activity specifically for one function, rather than acting in different ways at many different sites throughout the body. Additionally, the molecular intricacy allows for significantly more complex functions that simply cannot be replicated with small molecule drugs—the main reason missing or misfolded proteins cause diseases that cannot be easily treated without protein or gene therapy (which is not currently available as a treatment option). Finally, because proteins are often found

naturally throughout the body, proteins are generally well-tolerated and display low immunogenicity.[7] In short, the field of protein therapeutics has grown so rapidly because proteins are nearly ideal therapeutics: they perform their specific function, they perform it very well, and they do almost nothing else until they are degraded and removed from the body.

Despite already staggering sales, the technology is still in its infancy. The human genome contains genes encoding for 25,000 to 40,000 different proteins, and post-translational modifications allow for multiple functionally different proteins to result from the same gene.[7] Thus, compared to the many tens of thousands of proteins present in the human proteome, 150 drugs is but a small drop in the bucket. As a result, there are many thousands of proteins native to the human proteome remaining to be utilized in treatment of many different diseases, as well as a nearly unlimited number of synthetic proteins. Although advancement in synthetic protein synthesis would undoubtedly usher in a boom era in protein research and new drugs, much like what has occurred with nucleic acid research following the invention of PCR, the current potential for advancement with novel drugs is still pushing protein therapy forward at an impressive pace: the market is projected to grow by 10-30% per year for at least the next decade.[8] This expansion is aided by the fact that pharmaceutical companies have strong incentive to develop new protein therapeutics. Due to the reduced number of systemic side effects and low immunogenicity, protein drugs have on average a much shorter FDA-approval process than small molecule drugs—3 years on average compared to roughly 7.[7] Patent protection of recombinant protein drugs is also quite extensive, allowing companies to avoid having generic competitors on new drugs for many years. With all of the benefits associated with protein therapy, the rapid expansion of the market is expected to

continue, making now the best time to develop not only new drugs, but also better systems for delivering the protein therapeutics into the body.

2.2 ADMINISTRATION OF PROTEIN THERAPEUTICS

Currently, nearly all protein therapeutics are delivered by intravenous, subcutaneous, or intramuscular injection. Although comparatively simple and straightforward, injections have major drawbacks. Injections are often painful and/or frightening to the user, embarrassing to administer in public, and relatively costly. Injections require highly sterile, clean-room manufacturing facilities and sterile syringes, and intravenous injections must be administered by a healthcare professional, all of which adds greatly to the cost of the treatment and requires significantly more time from the patient's day. All of these drawbacks have been shown to adversely affect patient compliance with prescribed treatment. In one study, it was reported that over half of insulin users have intentionally skipped injections at some point, and 20% regularly do so to avoid the pain and embarrassment of the injection.[9] Skipping injections greatly reduces the efficacy of the treatment plan and can be quite dangerous. As a result, a more amenable delivery option would not only improve patient quality of life, but would also improve treatment efficacy if users do not feel inclined to skip injections.

Delivery via the oral route is a more preferred method of administration. It offers a much more convenient pathway that is very familiar to all users and eliminates the fear, pain, and embarrassment that is associated with injections. Additionally, delivery via the oral pathway in a pill form typically helps reduce the cost of the treatment. Orally-delivered drugs need not be produced in such a highly sterile cleanroom environment as required for injections because potential contaminants are unlikely to survive through the proteolytic environment of the stomach.[10] This significantly reduces the production cost

of the drug and eliminates costs of sterile syringes and professional application (for intravenous injection). Protein therapy can be cost-prohibitive, with the average treatment cost being around $100,000 per year,[7] so even a slight reduction in cost can be significant in allowing wider access to highly effective treatments.

2.2.1 Obstacles to Oral Delivery

Unfortunately, there are significant obstacles that have prevented oral delivery of protein therapeutics thus far. The path that a drug must take when delivered orally is fraught with peril. When ingested, a drug first passes down the esophagus into the stomach. There, it encounters an environment that is highly acidic and contains many proteolytic enzymes seeking to degrade the protein. This environment of course allows for humans to ingest animal or plant proteins, break them down into their substituent amino acids, and absorb these building blocks as nutrients for constructing our own proteins as needed. However, this function also prevents therapeutic proteins from reaching the bloodstream intact, as naked proteins exhibit almost negligible bioavailability without some means of protection.[11–13]

The average residence time in the human stomach is approximately 3.5 hours.[14] Within this time, the protein is digested by the digestive system's primary proteolytic enzyme, pepsin. Pepsin comes from an inactive precursor molecule, pepsinogen, a 44-amino acid zymogen that is secreted by chief cells in the stomach. Pepsinogen is then activated by the hydrochloric acid released from parietal cells in the stomach through an autocatalytic cleavage, yielding the active enzyme pepsin. Pepsin remains active in acidic conditions (pH < 6.5), with maximal activity at pH 2.0. It typically cleaves approximately 20% of amide bonds in ingested proteins, with preference for cleaving the

N-terminal side of aromatic amino acid residues such as phenylalanine, tryptophan, and tyrosine.[15,16]

In addition to cleavage by pepsin, the hydrochloric acid responsible for activating pepsin also acts to denature proteins. A study on the effects of acid on protein denaturation by Fink et al.[17] revealed three classes of responses depending on the strength of the acid, the temperature, and the presence of salts or other denaturants. Proteins may: 1) initially unfold at pH 3-4 and then refold into a molten, globule-like state at lower pH; 2) not fully unfold, but directly transition to the molten, globule-like state; 3) show no significant unfolding with pH as low as 1. However, the presence of salts or denaturants such as urea can significantly affect such behavior. Therefore, although some proteins will naturally be resistant to denaturation by acid, many will deform and lose tertiary structure, at least to some degree.

The median gastric pH for healthy people in the fasted state has been found to be 1.7; after a meal, the pH briefly raises to a median peak of 6.7 and declines back to the fasted state pH over 2 h.[18] This means that the drug will most likely spend roughly 1.5 h in highly acidic conditions (pH 1.7) and another 2 h in harsh to mild acidic conditions (pH 1.7 - 6.7). Thus, a functioning drug delivery system for enabling oral delivery of protein therapeutics requires that it both protect the protein from pepsin and provide some sort of support for secondary and tertiary structure so that the drug is not denatured in the highly acidic environment. Of course, all of this is needed to overcome the obstacles in just the stomach!

After the stomach, the drug the passes on to the small intestine, where nutrient absorption into the bloodstream occurs. This is the ideal site for transport of an orally-delivered protein into the bloodstream where it can be active as though it were injected. The pH of the small intestine is decidedly more neutral than that of the stomach: in the

fasted state, the median duodenal pH is 6.1; after a meal, the pH decreases to pH 5.4 and then fluctuates between 5 and 6.2 for over 4 h.[18] Thus, the primary concern in the small intestine is not acidic denaturation, although significant obstacles do remain.

One obstacle presented by the small intestine is the presence of additional proteolytic enzymes, primarily trypsin and chymotrypsin. Together with pepsin, these enzymes comprise the primary proteolytic enzymes of the gastrointestinal tract. Trypsin predominantly degrades proteins at the carboxyl side of lysine or arginine residues.[19] Chymotrypsin has similar cleavage sites as pepsin, preferentially cleaving on the N-terminal side of tyrosine, tryptophan, and phenylalanine residues, with slower cleavage of leucine and methionine residues, and therefore acts as a second screen for ensuring protein degradation.[20]

In addition to surviving potential degradation by these additional enzymes, the protein must cross the intestinal mucosa and epithelial cell layer to reach the bloodstream and enter systemic circulation. As shown graphically in Figure 2-1, there are two primary means of crossing the epithelium: paracellular transport, as the protein diffuses through the tight junctions between cells, or transcellular transport through the cells by active or passive means. Many small molecules such as amino acids are readily absorbed across the intestine, but the intestine has evolved to keep foreign proteins, viruses, and bacteria (i.e., large molecules or organisms) out of the bloodstream in an effort to prevent invasion by foreign parasites. Therefore, although there are some naturally occurring proteins that readily cross by active transcellular transport, such as transferrin[21] and IgG antibodies,[22] the primary means of transport for macromolecules is through paracellular transport,[23] which limits most proteins to 0-10% absorption.[24,25] As a result, even a hypothetical delivery system capable of delivering 100% of encapsulated drug to the small intestine would still fail to achieve high bioavailability without promoting intestinal

absorption through some mechanism. Thus, the problem of intestinal permeability is a highly significant obstacle to overcome in terms of achieving high bioavailability of orally delivered proteins. As such, in addition to offering protection throughout the gastric environment, an ideal oral protein drug delivery system would also offer some protection from trypsin and chymotrypsin as well as promote intestinal absorption.

2.3 HYDROGELS FOR DRUG DELIVERY

The numerous obstacles presented by human physiology have kept orally-delivered protein therapeutics from entering the market thus far. However, recent research has led to promising advances for enabling oral delivery. Peppas and collaborators have previously studied pH-responsive hydrogels based on methacrylic acid that show promise as protein delivery vehicles.[21,27–31] In these systems, methacrylic acid is copolymerized with poly(ethylene glycol) monomethyl ether monomethacrylate (PEGMMA) or N-vinyl pyrrolidone (NVP)—two hydrophilic and biocompatible monomers—and a crosslinking agent such as tetra(ethylene glycol) dimethacrylate (TEGDMA) to form a pH-responsive hydrogel. The structure of these molecules and a resulting gel network are shown in Figure 2-2.

The carboxylic acid group on methacrylic acid provides the pH-responsive activity. The pK_a of methacrylic acid is 4.65, which leads to the acid group being protonated (-COOH) at highly acidic pH below the pK_a, as found in the stomach, and deprotonated ($-COO^-$) at neutral or basic pH above the pK_a, as found in the small intestine. When protonated, the hydrogen groups are available for hydrogen bonding with the oxygen atoms in the poly(ethylene glycol) chains or on the N-vinyl pyrrolidone side group. This complexation causes the hydrogel to adopt a smaller, collapsed state, reducing the pore sizes of the hydrogel network and allowing the gel to effectively

encapsulate a protein drug for protection throughout the stomach. When entering the neutral pH of the small intestine, the acid groups deprotonate and lose their hydrogen bonding abilities, causing swelling throughout the hydrogel network due to a combination of entropic interactions, favorable water imbibition by osmotic pressure, and anionic repulsion of the $–COO^-$ groups.[32] The increased pore size allows for diffusive release of an encapsulated drug within the small intestine.

Methacrylic acid-based gels copolymerized with poly(ethylene glycol) monomethyl ether monomethacrylate or N-vinyl pyrrolidone, designated P(MAA-*g*-EG) or P(MAA-*co*-NVP) respectively, have been synthesized and studied as potential protein delivery vehicles. pH-Responsive swelling has been shown to cause up to a 30-fold increase in weight when comparing the collapsed and swollen states of the polymers.[33] Both polymers have also shown ability to effectively encapsulate and release insulin in *in vitro* loading and release experiments and *in vivo*, closed-loop animal models.[27,31,33–35]

While this system has been promising for insulin, proteins represent an extremely broad class of molecules. Importantly for polymer-based delivery, proteins differ widely in terms of size, shape, chemical stability, hydrophilicity or hydrophobicity, and isoelectric point. For example, proteins range in size from a few kDa to several hundred kDa, which may require pore sizes to accommodate different diameters spanning over an order of magnitude. As a result, the polymer system used to deliver the protein needs to be tailored to meet the demands of the specific therapeutic being delivered.

One of the properties that must be accommodated is the isoelectric point. The isoelectric point (pI) is the pH at which the protein has no net charge. Above a protein's pI, the protein will have a net negative charge; below the pI, the protein will have a net positive charge. Insulin has a pI of 5.39, meaning that it will be cationic in the low pH environment of the stomach and anionic in the neutral environment of the small

intestine.[36] Because the P(MAA-*g*-EG) swells based on an anionic functional group (-COO^-), the charge on insulin works advantageously, repelling insulin from the hydrogel mesh by anionic interactions when in the desired release site of the small intestine and assisting with diffusive release.

Unfortunately, the human proteome is split approximately evenly between proteins with low isoelectric points (pI < 7.4), like insulin, and proteins with high isoelectric points (pI > 7.4).[37] For high isoelectric point-exhibiting proteins, the charge interaction works disadvantageously. In the small intestine, the environmental pH remains below the pI of the protein, making the protein cationically charged while the hydrogel is anionically charged. This leads to coulombic charge interactions that bind the protein to the hydrogel mesh, hampering diffusive release. Therefore, the P(MAA-*g*-EG) and P(MAA-*co*-NVP) systems developed previously are not as ideally suited for achieving high bioavailability when delivering high isoelectric point-exhibiting proteins via the oral route. Studies have shown that a high isoelectric point-exhibiting protein used for treating osteoporosis called salmon calcitonin can achieve complete release from the hydrogel over the time span of days;[38] unfortunately, the average residence time in the small intestine is only 4 hours,[39] over which time the release is less than 20%.[28] Therefore, to achieve high bioavailability via the oral route with any of the tens of thousands of high pI-exhibiting proteins, adjustments to the proteins or the hydrogel vehicle are needed.

Of the over 150 currently FDA-approved protein therapeutics, at least 46 exhibit high isoelectric points (likely more, as not all of the approved drugs have accepted pI values available).[7,36] These therapeutics are used to treat a wide variety of diseases: breast, lung, colorectal, and head and neck cancers; rheumatoid arthritis; osteoporosis; Crohn's disease; infertility; non-Hodgkin's lymphoma; multiple sclerosis; macular

degeneration; anemia; and growth failure, among others.[7] Because these diseases together account for many millions of patients who may benefit from repeated administration of protein therapeutics, it is imperative that any oral delivery strategy be able to accommodate the high isoelectric point exhibited by the proteins.

The aims of this thesis are to explore different strategies for achieving high bioavailability of therapeutic proteins delivered via the oral route in general, with emphasis on seeking innovations that could allow the previously studied systems to be expanded or modified to function with high isoelectric point exhibiting proteins. The focus will be on salmon calcitonin—a protein used for treating osteoporosis and Paget's disease—as a model, as it exhibits a high isoelectric point of 8.86 and has a small size similar to insulin (3.4 kDa compared to 5.8 kDa),[36] thereby isolating isoelectric point as the primary difference between proteins and eliminating significant differences that would arise from vastly different sizes. However, experiments with other high pI proteins urokinase and rituximab are also described.

2.4 BIOCONJUGATION

Bioconjugation refers to the attachment of additional molecules to a biomolecule such as a protein via covalent linkages. It is widely used across various fields in order to impart additional functionality to a biomolecule without significantly inhibiting its original activity. Bioconjugation reactions are used for a broad variety of purposes, finding uses in research, medicine, and materials synthesis.

2.4.1 PEGylation and Its Utility in Medicine

For one relevant and illustrative example, in medicine, attachment of a hydrophilic chain of poly(ethylene glycol) has shown to be an effective means of

providing stealth properties to proteins, particles, and surfaces, preventing rapid protein recognition by opsonins which cause protein removal by the reticuloendothelial system. This reaction, termed "PEGylation," has multiple advantages; it can: increase the hydrophilicity and solubility of highly hydrophobic drugs; increase the residence time of proteins by protecting against proteolysis and opsonization; protect against immunological reaction to the injected drug; or provide charge shielding interactions for ionic or dipolar molecules.[40–51]

Such beneficial effects were first reported in a 1977 paper by Abuchowski et al.[52] in the lab of Dr. Frank Davis, where attachment of 1900 and 5000 Da PEG chains to bovine liver catalase prevented reaction with antiserum, granted protection from enzymatic degradation, and enhanced circulation time in mice, even as the catalase retained 93 and 95% of its native activity. Since this seminal work, PEGylation has become a common approach to enhancing the efficacy of biotherapeutics, and is now used as a fundamental feature in many pharmaceuticals, including Movantik, Omontys, Krystexxa, Cimzia, Mircera, Macugen, Neulasta, Somavert, Pegasys, Doxil, PegIntron, Oncaspar, and Adagen. Further, it has been used as a surface treatment for implants, preventing protein adhesion and therefore improving biocompatibility.

2.4.2 Bioconjugation reactions

Although bioconjugation reactions such as PEGylation have broad applicability, conjugation is typically performed through one of several common reactions. With protein therapeutics, one of the most common reactions employed is reaction of the primary amines in lysine residues with N-hydroxysuccinimide (NHS) esters through nucleophilic substitution. The NHS-ester is often formed from carboxylic acids using 1-ethyl-3-(3-dimethylaminopropyl)carbodiimide (EDC) and NHS (thus often referred to as

EDC/NHS chemistry). The reaction proceeds as shown in Figure 2-3. A carboxylic acid is first activated by EDC to form a urea intermediate that is then susceptible to nucleophilic attack, either directly by a primary amine (such as that found in lysine) or by NHS or sulfo-NHS. Attack by an NHS forms a stable intermediate that remains susceptible to nucleophilic attack by a primary amine while also increasing overall conjugation efficiency to over 90% and allowing storage of intermediates in a dry state.[53–57] This reaction is slightly pH sensitive, with optimal pH between 4.7 and 6.0, although pH can go as high as 7.5 without significant yield loss.[58]

The EDC/NHS reaction is especially useful for protein modification, as lysines are one of the most commonly observed amino acids in multiple, well-studied proteomes, upregulated consistently compared to what random probability would suggest and highly upregulated in the terminal position.[60–65] As a result, there are many sites available in a typical protein for the EDC/NHS coupling reaction, and upregulation at the terminal position makes attachment to a terminal site frequently possible, enabling conjugation at a location that generally does not cause steric interference with the active site of the protein. In addition, as can be seen in Figure 2-3, the reaction is a "zero-length" crosslinking reaction, in that the final product contains no portions of the EDC or NHS (i.e., no spacer), and the carboxylic acid-containing molecule and the amine containing molecule are directly attached. For these reasons, this highly versatile and valuable reaction will be utilized both for PEGylation and crosslinking in this dissertation as described later.

Although the ubiquity of lysine residues makes EDC/NHS coupling work with most proteins, it also has the drawback of having generally low selectivity with regard to particular reaction sites since most proteins will have multiple lysines. Therefore, other reactions exist to take advantage of less common amino acids. One particular reaction, as

seen in Figure 2-4, utilizes the thiol groups that are found only on cysteine—one of the (generally) least common amino acids[60,66]—which can therefore greatly increase site-specificity. In the reaction, a reagent with a maleimide functional group reacts with the thiol group present on cysteine via a Michael addition, forming a stable product with a thioether linker.[58,59,67,68] Maleimides will also react with amines, although tight control of the reaction pH between 6.5-7.5 can yield specificity toward thiol groups, as reaction with thiols proceeds 1000 times faster than with amines at pH 7; at higher pH values above 7.5, cross-reaction with amines becomes more common.[69–73]

Although the maleimide reaction with cysteine enables facile conjugation with greater site specificity than EDC/NHS chemistry with lysine, many cysteine residues present in proteins are coupled together with other cysteine residues (forming cystine residues) through disulfide bridges, especially in proteins typically found in the extracellular milieu.[66,74] These linkages are at times a mere structural motif to enhance stability, but also can either impart tertiary structure to proteins that is vital to proper function or be simply an inert structural motif.[74] If conjugation with a disulfide-linked cysteine does not impair functionality, the cystine will first need to be reduced to cysteines, as maleimides do not react with disulfides.[75] Common reducing agents are dithiothreitol (DTT), 2-mercaptoethanol, or tris(2-carboxyethyl)phosphine (TCEP). Following reduction, the maleimide-thiol reaction can proceed as described. In the event that reducing the disulfide does impair protein function, a dibromomaleimide may be used, which reacts with both sulfhydryls, maintaining the approximate disulfide-bonded structure through a two carbon linker while also attaching the desired conjugate, as seen in the PEGylation of salmon calcitonin scheme shown in Figure 2-5.[76–78]

Many additional reactions are available for bioconjugation which take advantage of different functional groups for improved reaction selectivity with various molecules.

Hermanson has written an excellent compendium of these reactions.[58] Due to the ease and versatility of EDC/NHS chemistry, it will be used as the predominant conjugation technique in this dissertation, with brief mention of the maleimide-thiol chemistry.

2.5 APTAMERS

Aptamers are single-stranded oligonucleotide (RNA or DNA) sequences that form tertiary structures based on complementary base-pair hybridization which allow the resulting molecule to bind to and interact with virtually any class of target molecule with high specificity and affinity.[79] They are analogous to antibodies, which have been utilized for over four decades for molecular recognition, with the difference that they are comprised of nucleotides instead of amino acids.

This distinction makes aptamers very appealing, because the polymerase chain reaction (PCR) allows rapid, exponential amplification of oligonucleotides through simple chemical means, enabling aptamers to be developed and reproduced rapidly and cheaply. Antibodies are not easily amplified by chemical means and require a biological system because of the numerous potential components (20 unique amino acids versus 4 unique nucleotides) and the lack of natural enzymes for reproduction since natural protein production consists of translation of mRNA into a protein rather than copying proteins already present.[80] Additionally, aptamers are significantly smaller in size than antibodies. Aptamers are often successfully selected using 15 to 40 random nucleotides, thus ranging in molecular weight from only 5 to 40 kDa;[80] antibodies are regularly on the order of 150 kDa in size, which can prevent them from being used effectively in many applications. Finally, aptamers are advantageous for having unlimited shelf-life and no immunogenicity; antibodies can denature in time and have significant immunogenicity in many cases.[80]

Aptamers became a popular class of molecules for the reasons described above following the description of the SELEX process in 1990.[81,82] SELEX, standing for "systematic evolution of ligands by exponential enrichment," also known as "*in vitro* selection" or "*in vitro* evolution," is a powerful tool for designing aptamers tailored for specific targets or specific functions. It is essentially a directed evolution process for chemicals rather than organisms. A large library of DNA or RNA strands, each containing a long random sequence in between primer sequences, is generated. The library is then screened by placing the library in the presence of the target molecule, allowing the small fraction of aptamers that will bind the target molecule to bind, and isolating the bound nucleic acids from the non-functioning nucleic acids by washing or some other process. The bound aptamers are then amplified by PCR and the process is repeated 5-15 times. Because PCR exponentially amplifies the nucleic acids isolated by the selection step, it will widen the gap in moles of aptamers binding with high affinity and those binding with low affinity such that after repeated cycles, the most suitable nucleic acid sequence is almost exclusively selected.[83–85] This process has been used for selection of many high affinity detection molecules with dissociation constants in the low picomolar to low nanomolar range.[80]

One of the limitations of using nucleic acids is their rapid degradation *in vivo* by RNases and DNases. An unmodified RNA aptamer, for example, has a half-life of a mere 8 s *in vivo*, far too short for any sort of therapeutic use.[86] Fortunately, there are several approaches to greatly improve the longevity of aptamers in a living system. The most common modification is to use nucleotides containing either amine (2'-NH_2) or fluoride (2'-F) substitutions at the 2'-OH site of the pyrimidines.[87,88] Using 2'-F-RNAs has been shown to extend the half-life of the RNA *in vivo* by up to 38,700 times to 86 h, more than sufficient for therapeutic use.[86] The first FDA-approved aptamer therapeutic,

Macugen for treatment of wet age-related macular degeneration (approved in December 2004), is made with 2'-F-pyrimidines and is conjugated to PEG to slow renal clearance.[89]

An interesting alternative method of improving half-life is to exploit the chirality of nature to avoid degradation by nucleases. Naturally occurring nucleases are all made of L-amino acids which only recognize D-nucleotides. As such, L-nucleotides will escape degradation by nucleases present *in vivo*. Aptamers taking advantage of this are termed Spiegelmers, and display half-lives *in vivo* upwards of 24 h.[89] Selecting the proper enantiomeric L-nucleotide is performed not with L-nucleotides, but with D-nucleotides binding the enantiomer of the desired target protein. In other words, since PCR works with D-nucleotides alone, the amplification step would be impossible with the Spiegelmer; however, by targeting the mirror image of the desired target, the selected aptamer's mirror image will bind the actual target.[90,91] While this is perhaps the most elegant solution to achieving long half-lives *in vivo*, the formation of the D-protein target for the SELEX process must be performed synthetically, which limits the size of the target to something that may be synthesized by peptide synthesis. Therefore, in this work, aptamer selection for therapeutic use will be performed using more simple 2'-F-modified pyrimidines.

While aptamers have been primarily used as immobilizing agents or signaling ligands for detection assays, they are also useful as therapeutic inhibitors (such as Macugen) and can even have enzymatic activity. Riboswitches and ribozymes are a natural example of RNA aptamers that contain catalytic and regulatory activity.[92]

Because aptamers can exhibit these widely varying functions, it is hypothesized in this work that they may similarly be designed for improving transport capabilities of protein therapeutics across the intestinal epithelium. Transport of antigens across the intestinal epithelium is accomplished naturally by IgA antibodies,[93] and previous work in

the lab has shown that transferrin (a protein for iron transport) may be used to improve protein transport by up to 15 times,[21] so it is expected that an aptamer analog of antibodies/proteins can be designed to have similar transcytosis-initiating capabilities to significantly enhance transport into the bloodstream. Choosing a known transporter like transferrin targets only a single receptor which can rapidly become saturated, limiting transport,[94] despite there being many different potential transcytosis-initiating binding receptors on a cell. Therefore, aptamer selection using a cellular-based modification of the SELEX process will utilize the multiple potential cellular receptors and systematically select the optimal receptor to target for the greatest improvement in transport capability without requiring detailed understanding of each available receptor.

2.6 PROPOSED DELIVERY SYSTEMS

2.6.1 Redesigned Hydrogels

While the previously studied anionic hydrogels P(MAA-g-EG) and P(MAA-*co*-NVP) have been shown to be capable of delivering insulin—a relatively low molecular weight (5.8 kDa) protein therapeutic with low isoelectric point of 5.39—studies using this technology platform to release proteins with high isoelectric points such as salmon calcitonin have identified drug delivery problems associated with charge interactions. Therefore, further design and investigation of different hydrogel formulations is needed to allow for high bioavailability of high pI proteins via the oral route.

Because one of the limiting factors in releasing sCT within the small intestine is the charge interaction between the anionic hydrogel and the net cationic protein, one possibility would be to use a cationic or neutral hydrogel. Unfortunately, with pH-responsive cationic gels, due to the nature of the pH-responsive behavior (transitioning

from a protonated $-NH_3^+$ group at low pH to a deprotonated $-NH_2$ group at neutral pH), the gel is in the swollen state at the low pH found in the stomach and collapsed at neutral pH, with an idealized pH-swelling profile seen in Figure 2-6.

While this behavior may work for small molecule delivery by acting as a sponge that "squeezes out" the drug upon shrinking, proteins are much larger, so a gel with sufficiently small pore size to protect proteins from enzymes in the stomach would only entrap the protein drug to a greater degree upon collapse in the small intestine. Therefore, although the anionic nature of the gel is largely to blame for the observed release issues, it is also an unavoidable consequence of utilizing pH-responsiveness as the targeting strategy.

Furthermore, is has been proposed that the anionic nature of the gel allows binding of extracellular Ca^{2+} ions in the small intestine, causing reversible opening of the tight junctions between epithelial cells and enhancing transport of the drug to the blood via paracellular transport.[21,23,96–98] The anionic nature thus may be beneficial after the protein has been released in the small intestine. Therefore, this dissertation details efforts to mitigate, rather than eliminate, the negative effects of the ionic interactions while simultaneously taking advantage of these interactions in appropriate situations.

Increasing the overall swelling and swelling speed would yield larger pore sizes, providing greater diffusivity through the polymer matrix and reduced average coulombic forces, and a longer timeframe for diffusive release, thus increasing the probability of protein release. Coulomb's law (Equation 2-1) states that the force is inversely proportional to the square of the distance between charged particles, so even a small increase in pore size can allow for significantly reduced coulombic attraction to the hydrogel's carboxylic acid groups.

$$|F| = k_e \frac{|q_1 q_2|}{r^2}$$ Equation 2-1

To achieve a greater distance between charges, the methacrylic acid pH-responsive moiety will be exchanged for its diprotic analogue, itaconic acid. Itaconic acid shares a similar structure, with the exception of a second –COOH group present, as seen in Figure 2-7. The expected result of this monomeric substitution is that the second acid group, although providing a second anion per monomer unit for protein binding, will yield greater complexation behavior and increased anionic repulsion between monomer units, resulting in improved swelling and significantly reduced swelling response time. Furthermore, if the number of acid groups per unit volume is kept constant between methacrylic acid and itaconic acid-based gels, the itaconic acid offers the advantage of more localized anionic groups, since two anions are attached to the same monomer rather than being spread out across two separate monomers. This yields a larger distance between anionic groups, and because, per Coulomb's law (Equation 2-1), force is directly proportional to charge while inversely proportional to the square of the distance, increasing distance has a more significant effect than increasing charge, meaning a greater distance of approach will typically yield smaller attractive forces, even if the charge difference is increased proportionally.

This dissertation therefore focuses on gels based on itaconic acid, such as poly(itaconic acid-co-N-vinylpyrrolidone) (P(IA-co-NVP)) and poly(itaconic acid-grafted-poly(ethylene glycol)) (P(IA-g-EG)), and the resulting effects on the delivery of high pI protein therapeutics.

2.6.2 Effects of Protein Conjugation

As described in section 2.4, conjugation of proteins can lead to substantially improved properties, such as longer half-life, improved solubility, and multiple functions. PEGylation of proteins is quite common, but the increased size and different properties of the conjugate may alter protein delivery capability. The increased size is likely to affect oral delivery by decreasing the diffusion rate, especially in the tortuous pathways out of the hydrogel mesh and through the size-selective tight junctions in the intestinal epithelium. However, there may be a beneficial response to PEG as well, as the formation of a water cage around the protein can act to shield charge interactions between the protein and the hydrogel, preventing the electrostatic binding that has limited the oral delivery of high isoelectric point proteins with pH-responsive systems.

In order to examine the effects of PEGylation on protein delivery, salmon calcitonin was PEGylated and evaluated using *in vitro* techniques to assess the impact on loading and release inside of the hydrogels as well as intestinal transport. The experimental protocols used and the ensuing results are discussed in Chapters 6 and 7.

2.6.3 Design of Aptamers for Enhancing Intestinal Absorption

The final obstacle preventing a protein from reaching the bloodstream for therapeutic action is the small intestinal epithelium. The epithelium is a size selective barrier designed to absorb digested nutrients while preventing uptake of macromolecules and foreign organisms that can cause sickness. As such, the absorption of whole proteins is almost negligible. However, some proteins such as transferrin or some IgA antibodies have biological function that requires active transport across the intestinal epithelium, and receptor proteins enable the selective uptake of these proteins by transcellular transport.

I hypothesized that one of these transcellular pathways can be used by designing an aptamer ligand that selectively binds to transcellular transport receptors on the cell surface, initiating active transport of proteins into the bloodstream. Aptamers are well suited for this task because the chemical amplification through PCR (which is not available with proteins) enables a facile, evolutionary approach (SELEX) to discovery that requires minimal prior knowledge about the target and thus the ideal characteristics of the ligand.

In this work, a modified selection protocol is used to enable the selection of aptamers achieving high levels of absorption across the epithelium by using a Caco-2 model of the intestine. Modified pyrimidine nucleotides containing fluorine atoms at the 2' position were used to prevent rapid degradation by RNases, and transport across the monolayer was used as the selection step to separate sequences that bind transcellular transport receptors from those that are not adequately transported. Incorporating high throughput sequencing is used in favor of traditional Sanger sequencing as the final step of the protocol, enabling a faster selection cycle by reducing the required number of cycles. In sum, the presented work aims to achieve an aptamer ligand that can be used to

significantly enhance the transport of therapeutic proteins across the intestinal epithelium, effectively overcoming the final and most significant barrier to high bioavailability via the oral route.

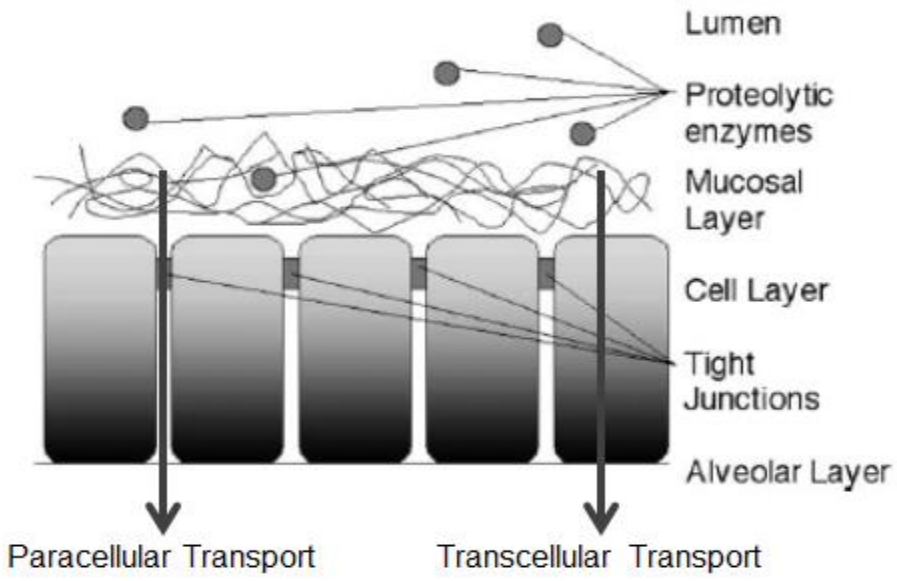

Figure 2-1: Intestinal Epithelium and Methods of Transport. Adapted from Blanchette et al.[26]

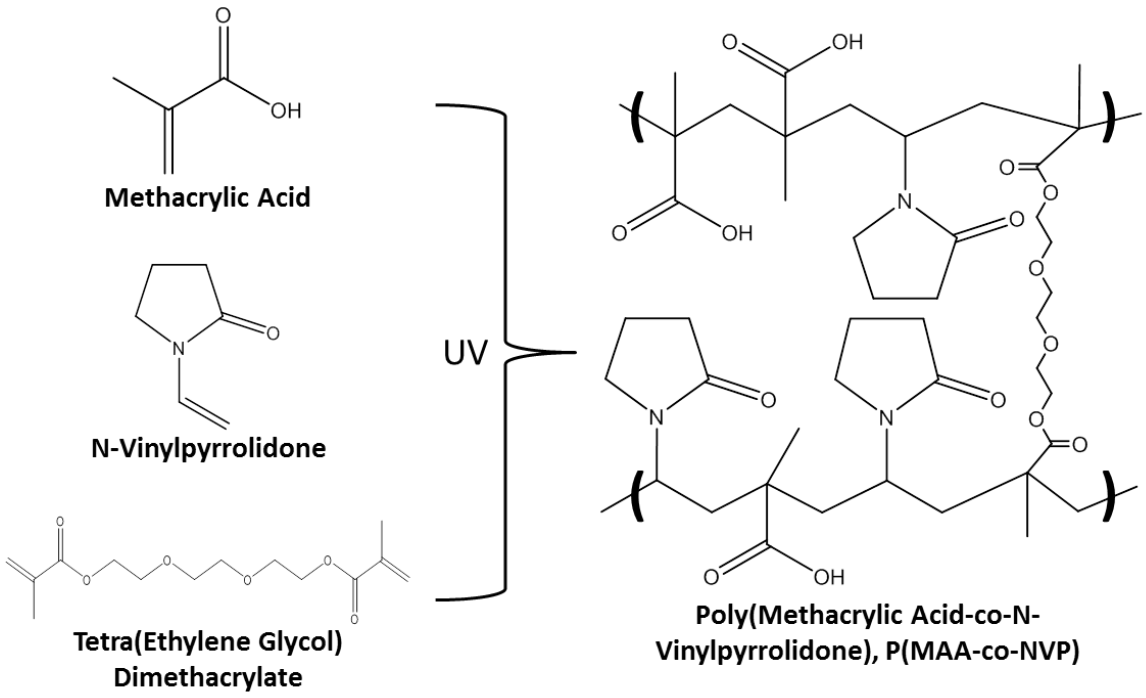

Figure 2-2: Chemical Structures of Monomers and Polymer Network of P(MAA-co-NVP) Hydrogels.

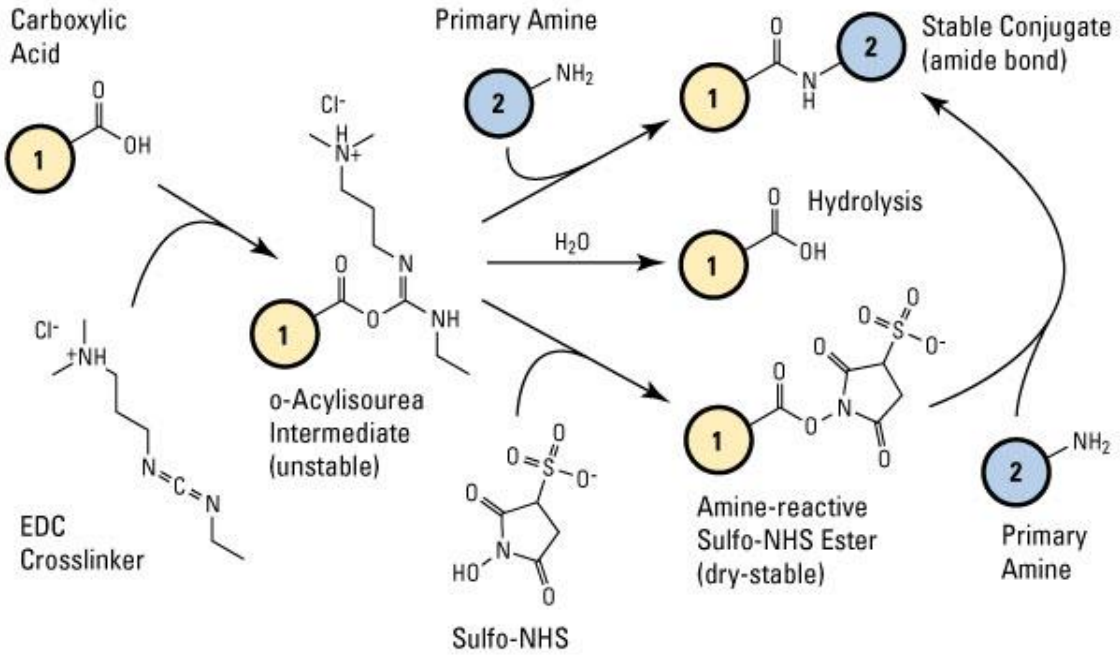

Figure 2-3: EDC/NHS Conjugation Reaction Scheme. Reprinted from Thermo Scientific Pierce.[59]

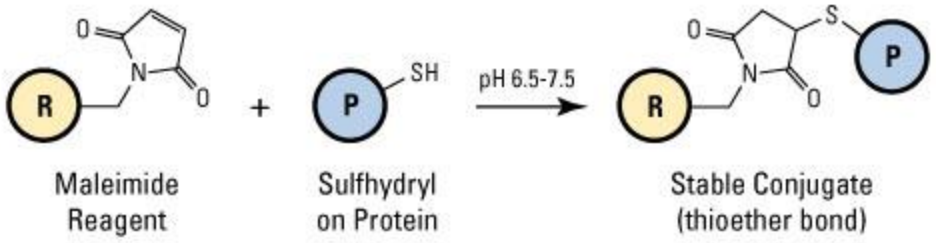

Figure 2-4: Maleimide-Thiol Conjugation Reaction Scheme. Reprinted from Thermo Scientific Pierce.[59]

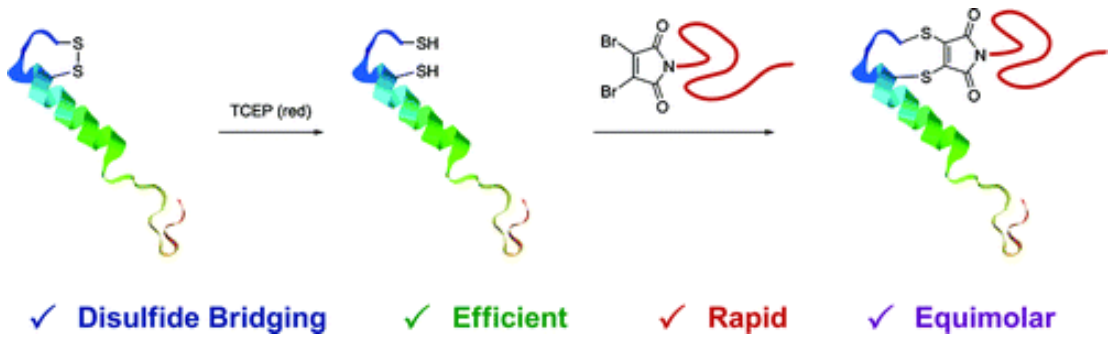

Figure 2-5: PEGylation of Salmon Calcitonin Using Dibromomaleimide to Maintain Disulfide Bridge. Reprinted with permission from Jones et al., J. Am. Chem. Soc., 2011.[76] Copyright 2011 American Chemical Society.

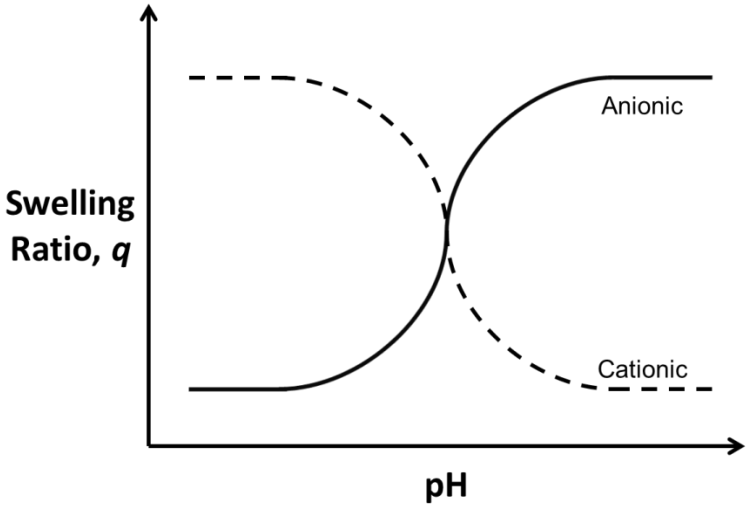

Figure 2-6: Characteristic Swelling Profiles for Anionic and Cationic pH-Responsive Hydrogels.

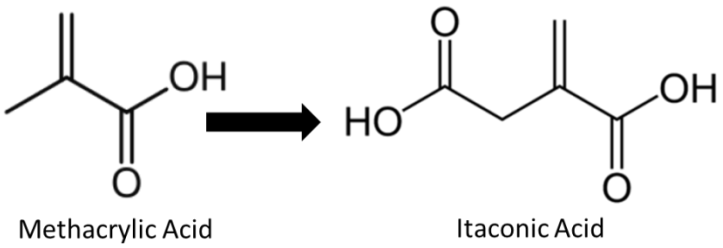

Figure 2-7: pH-Responsive Monomers: Methacrylic Acid and Itaconic Acid. Molecular structure of itaconic acid (right), which will be substituted for methacrylic acid (left) in pH-responsive hydrogels.

Table 2-1: Protein Therapeutics Appearing in the Top 20 Best-Selling Drug Products.

Rank	Drug Name	Protein	Manufacturer	Indications	Sales (Q4 2013, $MM)
3	Humira	Adalimumab	AbbVie	Crohn's disease; Rheumatoid arthritis; Plaque psoriasis; Ulcerative colitis; Ankylosing spondylitis	1,461.9
6	Enbrel	Etanercept	Amgen	Rheumatoid arthritis	1,189.8
8	Remicade	Infliximab	Centocor Ortho Biotech, Inc.	Crohn's disease; Rheumatoid arthritis	994.0
9	Neulasta	Filgrastim (G-CSF)	Amgen	Neutropenia	854.5
11	Lantus Solostar	Insulin glargine	Sanofi	Diabetes mellitus	839.7
12	Rituxan	Rituximab	Genentech	Non-Hodgkin's lymphoma; rheumatoid arthritis	746.8
16	Lantus	Insulin glargine	Sanofi	Diabetes mellitus	675.5
17	Avastin	Bevacizumab	Genentech	Cancers	650.2
20	Epogen	Epoetin alfa	Amgen	Anemia	503.5

2.7 REFERENCES

(1) Mullard, A. 2012 FDA Drug Approvals. *Nat. Rev. Drug Discov.* **2013**, *12*, 87–90.
(2) *FY 2011 Innovative Drug Approvals*; U.S. Food and Drug Administration, 2012; pp. 1–28.
(3) Dimitrov, D. S. Therapeutic Proteins. In; Voynov, V.; Caravella, J. A., Eds.; Methods in Molecular Biology; Humana Press, 2012.
(4) RNCOS. *Global Protein Therapeutics Market Outlook 2018*; 2014; p. 140.
(5) *Global Protein Therapeutics Market Analysis*; RNCOS, 2011; pp. 1–180.
(6) Drugs.com. Top 100 Drugs for Q4 2013 by Sales - U.S. Pharmaceutical Statistics http://www.drugs.com/stats/top100/sales.
(7) Leader, B.; Baca, Q. J.; Golan, D. E. Protein Therapeutics: A Summary and Pharmacological Classification. *Nat. Rev. Drug Discov.* **2008**, *7*, 21–39.
(8) Hiller, A. Fast Growth Foreseen for Protein Therapeutics. *Genet. Eng. Biotechnol. News* **2009**, *29*, 1–2.
(9) Peyrot, M.; Rubin, R. R.; Kruger, D. F.; Travis, L. B. Correlates of Insulin Injection Omission. *Diabetes Care* **2010**, *33*, 240–245.
(10) Fasano, A. Innovative Strategies for the Oral Delivery of Drugs and Peptides. *Trends Biotechnol.* **1998**, *16*, 152–157.
(11) Morishita, M.; Peppas, N. A. Is the Oral Route Possible for Peptide and Protein Drug Delivery? *Drug Discov. Today* **2006**, *11*, 905–910.
(12) Renukuntla, J.; Vadlapudi, A. D.; Patel, A.; Boddu, S. H. S.; Mitra, A. K. Approaches for Enhancing Oral Bioavailability of Peptides and Proteins. *Int. J. Pharm.* **2013**, *447*, 75–93.
(13) Gupta, S.; Jain, A.; Chakraborty, M.; Sahni, J. K.; Ali, J.; Dang, S. Oral Delivery of Therapeutic Proteins and Peptides: A Review on Recent Developments. *Drug Deliv.* **2013**, *20*, 237–246.
(14) Mojaverian, P.; Vlasses, P. H.; Kellner, P. E.; Jr, M. L. R. Effects of Gender, Posture, and Age on Gastric Residence Time of an Indigestible Solid: Pharmaceutical Considerations. *Pharm. Res.* **1988**, *5*, 639–644.
(15) Dunn, B. M. Overview of Pepsin-like Aspartic Peptidases. In *Current Protocols in Protein Science*; John Wiley & Sons, Inc., 2001.
(16) Cox, M.; Nelson, D. R.; Lehninger, A. L. *Lehninger Principles of Biochemistry*; 5th ed.; W. H. Freeman: San Francisco, 2008.
(17) Fink, A. L.; Calciano, L. J.; Goto, Y.; Kurotsu, T.; Palleros, D. R. Classification of Acid Denaturation of Proteins: Intermediates and Unfolded States. *Biochemistry (Mosc.)* **1994**, *33*, 12504–12511.
(18) Dressman, J. B.; Berardi, R. R.; Dermentzoglou, L. C.; Russell, T. L.; Schmaltz, S. P.; Barnett, J. L.; Jarvenpaa, K. M. Upper Gastrointestinal (GI) pH in Young, Healthy Men and Women. *Pharm. Res.* **1990**, *7*, 756–761.
(19) Rodriguez, J.; Gupta, N.; Smith, R. D.; Pevzner, P. A. Does Trypsin Cut Before Proline? *J. Proteome Res.* **2007**, *7*, 300–305.

(20) Appel, W. Chymotrypsin: Molecular and Catalytic Properties. *Clin. Biochem.* **1986**, *19*, 317–322.
(21) Kavimandan, N. J.; Losi, E.; Peppas, N. A. Novel Delivery System Based on Complexation Hydrogels as Delivery Vehicles for Insulin–transferrin Conjugates. *Biomaterials* **2006**, *27*, 3846–3854.
(22) Jones, E. A.; Waldmann, T. A. The Mechanism of Intestinal Uptake and Transcellular Transport of IgG in the Neonatal Rat. *J. Clin. Invest.* **1972**, *51*, 2916–2927.
(23) Kavimandan, N. J.; Peppas, N. A. Confocal Microscopic Analysis of Transport Mechanisms of Insulin across the Cell Monolayer. *Int. J. Pharm.* **2008**, *354*, 143–148.
(24) Artursson, P.; Karlsson, J. Correlation between Oral Drug Absorption in Humans and Apparent Drug Permeability Coefficients in Human Intestinal Epithelial (Caco-2) Cells. *Biochem. Biophys. Res. Commun.* **1991**, *175*, 880–885.
(25) Yee, S. In Vitro Permeability Across Caco-2 Cells (Colonic) Can Predict In Vivo (Small Intestinal) Absorption in Man—Fact or Myth. *Pharm. Res.* **1997**, *14*, 763–766.
(26) Blanchette, J.; Kavimandan, N.; Peppas, N. A. Principles of Transmucosal Delivery of Therapeutic Agents. *Biomed. Pharmacother.* **2004**, *58*, 142–151.
(27) Lowman, A. M.; Morishita, M.; Kajita, M.; Nagai, T.; Peppas, N. A. Oral Delivery of Insulin Using pH-Responsive Complexation Gels. *J. Pharm. Sci.* **1999**, *88*, 933–937.
(28) Carr, D. A.; Gómez-Burgaz, M.; Boudes, M. C.; Peppas, N. A. Complexation Hydrogels for the Oral Delivery of Growth Hormone and Salmon Calcitonin. *Ind. Eng. Chem. Res.* **2010**, *49*, 11991–11995.
(29) Carr, D. A.; Peppas, N. A. Assessment of Poly(methacrylic Acid-Co-N-Vinyl Pyrrolidone) as a Carrier for the Oral Delivery of Therapeutic Proteins Using Caco-2 and HT29-MTX Cell Lines. *J. Biomed. Mater. Res. A* **2010**, *92A*, 504–512.
(30) Foss, A. C.; Peppas, N. A. Investigation of the Cytotoxicity and Insulin Transport of Acrylic-Based Copolymer Protein Delivery Systems in Contact with Caco-2 Cultures. *Eur. J. Pharm. Biopharm.* **2004**, *57*, 447–455.
(31) Kamei, N.; Morishita, M.; Chiba, H.; Kavimandan, N. J.; Peppas, N. A.; Takayama, K. Complexation Hydrogels for Intestinal Delivery of Interferon B and Calcitonin. *J. Controlled Release* **2009**, *134*, 98–102.
(32) Brannon-Peppas, L.; Peppas, N. A. Equilibrium Swelling Behavior of Dilute Ionic Hydrogels in Electrolytic Solutions. *J. Controlled Release* **1991**, *16*, 319–329.
(33) López, J. E.; Peppas, N. A. Effect of Poly (Ethylene Glycol) Molecular Weight and Microparticle Size on Oral Insulin Delivery from P(MAA-g-EG) Microparticles. *Drug Dev. Ind. Pharm.* **2004**, *30*, 497–504.
(34) Morishita, M.; Goto, T.; Takayama, K.; Peppas, N. A. Oral Insulin Delivery Systems Based on Complexation Polymer Hydrogels. *J. Drug Deliv. Sci. Technol.* **2006**, *16*, 19–24.

(35) Tuesca, A.; Nakamura, K.; Morishita, M.; Joseph, J.; Peppas, N.; Lowman, A. Complexation Hydrogels for Oral Insulin Delivery: Effects of Polymer Dosing on in Vivo Efficacy. *J. Pharm. Sci.* **2008**, *97*, 2607–2618.
(36) Knox, C.; Law, V.; Jewison, T.; Liu, P.; Ly, S.; Frolkis, A.; Pon, A.; Banco, K.; Mak, C.; Neveu, V.; *et al.* DrugBank 3.0: A Comprehensive Resource for "Omics" Research on Drugs. *Nucleic Acids Res.* **2011**, *39*, D1035–D1041.
(37) Wu, S.; Wan, P.; Li, J.; Li, D.; Zhu, Y.; He, F. Multi-Modality of pI Distribution in Whole Proteome. *Proteomics* **2006**, *6*, 449–455.
(38) Torres-Lugo, M.; Peppas, N. A. Molecular Design and in Vitro Studies of Novel pH-Sensitive Hydrogels for the Oral Delivery of Calcitonin. *Macromolecules* **1999**, *32*, 6646–6651.
(39) Dressman, J. B.; Krämer, J. *Pharmaceutical Dissolution Testing*; Taylor & Francis: Boca Raton, FL, 2005.
(40) Roberts, M. J.; Bentley, M. D.; Harris, J. M. Chemistry for Peptide and Protein PEGylation. *Adv. Drug Deliv. Rev.* **2012**, *64, Supplement*, 116–127.
(41) Veronese, F. M. Peptide and Protein PEGylation: A Review of Problems and Solutions. *Biomaterials* **2001**, *22*, 405–417.
(42) Veronese, F. M.; Pasut, G. PEGylation, Successful Approach to Drug Delivery. *Drug Discov. Today* **2005**, *10*, 1451–1458.
(43) Jevševar, S.; Kunstelj, M.; Porekar, V. G. PEGylation of Therapeutic Proteins. *Biotechnol. J.* **2010**, *5*, 113–128.
(44) Harris, J. M.; Chess, R. B. Effect of Pegylation on Pharmaceuticals. *Nat. Rev. Drug Discov.* **2003**, *2*, 214–221.
(45) Harris, D. J. M.; Martin, N. E.; Modi, M. Pegylation. *Clin. Pharmacokinet.* **2012**, *40*, 539–551.
(46) Owens III, D. E.; Peppas, N. A. Opsonization, Biodistribution, and Pharmacokinetics of Polymeric Nanoparticles. *Int. J. Pharm.* **2006**, *307*, 93–102.
(47) Aggarwal, P.; Hall, J. B.; McLeland, C. B.; Dobrovolskaia, M. A.; McNeil, S. E. Nanoparticle Interaction with Plasma Proteins as It Relates to Particle Biodistribution, Biocompatibility and Therapeutic Efficacy. *Adv. Drug Deliv. Rev.* **2009**, *61*, 428–437.
(48) Youn, Y. S.; Jung, J. Y.; Oh, S. H.; Yoo, S. D.; Lee, K. C. Improved Intestinal Delivery of Salmon Calcitonin by Lys18-Amine Specific PEGylation: Stability, Permeability, Pharmacokinetic Behavior and in Vivo Hypocalcemic Efficacy. *J. Controlled Release* **2006**, *114*, 334–342.
(49) Gorochovceva, N.; Makuška, R. Synthesis and Study of Water-Soluble Chitosan-O-Poly(ethylene Glycol) Graft Copolymers. *Eur. Polym. J.* **2004**, *40*, 685–691.
(50) Toncheva, V.; Wolfert, M. A.; Dash, P. R.; Oupicky, D.; Ulbrich, K.; Seymour, L. W.; Schacht, E. H. Novel Vectors for Gene Delivery Formed by Self-Assembly of DNA with Poly(l-Lysine) Grafted with Hydrophilic Polymers. *Biochim. Biophys. Acta BBA - Gen. Subj.* **1998**, *1380*, 354–368.
(51) Nguyen, H.-K.; Lemieux, P.; Vinogradov, S. V.; Gebhart, C. L.; Guérin, N.; Paradis, G.; Bronich, T. K.; Alakhov, V. Y.; Kabanov, A. V. Evaluation of

Polyether-Polyethyleneimine Graft Copolymers as Gene Transfer Agents. *Gene Ther.* **2000**, *7*, 126–138.
(52) Abuchowski, A.; McCoy, J. R.; Palczuk, N. C.; Es, T. van; Davis, F. F. Effect of Covalent Attachment of Polyethylene Glycol on Immunogenicity and Circulating Life of Bovine Liver Catalase. *J. Biol. Chem.* **1977**, *252*, 3582–3586.
(53) Staros, J. V.; Wright, R. W.; Swingle, D. M. Enhancement by N-Hydroxysulfosuccinimide of Water-Soluble Carbodiimide-Mediated Coupling Reactions. *Anal. Biochem.* **1986**, *156*, 220–222.
(54) Grabarek, Z.; Gergely, J. Zero-Length Crosslinking Procedure with the Use of Active Esters. *Anal. Biochem.* **1990**, *185*, 131–135.
(55) Sehgal, D.; Vijay, I. K. A Method for the High Efficiency of Water-Soluble Carbodiimide-Mediated Amidation. *Anal. Biochem.* **1994**, *218*, 87–91.
(56) Nakajima, N.; Ikada, Y. Mechanism of Amide Formation by Carbodiimide for Bioconjugation in Aqueous Media. *Bioconjug. Chem.* **1995**, *6*, 123–130.
(57) Pierce Protein Biology Products. Carbodiimide Crosslinker Chemistry http://www.piercenet.com/method/carbodiimide-crosslinker-chemistry (accessed Jan 22, 2015).
(58) Hermanson, G. T. *Bioconjugate Techniques*; Academic press, 2013.
(59) Pierce Protein Biology Products. Protein Crosslinking Applications http://www.piercenet.com/method/crosslinking-applications#proteindna (accessed Jan 22, 2015).
(60) King, J. L.; Jukes, T. H. Non-Darwinian Evolution. *Science* **1969**, *164*, 788–798.
(61) Arkov, A. L.; Korolev, S. V.; Kisselev, L. L. Termination of Translation in Bacteria May Be Modulated via Specific Interaction between Peptide Chain Release Factor 2 and the Last Peptidyl-tRNASer/Phe. *Nucleic Acids Res.* **1993**, *21*, 2891–2897.
(62) Alff-Steinberger, C.; Epstein, R. Codon Preference in the Terminal Region of E. Coli Genes and Evolution of Stop Codon Usage. *J. Theor. Biol.* **1994**, *168*, 461–463.
(63) Arkov, A. L.; Korolev, S. V.; Kisslev, L. L. 5′ Contexts of Escherichia Coli and Human Termination Codons Are Similar. *Nucleic Acids Res.* **1995**, *23*, 4712–4716.
(64) Berezovsky, I. N.; Kilosanidze, G. T.; Tumanyan, V. G.; Kisselev, L. L. Amino Acid Composition of Protein Termini Are Biased in Different Manners. *Protein Eng.* **1999**, *12*, 23–30.
(65) DePristo, M. A.; Zilversmit, M. M.; Hartl, D. L. On the Abundance, Amino Acid Composition, and Evolutionary Dynamics of Low-Complexity Regions in Proteins. *Gene* **2006**, *378*, 19–30.
(66) Fahey, R. C.; Hunt, J. S.; Windham, G. C. On the Cysteine and Cystine Content of Proteins. Differences between Intracellular and Extracellular Proteins. *J. Mol. Evol.* **1977**, *10*, 155–160.
(67) Ghosh, S. S.; Kao, P. M.; McCue, A. W.; Chappelle, H. L. Use of Maleimide-Thiol Coupling Chemistry for Efficient Syntheses of Oligonucleotide-Enzyme Conjugate Hybridization Probes. *Bioconjug. Chem.* **1990**, *1*, 71–76.

(68) Brinkley, M. A Brief Survey of Methods for Preparing Protein Conjugates with Dyes, Haptens and Crosslinking Reagents. *Bioconjug. Chem.* **1992**, *3*, 2–13.
(69) Smyth, D. G.; Blumenfeld, O. O.; Konigsberg, W. Reactions of N-Ethylmaleimide with Peptides and Amino Acids. *Biochem. J.* **1964**, *91*, 589–595.
(70) Gorin, G.; Martic, P. A.; Doughty, G. Kinetics of the Reaction of N-Ethylmaleimide with Cysteine and Some Congeners. *Arch. Biochem. Biophys.* **1966**, *115*, 593–597.
(71) Heitz, J. R.; Anderson, C. D.; Anderson, B. M. Inactivation of Yeast Alcohol Dehydrogenase by N-Alkylmaleimides. *Arch. Biochem. Biophys.* **1968**, *127*, 627–636.
(72) Partis, M. D.; Griffiths, D. G.; Roberts, G. C.; Beechey, R. B. Cross-Linking of Protein by Ω-Maleimido Alkanoyl N-Hydroxysuccinimido Esters. *J. Protein Chem.* **1983**, *2*, 263–277.
(73) Brewer, C. F.; Riehm, J. P. Evidence for Possible Nonspecific Reactions between N-Ethylmaleimide and Proteins. *Anal. Biochem.* **1967**, *18*, 248–255.
(74) Hogg, P. J. Disulfide Bonds as Switches for Protein Function. *Trends Biochem. Sci.* **2003**, *28*, 210–214.
(75) Gorman, J. J.; Corino, G. L.; Mitchell, S. J. Fluorescent Labeling of Cysteinyl Residues. *Eur. J. Biochem.* **1987**, *168*, 169–179.
(76) Jones, M. W.; Strickland, R. A.; Schumacher, F. F.; Caddick, S.; Baker, J. R.; Gibson, M. I.; Haddleton, D. M. Polymeric Dibromomaleimides As Extremely Efficient Disulfide Bridging Bioconjugation and Pegylation Agents. *J. Am. Chem. Soc.* **2012**, *134*, 1847–1852.
(77) Smith, M. E. B.; Schumacher, F. F.; Ryan, C. P.; Tedaldi, L. M.; Papaioannou, D.; Waksman, G.; Caddick, S.; Baker, J. R. Protein Modification, Bioconjugation, and Disulfide Bridging Using Bromomaleimides. *J. Am. Chem. Soc.* **2010**, *132*, 1960–1965.
(78) Tedaldi, L. M.; Smith, M. E. B.; Nathani, R. I.; Baker, J. R. Bromomaleimides: New Reagents for the Selective and Reversible Modification of Cysteine. *Chem. Commun.* **2009**, 6583–6585.
(79) Jayasena, S. D. Aptamers: An Emerging Class of Molecules That Rival Antibodies in Diagnostics. *Clin. Chem.* **1999**, *45*, 1628–1650.
(80) Nimjee, S. M.; Rusconi, C. P.; Sullenger, B. A. Aptamers: An Emerging Class of Therapeutics. *Annu. Rev. Med.* **2005**, *56*, 555–583.
(81) Tuerk, C.; Gold, L. Systematic Evolution of Ligands by Exponential Enrichment: RNA Ligands to Bacteriophage T4 DNA Polymerase. *Science* **1990**, *249*, 505–510.
(82) Ellington, A. D.; Szostak, J. W. In Vitro Selection of RNA Molecules That Bind Specific Ligands. *Nature* **1990**, *346*, 818–822.
(83) Klug, S. J.; Famulok, M. All You Wanted to Know about SELEX. *Mol. Biol. Rep.* **1994**, *20*, 97–107.
(84) Stoltenburg, R.; Reinemann, C.; Strehlitz, B. SELEX—A (r)evolutionary Method to Generate High-Affinity Nucleic Acid Ligands. *Biomol. Eng.* **2007**, *24*, 381–403.

(85) Shamah, S. M.; Healy, J. M.; Cload, S. T. Complex Target SELEX. *Acc. Chem. Res.* **2008**, *41*, 130–138.
(86) Ulrich, H.; Martins, A. H. B.; Pesquero, J. B. RNA and DNA Aptamers in Cytomics Analysis. *Cytometry A* **2004**, *59A*, 220–231.
(87) Lin, Y.; Qiu, Q.; Gill, S. C.; Jayasena, S. D. Modified RNA Sequence Pools for in Vitro Selection. *Nucleic Acids Res.* **1994**, *22*, 5229–5234.
(88) Pagratis, N. C.; Bell, C.; Chang, Y.-F.; Jennings, S.; Fitzwater, T.; Jellinek, D.; Dang, C. Potent 2′-Amino-, and 2′-Fluoro-2′- Deoxyribonucleotide RNA Inhibitors of Keratinocyte Growth Factor. *Nat. Biotechnol.* **1997**, *15*, 68–73.
(89) Eulberg, D.; Klussmann, S. Spiegelmers: Biostable Aptamers. *ChemBioChem* **2003**, *4*, 979–983.
(90) Klußmann, S.; Nolte, A.; Bald, R.; Erdmann, V. A.; Fürste, J. P. Mirror-Image RNA That Binds D-Adenosine. *Nat. Biotechnol.* **1996**, *14*, 1112–1115.
(91) Nolte, A.; Klußmann, S.; Bald, R.; Erdmann, V. A.; Fürste, J. P. Mirror-Design of L-Oligonucleotide Ligands Binding to L-Arginine. *Nat. Biotechnol.* **1996**, *14*, 1116–1119.
(92) Wieland, M.; Benz, A.; Klauser, B.; Hartig, J. S. Artificial Ribozyme Switches Containing Natural Riboswitch Aptamer Domains. *Angew. Chem.* **2009**, *121*, 2753–2756.
(93) Lamm, M. E. Current Concepts in Mucosal Immunity. IV. How Epithelial Transport of IgA Antibodies Relates to Host Defense. *Am. J. Physiol. - Gastrointest. Liver Physiol.* **1998**, *274*, G614–G617.
(94) Brewer, E.; Lowman, A. Characterization of Drug Delivery Systems Utilizing Receptor-Mediated Transport. *Bioeng. Conf. NEBEC 201238th Annu. Northeast* **2012**, 105–106.
(95) Peppas, N. A.; Donini, C. Protein Delivery Systems. In *Encyclopedia of Biomaterials and Biomedical Engineering*; Taylor & Francis, 2013; pp. 1–13.
(96) Fisher, O. Z.; Peppas, N. A. Quantifying Tight Junction Disruption Caused by Biomimetic pH-Sensitive Hydrogel Drug Carriers. *J. Drug Deliv. Sci. Technol.* **2008**, *18*, 47–50.
(97) Madsen, F.; Peppas, N. A. Complexation Graft Copolymer Networks: Swelling Properties, Calcium Binding and Proteolytic Enzyme Inhibition. *Biomaterials* **1999**, *20*, 1701–1708.
(98) Ichikawa, H.; Peppas, N. A. Novel Complexation Hydrogels for Oral Peptide Delivery: In Vitro Evaluation of Their Cytocompatibility and Insulin-Transport Enhancing Effects Using Caco-2 Cell Monolayers. *J. Biomed. Mater. Res. A* **2003**, *67A*, 609–617.

Chapter 3: Specific Aims

The use of pH-responsive hydrogels as delivery carriers for the oral delivery of therapeutic proteins is quite promising, and much work has been done to design and study such systems, such as poly(methacrylic acid-grated-poly(ethylene glycol)) (P(MAA-g-EG)) or poly(methacrylic acid-co-N-vinylpyrrolidone) (P(MAA-co-NVP)). However, proteins exhibiting high isoelectric point have shown limited bioavailability in these systems due to electrostatic interactions with the hydrogels. Furthermore, the intestinal epithelium presents another significant obstacle to effective oral delivery at the current time, and therefore needs to be addressed in order to make an effective protein delivery platform.

The objective of this work was to make judicious modifications to previously studied P(MAA-g-EG) or P(MAA-co-NVP) hydrogel systems to overcome the limitations that have prevented oral delivery of protein therapeutics thus far. Substitution of itaconic acid as the pH-responsive moiety and incorporation of degradable peptide crosslinks targeted to degrade in the small intestine were explored as methods of enhancing the delivery of high isoelectric point-exhibiting proteins to the small intestine. Numerous design parameters were tested to determine the most important design criteria for proteins and suggest design rules for tailoring the systems to different proteins. Additionally, conjugation using PEG (PEGylation) is a common method of improving therapeutic bioavailability by enhancing *in vivo* half-life. The effects of this modification on delivery and intestinal absorption were elucidated. Finally, in an effort to overcome

the final barrier of limited intestinal absorption of macromolecules, a discovery protocol for transcellular transport initiating aptamer ligands was developed and used to identify optimal nucleic acid sequences for this purpose. The subsequently described experiments were designed to systematically investigate these strategies and thereby develop a safe and effective oral delivery platform for delivery of high isoelectric point-exhibiting proteins.

Therefore, the specific aims of the research presented herein were to:

1. Synthesize, characterize, and evaluate pH-responsive hydrogels and enzymatically-degraded hydrogels as vehicles for the oral delivery of protein therapeutics exhibiting high isoelectric point;
2. Optimize available hydrogel design parameters—such as monomer ratios, crosslinking density, particle size, and drug loading procedure—to achieve high bioavailability of protein therapeutics;
3. Evaluate the effects of bioconjugation on oral protein delivery properties;
4. Develop a novel aptamer ligand to target transcellular transport receptors in order to enhance protein transport across the intestinal epithelium;
5. Investigate the performance of designed oral delivery platforms *in vivo* using a closed-loop rat model.

Chapter 4: Synthesis and Characterization of Responsive Hydrogels[1]

4.1 INTRODUCTION

Numerous techniques have been studied in an effort to enable site-specific delivery of therapeutics, often with controlled or extended release capabilities. Although some of these systems have been inspired by natural processes found in the body, such as liposomes or micelles, the use of synthetic hydrogel matrices as drug carriers has been one of the foremost areas of research. Hydrogels have a wide range of properties that are easily tailored to the desired application. The nearly limitless spectrum of monomers that may be incorporated into the polymer backbone can give wide differences in function, based on variations in electronegativity, hydrophilicity, acidity, bond motility, etc. Furthermore, the structure plays a fundamental role in the behavior of the hydrogel. For example, low crosslinking density yields increased translational degrees of freedom for the polymer chains and larger effective mesh size, and may therefore be used to increase hydrogel swelling, to speed the release of compounds from the matrix, or to enable delivery of larger molecules. Furthermore, randomly ordered polymers will have significantly different behavior than block copolymers or those formed with isotactic backbones. Because both the chemical moieties and the physical structure of the

[1] Portions of this chapter have been previously published in Koetting, M. C.; Peppas, N. A. pH-Responsive Poly(itaconic Acid-Co-N-Vinylpyrrolidone) Hydrogels with Reduced Ionic Strength Loading Solutions Offer Improved Oral Delivery Potential for High Isoelectric Point-Exhibiting Therapeutic Proteins. International Journal of Pharmaceutics 2014, 471, 83–91.[1] Writing is reprinted herein with permission.

hydrogel have such strong effect on function, the range of behaviors observed in hydrogels is highly varied and highly customizable.

One of the most interesting and useful classes of hydrogels is stimulus-responsive hydrogels. Such hydrogels utilize chemical moieties in the polymer backbones or crosslinks that are chosen to yield a change in hydrogel behavior upon changes in the environment. Hydrogels have been successfully produced that exhibit responsiveness to a wide variety of stimuli, including pH, temperature, light, electromagnetic fields, and specific chemicals or analytes.[2–4]

Such hydrogels have obvious implications for drug delivery. The responsive behavior enables site-specific delivery of drug compounds by yielding a protecting or encapsulating phase that is wholly separate from the drug release phase, as well as a mechanism by which these phases may be easily switched. Site-specific drug delivery is ideal as it assures high concentration of therapeutic at the desired site of action while limiting off-target side effects associated with systemic application. It also enables precise temporal control of drug release, allowing for pulsatile release kinetics to keep drug concentrations within therapeutic ranges, as illustrated in Figure 4-1, or feedback-controlled release so that the drug is only released when needed (e.g., insulin released only when glucose levels are high; anti-inflammatory drugs released only in presence of inflammatory cytokines).[2,5–7] By offering control over the spatial and the temporal delivery of drugs, stimulus-responsive hydrogels will enable currently used therapeutics to be more effective and have fewer side effects while also enabling use of effective

potential therapeutics that would otherwise be unusable due to systemic toxicity concerns.

For enabling the oral delivery of protein therapeutics, pH-responsive hydrogels are especially auspicious because the wide transition in pH from the stomach to the small intestine offers a simple and effective triggering mechanism for site-specific drug release in the small intestine. Research in the Peppas lab over the past two decades has identified pH-responsive hydrogels of poly(methacrylic acid-grafted-poly(ethylene glycol)) (P(MAA-*g*-EG)) or poly(methacrylic acid-*co*-N-vinylpyrrolidone) (P(MAA-*co*-NVP) as suitable drug delivery carriers for enabling the oral delivery of insulin and human growth hormone. These systems exhibit a collapsed state at low pH as found in the stomach, effectively encapsulating and protecting the protein therapeutic, and transition to a swollen state at neutral pH as found in the small intestine, increasing the effective mesh size significantly and therefore releasing the protein therapeutic by diffusion for transport across the intestinal epithelium into the bloodstream. However, these systems still suffer from low bioavailability compared to injection, resulting in wasted drug and therefore higher cost.[8–13] Additionally, studies seeking to deliver proteins exhibiting high isoelectric points (pI) have been hampered by coulombic interactions in the small intestine between the anionic hydrogel and cationic protein, resulting in binding rather than release for uptake into the bloodstream.[9]

In this work, I focus on enabling oral delivery of salmon calcitonin as a model for high pI therapeutic proteins. Our group has previously synthesized and characterized pH-sensitive copolymer hydrogels comprised of poly(itaconic acid-grafted-poly(ethylene

glycol)) (P(IA-*g*-EG)) which showed potential as drug delivery carriers due to their favorable equilibrium swelling behavior in acidic and neutral pH environments.[14] The additional carboxylic acid residue present in itaconic acid compared to methacrylic acid can yield superior swelling behavior and drug delivery capability that would assist in delivery of high pI proteins. However, these hydrogels were initially studied on their own and not compared directly against previous P(MAA-*g*-EG) or P(MAA-*co*-NVP) systems, and were not tested in drug loading and release experiments, so I herein extend work with these systems by determining their swelling behavior in time-limited, dynamic-pH swelling experiments, by comparing against P(MAA-*g*-EG) and P(MAA-*co*-NVP) systems, and by utilizing them in *in vitro* drug loading and release experiments.

Furthermore, our group has previously demonstrated improved drug delivery behavior resulting from use of N-vinylpyrrolidone as a hydrogen-bond accepting comonomer instead of poly(ethylene glycol), as it offers stronger complexation behavior for improved protein protection and faster diffusive drug release.[9,15] Therefore, we also synthesize and test P(IA-co-NVP) hydrogels alongside P(MAA-*g*-EG), P(MAA-*co*-NVP), and P(IA-*g*-EG) hydrogels with the expectation that the stronger complexation behavior will also assist in enabling the oral delivery of high pI proteins.

In this chapter, I discuss the synthesis and characterization procedures of the proposed hydrogel systems (P(IA-co-NVP) and P(IA-g-EG) microparticles, as well as peptide-degradable hydrogels) and demonstrate improved material responsiveness as compared to previous systems.

4.2 MATERIALS AND METHODS

4.2.1 Synthesis and Purification of pH-Responsive Hydrogels

Seven different hydrogels were formed via UV-initiated free radical polymerization. Each hydrogel was comprised of a pH-responsive moiety—either methacrylic acid (MAA) (Sigma-Aldrich, St. Louis, MO) or itaconic acid (IA) (Acros Organics, Fair Lawn, NJ)—copolymerized with a hydrophilic comonomer containing a hydrogen bond-acceptor for complexation behavior—either N-vinyl pyrrolidone (NVP) (Sigma-Aldrich) or poly(ethylene glycol) monomethyl ether monomethacrylate (PEGMMA, molecular weight 1000) (Poly-sciences, Warrington, PA). Methyl methacrylate (MMA) (Sigma-Aldrich) was also incorporated as a third monomer in one formulation. Hydrogels were crosslinked using tetra(ethylene glycol) dimethacrylate (TEGDMA) (Sigma-Aldrich) or poly(ethylene glycol) dimethacrylate (PEGDMA, molecular weight 1000) (Sigma-Aldrich). Irgacure 2959 (Ciba Specialty Chemicals Corp., Tarrytown, NY) was used as the UV-initiator.

All polymerizations were carried out in a 50:50 w/w mixture of aqueous sodium hydroxide (NaOH) and ethanol. Sodium hydroxide was prepared at a concentration such that there was a 1:2 molar ratio of NaOH to IA. No NaOH was required for MAA-based gels. Within this co-solvent, monomers were added at various molar ratios as shown in Table 4-1, along with crosslinker (3-5 mol% for IA-based gels; 1 mol% for MAA-based gels) and 1 mol% initiator. Molar percent is defined with regard to the total moles of monomers and crosslinker.

The monomer solution was then introduced into a nitrogen environment in an MBraun Labmaster 130 glove box (MBraun, Garching, Germany) and purged with nitrogen for 10 minutes to remove oxygen, a free radical scavenger. The solution was pipetted between two quartz glass plates (15 x 15 x 0.3 cm) separated by a 0.7 mm thick Teflon spacer, and then polymerized for 75 minutes in 35 mW/cm^2 UV light using an IntelliRay 600 UV flood source (Uvitron International, West Springfield, MA).

Disks 12 mm in diameter were collected from the resulting films immediately following polymerization for use in swelling studies. The remaining hydrogel was then removed from the glass plates and washed in 1 L of 18.2 MΩ-cm deionized water, changed daily for 10 days to remove unreacted monomers. Following washing, the films were dried under vacuum at 29 °C for at least 2 days, crushed into microparticles with a mortar and pestle, and sieved to 90–150 μm in size.

4.2.2 Synthesis of Enzymatically Degradable Hydrogels

Enzymatically degradable hydrogels using peptide crosslinks were prepared as described by Knipe et al.[16] Uncrosslinked P(MAA-co-NVP) polymer was prepared by UV-initiated free radical polymerization. Methacrylic acid (Sigma-Aldrich) and N-vinylpyrrolidone (Sigma-Aldrich) were added to a 50:50 w/w mixture of water and ethanol at a molar ratio of 1:1 MAA:NVP and 30 wt% monomer to total solution weight. Irgacure 2959 (Ciba Specialty Chemicals Corp.) was added as a photoinitiator at 1 wt% relative to total monomer weight. The solution was purged with nitrogen for 5 min and polymerized for 30 min in 35 mW/cm^2 UV light using an IntelliRay 600 UV flood source

(Uvitron International). After polymerization, the polymer was purified using 1 N hydrochloric acid (Fisher Scientific, Fair Lawn, NJ) and acetone to cause precipitation of the polymer, followed by centrifugation and resuspension in deionized water 3 times. The purified polymer was dried by lyophilization.

The degradable P(MAA-co-NVP) hydrogel was formed by crosslinking using a synthetic peptide. Uncrosslinked P(MAA-co-NVP) polymer was dissolved in a 50:50 w/w mixture of water and ethanol at a concentration of 50 mg/mL. 1-ethyl-3-(3-dimethylaminopropyl)carbodiimide hydrochloride (EDC) (Sigma-Aldrich) was dissolved in ethanol at 50 mg/mL concentration. N-hydroxysuccinimide (NHS) (Thermo Scientific Pierce, Waltham, MA) was dissolved separately in ethanol at 16 mg/mL concentration. The EDC and NHS solutions were added to the polymer solution at a 6:3:1 ratio of polymer:EDC:NHS by weight, vortexed briefly, and reacted for 3 min. The solution pH was raised to pH 8 using 1 N sodium hydroxide (Fisher Scientific). A synthetic peptide with the sequence MMRRRKK (CHI Scientific, Maynard, MA) was dissolved in ethanol at a concentration of 100 mg/mL and added to the polymer solution at a 2:1 weight ratio of polymer:peptide. The mixture reacted for 12 h, and the product was isolated by centrifugation. The polymer was resuspended in deionized water and then isolated by centrifugation 3 times to remove remaining reactants. The hydrogel was then dried by lyophilization, crushed using a mortar and pestle, and sieved to microparticles 90-150 μm in size for use in studies.

4.2.3 Hydrogel Characterization Studies

4.2.3.1 Equilibrium Swelling Studies

Hydrogel disks 12 mm in diameter were acquired from the 1:1 P(IA-*co*-NVP), 1:9 P(IA-*co*-NVP), P(IA-*co*-NVP-*co*-MMA), and P(MAA-*co*-NVP) hydrogel formulations immediately following polymerization. These disks were weighed in air and in heptane to obtain the relaxed state weight of the disk. The disks were washed in deionized water for 10 days and dried at 30 °C under vacuum. The dry weight of each disk was determined in air and heptane using an Ohaus Analytical Plus scale (Ohaus, Parsippany, NJ). Disks were then placed in either a standard PBS buffer (0.150 M, pH 7.4) (Fisher Scientific) to simulate neutral small intestine conditions or a 0.01 N hydrochloric acid (HCl) solution (Sigma-Aldrich) (pH 2.0) to simulate acidic stomach conditions at 37 °C for 72 h, allowing the disks to swell to equilibrium. The swelled disks were then removed from solution and weighed in air and heptane to obtain the swollen weight of the disks.

4.2.3.2 Dynamic Swelling Studies

Dry disks were weighed in air and subsequently swelled at 37 °C for 3 h in 0.01 N HCl (pH 2.0). Ten dimethylglutaric acid (DMGA) buffers spanning a pH range from 3.2 to 7.6 were prepared and preheated to 37 °C. Following swelling in HCl, the disks were moved into the first of these ten buffers (pH 3.2), allowed to swell for 7 minutes, removed from the buffer, and weighed in air. The disks were then moved to the next

buffer (in order of increasing pH), and the swelling and weighing process was repeated through all 10 buffers with 7 minute swelling intervals.

4.2.3.3 Mesh Size Calculations

Mesh sizes were calculated using a mixture of polymer swelling theory and rubber elasticity theory. Polymer swelling behavior was modeled using three different equations for the 1:1 P(IA-co-NVP) hydrogel for comparison of the models. These three models are the Peppas-Merrill equation (Equation 4-1),[17] the Brannon-Peppas equation (Equation 4-2),[18] and the Şen-Güven model (Equation 4-3).[19] The Peppas-Merrill equation is the earliest and most easily used, but is valid for neutral hydrogel networks only:

$$\frac{1}{\overline{M_c}} = \frac{2}{\overline{M_n}} - \frac{\left(\frac{\bar{v}}{V_1}\right)\left[\ln\left(1 - v_{2,s}\right) + v_{2,s} + \chi_1 {v_{2,s}}^2\right]}{v_{2,r}\left[\left(\frac{v_{2,s}}{v_{2,r}}\right)^{1/3} - \left(\frac{v_{2,s}}{2v_{2,r}}\right)\right]} \qquad \text{Equation 4-1}$$

In this model, $\overline{M_c}$ is the average molecular weight of polymer between crosslinks [g/mol], $\overline{M_n}$ is the number average molecular weight of the linear polymer chains [g/mol], $\bar{v}$ is the specific volume of the dry polymer [mL/g], V_1 is the molar volume of the solvent (water, 18.1 mL/mol), $v_{2,s}$ is the volume fraction of the polymer in the swollen state, $v_{2,r}$ is the volume fraction of the polymer in the relaxed state (immediately after polymerization), and χ_1 is the Flory interaction parameter for the polymer and the solvent.

The Brannon-Peppas model (Equation 4-2) was derived for polyelectrolyte networks with monoprotic ionizable moieties such as poly(methacrylic acid):

$$\frac{V_1}{4I}\cdot\left(\frac{10^{-pKa}}{10^{-pH}+10^{-pKa}}\right)^2\cdot\left(\frac{v_{2,s}\cdot X}{\bar{v}\cdot M_r}\right)^2 = \left[\ln\left(1-v_{2,s}\right)+v_{2,s}+\chi_1 {v_{2,s}}^2\right]+\left(\frac{V_1}{\bar{v}\cdot\overline{M_c}}\right)\cdot\left(1-\frac{2\overline{M_c}}{\overline{M_n}}\right)\cdot v_{2,r}\cdot\left[\left(\frac{v_{2,s}}{v_{2,r}}\right)^{\frac{1}{3}}-\frac{1}{2}\left(\frac{v_{2,s}}{v_{2,r}}\right)\right] \quad \text{Equation 4-2}$$

In this model, the terms are the same as in the Peppas-Merrill equation, with the additions that M_r is the molar average molecular weight of a repeat unit [g/mol], X is the molar fraction of ionizable monomers in the polymer, and I is the ionic strength of the solvent [mol/mL].[20] (By error, the X and M_r terms were omitted from the equation in the original paper. Without these terms, the units do not cancel appropriately and the concentration of ions is incorrect. The error has been propagated through subsequent literature, and I am unaware of papers citing the correct form of the equation. However, after rederivation of the ionic contribution, I am confident in the veracity of this form.) Although itaconic acid has two pK_a values (one for each acid group), only the pK_a most proximate to the conditions was used in applying this model (e.g., pK_a = 3.85 for acidic conditions; pK_a = 5.45 for neutral conditions).

Finally, the model of Şen and Güven[19] (Equation 4-3) follows the derivation of the Brannon-Peppas model and therefore looks quite similar, but is specifically for diprotic ionizing groups, such as in poly(itaconic acid), and should therefore be the most appropriate for itaconic acid-based gels:

$$\frac{V_1}{4I}\cdot\left(\frac{2\cdot 10^{-(pK_{a1}+pK_{a2})}+10^{-(pH+pK_{a1})}}{2\cdot[(10^{-pH})^2+10^{-(pH+pK_{a1})}+10^{-(pK_{a1}+pK_{a2})}]}\right)^2\cdot\left(\frac{v_{2,s}\cdot X}{\bar{v}\cdot M_r}\right)^2 = \left[\ln(1-v_{2,s})+v_{2,s}+\chi_1 {v_{2,s}}^2\right]+\left(\frac{V_1}{\bar{v}\cdot\overline{M_c}}\right)\cdot\left(1-\frac{2}{\varphi}\right)\cdot {v_{2,r}}^{2/3}\cdot {v_{2,s}}^{1/3} \quad \text{Equation 4-3}$$

In this model, variables are the same as in the Peppas-Merrill (Equation 4-1) and Brannon-Peppas (Equation 4-2) equations, with the additions of φ being the functionality of crosslinks, and pK_{a1} referring to the more acidic unit (3.85 for itaconic acid) and pK_{a2} referring to the less acidic unit (5.45 for itaconic acid). It should be noted that the M_r term was omitted from this model in the original paper, as was the case with the Brannon-Peppas model. To make units match, the authors erroneously cited the molar volume of water as being 18.1 g/cm^3, which one will note is a density, not a molar volume, and 18x the actual density of water. As with the Brannon-Peppas equation, the M_r term is needed to properly calculate the concentration of ions in the hydrogel and is therefore utilized in this work.

Equilibrium swelling results from the 1:1 P(IA-co-NVP) disks were used with all three to determine $\overline{M_c}$ for each disk. The equilibrium swelling results for the remaining

itaconic acid gels were analyzed with the Şen-Güven model only, while the methacrylic acid gel was analyzed with the Brannon-Peppas model. The Flory interaction parameter χ_1 was assumed to have a value of 0.5, as is true for poly(methacrylic acid) and poly(N-vinylpyrrolidone) in water.[21–23] $\overline{M_n}$ was assumed to have a value of 40000 g/mol. M_r was taken as a weighted average of the monomers present in the hydrogel. $\overline{M_c}$ was determined using a generalized reduced gradient (GRG) nonlinear solution method implemented in Microsoft Excel.

Using the calculated values of $\overline{M_c}$, rubber elasticity theory was applied to determine mesh sizes. Rubber elasticity theory shows that the mesh size, ξ, can be calculated by Equation 4-4,

$$\xi = {v_{2,s}}^{-\frac{1}{3}} \cdot \left(\frac{2 \cdot C_n \cdot \overline{M_c}}{M_r} \right)^{1/2} \cdot l \qquad \text{Equation 4-4}$$

where C_n is the Flory characteristic ratio and l is the carbon-carbon bond length (1.54 Å for vinyl polymers).[2,24] The value of C_n used was a molar weighted average of the characteristic ratios for pure poly(itaconic acid), poly(methacrylic acid), and poly(N-vinylpyrrolidone). Values of $\overline{M_c}$ and equilibrium disk swelling measurements were used with the above equation to determine average mesh size.

4.2.3.4 Cytotoxicity Studies

Caco-2 human colorectal adenocarcinoma cells (ATCC, Manassas, VA) were cultured normally up to a passage number of 60. The cells were then plated into a 96-

well plate at an initial concentration of $1.0x10^4$ cells/well in Dulbecco's Modified Eagle's Medium (DMEM) with 10% v/v fetal bovine serum, 1% v/v penicillin-streptomycin, and 1% v/v L-glutamine added. Each well received 200 μL DMEM (5.0×10^4 cells/mL). Cells were incubated for 72 h at 37 °C. Microparticles of the 1:1 P(IA-*co*-NVP), 1:1 P(IA-*g*-EG), and 1:1 P(MAA-*g*-EG) hydrogels ranging from 90-150 μm in size were sterilized by exposure to ultraviolet light and then suspended in DMEM at concentrations of 5.000, 2.500, 1.250, 0.625, 0.312, 0.156, 0.078, and 0.039 mg/mL. DMEM was removed from all wells by vacuum aspiration and replaced with 120 μL of microparticle suspension (n=3 for each concentration of each hydrogel formulation), 1.5% v/v bleach in DMEM (negative control, n=8), or fresh DMEM (positive control, n=16). Cells were incubated in presence of hydrogel microparticles at 37 °C for 2 h. The microparticle suspensions were then removed from all wells by vacuum aspiration, and all wells were washed twice with 120 μL sterile phosphate-buffered saline. Cell viability was determined using an MTS assay: 20 μL (3-(4,5-dimethylthiazol-2-yl)-5-(3-carboxymethoxyphenyl)-2-(4-sulfophenyl)-2H-tetrazolium) (MTS) (Promega, Madison, WI) and 100 μL colorless DMEM were added to each well and incubated for 3 h before absorbance was measured at both 690 nm and 490 nm.

4.2.3.5 Thermogravimetric Analysis

The thermal degradation profiles of all the hydrogel formulations synthesized in section 4.2.1 were characterized using a Q500 thermogravimetric analyzer (TA Instruments, New Castle, DE). Hydrogel microparticles weighing 5-10 mg were heated

in a nitrogen environment from room temperature to 550 °C at a constant rate of 10 °C/min and maintained at 550 °C for 5 min before oxygen was added to eliminate any combustible degradation products.

4.3 RESULTS AND DISCUSSION

4.3.1 Synthesis of pH-Responsive Hydrogels

Itaconic acid presents several challenges to polymer synthesis: allylic hydrogen atoms act as chain transfer agents, inhibiting homopolymerization of itaconic acid;[25,26] the rate of homopolymerization is dependent on pH, with homopolymerization effectively halting above pH 4;[26] and the solubility of itaconic acid in water is only 0.083 g/mL, which is too low for creating a homogeneous hydrogel in water alone.[14] The pH-dependency is not as significant an issue with a copolymerization, as used here, but remains a key factor in determining the degree of incorporation of itaconic acid into the hydrogel. The solubility issue was overcome by Betancourt et al.[14] who achieved incorporation of IA up to 67 mol% by partially neutralizing acid groups in a sodium hydroxide, water, and ethanol solvent. The co-solvent and the partial neutralization allows for significantly improved solubility of IA, allowing for homogeneous hydrogel formation by UV-initiated free radical polymerization. Formulations of P(IA-*g*-EG) and P(IA-*co*-NVP) had been prepared by other groups prior to Betancourt et al., but these formulations required gamma ray irradiation as an initiation method and were unable to incorporate itaconic acid at greater than 9 mol% in the hydrogel.[27] Because of the cost

and hazards of gamma ray irradiation as a polymerization technique, the far more facile technique of UV-initiated polymerization is highly preferable, and was used here.

All hydrogels were successfully prepared by UV-initiated free radical polymerization using the procedures adapted from Betancourt et al.[14] Qualitatively, IA-based gels visibly required longer curing times than MAA-based gels. MAA-based gels had successfully cured within 30 min, whereas IA-based gels required up to 1 h to form a visible gel.

Qualitatively, IA-containing gels also exhibited lower mechanical strength than MAA-containing gels. The IA-based gels were softer and broke into smaller pieces readily upon mild agitation, such as moving the hydrogel film or refilling the rinse water. MAA-based gels did not tear nearly as readily and could easily be picked up and moved by hand without tearing. Methyl methacrylate was included as a third monomer in one formulation (P(IA-*co*-NVP-*co*-MMA)) at 10 mol% to add additional strength to the IA-based gel. The resulting gel did have improved strength, but was still softer and more easily broken than the MAA-based gels. Nevertheless, the reduced mechanical strength is a bulk property and does not significantly affect microparticle integrity. As a result, it is not expected to be a problem for end-use. Furthermore, the softness suggests higher porosity or greater water imbibition, which would be beneficial for improving bioavailability of proteins by aiding in diffusive protein release from the microparticle carriers.

4.3.2 Synthesis of Enzymatically Degradable Hydrogels

Enzymatically degradable hydrogels containing MMRRRKK peptide crosslinks were successfully prepared by the described method. Use of degradable hydrogels is one potential method for enhancing the bioavailability of orally delivered therapeutic proteins. The limitation of using previously studied systems with high isoelectric point exhibiting proteins is the low bioavailability resulting from electrostatic interactions between the protein and the anionic carriers, preventing diffusive release into the intestinal lumen. However, if the hydrogel particles degrade around the encapsulated protein, the protein does not have to diffuse through the hydrogel, ensuring it will reach the lumen.

Peptide crosslinks provide a highly beneficial method for targeting protein release to the small intestine through degradation. Careful selection of peptide sequence enables use of the enzymatic environment of the small intestine as a triggering mechanism for degradation and protein release. Using the peptides as crosslinks rather than as the fundamental monomer in the network enables degradation while using a minimal quantity of peptide, which is expensive to synthesize at large scale, thus greatly reducing cost. Finally, use of the peptide as a crosslinker allows the hydrogel to add degradability as a property while retaining the beneficial properties of the primary monomers, namely hydrophilicity, biocompatibility, and pH-responsiveness—which will act as a secondary mechanism for protein release that simultaneously assists external enzymes in reaching degradation sites within the hydrogel.

In order to target degradation to the small intestine, the peptide sequence must be carefully selected. Pepsin is the primary digestive enzyme in the stomach and preferentially cleaves proteins at the N-terminal side of phenylalanine, tryptophan, and tyrosine residues.[28,29] Therefore, these amino acids cannot be used in the crosslinker, as their incorporation would allow rapid degradation in the stomach where the encapsulated proteins would also be digested, yielding negligible bioavailability. The digestive enzymes in the small intestine are primarily trypsin and chymotrypsin. Chymotrypsin degrades at the same preferential sites as pepsin, but also has activity on leucine and methionine residues. This similarity in degradation sites makes it difficult to utilize chymotrypsin for hydrogel degradation, but it can be used with the incorporation of methionine residues. Trypsin, on the other hand, cleaves proteins at the carboxyl side of lysine or arginine residues, and is therefore quite easy to utilize for hydrogel degradation.

To take advantage of the enzymatic profile of the small intestine, the peptide MMRRRKK was chosen as a crosslinker. The three amino acids in the center of the crosslinker are arginine residues, providing several potential cleavage sites for trypsin. The carboxyl end of the peptide is comprised of lysine residues, which also enable degradation at these sites by trypsin. Methionine residues are also incorporated at the N-terminus in order to also utilize chymotrypsin while avoiding amino acids most susceptible to cleavage by pepsin. Therefore, the crosslinker is designed to enable degradation at any of the seven amino acids and by either of the two primary intestinal enzymes.

The MMRRRKK peptide crosslinker was successfully incorporated into the hydrogel using EDC/NHS crosslinking chemistry, linking primary amines in the peptide to carboxylic acids present in the P(MAA-co-NVP) polymer. Primary amines will be found at the N-terminus, on the arginine side chains, and on the lysine side chains, providing multiple locations for crosslinking. Although this means that the length of the incorporated crosslink is variable, the fact that all amino acids are potential degradation sites ensures that degradation can occur regardless of the actual crosslinking location. As such, the successfully prepared hydrogels will exhibit degradation specific to the small intestine.

4.3.3 Hydrogel Characterization

4.3.3.1 Equilibrium Swelling Studies

The fundamental feature of our hydrogel systems is their pH-responsive behavior. At low pH, the carboxylic acid residues in MAA or IA are protonated, allowing hydrogen bonding complexation between these residues and the electronegative oxygen in NVP or PEG, yielding a collapsed conformation with small mesh size. At neutral pH, the carboxylic acid residues are deprotonated, losing the hydrogen bonding complexation behavior and becoming anionically charged, thus swelling to a larger conformation with large mesh size due to entropic and enthalpic mixing interactions, osmotic pressure, and coulombic repulsion. As a result, the protein can be imbibed into the hydrogel in neutral conditions, encapsulated by acidification, and released once in neutral conditions again. Without this environmentally-responsive behavior, the hydrogels do not yield protection

from proteolytic enzymes and therefore will not work for oral protein delivery. Furthermore, the extent to which swelling occurs is suggestive of the achievable delivery efficiency.

Equilibrium weight swelling experiments were performed to determine the suitability of the synthesized hydrogels. The swelling behavior of P(IA-g-EG) hydrogels was not measured due to low physical stability of the material at the macro-scale. Although the hydrogel remains crosslinked and highly stable as microparticles, the large bulk disks used in weight swelling studies are too prone to breaking, especially when swelled in neutral conditions, to be accurately measured with gravimetry. P(MAA-*g*-EG) disks were also not studied, as their swelling behavior has been previously very well-characterized.[30–33]

As shown in Figure 4-2, during equilibrium swelling studies, the weight swelling ratio, q, defined as the swelled weight divided by the dry weight of a hydrogel disk, is very low for all tested formulations at low pH. All tested formulations exhibit weight swelling ratios ranging from 1.3 to 2.2, indicating that the average mesh size remains small in the acidic conditions expected in the stomach, keeping proteins encapsulated inside the hydrogel and preventing proteolytic enzymes from entering and degrading the protein. When swelled at neutral pH, the disks all achieve significantly greater swelling ratios ranging from 13.7 to 23.1, approximately one full order of magnitude greater than at low pH. This result indicates that the mesh size is significantly increased in the neutral conditions expected in the small intestine, such that the protein may diffuse out into the small intestine to cross the epithelial cell layer and enter the bloodstream. All of the

tested IA-based gels swelled significantly more ($p < 0.01$) than the MAA-based hydrogel, up to a 69% increase observed with the 45:45:10 P(IA-*co*-NVP-*co*-MMA) terpolymer, indicating the potential for the IA-based gels to encapsulate and therefore deliver greater amounts of the protein drug.

4.3.3.2 Dynamic Swelling Studies

In dynamic swelling studies, the difference in swelling behavior between IA and MAA-based gels is even more apparent. Figure 4-3 shows the results of the dynamic swelling studies, where there are 7 minutes of swelling time between each data point. The IA-based gels all achieved swelling ratios ranging from 11.2 to 15.4 within the 70 min of cumulative swelling time—on the same order of magnitude as the equilibrium swelling ratios. However, the MAA-based gel exhibited nearly imperceptible swelling, achieving a swelling ratio of only 1.5—a full order of magnitude less than its equilibrium weight swelling ratio. Because the residence time in the small intestine is limited—approximately 4 h for both fasted and fed patients[34]—it is important that the microparticles undergo a rapid transition from collapsed to swollen states to maximize the available time in which the encapsulated protein may diffuse out into the small intestine. The significantly improved time-dependent swelling characteristics of the IA-based gels compared to the MAA-based gels should therefore assist in maximizing protein release in the target region by maximizing the time available for diffusive release of the drug.

4.3.3.3 Mesh Size Calculations

The mesh size of a hydrogel used for drug delivery is an important quantity to determine, as it helps predict the probability of successful drug encapsulation and release. The mesh sizes of all disks at equilibrium conditions were determined using the Şen-Güven model for determining the average polymer weight between crosslinks, $\overline{M_c}$, coupled with rubber elasticity theory. Only equilibrium swelling measurements were used. Although the mesh size correlates to the swelling ratio, q, the Şen-Güven and Brannon-Peppas models were derived using the condition of equilibrium as a basic assumption and are therefore only accurate when the gel has swelled to equilibrium.[19,20]

Despite the fact that the Brannon-Peppas and Şen-Güven models have been present in literature for nearly two decades, these equations have not yet been widely used in determining the mesh size of P(MAA-g-EG) or P(MAA-co-NVP) hydrogels, with researchers opting to use the more pliable Peppas-Merrill equation.[14,15,17,35,36] The shortcoming of this approach is that the Peppas-Merrill equation is derived specifically for neutral hydrogels and does not take into account the ionic contribution to the free energy change of swelling. Therefore, a model that takes such ionic interactions into account, such as the Brannon-Peppas or Şen-Güven model, is more appropriate. However, the Brannon-Peppas equation does not consider the effect of monomers with multiple ionizing groups (e.g, diprotic or triprotic acids). The Şen-Güven model is essentially a rederivation of the Brannon-Peppas equation that assumes a diprotic acid in calculating the degree of ionization, making it the most ideal for hydrogels based on itaconic acid, and uses a newer phantom network model developed by Erman[37] rather

than an affine model developed by Flory in calculating the elastic contribution to the free energy change. Because it takes into account ionic contributions from both acid groups, the Şen-Güven model was used here for calculation of average mesh size in all itaconic acid-containing hydrogels. The Peppas-Merrill and Brannon-Peppas equations were also used with the 1:1 P(IA-co-NVP) hydrogel for comparison of the models, and the Brannon-Peppas model was used with the methacrylic acid gel because it is based on a monoprotic acid.

A comparison of the results from the three models applied to the 1:1 P(IA-co-NVP) hydrogel formulation is provided in Table 4-2. The calculated mesh size and molecular weight between crosslinks for each gel are tabulated in Table 4-3.

Comparing the resulting mesh sizes and molecular weights between crosslinks for the 1:1 gel from the three models, one sees that the models give nearly identical results for mesh sizes in the acidic state. In the neutral conditions, the numbers vary widely from mesh sizes as high as 232 Å with the Peppas-Merrill model down to 70.6 Å with the Şen-Güven model. Most notably, the Peppas-Merrill equation is the outlier, with a calculated mesh size approximately 3x as large as the Brannon-Peppas and Şen-Güven models, which are in much closer agreement. This is an expected result, as the primary difference with the Peppas-Merrill equation is that it does not take into account the significant ionic contribution to swelling, which is not present at highly acidic conditions when the carboxylic acid groups on itaconic acid are all protonated. At neutral conditions, these acid groups deprotonate, resulting in ionic interactions that result in generally increased swelling.

Furthermore, the much larger values of $\overline{M_c}$ calculated at neutral conditions compared to acidic conditions is expected as well. The protonation of acid groups at acidic conditions leads to hydrogen bonding interactions between the hydrogen-bond donor (the carboxylic acids) and the hydrogen bond acceptor (the electronegative oxygen in NVP) that act as crosslinks, even though they are not covalent. Therefore, the molecular weight between crosslinks is significantly larger in neutral conditions because these hydrogen-bonding crosslinks are lost.

One question arises: why does the Peppas-Merrill equation so significantly overstate the mesh size compared to the other models if ionic interactions promote swelling? This effect arises because we are applying the model to the data rather than using the model to create data. Because the gel actually experiences significant swelling enhancement due to the ionic interactions that create osmotic pressure and coulombic repulsion that both promote swelling while the model does not account for this, it must assume that the improved swelling is due only to lower crosslinking density rather than due to ionic contributions. Thus the model calculates a significantly higher $\overline{M_c}$ than the Brannon-Peppas or Şen-Güven models, since it can only assume fewer crosslinks is the reason for the enhanced swelling, leading to significantly larger calculated mesh size.

These results therefore demonstrate several salient points. First, the ionic contributions to swelling are significant, leading to multi-fold differences in the calculated geometry of the hydrogels when taken into account. Therefore, although all models are useful when applied in the proper systems, it is vital that one take into consideration the limitations of the models. Using an incorrect model, such as the

Peppas-Merrill model for describing methacrylic acid or itaconic acid-based systems, can yield extreme error in the calculated mesh size which can then lead to overconfidence in the gel's drug delivery capability.[14,15,35] Therefore, it is important to use the most appropriate model. In this case, the most appropriate model for the itaconic acid gels studied herein is the Şen-Güven model, which also proves to yield the most conservative estimate of the mesh size. This is advantageous, as we want large mesh sizes to help enable better release of the protein in the small intestine, and therefore do not want to use a model that will overstate the function of our systems. As a result, the Şen-Güven was applied to all itaconic acid gels, while the Brannon-Peppas equation was used for the methacrylic acid gel.

Comparing the results of the different hydrogel formulations, one can see that the mesh sizes of all gels are quite small in acidic conditions, as implied by the swelling results and as expected. The largest mesh size is 12.7 Å in the 1:9 P(IA-co-NVP) hydrogel. Comparing this to the size of a model protein like bovine serum albumin (140 x 40 x 40 Å prolate ellipsoid), it is apparent that a typical protein will be effectively encapsulated within the hydrogel since even the largest mesh size is significantly smaller than the size of a typical protein, thus preventing diffusion. This also implies sufficient protection of encapsulated protein from pepsin, which has dimensions of 41 x 48 x 65 Å that are much larger than the mesh size.[38]

At neutral conditions, the mesh sizes are all significantly larger, ranging from 36.7 Å in the P(MAA-co-NVP) gel all the way to 280 Å in the 1:9 P(IA-co-NVP) formulation. Importantly, the mesh size for all itaconic acid hydrogels was calculated to

be significantly higher than the mesh size of the methacrylic acid gel, even with what proved to be the slightly more conservative model, which is a vital improvement for enhancing bioavailability of high pI proteins. The mesh sizes of these itaconic acid gels—70.6, 99.8, and 280 Å for the 1:1 P(IA-co-NVP), P(IA-co-NVP-co-MMA), and 1:9 P(IA-co-NVP) formulations, respectively—are sufficiently large to allow for diffusion of typical proteins. However, for larger proteins such as antibodies, which have typical dimensions on the order of 100 Å may have difficulty diffusing through the hydrogel mesh.[39]

In conclusion, these calculated mesh sizes are indicative of hydrogels that perform as desired. The mesh remains small in acidic conditions, offering encapsulation and protection of proteins from proteolytic enzymes in the stomach, while expanding to dimensions sufficient for diffusion of typical proteins in neutral conditions. While improvement may be needed for very large proteins, possibly by decreasing crosslinking density, these systems seem ideal for use with proteins like salmon calcitonin. Finally, these calculations show improved hydrogel architecture with the itaconic acid gels as compared to the methacrylic acid hydrogel. This improvement is most likely due to the additional ionic contribution that is offered by a diprotic acid monomer compared to a monoprotic monomer.

4.3.3.4 Cytotoxicity Studies

Having shown a modest improvement in pH-responsive swelling behavior and mesh size by utilizing IA as the pH-responsive moiety, cytotoxicity studies were

performed to assure that the polymers were biocompatible and safe for use. Using Caco-2 cells, a proven, effective model of the human small intestine,[40–42] a cell viability study was performed *in vitro*. After culturing cells, cells were exposed to varying microparticle concentrations (0.039 – 5 mg/mL) of all 7 hydrogels, and viability was measured using an MTS assay. The results of this study are shown in Figure 4-4, with all cell viability values normalized to the positive control.

Even at very high concentrations of 5 mg/mL, the microparticles are still well tolerated, achieving over 80% relative viability with nearly every formulation. Only the 1:9 P(IA-co-NVP) shows any indication of toxicity at concentrations of 1.25 and 5.00 mg/mL, achieving only 59% and 74% viability at these concentrations, respectively. However, since 99% viability is observed at 2.50 mg/mL, the potential toxicity at 1.25 mg/mL is likely a random artifact rather than true toxicity. Nevertheless, no significant decrease in cell viability was observed with any concentration tested with the other 6 formulations. Therefore, the results indicate a high degree of safety with regard to cytotoxicity, even at high concentrations.

4.3.3.5 Thermogravimetric Analysis

Thermogravimetric analysis was performed on the hydrogels to assure a thermally stable delivery system that could withstand temperatures likely to be experienced during processing and transport. The combined results of the analysis are shown in Figure 4-5. Results for methacrylic acid-based hydrogels only are shown in Figure 4-6, and results for itaconic acid-based hydrogels only are shown in Figure 4-7.

The degradation profiles for all polymer formulations indicate that all formulations are sufficiently stable that thermal degradation will not be a concern for end use. A delivery system that changes properties over time is likely to experience issues with FDA approval and limited shelf life, but the observed degradation profiles indicate that this is not a concern for the developed systems. A slight reduction in weight is observed in all formulations up to 100 °C representing the loss of residual water from the hydrogels. However, no degradation is observed in any hydrogel below 150 °C—a temperature well above what will be experienced for end use.

The methacrylic acid-containing formulations are slightly more thermally stable than the itaconic acid-containing hydrogels. The first instance of degradation occurs at 225 °C. This corresponds to formation of methacrylic anhydrides between adjacent methacrylic acid units with loss of CO_2, reported to occur in poly(methacrylic acid) at 220 - 240 °C.[43,44] The next degradation step begins at 290 °C, with maximum rate of decomposition at 400 °C, corresponding to full decomposition and generation of carbon monoxide, carbon dioxide, and various carbonyls.[43,44]

The itaconic acid-containing formulations are less thermally stable. Decomposition begins as low as 150 °C in the P(IA-g-EG) formulation, with a second degradation step occurring as low as 190 °C in the same P(IA-g-EG) formulation. While these degradation temperatures are much lower than those observed in the methacrylic acid-containing gels, they are still significantly above anything that would reasonably be achieved during hydrogel processing or transport. Therefore, the thermogravimetric

analysis reveals sufficient stability for the intended biological applications of these hydrogels.

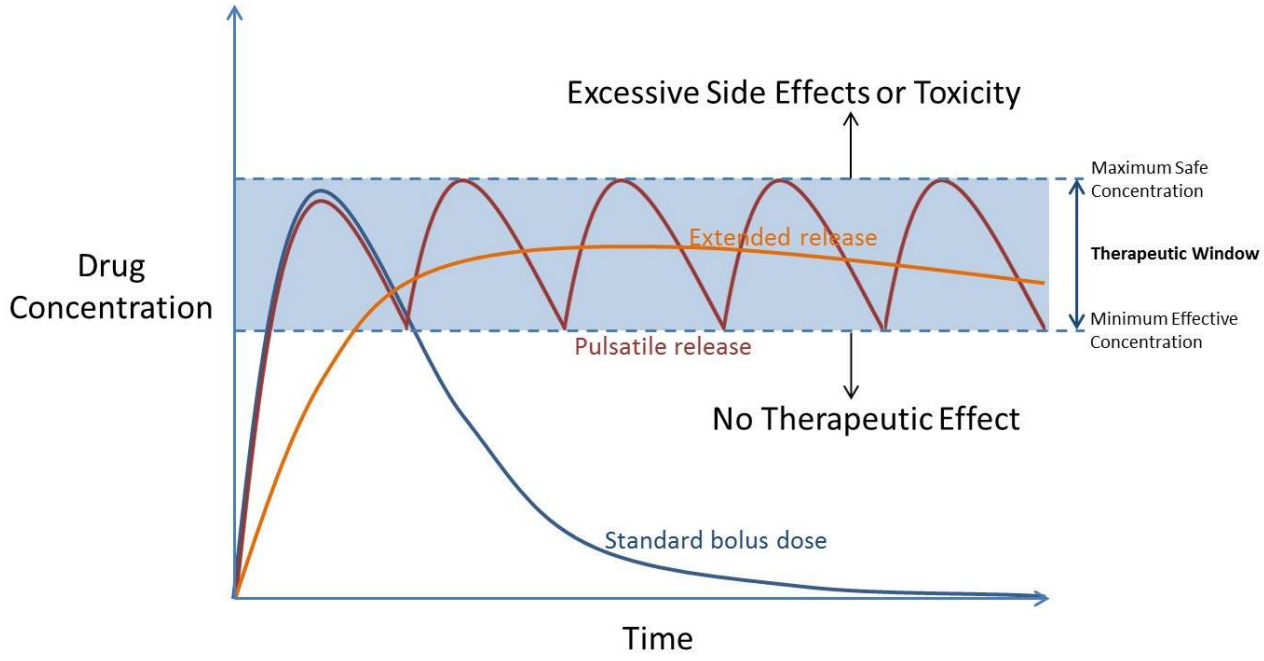

Figure 4-1: Drug concentration profiles for bolus, pulsatile, and extended release.

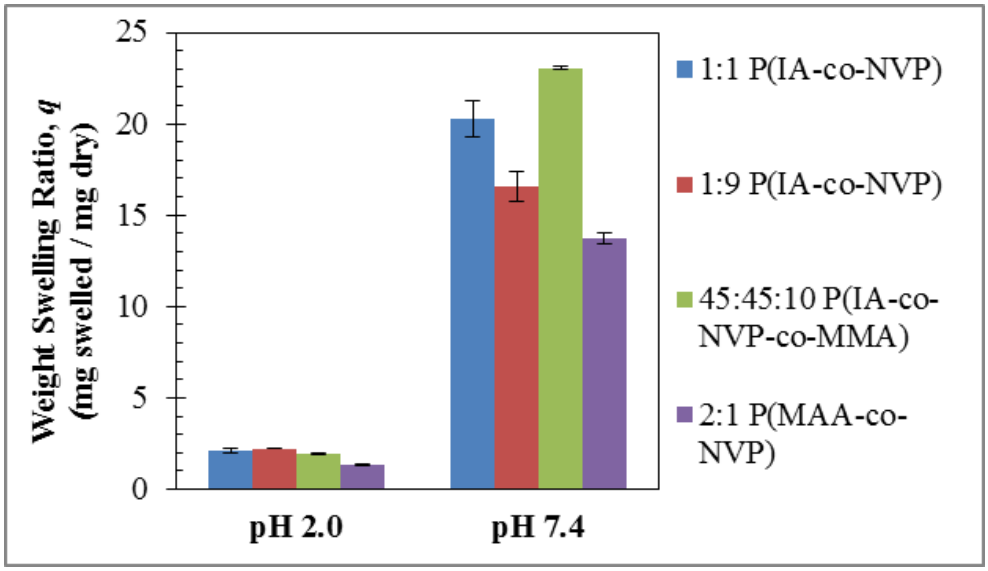

Figure 4-2: Equilibrium Weight Swelling Results. Swelling ratios (weight of swelled disk / weight of dry disk) recorded following 72 h swelling in 0.01 N HCl (pH 2.0) or 150 mM PBS buffer (pH 7.4). Reported as average ± standard deviation.

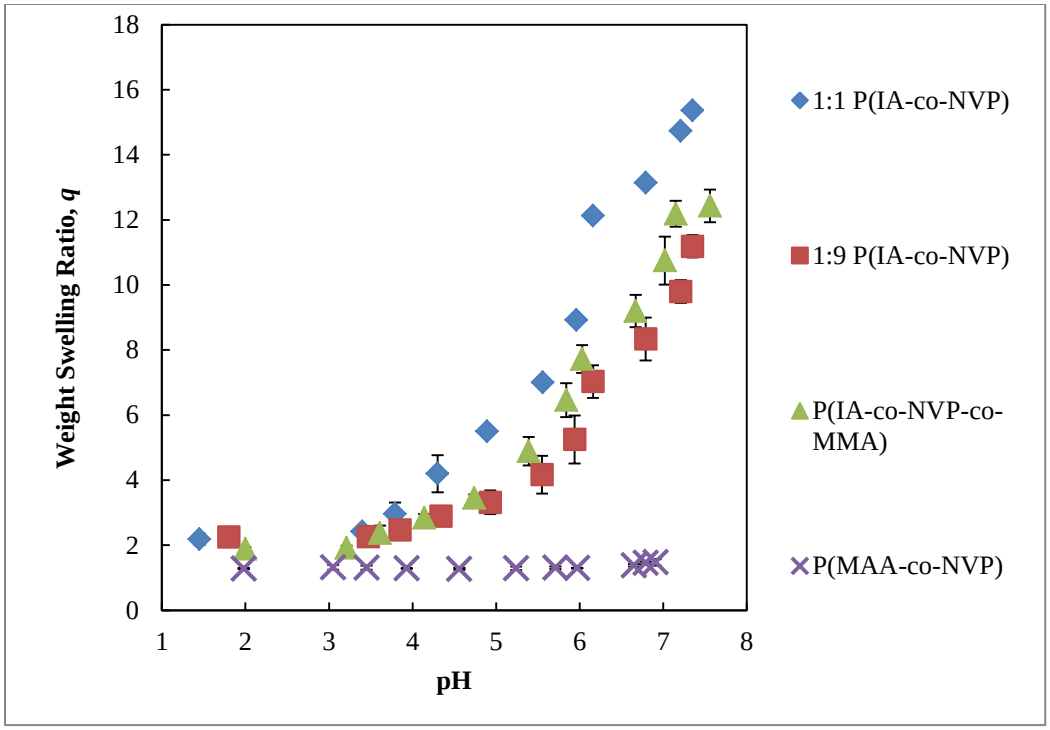

Figure 4-3: Dynamic Weight Swelling Results. Time-sensitive swelling results as disk transitioned between DMGA buffers in order of increasing pH. Swelling time was 7 minutes between each data point. Reported as average ± standard deviation.

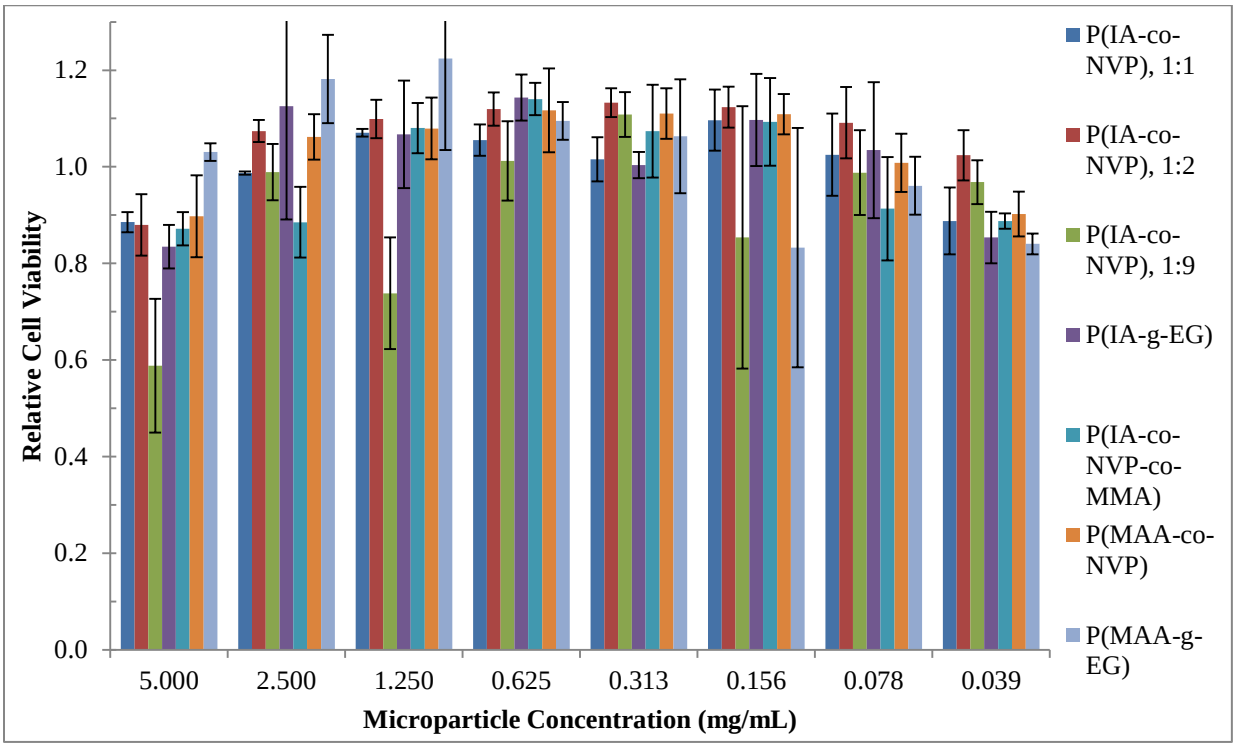

Figure 4-4: Caco-2 Cell Cytotoxicity. Relative cell viability following 2 h incubation with microparticles, as determined by MTA proliferation assay and normalized to positive control in Caco-2 cell culture. Each bar represents n=5 samples, and is reported as average ± standard deviation.

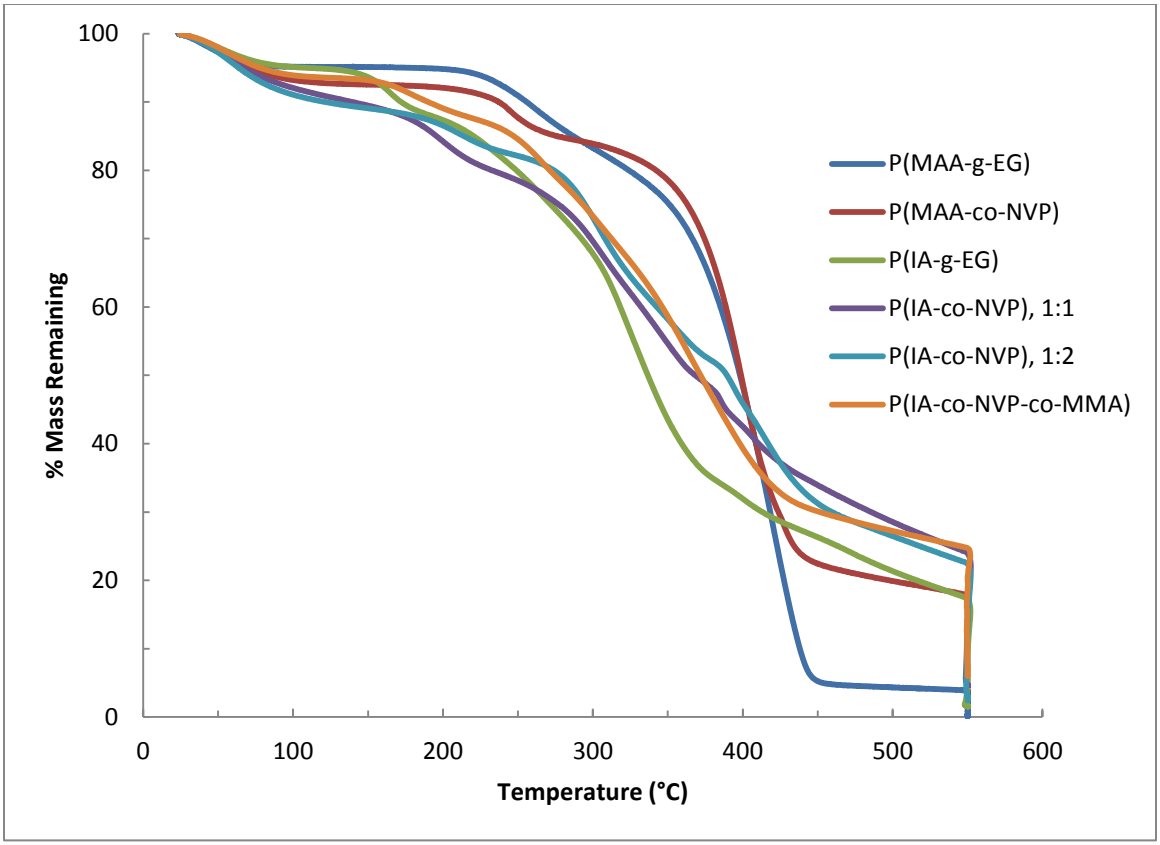

Figure 4-5: Thermogravimetric Analysis—Thermal Degradation Profiles for All Hydrogels.

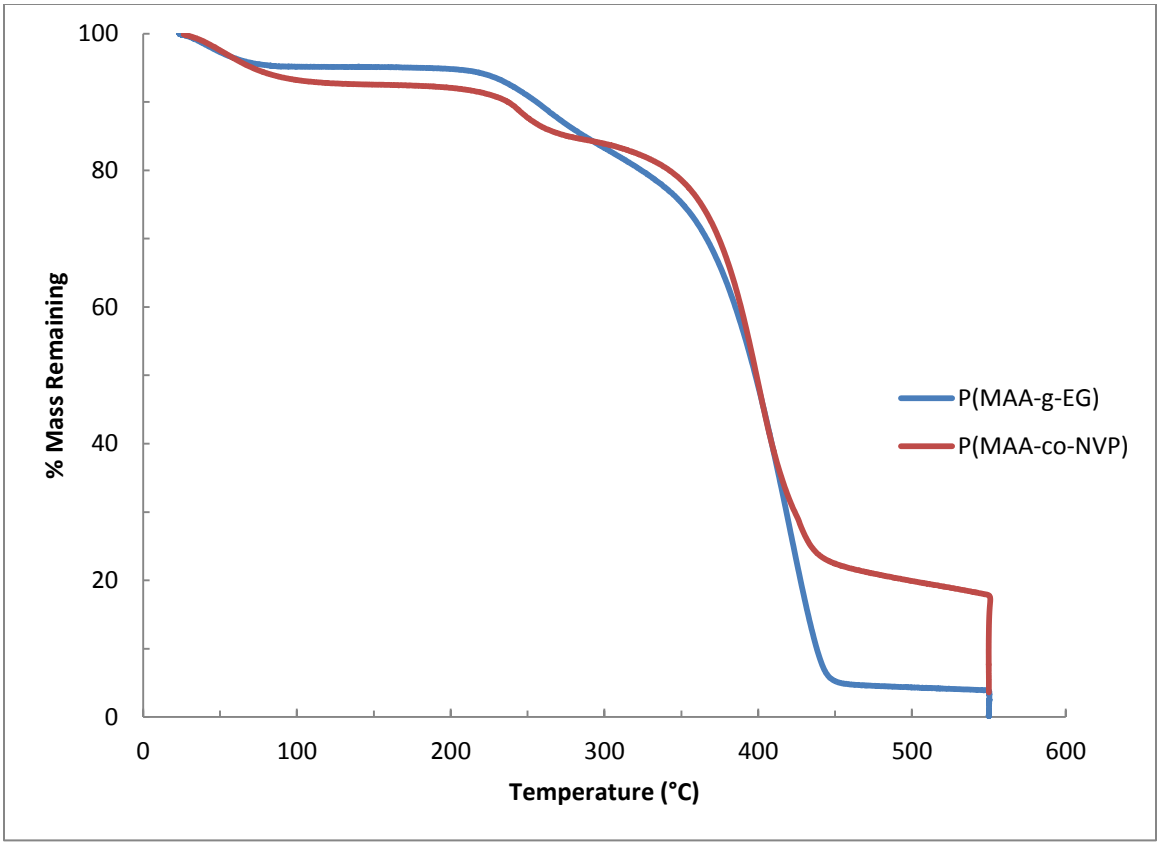

Figure 4-6: Thermogravimetric Analysis—Thermal Degradation Profiles for Methacrylic Acid-Based Hydrogels.

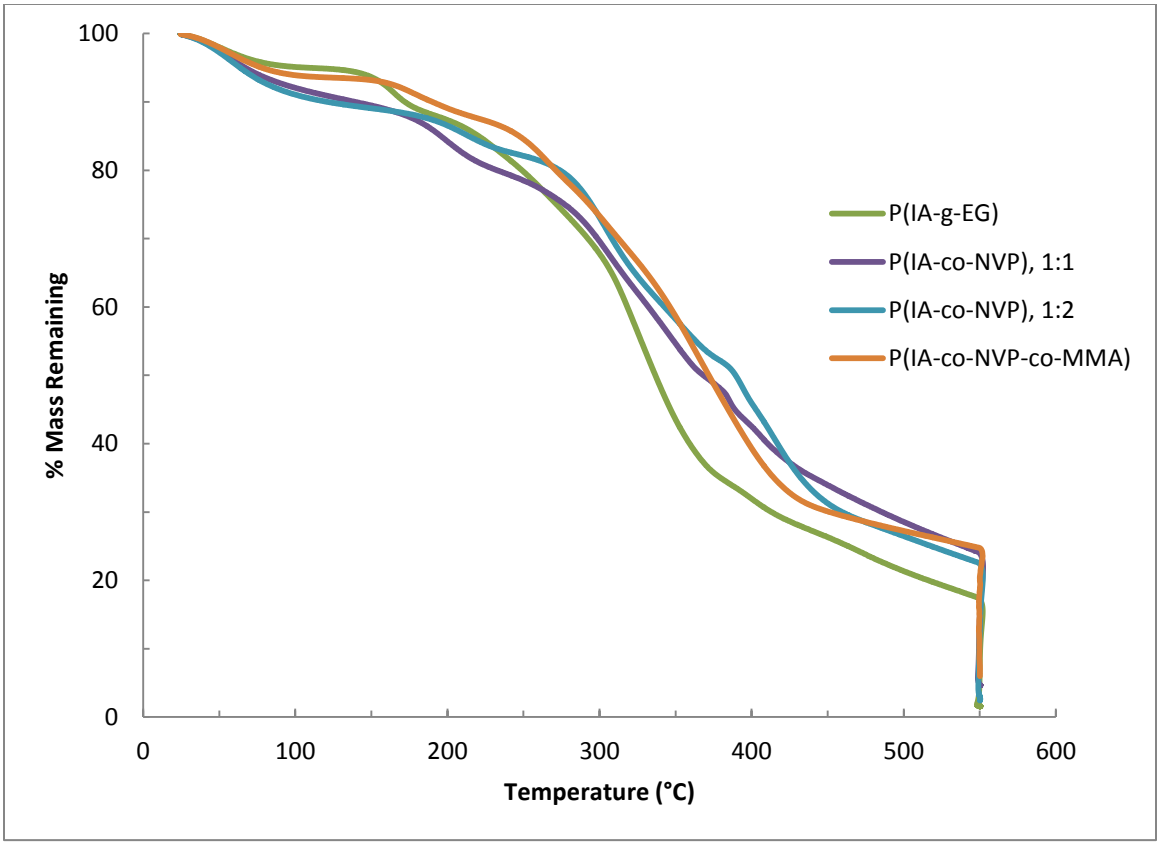

Figure 4-7: Thermogravimetric Analysis—Thermal Degradation Profiles for Itaconic Acid-Based Hydrogels.

Table 4-1: Hydrogel Feed Compositions.

Hydrogel Formulation	**Monomer Feed Ratio**	**Crosslinker**	**Molar % Crosslinker**
1:1 P(IA-*co*-NVP)	1:1 IA:NVP	TEGDMA	5
1:2 P(IA-*co*-NVP)	1:2 IA:NVP	TEGDMA	3
1:9 P(IA-*co*-NVP)	1:9 IA:NVP	TEGDMA	4
P(IA-*co*-NVP-*co*-MMA)	45:45:10 IA:NVP:MMA	PEGDMA	5
P(IA-*g*-EG)	1:1 IA:PEGMMA	PEGDMA	4
P(MAA-*co*-NVP)	2:1 MAA:NVP	TEGDMA	1
P(MAA-*g*-EG)	1:1 MAA:PEGMMA	TEGDMA	1

Table 4-2: Mesh Size and Molecular Weight Between Crosslinks for 1:1 P(IA-co-NVP) Hydrogel Calculated by Three Swelling Models.

	Acidic, pH 2		**Neutral, pH 7.4**	
	$\overline{M_c}$ **(g/mol)**	**Mesh Size, ξ (Å)**	$\overline{M_c}$ **(g/mol)**	**Mesh Size, ξ (Å)**
Peppas-Merrill	154 ± 22	9.69 ± 0.82	18177 ± 523	232 ± 9.9
Brannon-Peppas	153 ± 22	9.66 ± 0.81	2652 ± 220	88.5 ± 6.1
Şen-Güven	154 ± 18	9.72 ± 0.70	1688 ± 150	70.6 ± 5.1

Table 4-3: Comparison of Calculated Mesh Sizes for Hydrogel Formulations.

	Acidic, pH 2		**Neutral, pH 7.4**	
	$\overline{M_c}$ **(g/mol)**	**Mesh Size, ξ (Å)**	$\overline{M_c}$ **(g/mol)**	**Mesh Size, ξ (Å)**
1:1 P(IA-co-NVP)	154 ± 18.5	9.72 ± 0.70	1688 ± 150	70.6 ± 5.1
1:9 P(IA-co-NVP)	175 ± 3.3	12.7 ± 0.13	20661 ± 1040	280 ± 9.1
P(IA-co-NVP-co-MMA)	133 ± 2.4	8.94 ± 0.10	2985 ± 138	99.8 ± 2.4
P(MAA-co-NVP)	16.6 ± 2.8	3.68 ± 0.35	310 ± 16.6	36.7 ± 1.36

4.4 REFERENCES

(1) Koetting, M. C.; Peppas, N. A. pH-Responsive Poly(itaconic Acid-Co-N-Vinylpyrrolidone) Hydrogels with Reduced Ionic Strength Loading Solutions Offer Improved Oral Delivery Potential for High Isoelectric Point-Exhibiting Therapeutic Proteins. *Int. J. Pharm.* **2014**, *471*, 83–91.

(2) Peppas, N. A.; Bures, P.; Leobandung, W.; Ichikawa, H. Hydrogels in Pharmaceutical Formulations. *Eur. J. Pharm. Biopharm.* **2000**, *50*, 27–46.

(3) Yong Qiu; Kinam Park. Environment-Sensitive Hydrogels for Drug Delivery. *Adv. Drug Deliv. Rev.* **2001**, *53*, 321–339.

(4) Allan S Hoffman. Stimuli-Responsive Polymers: Biomedical Applications and Challenges for Clinical Translation. *Adv. Mater.* **2013**, *65*, 10–16.

(5) Horbett, T. A.; Ratner, B. D.; Kost, J.; Singh, M. A Bioresponsive Membrane for Insulin Delivery. In *Recent Advances in Drug Delivery Systems*; Anderson, J. M.; Kim, S. W., Eds.; Springer US, 1984; pp. 209–220.

(6) Horbett, T. A.; Kost, J.; Ratner, B. D. Swelling Behavior of Glucose Sensitive Membranes. In *Polymers as Biomaterials*; Shalaby, S. W.; Hoffman, A. S.; Ratner, B. D.; Horbett, T. A., Eds.; Springer US, 1984; pp. 193–207.

(7) Albin, G.; Horbett, T. A.; Ratner, B. D. Glucose Sensitive Membranes for Controlled Delivery of Insulin: Insulin Transport Studies. *J. Controlled Release* **1985**, *2*, 153–164.

(8) Lowman, A. M.; Morishita, M.; Kajita, M.; Nagai, T.; Peppas, N. A. Oral Delivery of Insulin Using pH-Responsive Complexation Gels. *J. Pharm. Sci.* **1999**, *88*, 933–937.

(9) Carr, D. A.; Gómez-Burgaz, M.; Boudes, M. C.; Peppas, N. A. Complexation Hydrogels for the Oral Delivery of Growth Hormone and Salmon Calcitonin. *Ind. Eng. Chem. Res.* **2010**, *49*, 11991–11995.

(10) Carr, D. A.; Peppas, N. A. Assessment of Poly(methacrylic Acid-Co-N-Vinyl Pyrrolidone) as a Carrier for the Oral Delivery of Therapeutic Proteins Using Caco-2 and HT29-MTX Cell Lines. *J. Biomed. Mater. Res. A* **2010**, *92A*, 504–512.

(11) Foss, A. C.; Peppas, N. A. Investigation of the Cytotoxicity and Insulin Transport of Acrylic-Based Copolymer Protein Delivery Systems in Contact with Caco-2 Cultures. *Eur. J. Pharm. Biopharm.* **2004**, *57*, 447–455.

(12) Kamei, N.; Morishita, M.; Chiba, H.; Kavimandan, N. J.; Peppas, N. A.; Takayama, K. Complexation Hydrogels for Intestinal Delivery of Interferon B and Calcitonin. *J. Controlled Release* **2009**, *134*, 98–102.

(13) Kavimandan, N. J.; Losi, E.; Peppas, N. A. Novel Delivery System Based on Complexation Hydrogels as Delivery Vehicles for Insulin–transferrin Conjugates. *Biomaterials* **2006**, *27*, 3846–3854.

(14) Betancourt, T.; Pardo, J.; Soo, K.; Peppas, N. A. Characterization of pH-Responsive Hydrogels of Poly(itaconic Acid-G-Ethylene Glycol) Prepared by UV-Initiated Free Radical Polymerization as Biomaterials for Oral Delivery of Bioactive Agents. *J. Biomed. Mater. Res. A* **2010**, *93A*, 175–188.

(15) Carr, D. A.; Peppas, N. A. Molecular Structure of Physiologically-Responsive Hydrogels Controls Diffusive Behavior. *Macromol. Biosci.* **2009**, *9*, 497–505.
(16) Knipe, J. M.; Chen, F.; Peppas, N. A. Enzymatic Biodegradation of Hydrogels for Protein Delivery Targeted to the Small Intestine. *Biomacromolecules* **2015**, *16*, 962–972.
(17) Peppas, N. A.; Merrill, E. W. Poly(vinyl Alcohol) Hydrogels: Reinforcement of Radiation-Crosslinked Networks by Crystallization. *J. Polym. Sci. Polym. Chem. Ed.* **1976**, *14*, 441–457.
(18) Brannon-Peppas, L.; Peppas, N. A. Equilibrium Swelling Behavior of pH-Sensitive Hydrogels. *Chem. Eng. Sci.* **1991**, *46*, 715–722.
(19) Şen, M.; Güven, O. Prediction of Swelling Behaviour of Hydrogels Containing Diprotic Acid Moieties. *Polymer* **1998**, *39*, 1165–1172.
(20) Brannon-Peppas, L.; Peppas, N. A. Equilibrium Swelling Behavior of Dilute Ionic Hydrogels in Electrolytic Solutions. *J. Controlled Release* **1991**, *16*, 319–329.
(21) Orwoll, R. A.; Arnold, P. A. Polymer–Solvent Interaction Parameter X. In *Physical Properties of Polymers Handbook*; Mark, J. E., Ed.; Springer New York, 2007; pp. 233–257.
(22) Şen, M.; Yakar, A.; Güven, O. Determination of Average Molecular Weight between Cross-Links (Mc) from Swelling Behaviours of Diprotic Acid-Containing Hydrogels. *Polymer* **1999**, *40*, 2969–2974.
(23) Silberberg, A.; Eliassaf, J.; Katchalsky, A. Temperature-Dependence of Light Scattering and Intrinsic Viscosity of Hydrogen Bonding Polymers. *J. Polym. Sci.* **1957**, *23*, 259–284.
(24) Brock Thomas, J.; Tingsanchali, J. H.; Rosales, A. M.; Creecy, C. M.; McGinity, J. W.; Peppas, N. A. Dynamics of Poly(ethylene Glycol)-Tethered, pH Responsive Networks. *Polymer* **2007**, *48*, 5042–5048.
(25) Marvel, C. S.; Shepherd, T. H. Polymerization Reactions of Itaconic Acid and Some of Its Derivatives. *J. Org. Chem.* **1959**, *24*, 599–605.
(26) Tate, B. E. Polymerization of Itaconic Acid and Derivatives. *Fortschritte Hochpolym.-Forsch.* **1967**, *5*, 214–232.
(27) Şen, M.; Yakar, A. Controlled Release of Antifungal Drug Terbinafine Hydrochloride from poly(N-Vinyl 2-Pyrrolidone/itaconic Acid) Hydrogels. *Int. J. Pharm.* **2001**, *228*, 33–41.
(28) Dunn, B. M. Overview of Pepsin-like Aspartic Peptidases. In *Current Protocols in Protein Science*; John Wiley & Sons, Inc., 2001.
(29) Cox, M.; Nelson, D. R.; Lehninger, A. L. *Lehninger Principles of Biochemistry*; 5th ed.; W. H. Freeman: San Francisco, 2008.
(30) López, J. E.; Peppas, N. A. Effect of Poly (Ethylene Glycol) Molecular Weight and Microparticle Size on Oral Insulin Delivery from P(MAA-g-EG) Microparticles. *Drug Dev. Ind. Pharm.* **2004**, *30*, 497–504.
(31) Torres-Lugo, M.; Peppas, N. A. Molecular Design and in Vitro Studies of Novel pH-Sensitive Hydrogels for the Oral Delivery of Calcitonin. *Macromolecules* **1999**, *32*, 6646–6651.

(32) Nakamura, K.; Murray, R. J.; Joseph, J. I.; Peppas, N. A.; Morishita, M.; Lowman, A. M. Oral Insulin Delivery Using P(MAA-G-EG) Hydrogels: Effects of Network Morphology on Insulin Delivery Characteristics. *J. Controlled Release* **2004**, *95*, 589–599.
(33) Foss, A. C.; Goto, T.; Morishita, M.; Peppas, N. A. Development of Acrylic-Based Copolymers for Oral Insulin Delivery. *Eur. J. Pharm. Biopharm.* **2004**, *57*, 163–169.
(34) Dressman, J. B.; Berardi, R. R.; Dermentzoglou, L. C.; Russell, T. L.; Schmaltz, S. P.; Barnett, J. L.; Jarvenpaa, K. M. Upper Gastrointestinal (GI) pH in Young, Healthy Men and Women. *Pharm. Res.* **1990**, *7*, 756–761.
(35) Carr, D. A. *Molecular Design of Biomaterial Systems for the Oral Delivery of Therapeutic Proteins*; ProQuest, 2008.
(36) Peppas, N. A.; Wood, K. M.; Thomas, J. B. Membranes in Controlled Release. In *Membranes for the Life Sciences*; Peinemann, K.-V.; Nunes, S. P., Eds.; Wiley-VCH Verlag GmbH & Co. KGaA, 2007; pp. 175–190.
(37) Erman, B.; Mark, J. E. *Structures and Properties of Rubberlike Networks*; Topic in polymer science; Oxford University Press: Oxford, 1997.
(38) Giussani, L.; Fois, E.; Gianotti, E.; Tabacchi, G.; Gamba, A.; Coluccia, S. On the Compatibility Criteria for Protein Encapsulation inside Mesoporous Materials. *ChemPhysChem* **2010**, *11*, 1757–1762.
(39) Reth, M. Matching Cellular Dimensions with Molecular Sizes. *Nat. Immunol.* **2013**, *14*, 765–767.
(40) Sambuy, Y.; De Angelis, I.; Ranaldi, G.; Scarino, M. L.; Stammati, A.; Zucco, F. The Caco-2 Cell Line as a Model of the Intestinal Barrier: Influence of Cell and Culture-Related Factors on Caco-2 Cell Functional Characteristics. *Cell Biol. Toxicol.* **2005**, *21*, 1–26.
(41) Pinto, M.; Robine-Leon, S.; Appay, M.-D.; Kedinger, M.; Triadou, N.; Dussaulx, E.; Lacroix, B.; Simon-Assmann, P.; Haffen, K.; Fogh, J.; *et al.* Enterocyte-like Differentiation and Polarization of the Human Colon Carcinoma Cell Line Caco-2 in Culture. *Biol. Cell* **1983**, *47*, 323–330.
(42) Hidalgo, I. J.; Raub, T. J.; Borchardt, R. T. Characterization of the Human Colon Carcinoma Cell Line (Caco-2) as a Model System for Intestinal Epithelial Permeability. *Gastroenterology* **1989**, *96*, 736–749.
(43) Ho, B.-C.; Lee, Y.-D.; Chin, W.-K. Thermal Degradation of Polymethacrylic Acid. *J. Polym. Sci. Part Polym. Chem.* **1992**, *30*, 2389–2397.
(44) Schild, H. G. Thermal Degradation of Poly(methacrylic Acid): Further Studies Applying TGA/FTIR. *J. Polym. Sci. Part Polym. Chem.* **1993**, *31*, 2403–2405.

Chapter 5: Evaluation and Optimization of Hydrogel Drug Delivery Vehicles

5.1 INTRODUCTION

After successful synthesis and characterization of the hydrogel systems, beneficial changes in the hydrogel response were observed in terms of mesh size, equilibrium swelling ratio, and speed of swelling response, as well as strong evidence of biocompatibility of the materials. However, the enhanced material properties may not necessarily translate into improvements in drug delivery capability or final bioavailability.

The problems observed with delivery of high isoelectric point exhibiting therapeutic proteins to the small intestine using previous P(MAA-g-EG) or P(MAA-co-NVP) systems arise primarily from charge interactions between the anionic carriers and the cationic proteins in the neutral conditions of the small intestine. Unfortunately, the anionic character of the hydrogels cannot be removed without adversely affecting the direction of the pH-responsive swelling profile, so we must therefore mitigate these adverse effects through charge localization and increased swelling. Therefore, the actions taken to improve material properties rely on a delicate balance of increasing charge while increasing distance from the charges in the expectation that the benefits will outweigh the limitations. In this chapter, the *in vitro* experiments used to test the protein delivery capabilities of the modified hydrogel systems are discussed, as well as various

studies to elucidate the possible improvements in protein delivery available from mechanical and procedural changes.

Multiple factors that could affect the delivery of proteins theoretically are explored in this chapter. The monomers used in making a polymer are the primary determinants of the resulting behavior of the system, and should therefore have a large impact on drug delivery capability. For example, previous work has shown that the electronegativity of the lactam oxygen in N-vinylpyrrolidone yields stronger complexation behavior with methacrylic acid, allowing for wider shifts in swelling ratio, and imparts some mucoadhesive capability.[1–5] Although the monomers used in this work are functionally and structurally similar to those used in previous systems of P(MAA-g-EG) or P(MAA-co-NVP), as shown in Chapter 4, even a small change in the structure of the monomers (IA instead of MAA) or the ratio of monomers had a profound effect on swelling behavior—both in terms of magnitude and kinetic rate. The improved swelling dynamics shown in Chapter 4 should result in preferable delivery of high isoelectric point-exhibiting proteins due to both increased mesh size and more time available for diffusional release. Thus, the effect of monomers and monomer ratios on *in vitro* delivery is explored.

Another variable explored is the size of the microparticles used. With the primary mechanism of release in these systems being diffusion through the hydrogel mesh after swelling, the diffusional distance the protein must travel through the hydrogel determines the time needed for release. Because the residence time in the small intestine is typically only 4 h,[6] a rapid release must be attained. Reducing the size of the particle may

therefore benefit the delivery potential of the system by reducing the average diffusional distance to the exterior of the particle. However, due to the complications presented by coulombic interaction between the drug and the delivery vehicle, an improvement in delivery resulting from reduced particle size may not manifest itself at the micrometer length scale. Therefore, an experiment to test the effect of microparticle size on protein delivery is presented here.

Another structural characteristic of the hydrogels that could potentially be used for tailoring drug delivery is the crosslinking density. Qualitatively, with higher crosslinking density, the hydrogel mesh size decreases due to a greater number of tie points between polymer chains that inhibit entropic swelling. Although large mesh size is desirable in the small intestine to maximize protein release, it is not ideal in the stomach, where proteins must be protected from proteolytic enzymes. Furthermore, the mesh size affects diffusive release relative to the size of the protein. Large proteins may require very low crosslinking density for sufficient mesh size to diffuse through, whereas very small proteins may benefit from high crosslinking density to promote encapsulation through the stomach. As a result, the crosslinking density that works best for one protein may not work well for a different protein. However, crosslinking density provides a facile potential method for tuning the physical properties of the hydrogel to enable delivery of different proteins. Experiments testing the effect of crosslinking ratio and protein size are presented in this chapter seeking to determine if protein size is a potential limiting factor and if so, to determine if crosslinking density provides a control knob for tuning the vehicle to a particular protein.

5.2 MATERIALS AND METHODS

5.2.1 Effect of Hydrogel Formulation on Protein Delivery

A solution of salmon calcitonin (sCT) (Selleck Chemicals, Houston, TX) was prepared at a concentration of 0.40 mg/mL in 0.0150 M PBS buffer (pH 7.4), and 1.5 mL of this solution was added to each of 21 (n=3 per hydrogel formulation), 2.0 mL, low-adhesion microcentrifuge tubes. Microparticles 90-150 μm in size were added to this solution at 10 mg of dry hydrogel per tube. The mixture was agitated for 1 h using an Eppendorf Thermomixer (Eppendorf, Hauppauge, NY), allowing the microparticles to swell and sCT to diffuse into the interior of the particles. The particles were collapsed using 75 μL of 0.1 N HCl and isolated by centrifugation and decanting. The supernatant was collected for analysis. The particles were resuspended in two subsequent washes consisting of 1.0 mL of 0.01 N HCl to remove surface-bound protein. After each wash, the particles were isolated by centrifugation and decanting, and the rinse was collected for analysis. The isolated microparticles with encapsulated sCT were lyophilized until dry. Samples of the stock solution, the supernatant following particle collapse, and the two acid rinses were analyzed by a Micro BCA protein concentration assay (Thermo Fisher Scientific, Rockford, IL).

Once the microparticles were dry from lyophilization, 1.0 mL of 0.150 M PBS buffer at a pH of 3.0 (from adding HCl) was added to each microcentrifuge tube and agitated for 1 h at 37 °C. A 150 μL sample was removed for analysis and replaced with 150 μL fresh, pH 3.0 PBS before raising the pH back to 7.4 by addition of 1 N NaOH.

The neutralized mixture was agitated for 24 h at 37 °C, with 150 μL samples collected at time points of 1, 2, 4, and 24 h, each time being replaced by 150 μL fresh PBS (pH 7.4). All samples were analyzed for sCT concentration using a Micro BCA protein concentration assay.

5.2.2 Effect of Ionic Strength on Protein Delivery

Three separate trials were undertaken to examine the effects of changing the ionic strength of the loading solution on salmon calcitonin delivery. In the first trial, three different concentrations of PBS buffer at pH 7.4 were used: 1.5 M (10x concentrated PBS), 150 mM (1x standard PBS), and 15 mM (0.1x concentrated PBS). In these solutions, salmon calcitonin was dissolved at a concentration of 0.1 mg/mL. Using 40 mL of each solution, 100 mg of purified 1:1 P(IA-co-NVP) microparticles, sieved to 90-150 μm in size, were added to each solution and mixed for 1 h. Particles were collapsed by addition of 1 N HCl to reduce pH to 2.0, isolated by decanting, and lyophilized. Samples of the stock solutions and post-collapse supernatant were analyzed for sCT concentration using high performance liquid chromatography to determine sCT loading levels. After lyophilization, 30 mg of each sample were added to 30 mL of 150 mM (1x), pH 3.0 PBS buffer and stirred for 1 h at a temperature of 37.0 °C using a Distek dissolution apparatus (Distek, North Brunswick, NJ). After 1 h, a 500 μL sample was taken for analysis and replaced with fresh, pH 3.0 PBS. The pH was then raised to pH 7.4 by addition of 1 N NaOH. Samples were collected at time points of 45, 75, and 120

minutes following neutralization. Salmon calcitonin concentration in all samples was determined by a Micro BCA protein assay.

In the second trial, another sCT solution in 1.5 mM PBS (0.01x) was added for study. The four solutions (0.01x, 0.1x, 1x, and 10x PBS) were prepared, and salmon calcitonin was dissolved in 7 mL of each solution at a concentration of 250 μg/mL. To each of these solutions, 10 mg of purified 1:1 P(IA-co-NVP) microparticles were added and allowed to imbibe sCT for 1 h while agitated. The particles were then collapsed by addition of 1 N HCl to reduce pH to 2.0 and were collected by centrifugation and decanting. Samples from the stock solutions and supernatant were analyzed for sCT concentration by HPLC. The collected particles were dried by lyophilization. Following drying, the microparticle samples were added to 2.0 mL microcentrifuge tubes containing 1.75 mL of 150 mM (1x), pH 3.0 PBS buffer and agitated at 37 °C using an Eppendorf Thermomixer. After 1 h, 150 μL samples of the solutions were collected for analysis and replaced with fresh PBS (pH 3.0). The solutions were then neutralized by addition of 0.2 N NaOH to a pH of 7.4. Release at neutral conditions was carried out for 2 h, with samples acquired at time points of 1 and 2 h. All samples were analyzed for sCT concentration using a Micro BCA protein concentration assay.

In the third trial, the same four solutions were used as in the second trial. Calcitonin was dissolved in 30 mL of each solution at a concentration of 0.20 mg/mL. To each solution, 100 mg of 1:1 P(IA-co-NVP) microparticles were added, and the pH was maintained at 7.0 by addition of NaOH. The solutions were mixed for 18 h at room temperature to allow for drug loading prior to collapse by acidification to pH 2.5 with

HCl. The particles were isolated by decanting, washed twice with 1 mL 0.01 N HCl, and lyophilized. Following drying, 20 mg of each of the dried, drug-loaded microparticle samples were added to 40 mL of pH 3, 0.150 M PBS buffer (acidified with HCl) and stirred for 1 h in a Distek dissolution apparatus at 37 °C. The solutions were then neutralized to pH 7.4 by addition of NaOH and stirred for 2 h. Samples were acquired at time points of 1 h during acidic conditions, 1h following neutralization, and 2 h following neutralization. The samples were analyzed for sCT concentration by a Micro BCA protein concentration assay.

5.2.3 Effect of Particle Size on Protein Delivery

A solution of salmon calcitonin (sCT) (Selleck Chemicals, Houston, TX) was prepared at a concentration of 0.40 mg/mL in 0.00150 M PBS buffer (pH 7.4), and 1.5 mL of this solution was added to each of 15 x 2.0 mL, low-adhesion microcentrifuge tubes. Microparticles of the 1:2 P(IA-co-NVP) formulation were added to this solution at 10 mg of dry hydrogel per tube, with particles sieved into size ranges of 45-75 μm, 75-90 μm, and 90-150 μm (n = 5 per size range). The mixture was agitated for 24 h using an Eppendorf Thermomixer, allowing the microparticles to swell to equilibrium and sCT to diffuse into the interior of the particles. The particles were collapsed using 25 μL of 1 N HCl and isolated by centrifugation and decanting. The supernatant was collected for analysis. The particles were resuspended in two subsequent washes consisting of 1.0 mL of 0.01 N HCl to remove surface-bound protein. After each wash, the particles were isolated by centrifugation and decanting, and the rinse was collected for analysis. The

isolated microparticles with encapsulated sCT were lyophilized until dry. Samples of the stock solution, the supernatant following particle collapse, and the two acid rinses were analyzed by a Micro BCA protein concentration assay (Thermo Fisher Scientific, Rockford, IL).

Once the microparticles were dry from lyophilization, 1.5 mL of 0.150 M PBS buffer at pH 3 (from adding HCl) was added to each microcentrifuge tube and agitated for 1 h at 37 °C. A 150 μL sample was removed for analysis and replaced with 150 μL fresh, pH 3.0 PBS before raising the pH back to 7.4 by addition of 1 N NaOH. The neutralized mixture was agitated for 4 h at 37 °C. A 250 μL sample was collected after 4 h to test end point release. All samples were analyzed for sCT concentration using a Micro BCA protein concentration assay.

5.2.4 Effect of Crosslinking Density on Protein Delivery

A solution of salmon calcitonin (sCT) (Selleck Chemicals, Houston, TX) was prepared at a concentration of 0.20 mg/mL in 0.00150 M PBS buffer (pH 7.4), and 1.0 mL of this solution was added to each of 12 x 2.0 mL, low-adhesion microcentrifuge tubes. Microparticles of three hydrogels were added to this solution at 5 mg of dry hydrogel per tube. All hydrogels were 1:2 IA:NVP monomer molar ratio P(IA-co-NVP) hydrogels prepared as described in Chapter 2, crushed and sieved into 90-150 μm microparticles, with varying crosslinker mole percent in the monomer feed: 1%, 5%, and 10% TEGDMA crosslinking (n = 4 per formulation). The mixture was agitated for 24 h using an Eppendorf Thermomixer, allowing the microparticles to swell to equilibrium

and sCT to diffuse into the interior of the particles. The particles were collapsed using 1 N HCl to reduce pH to 2.0 and isolated by centrifugation and decanting. The supernatant was collected for protein quantification. The particles were resuspended in two subsequent washes consisting of 1.0 mL of 0.01 N HCl to remove surface-bound protein. After each wash, the particles were isolated by centrifugation and decanting, and the rinse was collected for analysis. The isolated microparticles with encapsulated sCT were dried overnight in air. Samples of the stock solution, the supernatant following particle collapse, and the two acid rinses were analyzed by a Micro BCA protein concentration assay (Thermo Fisher Scientific, Rockford, IL).

Once the microparticles were dry, 1.0 mL of 0.150 M PBS buffer at pH 3 (from adding HCl) was added to each microcentrifuge tube and agitated for 1 h at 37 °C. A 150 μL sample was removed for analysis and replaced with 150 μL fresh, pH 3.0 PBS before raising the pH back to 7.4 by addition of 1 N NaOH. The neutralized mixture was agitated for 24 h at 37 °C, with 150 μL samples collected at time points of 1, 2, 4, and 24 h, each time being replaced by 150 μL fresh PBS (pH 7.4). All samples were analyzed for sCT concentration using a Micro BCA protein concentration assay.

5.2.5 Loading and Release of Larger Proteins

A protocol identical to that presented in section 5.2.4 was used, with a 0.40 mg/mL solution of Rituxan (rituximab) substituted for the 0.20 mg/mL sCT. Rituxan was generously provided for our research by Genentech. The same 1%, 5%, and 10%

TEGDMA crosslinked, 1:2 P(IA-co-NVP) microparticles were used in identical loading and release conditions. Protein samples were quantified using a MicroBCA assay.

Additionally, a second experiment was performed using salmon calcitonin, urokinase, and rituximab as high pI proteins. Solutions of the three proteins were prepared at 200 μg protein/mL concentration in 1.5 mM PBS (0.01x). In 15 x 2.0 mL low adhesion tubes, 5 mg of 1:2 P(IA-co-NVP) hydrogel microparticles (90-150 μm in size) was added to each tube and incubated with 1.5 mL of protein solution (n = 5 per protein) for 24 h at pH 7.4. The solutions were collapsed using 1 N HCl to reduce the pH to 2, isolated by centrifugation and decanting, washed two times with 0.5 mL of 0.01 N HCl, and lyophilized. Following drying, 1.0 mL of 150 mM PBS (1x) at pH 3 was added to each tube and incubated at 37 °C for 1 h. A 150 μL sample was taken and replaced with pH 3 PBS, and the solutions were then raised to pH 7.4 using 1 N NaOH. The solutions were stirred at 37 °C for 24 h, with 150 μL samples acquired and replaced with fresh PBS at time points of 1, 2, 4, and 24 h. All loading and release samples were analyzed for protein concentration using a MicroBCA assay.

5.2.6 Degradable Hydrogel Loading and Release

In a study with salmon calcitonin, 10 mg of purified, degradable P(MAA-co-NVP) microparticles crosslinked with MMRRRKK and sieved to 90-150 μm in size were added to 1.5 mL of a 400 μg/mL solution of salmon calcitonin (Selleck Chemicals) in 1.50 mM PBS buffer at pH 7.4 (n = 3). The mixture was agitated for 24 h using an Eppendorf Thermomixer, allowing the microparticles to swell to equilibrium and sCT to

diffuse into the interior of the particles. The particles were collapsed using 25 μL of 1 N HCl and isolated by centrifugation and decanting. The supernatant was collected for analysis. The particles were resuspended in two subsequent washes consisting of 1.0 mL of 0.01 N HCl to remove surface-bound protein. After each wash, the particles were isolated by centrifugation and decanting, and the rinse was collected for analysis. The isolated microparticles with encapsulated sCT were lyophilized until dry. Samples of the stock solution, the supernatant following particle collapse, and the two acid rinses were analyzed for sCT concentration using high performance liquid chromatography.

Once the microparticles were dry from lyophilization, 1.5 mL of USP-standard simulated gastric fluid (containing 3.2 mg/mL pepsin) at pH 1.2 was added to each microcentrifuge tube and agitated for 1 h at 37 °C. The particles were isolated by centrifugation, and the simulated gastric fluid supernatant was removed. The microparticles were resuspended in 1.5 mL of USP-standard simulated intestinal fluid (containing 10 mg/mL pancreatin) at pH 6.8 and agitated for 4 h at 37 °C. 250 μL samples were collected at times of 1 h, 4 h, and 48 h after adding simulated intestinal fluid and subsequently replaced with fresh simulated intestinal fluid. All samples were analyzed for sCT concentration using high performance liquid chromatography.

5.3 RESULTS AND DISCUSSION

5.3.1 Effect of Hydrogel Formulation on Protein Delivery

The ultimate goal of this work is to develop a system enabling oral delivery of high isoelectric point-exhibiting proteins with high bioavailability. The swelling and cytotoxicity studies show that the developed systems exhibit the proper behavior and are biocompatible for use with human cells, but a direct test of delivery capability with high isoelectric point-exhibiting therapeutic proteins was needed. For this test, salmon calcitonin was encapsulated in microparticles of the 7 hydrogel formulations by imbibition and subsequently released by diffusion out of the polymer matrix following swelling in neutral conditions. The observed delivery potential for sCT (mg of sCT released at a certain time per mg of hydrogel used) for each of the hydrogel formulations is shown in Figure 5-1 and tabulated in Table 5-1.

The ideal behavior would be to have zero protein release at the 1 h time point, which is taken at the end of the acidic portion of the release, meaning no protein is lost due to premature release in the stomach, and to have very high delivery potential at the 4 h time point that is of similar magnitude as the 24 h time point, indicating fast and complete release in a timeframe and pH similar to what would be observed in the small intestine. None of the systems studied exhibited such ideal behavior, as all tested systems released a fraction of encapsulated sCT in acidic conditions; however, subtracting the amount of sCT released at 1 h from that released at 4 h provides a good indication of which formulation best approximates ideal behavior. The best candidate is the 1:2

formulation of P(IA-*co*-NVP), which released 12.4 μg sCT/mg hydrogel after 3 h in neutral conditions—2.7 times more than the previously studied P(MAA-*g*-EG) hydrogel, and 16.8 times more than the previously studied P(MAA-*co*-NVP) hydrogel. Although 6.26 μg sCT/mg hydrogel were released in stomach conditions, the remaining 6.15 μg sCT/mg hydrogel delivered in subsequent small intestinal conditions far exceed the 1.7 μg sCT/mg hydrogel that the P(MAA-*g*-EG) hydrogel delivered in the same conditions.

The large, significant ($p < 0.01$) increase in delivery potential observed with the 1:2 molar ratio of IA to NVP compared to the other formulations shows that the 1:2 ratio of monomer reactants optimizes swelling and binding behavior to best accommodate oral delivery of sCT, likely due to the localization of anions through the hydrogel.

The anionic groups in the polymer backbone are useful in achieving high drug loading by taking advantage of the same coulombic interactions that are best avoided during release and by improving hydrogel swelling via anionic repulsion for greater loading and release. The important distinction between IA and MAA is that IA has two potential anions ($–COO^-$) present per molecule while MAA possesses only one. Therefore, by having 1 in 3 monomer subunits ionizable (IA) in the 1:2 P(IA-*co*-NVP) hydrogel versus 2 in 3 ionizable subunits (MAA) in the 2:1 P(MAA-*co*-NVP) hydrogel, the overall number of anions will be identical between the two gels, yielding identical levels of osmotic pressure and hydrogen bond crosslinking to drive swelling. However, with IA, the 2 anions are localized on a single subunit rather than spread out among 2 different monomers, which results in a greater average distance between anionic regions for the sCT to diffuse through during release. Coulombic forces decrease by the square

of the distance between ions while only increasing linearly with charge; therefore, any significant increase in distance of approach during diffusion will have a significant effect in assisting diffusive release, even if it comes at the cost of having additional ions.

Therefore, the localization of anions to a single monomer is likely to be a contributing factor in the improved delivery potential observed with the 1:2 P(IA-*co*-NVP) hydrogel formulation. Coupled with faster and greater overall swelling response, which further increase the average approach distance and maximize time available for diffusive release, the 1:2 molar ratio experimentally proves to best take advantage of these multiple factors to achieve improved delivery potential.

5.3.2 Effect of Ionic Strength on Protein Delivery

In addition to using different materials based on IA instead of MAA, there may be delivery improvements available from a procedural standpoint without requiring all new materials. Unfortunately, the release environment is set entirely by the small intestine and is not easily or safely alterable. Therefore, only variables involved in the loading are easily utilized for improving bioavailability of high isoelectric point-exhibiting proteins.

One of the ideal variables available for study is the ionic strength of the loading solution. The ionic strength can affect the loading of the drug into the hydrogel in two ways. First, ionic strength strongly affects the swelling behavior of the pH-responsive hydrogel as described by Brannon-Peppas and Peppas,[7,8] with higher ionic strength resulting in decreased swelling and lower ionic strength resulting in increased swelling, since more medium must be imbibed to equilibrate the osmotic pressure of the hydrogel-

generated ions if the medium has low ion concentration. Therefore, by reducing the ionic strength of the loading solution, the hydrogel will swell to a greater degree, allowing it to imbibe a greater amount of the protein. With more drug loaded, the driving force for diffusive release is increased, resulting in greater delivery capability.

Second, the ionic strength affects the degree to which coulombic interactions take place, as described by the Debye length. The Debye length is the effective distance over which an ion's charge is offset by the charges of ions present in the surrounding medium. The Debye length can be calculated using Equation 5-1,

$$\lambda_D = \sqrt{\frac{\varepsilon k_B T}{2 N_A e^2 I}} \propto \sqrt{\frac{1}{I}} \qquad \text{Equation 5-1}$$

where I is the ionic strength (mol/m^3), ε is the permittivity of the medium, k_B is the Boltzmann constant, T is the absolute temperature, N_A is Avogadro's number, and e is the elementary charge. The important relationship is that the Debye length is inversely proportional to the square root of the ionic strength. Therefore, by decreasing the ionic strength of the loading solution, in addition to increasing swelling, the distance over which ionic interactions are expected to occur increases, meaning there is a greater likelihood of coulombic binding. Although we hope to avoid such interactions during drug release, they can be used beneficially during loading by encouraging binding to the interior of the microparticles, further increasing the driving force for diffusive release.

To test the hypothesis that reducing the ionic strength of the loading solution may be beneficial for high pI protein delivery, an experiment involving loading and releasing

sCT in four loading solutions of different ionic strength was performed in three different trials. The results are shown below in Figures 5-2 through 5-4 and Tables 5-2 through 5-4.

In Trial 1 (Figure 5-2, Table 5-2), it is observed that lower ionic strength loading solution (0.1x PBS) results in an overall improvement in delivery potential compared to the previously used standard (1x) PBS solution. The loading level is 54% lower in the 0.1x PBS buffer compared to the 1x PBS buffer, contrary to expectations, but the percent release is 164% greater, yielding 20% greater overall delivery potential. This result is preferable, because it means that less hydrogel is required to deliver a therapeutic dose of drug and that less of the drug is being wasted by remaining in the hydrogel—both of which are benefits that will help decrease cost of an oral drug formulation.

In Trial 2 (Figure 5-3, Table 5-3), the experiment was extended to include an even lower ionic strength loading solution (0.01x PBS). The results show that the further reduction provides even greater benefits to the delivery potential. Within three hours of release (2 h at neutral pH), the 0.01x-PBS-loaded sample delivered 48.4 μg sCT/mg hydrogel, compared to the 0.1x-PBS-loaded sample delivering 16.1 μg sCT/mg (a 3.0-fold improvement) and the 1x-PBS-loaded sample delivering only 0.6 μg sCT/mg (an 83-fold improvement). Percent release also increased with decreasing ionic strength in the loading solution. Again, lower ionic strength loading solutions yielded greater percent release and greater overall delivery, which results in a smaller pill for the user at cheaper cost due to less wasted drug.

Finally, in Trial 3 (Figure 5-4, Table 5-4), similar, but less pronounced behavior is observed. The 0.01x-PBS-loaded sample releases 6.18 mg sCT/mg hydrogel within 2 h at neutral pH, compared to the 0.1x-PBS-loaded sample delivering 4.67 μg sCT/mg (a 1.3-fold improvement) and the 1x-PBS-loaded sample delivering only 2.23 μg sCT/mg (a 2.8-fold improvement). Additionally, the percent release increases with decreasing ionic strength of the loading solution. Once again, this data collectively shows that a small procedural change using a reduced ionic strength loading solution yields a cheaper, better delivery system that requires less hydrogel and wastes less of the drug.

Unfortunately the degree of improvement achieved by utilizing a lower ionic strength loading solution was not consistent across all three trials, ranging from a 2.8-fold improvement to an 83-fold improvement by moving to the 0.01x PBS loading solution from the 1x. However, the general trend is consistent across all three trials: that a reduced ionic strength loading solution yields higher delivery potential and a higher percentage of encapsulated drug being released, which holds true from the 0.01x solution to the 10x solution. Of course, this trend is only necessarily true for salmon calcitonin as tested here, not other proteins with different sizes and shapes. Nevertheless, given the core principles behind the improvement (altering swelling and coulombic binding properties), the trend is expected to extend to all high isoelectric point-exhibiting proteins.

The variation in improvement between trials is likely an artifact of using different protein concentrations and particle/protein ratios in the loading solutions, which as shown in section 5.3.5, strongly affects final delivery potential. Therefore, the differences

between trials are indicative of systemic differences rather than invalidity of the results. Inability to easily control the loading pH at the scales used could also lead to some of the variation in the final results. However, this is merely an issue at the laboratory scales used here, as pH control becomes significantly easier with larger quantities of solution.

Although not tested here, using a lower ionic strength loading solution may yield improvement for low isoelectric point-exhibiting proteins as well. Although the Debye length changes are unfavorable (encouraging repulsion from the microparticles rather than binding for loading), the improvement in swelling may be more beneficial than the slight increase in ionic repulsion will be detrimental, yielding improved delivery capability.

5.3.3 Effect of Particle Size on Protein Delivery

The mechanism for release of the therapeutic proteins from the hydrogel microparticles is based on diffusion through the hydrogel network, so it is reasonable to assume that length scales will be an important factor in drug delivery capability. During release, the protein must overcome charge interactions by diffusion or osmotic pressure. The further the drug must travel by diffusion through the hydrogel mesh to the exterior of the particle, the more likely it is to encounter strong ionic interactions that overwhelm the diffusional "force" and prevent its release. Likewise, the average time scale required for ordinary diffusion at a given distance scales as

$$t \propto \frac{l^2}{D} \qquad \text{Equation 5-2}$$

where l is the diffusional distance [m] and D is the diffusional coefficient [m^2/s]. As a result, even in the case where coulombic interactions are not present and therefore do not impede release, a longer diffusional distance will require significantly more time, scaling by the square of the distance. For example, if encapsulated proteins are distributed uniformly through a particle, those proteins near the center of a 50 μm particle would be expected to take 4 times as long to escape as those near the center of a 100 μm particle. Because there is a limited time frame available for release in the small intestine (approximately 4 h total through the duodenum, jejunum, and ileum[6]), the diffusional time is limited, and particles too large in size will waste encapsulated protein due to incomplete release of protein within the biologically-imposed time constraints. Therefore, it is logical to hypothesize that using smaller particles, thus increasing the surface area to volume ratio and decreasing diffusional distance, will significantly enhance protein delivery capabilities.

To study the effect of decreased particle size on oral protein delivery, microparticles of the 1:2 P(IA-co-NVP) formulation (the best-performing formulation from the study in section 5.3.1) were crushed and sieved into size ranges of 45-75 μm, 75-90 μm, and 90-150 μm and used in a loading and release experiment using salmon calcitonin as the model high pI drug. The results of this experiment are shown in Figure 5-5.

The results do not show any statistically significant difference in the final delivery potential of the differently-sized hydrogel samples ($p > 0.23$ for all pair-wise

comparisons), either in acidic conditions or neutral conditions. In terms of loading levels, the 90-150 μm size range loaded the most amount of protein (29.0 μg sCT/mg hydrogel), significantly more than the 45-75 μm size range ($p = 0.03$) but not significantly more than the 75-90 μm size range, which is to be expected given the juxtaposed size boundaries. Thus, although there was no statistically significant difference in overall delivery levels on a per mass basis, the 45-75 μm size range exhibited a statistically significant increase in percent release (29.3%) of encapsulated protein compared to the 90-150 μm size range (22.3%).

The improved percent release does support the previous hypothesis that smaller particles could improve drug delivery, but the degree of improvement at this length scale is small. Nevertheless, the improved percent release is beneficial in that less protein is lost due to not releasing in the small intestine. Protein not loaded can be recovered and recycled for loading into other particles, but protein that is not released is forever lost, so percent release is important from the perspective of reducing cost of such a delivery system. Therefore, from a cost perspective, these results indicate moderate benefit to using smaller size microparticles.

That the overall release levels per mass of hydrogel are so similar is more difficult to explain. Presumably, the percent release is an accurate verification of the hypothesis that smaller particles improve delivery due to smaller diffusional distance and increased surface area to volume. However, the larger size range seems to make up for the lower percent release by having a higher loading level. This result is most likely due to the

washing steps employed during loading to minimize the burst release of surface-bound protein. A uniform weight of hydrogel particles is used across the different size ranges, meaning equal volume of hydrogel, since all particles are from the same formulation and therefore should have uniform density. As a result, the particles will load approximately the same amount of protein on a per mass basis if protein loads uniformly through the particles. However, the smaller particles will have a larger cumulative surface area than the larger particles, meaning more of the volume is made up of surface or near surface level binding sites. When the wash steps occur, therefore, a larger proportion of the protein is washed away, making the overall loading appear to be lower than with larger particles.

Therefore, the results of this experiment suggest that there is some benefit associated with use of smaller particles, although it may be limited to higher percent release rather than higher delivery per mass of hydrogel. This further shows that the protein release is limited by the diffusional time expected in the small intestine, so experiments that seek to increase the residence time of the particles in the small intestine, such as those by Wood et al.[9,10] or Schoener et al.,[11–13] can potentially improve the delivery system at the microparticle scale. However, even though the improvement in percent release is statistically significant, it is still not a large increase in efficiency. Large improvement may not be observed from reducing the size of the particles without using nano-scale particles, which require more complicated synthesis procedures.

5.3.4 Effect of Crosslinking Density on Protein Delivery

Another factor that could have a significant effect on the protein delivery capability of the hydrogel systems is the crosslinking density. Crosslinking density determines the value of $\overline{M_c}$, the average molecular weight between crosslinks which, as described by the swelling models in Chapter 4 and shown graphically in Figure 5-6,[8] directly affects the swelling of the hydrogel. Lower crosslinking density will lead to larger $\overline{M_c}$, which in turn leads to larger swelling ratios and larger mesh sizes. This effect can be highly beneficial in enabling the delivery of macromolecules and should grant the ability to tailor mesh sizes for delivery of differently sized molecules. For example, a small protein like salmon calcitonin (3.4 kDa) may benefit from high crosslinking density to prevent diffusion out of the mesh at low pH, whereas much larger monoclonal antibodies like rituximab (144 kDa) may need low crosslinking density to achieve sufficiently large mesh size for diffusion in and out of the hydrogel.

To test the effect of crosslinking density on protein delivery capability, a standard loading and release experiment was conducted using salmon calcitonin and Rituxan as test proteins loaded into 90-150 μm microparticles of 1:2 P(IA-co-NVP) using 1%, 5%, or 10% TEGDMA crosslinker. As expected, the hydrogels with higher crosslinking density exhibited qualitatively greater mechanical toughness; the 10% crosslinked gel was easily formed as a film and remained as a film throughout all wash steps, while the 5% broke after multiple water changes, and the 1% formulation rapidly broke into pieces sufficiently small to necessitate the use of a sieve during washes after hydration, even

with minimal shear stress. This implies successful incorporation of higher crosslinking densities in the gels as expected.

The results of the salmon calcitonin loading and release are shown in Table 5-5 and Figure 5-7. As shown by the release profiles, the 5% crosslinked formulation achieves the highest total release of sCT within 4 h at neutral conditions, while releasing no more than the 10% formulation in the 1 h at acidic conditions. The 1% formulation, although achieving similar loading level as the 10% formulation, did not release as much sCT at either acidic conditions or in neutral conditions. This may seem counterintuitive that a hydrogel with less crosslinker would release a lower percentage of its payload than more crosslinked hydrogels. However, lower crosslinking density also equates to higher concentrations of anions per unit of polymer backbone, yielding more binding sites for coulombic interactions. Thus, this implies that for a small, high pI protein like sCT, the release is determined by an interplay of mesh size and coulombic interactions, with the optimal crosslinking density appearing to be around 5% (somewhere between 1 and 10%).

5.3.5 Loading and Release of Larger Proteins

The results of the Rituxan loading and release experiment with different crosslinking densities are shown in Figure 5-8 and Table 5-6. Interestingly, despite the much larger size of Rituxan (144 kDa), the release levels and percent release seen in this experiment are higher than were observed with salmon calcitonin. This result is due to higher loading levels (56-64 μg/mg hydrogel) that result primarily from the higher

protein loading concentration used (400 μg/mL rather than 200 μg/mL), although other possible contributors could be greater coulombic interactions with the carriers, reduced penetration of the protein into the carriers (due to the size), or minor shifts in the pH during the loading step. Further experimentation with confocal microscopy or simply altering the loading pH could potentially elucidate the mechanisms for this result.

What this experiment clearly demonstrates, however, is the greatly enhanced delivery resulting from use of the 1% crosslinked hydrogels as compared to the 5% or 10% formulations. Although all profiles are nearly ideal in terms of limited release at the 1 h, acidic time point and enhanced release over a physiological time at neutral conditions, the release level observed by the 1% crosslinked formulation significantly exceeds that of the 5% and 10% formulations ($p = 0.0004$). Meanwhile, the 5% and 10% crosslinked formulations are not significantly different at any time point ($p > 0.35$). Unlike with the much smaller sCT, the release seems to be very strongly affected by the crosslinking density with the much larger rituximab protein. This further demonstrates that the release is determined by a competing combination of mesh size and coulombic interactions. While the coulombic interactions seemed to dominate with the much smaller protein, likely due to the large size of all the tested hydrogels' meshes compared to the protein, the mesh size appears to dominate with the much larger protein.

In conclusion, these two tests demonstrate two important points. First, these results indicate that the delivery potential for any given protein is largely specific to that protein due to wide differences in charge and size between proteins. While the 5% and 10% crosslinked formulations proved best for the small peptide salmon calcitonin, the

1% crosslinked formulation was vastly better for the large antibody rituximab. Second, these results also demonstrate that these P(IA-co-NVP) hydrogel systems may be easily tuned using varying crosslinking density to accommodate a wide range of proteins, ranging from the 3.4 kDa salmon calcitonin to the 144 kDa rituximab.

In an additional experiment, the loading and release of urokinase was also compared to that of sCT and rituximab using P(IA-co-NVP) microparticles synthesized with a monomer ratio of 1:2 IA to NVP. This experiment utilized urokinase as another high pI protein (pI = 8.66) with a molecular weight (54.0 kDa) between that of salmon calcitonin (3.4 kDa) and rituximab (144 kDa), allowing us to see the effects across a range of sizes, rather than just two endpoints. Urokinase is used clinically as a thrombolytic agent for myocardial infarction, pulmonary embolism, and deep vein thrombosis. As such, it is not a strong candidate for therapeutic use with our systems, due to the need for very fast application to the bloodstream, but does work well as a commercially available, medium-sized, high pI exhibiting drug.

The results of the experiment are shown in Figure 5-9 and Table 5-7. The loading level of the proteins vary considerably: salmon calcitonin had high loading levels with 44.8 μg sCT/mg hydrogel, while urokinase (19.0 μg/mg) and rituximab (24.1 μg/mg) exhibited similar, but significantly lower loading levels. This is likely due to mesh size limitations of the hydrogel that prevent easy access into the particle for larger proteins. Accordingly, both the amount of protein released and the percent release of urokinase and rituximab were lower than those of salmon calcitonin. This result further supports that protein size is a strong determining factor in the delivery potential of these hydrogels,

with larger proteins requiring larger mesh sizes in order to facilitate their diffusive transport through the tortuous paths into and out of the hydrogel mesh.

Another feature of the results of this experiment is that the Rituxan delivery potential is significantly lower than what was observed in the previous experiment. This difference arises from two results. First, the hydrogels used in this experiment were crosslinked using 3 mol% TEGDMA in the monomer feed. As a result, the rituximab release level observed is more similar to what was observed with the 5% crosslinked particles than the 1% crosslinked particles that exhibited such high release. Secondly, and most importantly, this experiment utilized loading solutions of proteins at only 200 μg/mL rather than at 400 μg/mL as was used in the preceding experiment. The lower concentration causes lower loading levels due to less protein being available for loading as well as reduced driving force for the protein to enter into the swollen hydrogels. With lower loading levels comes both lower overall delivery and lower percent release, as the lower loading level means less protein to be released even at 100% efficiency and, since concentration difference is the driving force for diffusion, less entropic gain due to diffusive release which therefore shifts the equilibrium toward coulombic binding rather than diffusive release.

These two factors account for the reduced loading and overall delivery of rituximab in this experiment, and thus show that the delivery capability of these gels is strongly dependent on the loading conditions. Higher concentration loading solutions can be used to promote higher percent release and overall delivery. The main limitation imposed by high concentration solutions is protein aggregation,[14,15] although this is

strongly dependent on the individual protein's structure and was not an observed issue at the relatively low concentrations studied here.

This experiment shows that the hydrogel delivery systems are capable of delivering high pI-exhibiting therapeutic proteins across a wide spectrum of molecular weights to the small intestine. However, in accordance with the results of the previous experiments, the system must be tailored for the individual protein being used, with molecular weight being one of the primary determining factors. The crosslinking density provides one simple means of tailoring these particles to the size of the protein, with larger proteins benefitting from lower crosslinking density (larger mesh size) and small proteins benefitting from higher crosslinking density (smaller mesh size). Additionally, the loading procedures used are also very important. Low ionic strength conditions (specifically for high pI proteins) and high protein concentrations in the imbibition loading procedure promote enhanced delivery capability and higher bioavailability.

5.3.6 Degradable Hydrogel Loading and Release

The results of the loading and release study are shown in Figure 5-10 and Table 5-8. The degradable hydrogels displayed reduced loading levels of sCT compared to what has been observed with the P(IA-co-NVP) systems, achieving only 12.4 μg sCT/mg hydrogel of encapsulated protein despite the relatively high concentration of sCT in the loading solution (400 μg/mL). The percent release of encapsulated protein, however, was approximately 100% at all time points in the simulated intestinal conditions. Although

the calculated averages are slightly above 100%, the values are not significantly different from 100% ($p > 0.064$), indicating complete release of encapsulated sCT.

The observed overall delivery level was only 13 μg sCT/mg hydrogel, necessitating the use of more hydrogel to accommodate a therapeutic dose of protein compared to the P(IA-co-NVP) system. However, because the entirety of the encapsulated protein is released by degradation of the hydrogel, the bioavailability of the protein by this method would be higher, as no protein drug would be wasted due to incomplete release in the small intestine. Furthermore, no release was observed in the simulated gastric fluid as measured by HPLC. Therefore, this system performed very well in terms of delivering protein to the small intestine, losing none of the encapsulated protein to degradation in the stomach conditions and achieving complete release in the small intestine conditions. As such, this hydrogel is very promising for achieving the highest possible bioavailability of therapeutic proteins via the oral route.

The primary limitation of the system, however, is that is difficult and costly to synthesize large quantities of the peptide crosslinker. Peptides are not easily manufactured at large scales and therefore generally are not. One notable exception is the HIV fusion inhibitor peptide, Fuzeon, which was manufactured at near-ton annual quantities because of the large daily dose needed.[16] However, the excessive cost of the manufacturing process prevented the drug from reaching blockbuster status. As a result of the high cost of peptide synthesis, this hydrogel is likely too costly to make a financially viable product at the current time. The system could find utility with protein drugs that are sufficiently expensive to manufacture that complete release in the small

intestine makes up for the increased cost of the hydrogel. However, until technological improvements in peptide synthesis are made, making inexpensive, large-scale synthesis of peptides a reality, this system may be limited to academic interest, despite its ideal performance in this *in vitro* experiment.

5.3.7 Pharmacological Feasibility

The normal recommended dosage of salmon calcitonin for a patient treating osteoporosis is 50-100 IU/day by injection, equating to 8.3-16.7 μg/day. Rituxan is used in multiple indications, but the highest recommended dose for any indication is 500 mg/m^2 (for chronic lymphocytic leukemia). For a typical adult male (50^{th} percentile of weight and height), the body surface area is 1.97 m^2, which amounts to 985 mg of Rituxan administered in a single infusion. Urokinase as used for pulmonary embolism and deep vein thrombosis is typically administered at 4400 IU/kg, which for a typical male (80 kg) and typical activity of 100,000 IU/mg amounts to 3.52 mg of urokinase. To deliver an equivalent amount of protein by the oral route, a greater amount will need to be delivered to the small intestine, which can be estimated by a simple calculation.

To ensure a conservative determination of feasibility, the required dose used in the calculation will be the high end values of 16.7 μg for sCT, 985 mg of Rituxan, and 3.52 mg of urokinase. Aside from limited delivery potential from the microparticle carriers, loss of bioavailability resulting from intestinal enzymatic degradation and low intestinal absorption must also be accounted for. Data from Youn et al.[17] showed 0.05% of unmodified sCT was transported across a Caco-2 monolayer in *in vitro* conditions over

60 min. Assuming a constant permeability (as is observed during those 60 min), this means 0.15% of released sCT can be expected to be transported across the intestinal epithelium into the bloodstream over the 3 h average residence time. The actual percentage will likely be significantly higher than this, as Caco-2 monolayers are reported to exhibit less permeable tight junctions than are observed *in vivo*.[18–22] Correlations between Caco-2 permeability and *in vivo* absorption[19,23] suggest that the apparent permeability of 1.5 x 10^{-7}/cm^2 reported by Youn et al.[17] lies in the range of poorly absorbed compounds (0-20% uptake); indeed, compounds with similar permeability in Caco-2 cultures such as doxorubicin (1.6 x 10^{-7}/cm^2) or 1-deamino-8-D-arginine-vasopressin (1.3 x 10^{-7}/cm^2) show 5% and 1% absorption respectively, so the actual absorption could be expected to be somewhere between 1 and 5%. Furthermore, the presence of P(MAA-g-EG) microparticles has been shown to inhibit enzymatic degradation following intestinal release and enhance permeability by reversible opening of the tight junctions in the intestinal epithelium, which would further enhance bioavailability and intestinal absorption.[24–27] However, for the purpose of maintaining a conservative estimate of feasibility, the very low 0.15% absorption for Caco-2 cultures over 3 h will be used.

With the selection of a high dosage and a low level of absorption, the approximate amount of polymer microparticles needed for a daily dose using the largest delivery potentials observed in experiment (48.2 μg sCT/mg hydrogel; 2.68 μg urokinase/mg hydrogel; and 81.7 μg Rituxan/mg hydrogel) are

$$\text{Hydrogel required (sCT)} = \frac{16.7\ \frac{\mu\text{g sCT}}{\text{day}}}{48.2\ \frac{\mu\text{g sCT}}{\text{mg hydrogel}} \times 0.0015} = 230\ \frac{\text{mg hydrogel}}{\text{day}}$$

$$\text{Hydrogel required (urokinase)} = \frac{3.52\ \text{mg urokinase}}{2.68\ \frac{\mu\text{g urokinase}}{\text{mg hydrogel}} \times 0.0015} = 876\ \text{g hydrogel}$$

$$\text{Hydrogel required (Rituxan)} = \frac{985\ \text{mg Rituxan}}{81.7\ \frac{\mu\text{g Rituxan}}{\text{mg hydrogel}} \times 0.0015} = 8.0\ \text{kg hydrogel}$$

Given a density of 0.66 g/mL for dry P(IA-*co*-NVP) microparticles, 230 mg will easily fit within a size 2 gel capsule (15.3 mm in length), meaning a daily dose of salmon calcitonin could be given with one pill that is smaller than a standard Tylenol gel capsule (19 mm in length) per day. Unfortunately, due to the comparatively large doses of urokinase and Rituxan, the amount of hydrogel required at this point is unreasonable. However, as stated previously, this estimation uses a low value of intestinal absorption that would be unlikely to be observed *in vivo*, and the enormous quantities of hydrogel required as calculated are due largely to this figure. It is likely that the actual amount required could be as much as 6–33x less than calculated (assuming 1-5% actual intestinal absorption), although a dose of Rituxan would still require an unreasonable 240 g of hydrogel.

Depending strongly on the actual absorption in the small intestine and the prescribed dosage, our results show that a normal regimen of salmon calcitonin may be received with our system with the improved loading procedures and delivery materials described herein, likely with no more than one or two pills taken per day. Unfortunately,

despite high delivery capability observed using low crosslinking ratio in the hydrogels with Rituxan, the delivery of proteins that require high doses does not seem to be reasonable without further improvement. Because crosslinking density and loading conditions can be used to overcome low levels of delivery to the small intestine, the passage across the intestinal epithelium is the primary remaining obstacle to oral protein delivery. Better intestinal absorption well beyond 0.15% absorption is needed to make both the amount of hydrogel ingested and the cost reasonable. Some improvement in absorption is expected to result from greater *in vivo* permeability compared to Caco-2 cultures, as described above, and from the reversible opening of tight junctions by the polymer microparticles. However, further improvement is likely necessary before such systems are pharmaceutically feasible.

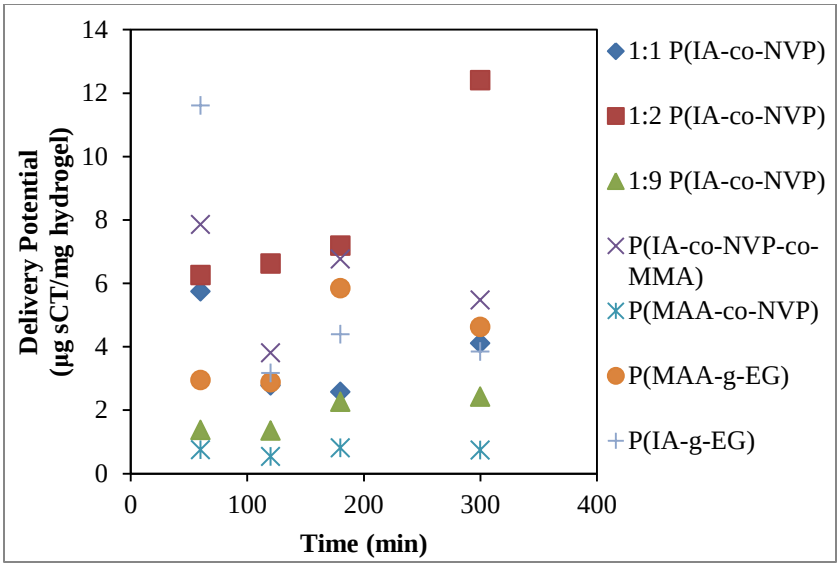

Figure 5-1: Salmon Calcitonin Release from pH-Responsive Hydrogel Microparticles Based on Methacrylic Acid or Itaconic Acid. Time point at 60 min is in acidic (pH 3.0) conditions immediately before neutralization with NaOH. All other time points were collected in neutral (pH 7.4) conditions. Delivery potential reported as mg sCT per mg hydrogel, as determined by Micro BCA assay.

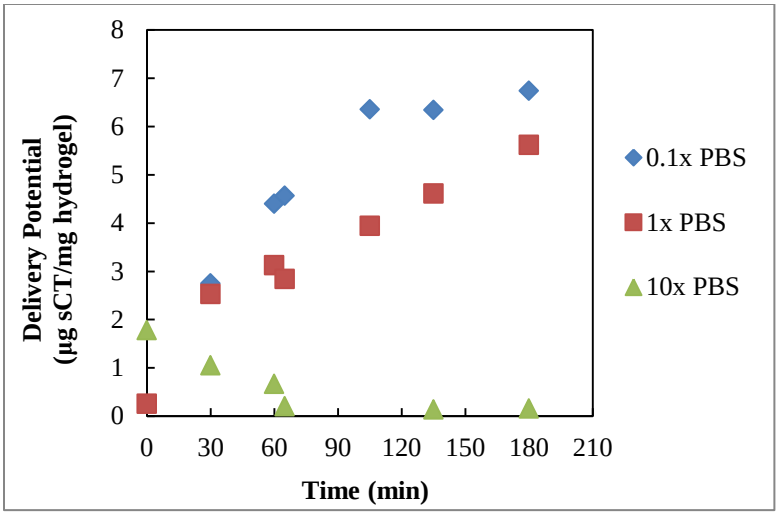

Figure 5-2: Salmon Calcitonin Release—Ionic Strength Trial 1. All profiles are for release of salmon calcitonin following loading into 1:1 P(IA-co-NVP) microparticles in 0.1x, 1x, or 10x concentrated PBS buffer. Time points from 0 – 60 min are in acidic conditions (pH 3.0) and time points from 65 – 180 minutes are in neutral conditions (pH 7.4).

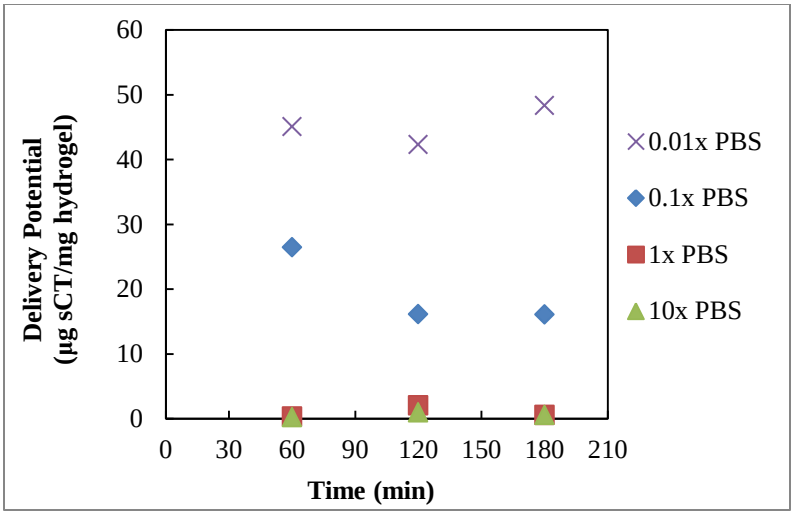

Figure 5-3: Salmon Calcitonin Release—Ionic Strength Trial 2. All profiles are for release of salmon calcitonin following loading into 1:1 P(IA-co-NVP) microparticles in 0.01x, 0.1x, 1x, or 10x concentrated PBS buffer. Time point at 60 min is in acidic conditions (pH 3.0), and time points at 120 and 180 minutes are in neutral conditions (pH 7.4).

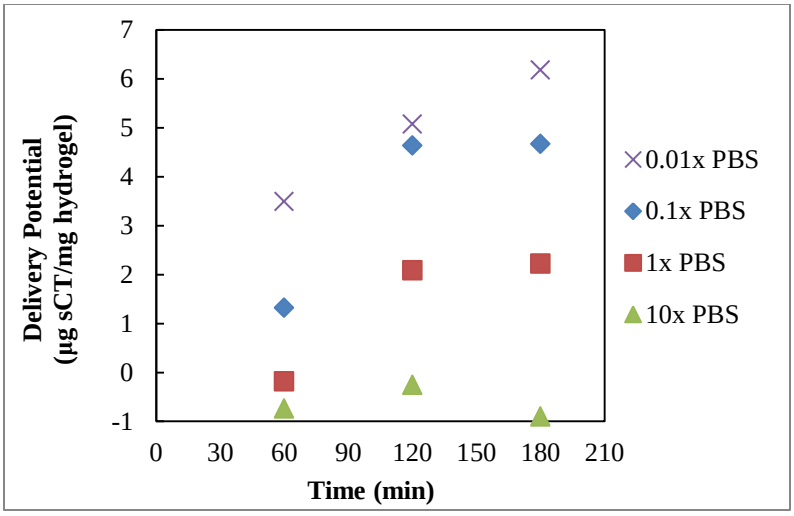

Figure 5-4: Salmon Calcitonin Release—Ionic Strength Trial 3. All profiles are for release of salmon calcitonin following loading into 1:1 P(IA-co-NVP) microparticles in 0.01x, 0.1x, 1x, or 10x concentrated PBS buffer. Time point at 60 min is in acidic conditions (pH 3.0), and time points at 120 and 180 minutes are in neutral conditions (pH 7.4).

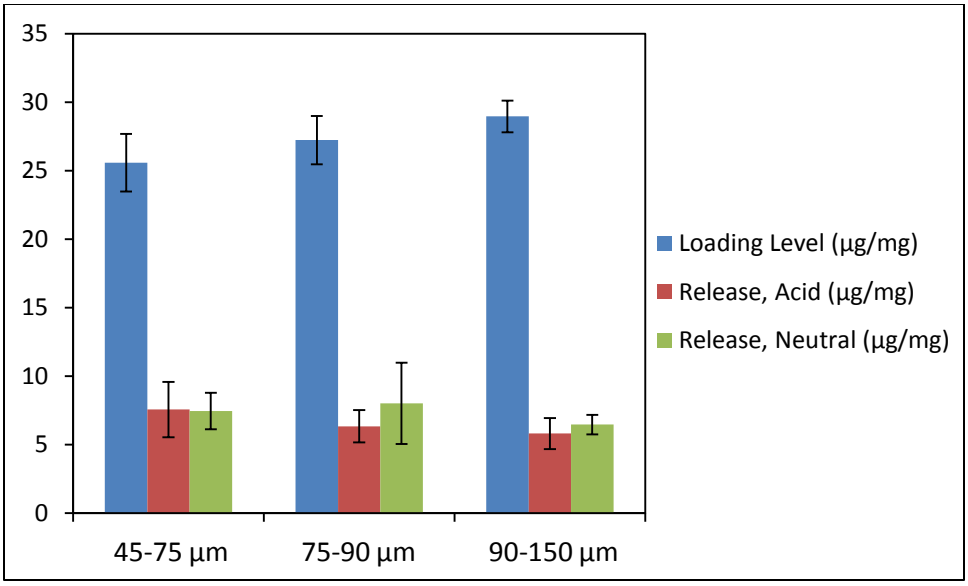

Figure 5-5: Loading and Release of Salmon Calcitonin from P(IA-co-NVP) Microparticles of Varying Sizes. All microparticles are comprised of 1:2 P(IA-co-NVP). Acidic release data reported after 1 h at pH 3, and neutral release data reported after 4 h at pH 7.4.

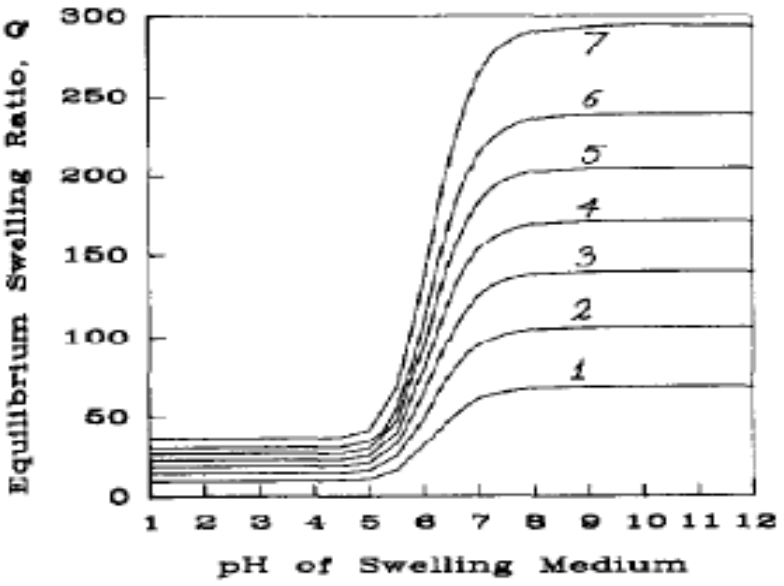

Figure 5-6: Theoretical Swelling of Anionic Hydrogel with Varying Crosslinking Density. Swelling profiles obtained by solution of Brannon-Peppas equation for varying values of $\overline{M_c}$: (1) $\overline{M_c}$ = 2000; (2) $\overline{M_c}$ = 4000; (3) $\overline{M_c}$ = 6000; (4) $\overline{M_c}$ = 8000; (5) $\overline{M_c}$ = 10,000; (6) $\overline{M_c}$ = 12,000; and (7) $\overline{M_c}$ = 15,000. Reprinted from Brannon-Peppas and Peppas[7] with permission from Elsevier.

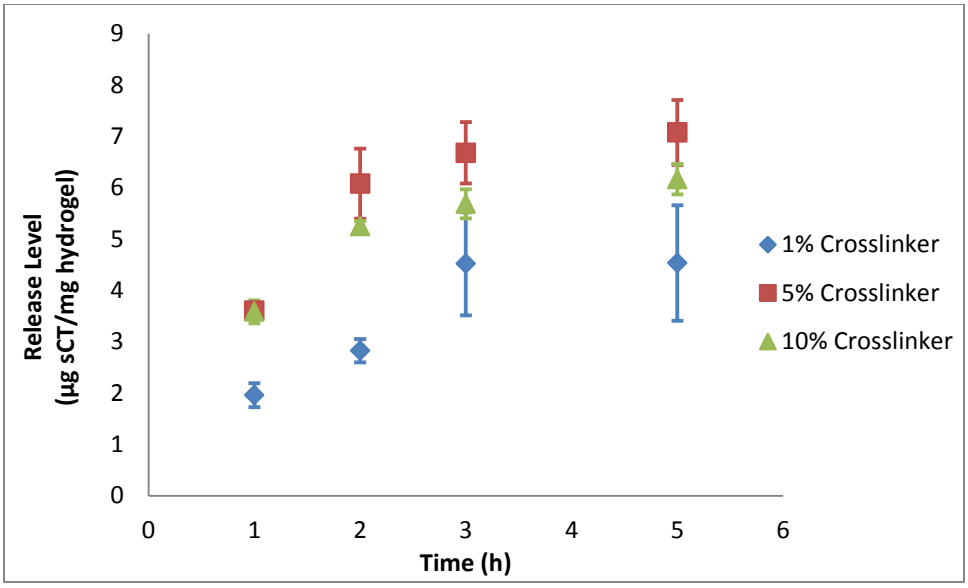

Figure 5-7: Effect of Crosslinking Density on Delivery of Salmon Calcitonin, Release Profiles. For t = 0-1 h, release conditions were acidic at pH 3. The release solutions were then neutralized, to pH 7.4 for t > 1 h.

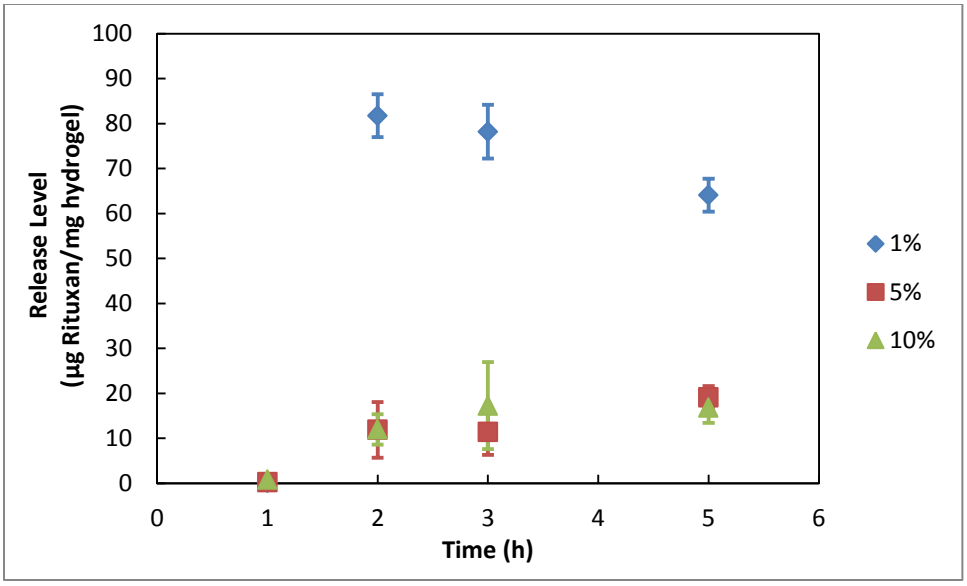

Figure 5-8: Release of Rituxan (rituximab) from 1:2 P(IA-co-NVP) Microparticles of Varying Crosslinking Density. For t = 0-1 h, release conditions were acidic at pH 3. The release solutions were then neutralized, to pH 7.4 for t > 1 h.

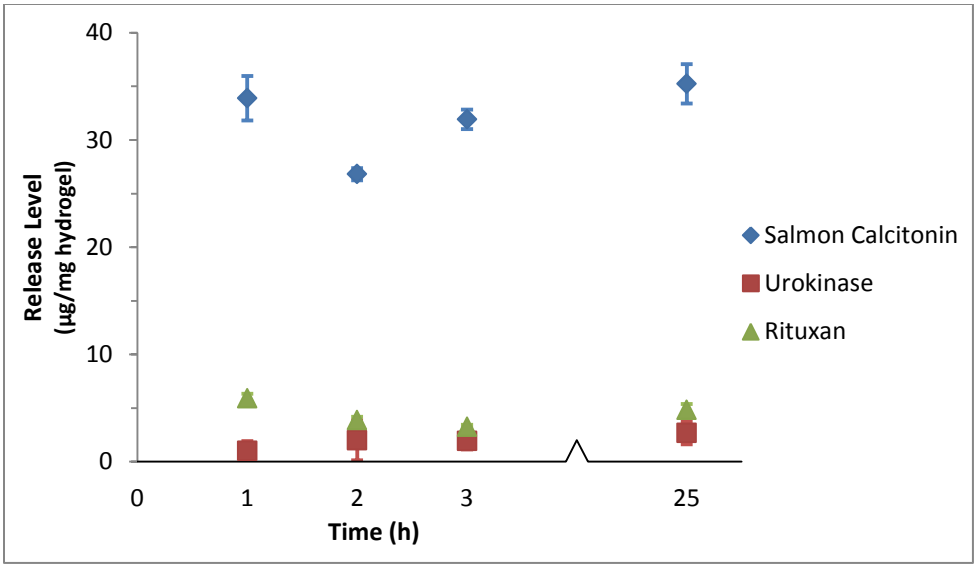

Figure 5-9: Release Profile of Calcitonin, Urokinase, and Rituxan from 1:2 P(IA-co-NVP) Hydrogel Microparticles. For t = 0-1 h, release conditions were acidic at pH 3. The release solutions were then neutralized, to pH 7.4 for $t >$ 1 h.

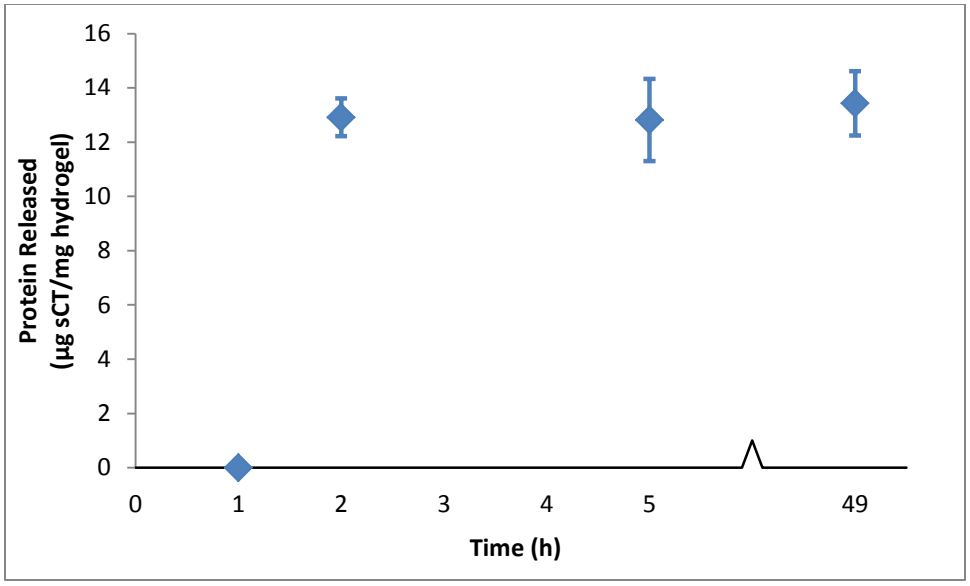

Figure 5-10: Salmon Calcitonin Release Profile from Enzymatically Degradable P(MAA-co-NVP) Hydrogel Microparticles Crosslinked with MMRRRKK Peptide. For t = 0-1 h, protein release occurred in USP-standard simulated gastric fluid (pH 1.2, 3.2 mg/mL pepsin). For t > 1 h, protein release occurred in USP-standard simulated intestinal fluid (pH 6.8, 10 mg/mL pancreatin). Salmon calcitonin release reported as average ± standard deviation (n = 3).

Table 5-1: Salmon Calcitonin Loading and Release Levels from Various Hydrogel Formulations.

Hydrogel Formulation	**Loading Level (µg sCT/mg hydrogel)**	**Delivery Potential, t=4 h (µg sCT/mg hydrogel)**	**Percent Release, t=4 h (%)**
1:2 P(IA-*co*-NVP)	45.0	12.4	27.7
P(IA-*co*-NVP-*co*-MMA)	29.1	5.5	19.0
P(MAA-*g*-EG)	23.4	4.6	19.8
1:1 P(IA-*co*-NVP)	22.3	4.1	12.3
P(IA-*g*-EG)	38.1	3.8	10.0
1:9 P(IA-*co*-NVP)	35.9	2.4	7.4
P(MAA-*co*-NVP)	9.8	0.7	8.0

Table 5-2: Salmon Calcitonin Loading and Release Levels, Ionic Strength Trial 1.

Loading Solution	**Loading Level (µg sCT/mg hydrogel)**	**Delivery Potential, t=180 min (µg sCT/mg hydrogel)**	**Percent Release, t=180 min (%)**
0.1x PBS (15 mM)	10.7	6.74	63.0
1x PBS (150 mM)	23.5	5.62	23.9
10x PBS (1500 mM)	7.4	0.16	2.1

Table 5-3: Salmon Calcitonin Loading and Release Levels, Ionic Strength Trial 2.

Loading Solution	**Loading Level (µg sCT/mg hydrogel)**	**Delivery Potential, t=180 min (µg sCT/mg hydrogel)**	**Percent Release, t=180 min (%)**
0.01x PBS (1.5 mM)	105.6	48.4	45.8
0.1x PBS (15 mM)	171.0	16.1	9.4
1x PBS (150 mM)	12.2	0.6	4.8
10x PBS (1500 mM)	53.4	0.6	1.1

Table 5-4: Salmon Calcitonin Loading and Release Levels, Ionic Strength Trial 3.

Loading Solution	**Loading Level (µg sCT/mg hydrogel)**	**Delivery Potential, t=180 min (µg sCT/mg hydrogel)**	**Percent Release, t=180 min (%)**
0.01x PBS (1.5 mM)	57.8	6.18	10.7
0.1x PBS (15 mM)	54.8	4.67	8.5
1x PBS (150 mM)	49.6	2.23	4.5
10x PBS (1500 mM)	47.3	-0.90	-1.9

Table 5-5: Loading and Release of Salmon Calcitonin from 1:2 P(IA-co-NVP) Microparticles with Varying Crosslinking Density.

Crosslinking Density	**Loading Level (µg sCT/mg hydrogel)**	**Protein Released, t=4 h (µg sCT/mg hydrogel)**	**Percent Release, t=4 h (%)**
1% TEGDMA	33.7 ± 0.4	4.53 ± 1.13	13.4 ± 3.2
5% TEGDMA	36.2 ± 0.4	7.08 ± 0.63	19.5 ± 1.6
10% TEGDMA	33.7 ± 0.3	6.17 ± 0.30	18.3 ± 0.9

Table 5-6: Loading and Release of Rituxan (rituximab) from 1:2 P(IA-co-NVP) Microparticles with Varying Crosslinking Density.

Crosslinking Density	**Loading Level (µg Rituxan/mg hydrogel)**	**Protein Released, t=4 h (µg Rituxan/mg hydrogel)**	**Percent Release, t=4 h (%)**
1% TEGDMA	56.3 ± 0.7	64.1 ± 3.7	113.8 ± 5.2
5% TEGDMA	60.4 ± 3.4	19.1 ± 2.5	31.5 ± 2.6
10% TEGDMA	64.1 ± 3.9	16.8 ± 3.4	26.4 ± 6.2

Table 5-7: Loading and Release of Salmon Calcitonin, Urokinase, and Rituxan from 1:2 P(IA-co-NVP) Microparticles.

Protein	**Loading Level (µg/mg hydrogel)**	**Protein Released, t = 24 h (µg/mg hydrogel)**	**Percent Release, t = 24 h (%)**
Salmon Calcitonin	44.8 ± 4.7	15.5 ± 1.8	35.2 ± 7.2
Urokinase	19.0 ± 1.1	2.7 ± 0.5	14.2 ± 3.2
Rituxan	24.1 ± 1.5	4.8 ± 1.1	20.0 ± 3.6

Table 5-8: Loading and Release of Salmon Calcitonin from Enzymatically Degradable P(MAA-co-NVP) Microparticles Crosslinked with MMRRRKK Peptide. Microparticles were incubated in USP simulated gastric fluid (pH 1.2, 3.2 mg/mL pepsin) for 1 h, then incubated in USP simulated intestinal fluid (pH 6.8, 10 mg/mL pancreatin) for 48 h. All values reported as average ± standard deviation (n = 3).

Release Conditions	**Time in Release Conditions (h)**	**Loading Level (μg sCT/mg hydrogel)**	**Protein Released (μg sCT/mg hydrogel)**	**Percent Release (%)**
Gastric	1	12.4 ± 0.7	0	0
Intestinal	1	12.4 ± 0.7	12.9 ± 0.7	103.8 ± 2.6
	4		12.8 ± 1.5	102.8 ± 9.5
	48		13.4 ± 1.2	107.9 ± 7.6

5.4 REFERENCES

(1) Lowman, A. M. The Dynamics of Complexation Graft Copolymers: Structural Analysis, NMR Spectroscopy, and Their Implications for Biomedical Applications. *Theses Diss. Available ProQuest* **1997**, 1–316.

(2) Feldstein, M. M. Adhesive Hydrogels: Structure, Properties, and Applications (a Review). *Polym. Sci. Ser. Chem. Phys.* **2004**, *46*, 1165–1191.

(3) Liu, S.; Fang, Y.; Hu, D.; Gao, G.; Ma, J. Complexation between Poly(methacrylic Acid) and Poly(vinylpyrrolidone). *J. Appl. Polym. Sci.* **2001**, *82*, 620–627.

(4) Bekturov, E. A.; Bimendina, L. A. Interpolymer Complexes. In *Speciality Polymers*; Advances in Polymer Science; Springer Berlin Heidelberg, 1981; pp. 99–147.

(5) Carr, D. A. *Molecular Design of Biomaterial Systems for the Oral Delivery of Therapeutic Proteins*; ProQuest, 2008.

(6) Dressman, J. B.; Krämer, J. *Pharmaceutical Dissolution Testing*; Taylor & Francis: Boca Raton, FL, 2005.

(7) Brannon-Peppas, L.; Peppas, N. A. Equilibrium Swelling Behavior of pH-Sensitive Hydrogels. *Chem. Eng. Sci.* **1991**, *46*, 715–722.

(8) Brannon-Peppas, L.; Peppas, N. A. Equilibrium Swelling Behavior of Dilute Ionic Hydrogels in Electrolytic Solutions. *J. Controlled Release* **1991**, *16*, 319–329.

(9) Wood, K. M.; Stone, Gregory M.; Peppas, N. A. Wheat Germ Agglutinin Functionalized Complexation Hydrogels for Oral Insulin Delivery. *Biomacromolecules* **2008**, *9*, 1293–1298.

(10) Wood, K. M.; Stone, Gregory M.; Peppas, N. A. In Vitro Investigation of Oral Insulin Delivery Systems Using Lectin Functionalized Complexation Hydrogels. *Adv. Med. Eng. Drug Deliv. Syst. Ther. Syst.* **2006**, 75–83.

(11) Schoener, C. A.; Hutson, H. N.; Peppas, N. A. pH-Responsive Hydrogels with Dispersed Hydrophobic Nanoparticles for the Oral Delivery of Chemotherapeutics. *J. Biomed. Mater. Res. A* **2013**, *101A*, 2229–2236.

(12) Schoener, C. A.; Hutson, H. N.; Peppas, N. A. Amphiphilic Interpenetrating Polymer Networks for the Oral Delivery of Chemotherapeutics. *AIChE J.* **2013**, *59*, 1472–1478.

(13) Schoener, C. A.; Peppas, N. A. pH-Responsive Hydrogels Containing PMMA Nanoparticles: An Analysis of Controlled Release of a Chemotherapeutic Conjugate and Transport Properties. *J. Biomater. Sci. Polym. Ed.* **2013**, *24*, 1027–1040.

(14) Fink, A. L. Protein Aggregation: Folding Aggregates, Inclusion Bodies and Amyloid. *Fold. Des.* **1998**, *3*, R9–R23.

(15) Shire, S. J.; Shahrokh, Z.; Liu, J. Challenges in the Development of High Protein Concentration Formulations. *J. Pharm. Sci.* **2004**, *93*, 1390–1402.

(16) Thayer, A. M. Making Peptides at Large Scale. *Chem. Eng. News* **2011**, *89*, 21–25.

(17) Youn, Y. S.; Jung, J. Y.; Oh, S. H.; Yoo, S. D.; Lee, K. C. Improved Intestinal Delivery of Salmon Calcitonin by Lys18-Amine Specific PEGylation: Stability,

Permeability, Pharmacokinetic Behavior and in Vivo Hypocalcemic Efficacy. *J. Controlled Release* **2006**, *114*, 334–342.
(18) Artursson, P. Cell Cultures as Models for Drug Absorption across the Intestinal Mucosa. *Crit. Rev. Ther. Drug Carrier Syst.* **1990**, *8*, 305–330.
(19) Artursson, P.; Karlsson, J. Correlation between Oral Drug Absorption in Humans and Apparent Drug Permeability Coefficients in Human Intestinal Epithelial (Caco-2) Cells. *Biochem. Biophys. Res. Commun.* **1991**, *175*, 880–885.
(20) Lennernäs, H. Regional Intestinal Drug Permeation: Biopharmaceutics and Drug Development. *Eur. J. Pharm. Sci.* **2014**, *57*, 333–341.
(21) Lennernäs, H.; Palm, K.; Fagerholm, U.; Artursson, P. Comparison between Active and Passive Drug Transport in Human Intestinal Epithelial (caco-2) Cells in Vitro and Human Jejunum in Vivo. *Int. J. Pharm.* **1996**, *127*, 103–107.
(22) Dantzig, A. H.; Bergin, L. Uptake of the Cephalosporin, Cephalexin, by a Dipeptide Transport Carrier in the Human Intestinal Cell Line, Caco-2. *Biochim. Biophys. Acta BBA - Biomembr.* **1990**, *1027*, 211–217.
(23) Yee, S. In Vitro Permeability Across Caco-2 Cells (Colonic) Can Predict In Vivo (Small Intestinal) Absorption in Man—Fact or Myth. *Pharm. Res.* **1997**, *14*, 763–766.
(24) Madsen, F.; Peppas, N. A. Complexation Graft Copolymer Networks: Swelling Properties, Calcium Binding and Proteolytic Enzyme Inhibition. *Biomaterials* **1999**, *20*, 1701–1708.
(25) Kavimandan, N. J.; Losi, E.; Peppas, N. A. Novel Delivery System Based on Complexation Hydrogels as Delivery Vehicles for Insulin–transferrin Conjugates. *Biomaterials* **2006**, *27*, 3846–3854.
(26) Kavimandan, N. J.; Peppas, N. A. Confocal Microscopic Analysis of Transport Mechanisms of Insulin across the Cell Monolayer. *Int. J. Pharm.* **2008**, *354*, 143–148.
(27) Ichikawa, H.; Peppas, N. A. Novel Complexation Hydrogels for Oral Peptide Delivery: In Vitro Evaluation of Their Cytocompatibility and Insulin-Transport Enhancing Effects Using Caco-2 Cell Monolayers. *J. Biomed. Mater. Res. A* **2003**, *67A*, 609–617.

Chapter 6: PEGylation of High Isoelectric Point Proteins and Its Effects on Oral Drug Delivery

6.1 INTRODUCTION

As discussed in section 2.4, bioconjugation has been a method explored by scientists and pharmaceutical developers for imbuing therapeutics with additional, beneficial properties that enhance the physiological properties of the molecule. The improvements achieved through bioconjugation are manifold. For example, many drug molecules are poorly soluble, with 25% of the medicines on the World Health Organization's Essential Medicines List being classified as poorly soluble[1] and many more promising candidates being unexplored because of poor solubility. The solubility can be enhanced by conjugation of a hydrophilic molecule to the poorly soluble molecule. Alternatively, attachment of an enzymatically non-degradable molecule to a protein may offer significantly enhanced half-life *in vivo* for enhanced efficacy. Conjugation of a targeting molecule, such as an antibody, can help ensure that a therapeutic reaches its desired location within the body or within a cell. Or, conjugation of two therapeutic agents to one another can provide multiple mechanisms of action while localizing the two compounds to the same delivery site to enhance efficacy. The possibilities are diverse and numerous.

However, one of the most widely used conjugation strategies involves attachment of a poly(ethylene glycol) chain to a protein—a process termed "PEGylation." PEGylation imparts many of the beneficial properties named above. PEG has several

interesting properties, including a surprisingly high degree of hydrophilicity compared to the largely hydrophobic poly(methylene oxide) and poly(butylene oxide), which are a mere carbon link different at the monomer level, as well as some hydrophobic character, exhibited by its tendency to form monolayers at air-water interfaces.[2] Nevertheless, the generally highly hydrophilic polymer has been widely used as a conjugate to increase the solubility of compounds.[3–8]

Furthermore, it has been shown that PEG demonstrates repulsive interactions with typical proteins at long distance, but can instead demonstrate an attractive interaction at close range.[9] The effect is thought to occur due to competitive binding of water molecules and the proteins, with the water molecules dominating due to the smaller size until the protein gets sufficiently close to bind. As such, the effect is often described as a water cage that forms around the PEG-protein conjugate.

The repulsive aspect is highly useful in biomedical applications, as it provides stealth properties to the protein by preventing binding of opsonins, therefore extending the half-life of the protein *in vivo* by preventing recognition and removal by macrophages. Because of the attractive interaction at close range, adsorption of proteins is kinetically, but not thermodynamically limited, meaning in time opsonins will eventually bind and cause the removal of the conjugate.[2,9] While this limits the therapeutic's half-life *in vivo*, this is beneficial, as it means therapeutics will not accumulate in the body over time and cause long acting side effects. PEGylation has therefore been used in 13 FDA-approved drugs and used extensively in research to extend the half-life of rapidly removed or degraded drugs.[3,4,6–8,10–16]

One final benefit of PEGylation that could prove useful in our drug delivery systems is the ability to provide charge shielding, limiting electrostatic interactions. This effect has been shown in several studies[15,17] and likely results from the formation of the water cage, which disperses electrostatic interactions via dipolar rearrangement of the water molecules. This effect could be beneficial for oral delivery of proteins using our systems; because high pI proteins are bound by electrostatic interactions between the anionic polymer and the cationic protein, charge shielding through PEGylation could promote protein release by reducing the strength of these interactions.

Because PEGylation is a widely used method of imparting numerous beneficial properties to biotherapeutics, I sought to determine what effects PEGylation would have on the delivery of high pI exhibiting proteins using the P(IA-co-NVP) delivery system. PEGylation often imbues additional hydrophilicity to particles and can shield charge interactions, which could promote release of proteins from our systems. However, the attachment of a PEG chain to a biotherapeutic agent necessarily increases the size of the protein, due to increased molecular weight and increased hydrodynamic radius from the water cage, which could potentially reduce the probability of diffusion through the tortuous pathway through the hydrogel mesh. Therefore, the effects of PEGylation on protein delivery were studied and are reported here in Chapter 6. Effect of PEGylation on the later process of intestinal absorption is subsequently reported in Chapter 7.

6.2 PEGylation Reaction

Salmon calcitonin consists of only 32 amino acids, so conjugation sites are inherently limited. At the N-terminus, there are two cysteine residues at the 1 and 7 positions bonded together by a disulfide linkage. Additionally, there are 2 lysines, at the 11 and 18 positions, and the N-terminus where primary amines are found.

The cysteine residues could potentially be reduced using dithiothreitol or TCEP and used as conjugation sites with a PEG-maleimide or PEG-dibromomaleimide. Using a PEG-maleimide would react with one of the thiols, providing PEGylation at the 1 or 7 amino acid, but would leave the disulfide broken, which could impair the structure and function of the protein. Use of PEG-dibromomaleimide would approximately maintain the disulfide with a two carbon linker in between sulfurs, and would provide site specific conjugation at the disulfide site.[18–20] However, the dibromomaleimide reactant is not commercially available and has a demanding synthesis procedure.

The primary amines in the protein may be used by EDC/NHS coupling, as described in Chapter 2. Monofunctional NHS esters of PEG are available commercially, making the PEGylation reaction a simple one-step procedure where the pre-activated NHS ester is mixed in solution with the protein, enabling it to react with primary amines and form a zero-length crosslink between the PEG and the amine. The drawback of this synthesis is that it does not provide site specificity. All three sites will readily react, and depending on molar ratio of the reactants, the degree of substitution could vary between proteins. For the sake of this research, the location of the conjugation is not important. Lee et al. have shown that conjugation to the Lys^{18} is preferable for maximizing

bioavailability,[21] so care to ensure conjugation to this site would be important if we were seeking to maximize bioavailability in a clinical setting.

However, the goal of this study is merely to study the effect of increased size and hydrophilicity on the drug delivery capability with the P(IA-co-NVP) hydrogel systems, which should not require site specificity. The degree of substitution is important, however, as the number of PEG chains conjugated to the protein determines the conjugate's size and hydrophilicity. Therefore, the more straightforward PEGylation procedure of conjugating to primary amines will be used in lieu of the cysteine conjugation, and the degree of substitution will be maintained at 1 PEG chain per sCT protein, as controlled by reactant ratio and verified by mass spectrometry.

6.3 MATERIALS AND METHODS

6.3.1 PEGylation of Salmon Calcitonin

An equimolar mixture of salmon calcitonin (Selleck Chemicals, Houston, TX) and methoxy poly(ethylene glycol) succinimidyl carboxy methyl ester ($mPEG_{2k}$-SCM, number average PEG molecular weight of 2 kDa) (NanoCS, Boston, MA) were dissolved in methanol (Sigma Aldrich, St. Louis, MO). Both reactants were added at a concentration of 0.873 mM. The reaction proceeded for 1 h on a rotary mixer. The PEGylated salmon calcitonin (sCT-PEG) was isolated by dialysis. The reaction mixture was placed inside a 10 mm regenerated cellulose membrane tube with a 3.5 – 5 kDa molecular weight cutoff (Spectrum Laboratories, Inc., Rancho Dominguez, CA), which was then placed in 1 L of deionized water. The water was changed every 24 h for 3 days,

at which time the sCT-PEG was removed from the inside of the tube, dried by lyophilization, and stored at -20 °C.

6.3.2 MALDI-TOF Characterization of sCT-PEG

The PEGylated product was characterized using matrix assisted laser desorption ionization time of flight (MALDI-TOF) mass spectrometry. Samples of both the final reactant mixture and the purified, isolated product were analyzed. The matrix solution used consisted of α-cyano-4-hydroxycinnamic acid (CHCA) at 10 mg/mL concentration in 40 vol% of 0.1% trifluoroacetic acid and 60 vol% of acetonitrile. 0.5 μL samples were placed on the spot plate and covered with 0.5 μL of matrix solution. Spots were allowed to dry at room temperature before being analyzed using an AB-Sciex Voyager-DE Pro MALDI-TOF mass spectrometer.

6.3.3 Loading and Release of sCT-PEG

Separate solutions of sCT and sCT-PEG were prepared at 500 μg protein/mL concentration in 1.5 mM PBS (0.01x). In 12 x 2.0 mL low adhesion tubes, 5 mg of 1:2 P(IA-co-NVP) hydrogel microparticles (90-150 μm in size) were added to each tube and incubated with 1.5 mL of protein solution (n = 6 per protein compound) for 24 h at pH 7.4. The solutions were collapsed using 1 N HCl to reduce the pH to 2, isolated by centrifugation and decanting, washed two times with 0.5 mL of 0.01 N HCl, and lyophilized. Following drying, 1.0 mL of 150 mM PBS (1x) at pH 3 was added to each tube and incubated at 37 °C for 1 h. A 300 μL sample was taken and replaced with pH 3

PBS, and the solutions were then raised to pH 7.4 using 1 N NaOH. The solutions were stirred at 37 °C for 24 h, with 200 μL samples acquired and replaced with fresh PBS at time points of 1, 2, 3, and 24 h. All loading and release samples were analyzed for protein concentration using a MicroBCA assay.

6.4 RESULTS AND DISCUSSION

6.4.1 PEGylation and MALDI-TOF Characterization

The most important aspect of the PEGylation reaction for the sake of this research was to demonstrate control over the degree of substitution, maintaining a uniform degree of substitution so that molecular weight and hydrophilicity would be consistent. In an initial trial, reactants were mixed at a molar ratio of 3 to 1 mPEG-SCM to sCT. A multi-fold molar excess of the NHS-ester reactant (mPEG-SCM) to the protein is recommended by several conjugation texts as standard procedure to drive the reaction to completion.[22,23] After reaction, the reaction mixture was analyzed by MALDI-TOF mass spectrometry, with the resulting molecular weight profile shown in Figure 6-1. The molecular weight distribution of unreacted $mPEG_{2k}$-SCM is clearly seen as a Gaussian distribution around 2200 Da. There is a small, broad peak around 7800 Da that corresponds to a degree of substitution of 2, and a larger broad peak around 10000 Da that corresponds to a degree of substitution of 3.

The relative sizes of these peaks indicates a high yield of protein with 3 conjugated PEG chains, with a small quantity of protein with only 2 PEG chains per molecule. Such a mixture of products is not ideal for study, and the high degree of

substitution would likely interfere with the activity of the protein for end use. Wu et al. have demonstrated that conjugate size can have an effect on activity of proteins,[24] and singly-PEGylated sCT has been shown to have an already reduced activity of 74% compared to unmodified sCT (although a 3-fold longer half-life yields overall better bioavailability),[12] so attachment of multiple PEG chains to sCT may yield a largely inactive molecule, making study irrelevant.

Therefore, the reactant ratio was reduced to a 1:1 molar ratio of $mPEG_{2k}$-SCM to sCT to limit degree of substitution to approximately 1. The final reaction mixture was analyzed using MALDI-TOF mass spectrometry, and the resulting mass profile is shown in Figure 6-2. The broad peak around 2200 Da is not seen in this spectrum, although a tall, narrow peak at 3432 Da is seen, corresponding to unreacted sCT. Although the height of the peak relative to all others may seem to indicate very low yield, the height of the sCT peak is misleading: all of the unreacted sCT is at exactly this molecular weight, giving that one mass a very tall peak, whereas the polydispersity of the PEG makes the conjugate appear lower in intensity at each point, but broader in terms of molecular weight. The areas under the peaks should be similar, indicating a similar number of unreacted sCT and PEG, but the broadness of the PEG peak makes it imperceptibly small. As a result, the perceptible peak seen at 5400 Da indicates that sCT-PEG is actually the dominant species, meaning a high yield of the desired product. Importantly, very little doubly-conjugated sCT is seen in the spectrum, so this molar ratio of reactants appears to provide a favorable combination of high yield of the desired product with minimal mixture of products due to excessive substitution per molecule.

The 1:1 molar ratio was then used at a larger scale to prepare sCT-PEG for experiments, and the product was purified by dialysis. The MALDI-TOF mass spectra of the product mixture and the dialyzed product are shown in Figures 6-3 and 6-4, respectively. Because the molecular weight cutoff of the dialysis tubing (3.5-5 kDa) is close to the molecular weights of the unreacted sCT (3.4 kDa) and the product (5.4 kDa), the process does not produce ideal separation of product from reactant. However, the peaks around 5.4 kDa become noticeably more prominent after dialysis, indicating some level of purification.

The ratios of identifiable peak areas at 3.4 kDa and 5.4 kDa ($A_{3.4\ kDa}$ / $A_{5.4\ kDa}$) before and after dialysis were 238 and 0.55 respectively. The peak areas are indicative of concentrations of species in the sample, but do not directly reflect the true ratio of concentrations due to different volatilities and susceptibilities to ionization between species. Therefore, a 0.55 ratio does not necessarily mean that there are nearly 2 sCT-PEG molecules for every sCT molecule; the actual ratio would likely favor sCT-PEG even more due to increased mass, requiring higher laser intensity to desorb from the matrix than sCT. Nevertheless, the fact that the peak area ratio decreases by such a large degree (a 432x reduction) indicates that the dialysis process provides suitable separation that strongly favors retention of sCT-PEG over unreacted sCT.

6.4.2 Loading and Release of sCT-PEG

The purified sCT-PEG was used alongside unmodified sCT in a loading and release experiment to study the effects of increased size and hydrophilicity on drug

delivery in the P(IA-co-NVP) systems. The results are shown in Figure 6-5 and Table 6-1. Figure 6-5 shows that the unmodified salmon calcitonin achieves significantly greater protein release levels at all time points ($p < 0.005$), with the difference increasing through the 4 h time point. However, as shown in Table 6-1, this greater release level is not due to greater loading level: the sCT-PEG had higher average loading levels than the unmodified sCT did in the 1:2 P(IA-co-NVP) microparticles, although the difference was not statistically significant ($p = 0.094$). The similar loading levels mean that the unmodified salmon calcitonin also exhibited significantly higher ($p = 0.000036$) percent release of encapsulated protein than the sCT-PEG did. Therefore, the PEGylation process does not appear to limit loading, but does cause reduced protein delivery levels, both in terms of quantity delivered and percent of encapsulated protein released.

The difference in release level could be due to several factors. The simplest explanation is that the increased size of the sCT-PEG compared to unmodified sCT impedes diffusion through the hydrogel mesh. This doubtlessly plays some role in the reduced delivery levels, but the similar loading level implies that the size was not an impediment during diffusion into the hydrogel, meaning it is likely not the foremost factor in why the release levels were reduced.

Another factor is that the protein loading solutions were identical in terms of weight concentration, rather than identical in terms of molar concentrations. Similar loading levels in terms of weight of protein mean that there are fewer molecules of the larger sCT-PEG in the hydrogels compared to the number of sCT molecules in the sCT-loaded microparticles. The sCT-PEG weighs roughly 60% more than the sCT, meaning

nearly 40% fewer molecules per mass of hydrogel as compared to the sCT. Because the entropic driving force for diffusion is based on molar concentration differences between the interior and exterior of the particles, rather than mass concentrations, the diffusional "force" for protein release from the hydrogel is smaller for the sCT-PEG loaded hydrogels compared to the sCT-loaded hydrogels at similar loading level. This alone could explain the observed difference in release; further experiments maintaining equal molar concentrations during loading would be useful in identifying if this is the primary cause.

Finally, the increased hydrophilicity of the sCT-PEG could be encouraging partitioning inside the highly hydrophilic interior of the hydrogel. This could explain the similar, though slightly larger loading level for the sCT-PEG inside the particles, even though the larger protein size should reduce the rate of diffusion into the interior of the particles if diffusion were the only mechanism for drug loading. Furthermore, with hydrophilicity promoting partitioning inside the hydrogel, the release level would be expected to be reduced due to more favorable free energy interactions for remaining in the hydrogel. Such behavior is consistent with what is observed, indicating that the hydrophilicity of the drug compound is likely an important characteristic in determining the loading and release expected for a drug using our pH-responsive systems.

This experiment clearly shows that PEGylation will have some effect on the drug delivery potential of our systems. For a 2 kDa PEG chain attached to salmon calcitonin, the impact was negative, yielding similar loading level but reduced release level. The difference was statistically significant, although even with the reduction, the sCT-PEG

still exhibited a respectable 27 μg/mg release level, which would not preclude its clinical use with our systems. Indeed, the 3-fold improvement in half-life of PEGylated sCT with only a 26% reduction in activity more than makes up for the reduction in delivery with our systems in terms of overall efficacy. Nevertheless, when coupled with the experiments with sCT, Rituxan, and urokinase discussed in Chapter 5, this experiment adds to the list of important characteristics to consider when tailoring our systems to a particular therapeutic: isoelectric point, molecular size, crosslinking density of the hydrogels, and now hydrophilicity.

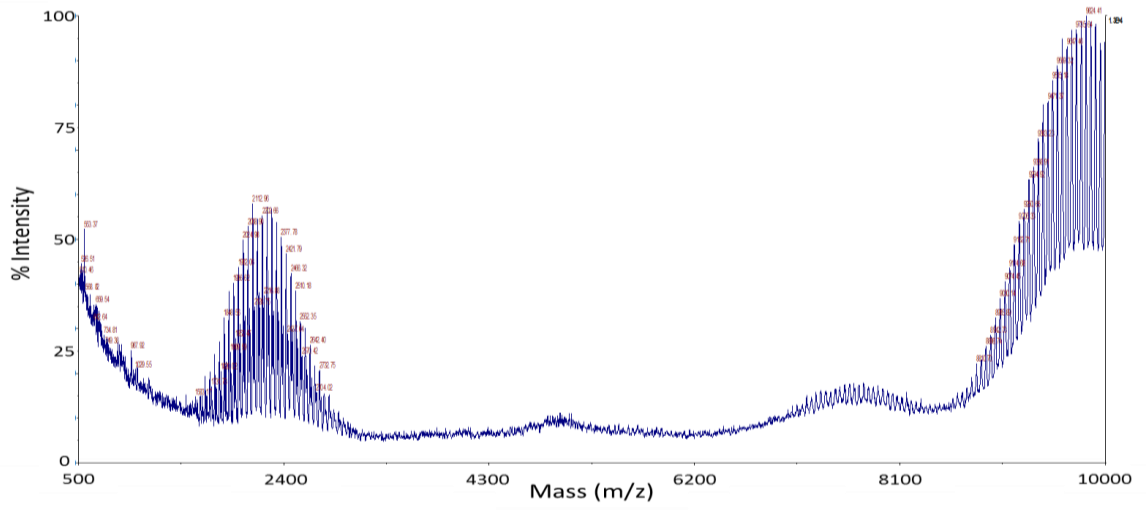

Figure 6-1: Mass Spectrum of PEG_{2k}SCM-sCT (3:1) Conjugation Product Mixture.

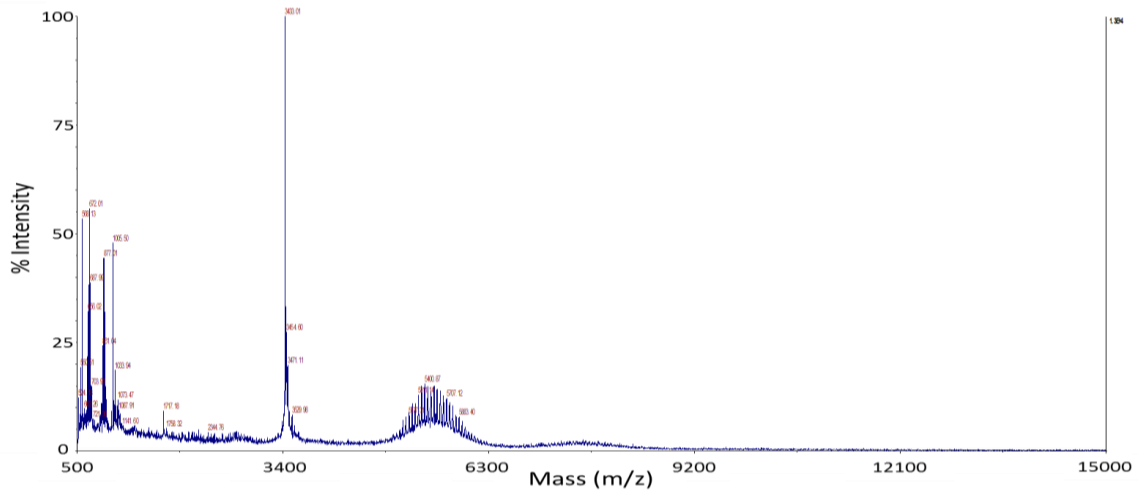

Figure 6-2: Mass Spectrum of PEG_{2k}SCM-sCT (1:1) Conjugation Product Mixture.

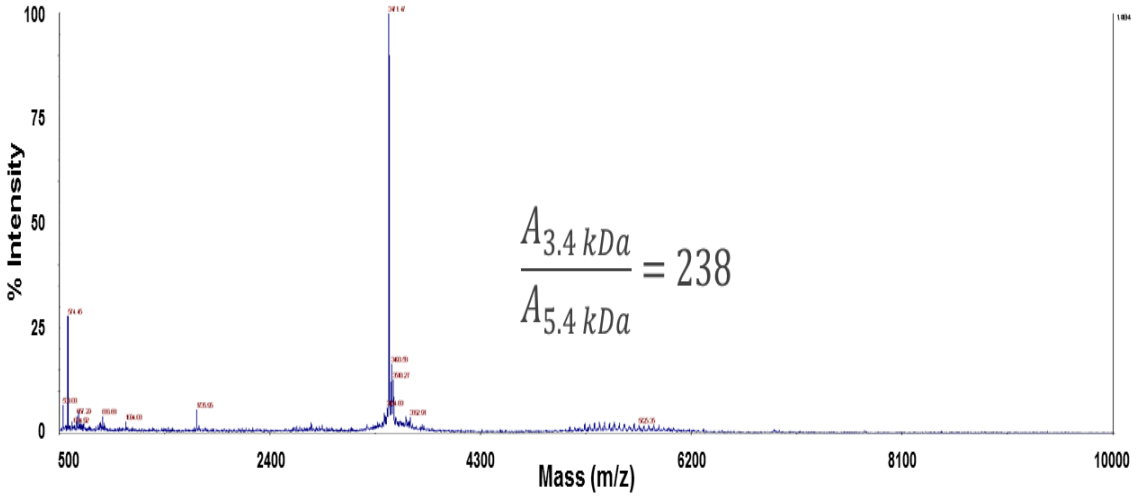

Figure 6-3: Mass Spectrum of Mono-PEGylated Salmon Calcitonin, Before Dialysis.

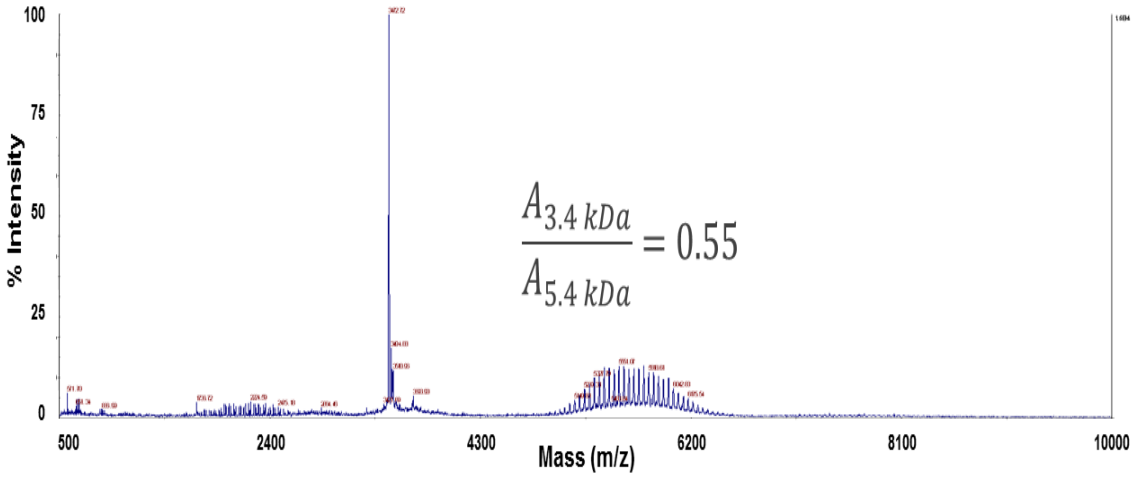

Figure 6-4: Mass Spectrum of Mono-PEGylated Salmon Calcitonin, After Dialysis.

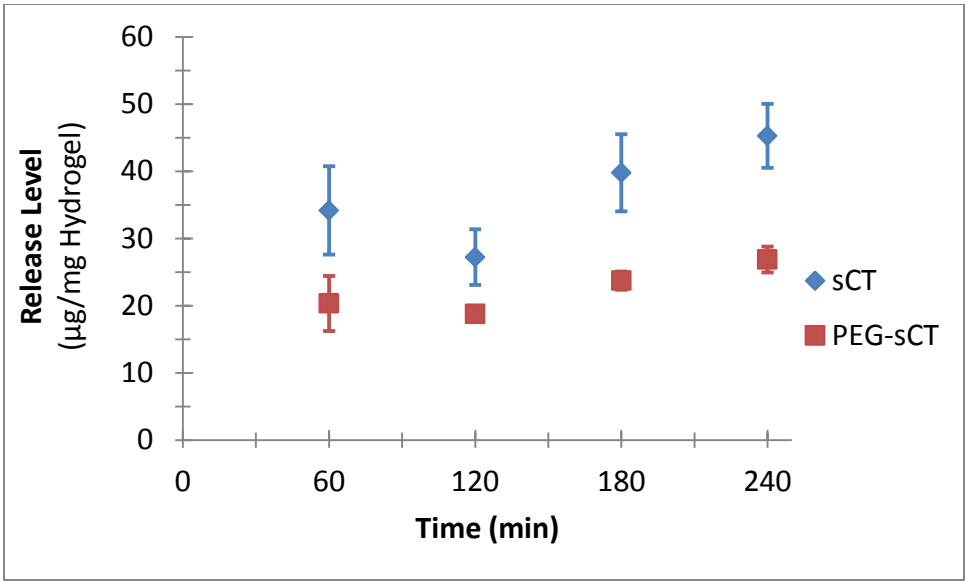

Figure 6-5: Release Profile of Salmon Calcitonin and PEGylated Salmon Calcitonin. From time t = 0-60 min, release conditions were acidic (pH 3). At t = 60 min, the release medium was neutralized and maintained at pH 7.4 for t > 60 min. Release levels reported as average ± standard deviation (n = 6).

Table 6-1: Loading and Release Levels of Unmodified and PEGylated Salmon Calcitonin Using 1:2 P(IA-co-NVP) Microparticles.

Protein	**Loading Level (µg/mg hydrogel)**	**Protein Released, t=4 h (µg/mg hydrogel)**	**Percent Release, t=4 h (%)**
sCT, Unmodified	103.0 ± 4.1	45.3 ± 4.8	43.9 ± 3.7
sCT-$PEG_{2\ kDa}$	108.1 ± 4.5	26.9 ± 1.9	24.9 ± 1.2
p-value	0.094	0.00013	0.000036

6.5 REFERENCES

(1) World Health Organization. Multisource (generic) Products and Interchangeability: Training Workshop on Dissolution, Pharmaceutical Product Interchangeability and Biopharmaceutical Classification System, 2007.

(2) Israelachvili, J. The Different Faces of Poly(ethylene Glycol). *Proc. Natl. Acad. Sci.* **1997**, *94*, 8378–8379.

(3) Roberts, M. J.; Bentley, M. D.; Harris, J. M. Chemistry for Peptide and Protein PEGylation. *Adv. Drug Deliv. Rev.* **2002**, *54*, 459–476.

(4) Veronese, F. M. Peptide and Protein PEGylation: A Review of Problems and Solutions. *Biomaterials* **2001**, *22*, 405–417.

(5) Veronese, F. M.; Pasut, G. PEGylation, Successful Approach to Drug Delivery. *Drug Discov. Today* **2005**, *10*, 1451–1458.

(6) Jevševar, S.; Kunstelj, M.; Porekar, V. G. PEGylation of Therapeutic Proteins. *Biotechnol. J.* **2010**, *5*, 113–128.

(7) Harris, J. M.; Chess, R. B. Effect of Pegylation on Pharmaceuticals. *Nat. Rev. Drug Discov.* **2003**, *2*, 214–221.

(8) Harris, D. J. M.; Martin, N. E.; Modi, M. Pegylation. *Clin. Pharmacokinet.* **2012**, *40*, 539–551.

(9) Sheth, S. R.; Leckband, D. Measurements of Attractive Forces between Proteins and End-Grafted Poly(ethylene Glycol) Chains. *Proc. Natl. Acad. Sci.* **1997**, *94*, 8399–8404.

(10) Owens III, D. E.; Peppas, N. A. Opsonization, Biodistribution, and Pharmacokinetics of Polymeric Nanoparticles. *Int. J. Pharm.* **2006**, *307*, 93–102.

(11) Aggarwal, P.; Hall, J. B.; McLeland, C. B.; Dobrovolskaia, M. A.; McNeil, S. E. Nanoparticle Interaction with Plasma Proteins as It Relates to Particle Biodistribution, Biocompatibility and Therapeutic Efficacy. *Adv. Drug Deliv. Rev.* **2009**, *61*, 428–437.

(12) Youn, Y. S.; Jung, J. Y.; Oh, S. H.; Yoo, S. D.; Lee, K. C. Improved Intestinal Delivery of Salmon Calcitonin by Lys18-Amine Specific PEGylation: Stability, Permeability, Pharmacokinetic Behavior and in Vivo Hypocalcemic Efficacy. *J. Controlled Release* **2006**, *114*, 334–342.

(13) Youn, Y. S.; Kwon, M. J.; Na, D. H.; Chae, S. Y.; Lee, S.; Lee, K. C. Improved Intrapulmonary Delivery of Site-Specific PEGylated Salmon Calcitonin: Optimization by PEG Size Selection. *J. Controlled Release* **2008**, *125*, 68–75.

(14) Gorochovceva, N.; Makuška, R. Synthesis and Study of Water-Soluble Chitosan-O-Poly(ethylene Glycol) Graft Copolymers. *Eur. Polym. J.* **2004**, *40*, 685–691.

(15) Toncheva, V.; Wolfert, M. A.; Dash, P. R.; Oupicky, D.; Ulbrich, K.; Seymour, L. W.; Schacht, E. H. Novel Vectors for Gene Delivery Formed by Self-Assembly of DNA with Poly(l-Lysine) Grafted with Hydrophilic Polymers. *Biochim. Biophys. Acta BBA - Gen. Subj.* **1998**, *1380*, 354–368.

(16) Abuchowski, A.; McCoy, J. R.; Palczuk, N. C.; Es, T. van; Davis, F. F. Effect of Covalent Attachment of Polyethylene Glycol on Immunogenicity and Circulating Life of Bovine Liver Catalase. *J. Biol. Chem.* **1977**, *252*, 3582–3586.
(17) Nguyen, H.-K.; Lemieux, P.; Vinogradov, S. V.; Gebhart, C. L.; Guérin, N.; Paradis, G.; Bronich, T. K.; Alakhov, V. Y.; Kabanov, A. V. Evaluation of Polyether-Polyethyleneimine Graft Copolymers as Gene Transfer Agents. *Gene Ther.* **2000**, *7*, 126–138.
(18) Jones, M. W.; Strickland, R. A.; Schumacher, F. F.; Caddick, S.; Baker, J. R.; Gibson, M. I.; Haddleton, D. M. Polymeric Dibromomaleimides As Extremely Efficient Disulfide Bridging Bioconjugation and Pegylation Agents. *J. Am. Chem. Soc.* **2012**, *134*, 1847–1852.
(19) Smith, M. E. B.; Schumacher, F. F.; Ryan, C. P.; Tedaldi, L. M.; Papaioannou, D.; Waksman, G.; Caddick, S.; Baker, J. R. Protein Modification, Bioconjugation, and Disulfide Bridging Using Bromomaleimides. *J. Am. Chem. Soc.* **2010**, *132*, 1960–1965.
(20) Tedaldi, L. M.; Smith, M. E. B.; Nathani, R. I.; Baker, J. R. Bromomaleimides: New Reagents for the Selective and Reversible Modification of Cysteine. *Chem. Commun.* **2009**, 6583–6585.
(21) Lee, K. C.; Moon, S. C.; Park, M. O.; Lee, J. T.; Na, D. H.; Yoo, S. D.; Lee, H. S.; DeLuca, P. P. Isolation, Characterization, and Stability of Positional Isomers of Mono-PEGylated Salmon Calcitonins. *Pharm. Res.* **1999**, *16*, 813–818.
(22) Hermanson, G. T. Chapter 3 - Zero-Length Crosslinkers. In *Bioconjugate Techniques (Second Edition)*; Hermanson, G. T., Ed.; Academic Press: New York, 2008; pp. 213–233.
(23) Brinkley, M. A Brief Survey of Methods for Preparing Protein Conjugates with Dyes, Haptens and Crosslinking Reagents. *Bioconjug. Chem.* **1992**, *3*, 2–13.
(24) Wu, C.-S.; Lee, C.-C.; Wu, C.-T.; Yang, Y.-S.; Ko, F.-H. Size-Modulated Catalytic Activity of Enzyme–nanoparticle Conjugates: A Combined Kinetic and Theoretical Study. *Chem. Commun.* **2011**, *47*, 7446–7448.

Chapter 7:

In Vitro Models of Intestinal Absorption of Protein Therapeutics

7.1 INTRODUCTION

In the course of enabling the oral delivery of protein therapeutics, numerous obstacles had to be overcome: protection from protein degradation in the stomach by hydrochloric acid or proteolytic enzymes; delivery to the small intestine (i.e., release from encapsulating delivery vehicles); protection from enzymatic degradation in the small intestine; and absorption of proteins into the bloodstream across the intestinal epithelium. The last of these obstacles, intestinal absorption, is arguably the most significant barrier to achieving high bioavailability of proteins via the oral route.

Intestinal cells have evolutionarily developed tight junctions—a collection of proteins between cells that regulate the permeability of the paracellular region—in order to control the absorption of compounds across the intestinal epithelium and prevent the transport of foreign molecules or organisms into the bloodstream. Multiple proteins are responsible for forming and maintaining these tight junctions, most notably occludin, as seen in Figure 7-1.[1] These proteins dynamically maintain the limited permeability between enterocytes, with permeability varying over multiple orders of magnitude between different epithelia and varying in response to numerous cellular signals, including: electrolytes such as H^+, Cl^-, Na^+, and Ca^{2+}; electrical current; pressure; and

chemical agents such as bile salts, amphotericin B, nystatin, various detergents, cholera toxin, and theophylline.[2]

In previous studies in our lab and other leading laboratories, Caco-2 cells have been widely used as a model of the small intestine. These cells are human colon carcinoma cells that exhibit the main characteristics of the small intestine: a polarized cell monolayer; tight junctions between cells; microvilli; and enzymes and transporter proteins characteristic of small intestinal enterocytes.[3–5] Interestingly, cell lines derived directly from small intestinal cells fail to produce the polarized monolayer and tight junctions typical of them *in vivo* when cultured *in vitro*.

Because it does express such features, the Caco-2 cell line provides one of the most accurate *in vitro* models of the small intestine, and its use has been widely adopted by the pharmaceutical industry and regulatory agencies as a result of Caco-2 models accurately predicting *in vivo* absorption of a wide range of compounds.[6–10] Although Caco-2 cell monolayers exhibit lower permeability than the small intestine does *in vivo*,[11–13] the observed permeabilities correlate strongly with observed *in vivo* absorption.[6,7] A Caco-2 model may therefore be used to determine expected protein absorption across the small intestine in humans by measurement of the apparent permeability of the protein *in vitro*.

Primarily due to their large size, macromolecules such as protein therapeutics ordinarily display very poor absorption across the small intestinal epithelium. Although there are a select few proteins such as transferrin or various IgA antibodies that are actively transported across the epithelium by receptor-mediated transcytosis, most

proteins will exhibit only 1-10% absorption across the small intestine. Caco-2 studies with insulin, a relatively small protein at only 5.8 kDa molecular weight, have shown only 0.05-0.1% absorption over 3 h (P_{app} = 1.1- 1.6 x 10^{-9} cm/s) across a monolayer in Transwell plates,[14,15] which correlates to negligible absorption across the small intestine *in vivo*.[6,7] Likewise, Youn et al.[16] reported 0.05% of unmodified salmon calcitonin transport across a Caco-2 monolayer in 1 h (P_{app} = 1.5 x 10^{-7} cm/s), which correlates to low absorption *in vivo*, ranging from 0-15%.

Such poor absorption of proteins, even small ones like insulin and salmon calcitonin, across the intestine results in very low bioavailability of orally delivered proteins. Even if a theoretical delivery system achieved perfect release of encapsulated protein in the small intestine, the overall bioavailability would still be capped at 0-15%. At best, 85% of the administered drug would be wasted due to incomplete absorption across the intestinal epithelium into the bloodstream, requiring a prohibitively expensive amount of drug be used to achieve therapeutic effect. As such, the intestinal barrier is a significant barrier to achieving high bioavailability of protein therapeutics delivered via the oral route.

Studies have shown that the primary mode of transport across the intestinal epithelium for unmodified proteins is via paracellular transport through the tight junctions.[17] The overall absorption can therefore be improved by either upregulating the paracellular pathway by opening of the tight junctions or enabling an active transport pathway through the cells. The tight junctions may be disrupted by administration of

detergents or chloride ions, but these can potentially damage the epithelium with repeated administration.

Several studies have shown that P(MAA-g-EG) microparticles can cause reversible opening of the tight junctions, increasing insulin permeability 1.5-fold to 9-fold.[14,15,18–20] In these studies, it has been hypothesized that chelation of Ca^{2+} ions by the anionic hydrogels is responsible for the opening of the tight junctions, especially since the apparent permeability increase is even greater (21-fold) when solutions with low Ca^{2+} concentration are used in the apical chamber.[18] The effect of the microparticles was also seen with salmon calcitonin, ^{14}C-mannitol, fluorescein sodium, and fluorescein isothiocyanate dextran, although the degree of upregulation seemed to be correlated to the presence of PEG chains in the hydrogels rather than the methacrylic acid; this was further shown by the fact that pure PEG nanospheres caused increased permeability while pure PMAA nanospheres did not have such an effect.[21] Because the methacrylic acid is responsible for the anionic charges that would bind Ca^{2+}, these results cast some doubt as to the mechanism of the upregulation, instead demonstrating that some interaction of PEG with the cellular monolayer is instead the mechanism for enhanced permeability.

Indeed, in a study by Carr and Peppas,[22] P(MAA-co-NVP) hydrogels did not cause cellular disruption (as monitored by transepithelial electrical resistance) and did not cause a significant increase in insulin permeability across a Caco-2 cellular monolayer. Therefore, it is likely that the beneficial, reversible opening of the tight junctions associated with use of P(MAA-g-EG) hydrogels is due solely to PEG interaction with the cell layer rather than due to Ca^{2+} binding.

Interestingly, Youn et al.[16] reported no significant change in salmon calcitonin permeability following conjugation with a 2 kDa PEG chain. Although the increased hydrodynamic radius of the conjugate should decrease permeability because of the narrow passage through the tight junctions, the presence of the PEG chain seems to have offset the decrease. It is unusual that the conjugated PEG merely offset the sCT permeability decrease in this study, while the presence of PEG in hydrogel particles enhanced insulin permeability multi-fold in other studies. This could be due to the overall amount of PEG chains or perhaps PEG chain length differences, or any number of other factors; however, the salient point is that PEG seems to have a beneficial effect on the intestinal absorption of proteins.

In this chapter, Caco-2 studies are presented to determine the effects of the hydrogel microparticles and/or PEGylation on the intestinal absorption of salmon calcitonin and Rituxan. Any changes in the intestinal absorption could significantly improve the overall bioavailability of protein therapeutics delivered via the oral route and therefore increase the clinical feasibility of the delivery system. Therefore, it is important to determine what factors are responsible for determining protein transport across the epithelium and obtain an estimate of the possible bioavailability.

7.2 MATERIALS AND METHODS

7.2.1 Caco-2 Cell Culture

Caco-2 human colorectal adenocarcinoma cells (ATCC, Manassas, VA) were cultured normally using Dulbecco's Modified Eagle's Medium (DMEM) (Sigma-

Aldrich, St. Louis, MO) with 10% v/v fetal bovine serum (Hyclone Laboratories, Logan, UT), 1% v/v penicillin-streptomycin (Fisher Scientific, Waltham, MA), and 1% v/v L-glutamine (Mediatech, Manassas, VA) added. Cells were cultured in 75 cm^2 flasks (Fisher Scientific) at 37 °C with 5% CO_2. The cells were passaged once the cells reached 80-90% confluence, involving removal of cells from the flask surface by addition of trypsin in ethylenediaminetetraacetic acid (Sigma-Aldrich) and transfer to a new flask at 3.0 x 10^3 cells/cm^2 seeding density.

7.2.2 Caco-2 Transwell Intestinal Absorption Study

At passage number 55, Caco-2 cells were seeded into Transwell plates (Corning, Tewksbury, MA), as shown in Figure 7-2. All wells contained a 1.12 cm^2 polycarbonate membrane with 0.4 μm mesh size. Cells were seeded on this membrane at a density of 1.0 x 10^5 cells/well, using 0.5 mL of DMEM in each apical chamber and 1.5 mL in each basolateral chamber. Cells were initially allowed to grow for 3 days before the media was changed. Media was then changed every 2 days for a total of 21 days. Over this time, the transepithelial electrical resistance (TEER) was monitored using a chopstick electrode and an ohmmeter to monitor the development of tight junctions within the monolayer.

After 21 days of culture in the Transwell plate, the cell monolayers were used as a model small intestine. The initial TEER of all wells was measured using a chopstick electrode and ohmmeter. Culture media was then removed and all wells were rinsed with Hank's Balanced Salt Solution (HBSS) (Life Technologies, Carlsbad, CA). Bovine

serum albumin (BSA) (Sigma-Aldrich) was dissolved in HBSS at a concentration of 0.5 mg/mL and added to the apical and basolateral chambers of all wells to adsorb to free binding sites on the polystyrene plates. The solution was allowed to incubate for 30 min at 37 °C.

Four solutions using either salmon calcitonin (sCT) (Selleck Chemicals, Houston, TX) or sCT-PEG (prepared and purified as described in Chapter 6) were prepared in BSA/HBSS solution at a concentration of 200 μg/mL, with or without 1 mg/mL of microparticles of the 1:2 P(IA-co-NVP) formulation (prepared and purified as described in Chapter 4). Thus, the four test groups were:

1. sCT only (200 μg/mL) in BSA/HBSS
2. sCT-PEG only (200 μg/mL) in BSA/HBSS
3. sCT (200 μg/mL) in BSA/HBSS + 1:2 P(IA-co-NVP) microparticles (1 mg/mL)
4. sCT-PEG (200 μg/mL) in BSA/HBSS + 1:2 P(IA-co-NVP) microparticles (1 mg/mL)

After the 30 min incubation of BSA/HBSS in the Transwell plates, the BSA/HBSS was removed from the apical chamber of all wells and replaced with 0.5 mL of the test solutions described above (n = 5 per study group). The plates were incubated at 37 °C and 5% CO_2 for 2 h. At time points of t = 0.5, 1, and 2 h, 250 μL samples were taken from the basolateral chamber of all wells and replaced with 250 μL of BSA/HBSS solution. At the end of the 2 h study, the final TEER of all wells was measured. The

concentration of sCT or sCT-PEG absorbed into the basolateral chamber at each time point was determined using a salmon calcitonin EIA kit (Phoenix Pharmaceuticals, Burlingame, CA). The apparent permeability of each well was calculated using Equation 7-1,

$$P_{app} = \frac{V_R}{A \cdot c_0} \frac{dc}{dt} \qquad \text{Equation 7-1}$$

where P_{app} is the apparent permeability coefficient of the protein transported through the Caco-2 monolayer [cm/s], V_R is the volume of the basolateral reservoir [cm^3], A is the surface area of the membrane [cm^2], c_0 is the initial concentration of protein in the apical chamber [ng/mL], and $\frac{dc}{dt}$ is the rate of concentration change in the basolateral chamber [ng/mL-s], calculated as the slope of the best-fit line running through the determined concentrations over the entire 2 h experiment. Student's *t*-test was used to test for group-to-group statistical significance, and ANOVA was used to test for statistical significance between all groups.

7.3 RESULTS AND DISCUSSION

The study described in section 7.2.2 was performed to determine the effects of the presence of PEG and the presence of the P(IA-co-NVP) microparticles on the intestinal absorption of salmon calcitonin. The inconsistent results of previous studies have led to confusion over whether the microparticles have inherent beneficial effects on the

intestinal absorption of proteins due to calcium chelation or whether PEG interacts with the cell layer in some manner, causing the increased permeability.

The study of Torres-Lugo et al.[21] indicated that the presence of PEG causes disruption of the tight junctions, rather than calcium binding by the anionic methacrylic acid residues present in the hydrogel. However, with a diprotic acid monomer like itaconic acid, the hydrogels developed for use with high pI-exhibiting therapeutic proteins may exhibit different Ca^{2+} binding capability than the methacrylic acid-based gels showed. Therefore, this study should provide some indication as to the overall bioavailability possible using the P(IA-co-NVP) hydrogel delivery system without further improvements to the intestinal absorption.

The average apparent permeability (P_{app}) for each study group is reported in Table 7-1. Wide variations in P_{app} were observed within each study group: calculated standard deviations were approximately equal in magnitude to the average values, ranging from 72 – 104% of the average values. As a result, the only statistically significant difference between study groups was between the sCT-PEG with microparticles group and the two groups using unmodified sCT, which was still not quite at the 95% confidence level ($p < 0.052$).

Despite the large standard deviations, the average values of P_{app} reveal an important distinction. The study groups using PEGylated sCT exhibited Caco-2 cell permeability two orders of magnitude greater than the groups using unmodified sCT. All 10 wells in the unmodified sCT groups exhibited apparent permeability on the order of 10^{-9} cm/s, while 7 of 10 wells in the sCT-PEG groups exhibited apparent permeability on

the order of 10^{-7} cm/s. (The other 3 wells were on the order of 10^{-9} cm/s, causing the very wide standard deviations.) Meanwhile, although the average P_{app} increased slightly due to the presence of the microparticles—a 33% increase for sCT groups and a 19% increase for sCT-PEG groups—the difference was not nearly as great as a full two orders of magnitude, and this difference could easily be due solely to intragroup variability rather than a true increase in permeability ($p > 0.70$).

These results therefore support the findings of Torres-Lugo et al.[21] that the presence of PEG causes increased intestinal permeability in Caco-2 cultures, while the presence of anionic hydrogels seems to have negligible effect. Although previous studies did show significantly increased permeability with use of P(MAA-g-EG) microparticles, this study and that of Torres-Lugo et al. demonstrate that the increased permeability is a result of some interaction of PEG with the monolayer rather than a result of the anionic hydrogel binding Ca^{2+} ions as hypothesized in these previous studies. Therefore, use of PEGylated proteins could lead to significantly improved bioavailability via the oral route due to increased intestinal absorption as well as increased half-life.

Furthermore, these results suggest that use of PEG-containing hydrogels may be preferable for enhancing oral protein delivery capability compared to gels with no PEG monomers. As reported in Table 5-1, three IA-based formulations with varying monomer ratios—namely the 1:2 and 1:1 molar monomer ratio formulations of P(IA-co-NVP) and the 45:45:10 P(IA-co-NVP-co-MMA) formulation—outperformed the lone P(IA-g-EG) hydrogel studied in terms of sCT loading and release in *in vitro* conditions. However, because the primary obstacle to oral delivery of therapeutic proteins is intestinal

absorption, the increased permeability resulting from PEG interaction with the cell layer could more than make up for the decreased loading and release efficiency, especially if the increased permeability is over two orders of magnitude as observed with PEGylated sCT in this study.

It is interesting to note that 4 kDa molecular weight PEG alone demonstrates 0% intestinal absorption *in vivo*,[6,7] while 0.9 kDa molecular weight PEG demonstrates 10% intestinal absorption.[7] This shows that the effect of PEG on intestinal absorption is size dependent. Thus, the 2 kDa PEG chain used in the sCT-PEG conjugate seems to enhance absorption, although a larger chain may not have the same effect. The PEG chain length should therefore be a well-controlled variable in the rational design of P(IA-g-EG) hydrogels for enhancing intestinal absorption: hydrogels with high monomer ratios of PEG to itaconic acid and with short PEG chains (~1 kDa) would be expected to demonstrate the best intestinal absorption of the delivered protein. However, the enhancement of intestinal absorption may be offset by reduced loading and release capability, necessitating a holistic study of both facets of the delivery system.

The TEER of all wells was measured before and after the study in order to have a quantified value that is indicative of the permeability of the cell monolayer. The compared average values for all groups are reported in Table 7-1. Prior to the study, there was no significant difference in TEER between groups (p = 0.30), indicating no difference between groups in terms of confluence or permittivity of the tight junctions that would have affected the results of this study. Likewise, after the study, the TEER values did not exhibit statistically significant difference between groups (p = 0.42). The

TEER values, however, did increase in 16 of the 20 studied wells and for all group averages.

TEER does not provide a complete picture of the integrity of the tight junctions since it measures the resistance to ion transport which can occur by paracellular or transcellular pathways and because the molecular bases for ion-selective and size-selective paracellular transport have proven to be distinct.[23–25] Therefore, it is not unexpected that PEGylation yields greater absorption despite the increased size while simultaneously increasing resistance to ion transport. Nevertheless, a significant decrease in the TEER would be expected if the cellular layer was being harmed; thus an increase in TEER that is similar for all groups corroborates the previously described cytotoxicity studies that indicated good biocompatibility with P(IA-co-NVP) microparticles with Caco-2 cells (Chapter 4) and indicates that the interaction between PEG and the monolayer, whatever the mechanism may be, does not cause unusual and potentially dangerous changes to ion-selective permeability of the intestinal epithelium.

The increased apparent permeability in response to the presence of PEG could have a great impact on the feasibility of the overall system. Although Caco-2 permeability tends to correlate well with human *in vivo* intestinal absorption, it is a rough correlation rather than a perfect match. The apparent permeability on the order of 10^{-9} cm/s observed the unmodified protein test groups correlates to *in vivo* absorption on the order of 0-5%, severely limiting the economic feasibility of these delivery systems. However, the 2 order of magnitude increase in apparent permeability observed due to

PEGylation correlates to a wide range of possible *in* vivo absorption, ranging from 15-75% absorption *in vivo*.[6,7,9]

Because of the wide variability in intestinal absorption with compounds within this range of Caco-2 permeability, it is difficult to ascertain the true economic feasibility of the delivery system. Nevertheless, it is clear that the increased permeability observed resulting from PEG will greatly enhance the ability of such delivery systems to reach clinical use. Indeed, even though the 1:2 P(IA-co-NVP) hydrogel formulation showed over 3x better delivery capability of sCT compared to P(IA-g-EG) microparticles, as shown in Table 5-1, if the presence of PEG in the P(IA-g-EG) microparticles results in absorption closer to 75% compared to 5%, the increase in intestinal permeability would clearly yield greater benefit and enable higher, clinically useful bioavailability via the oral route.

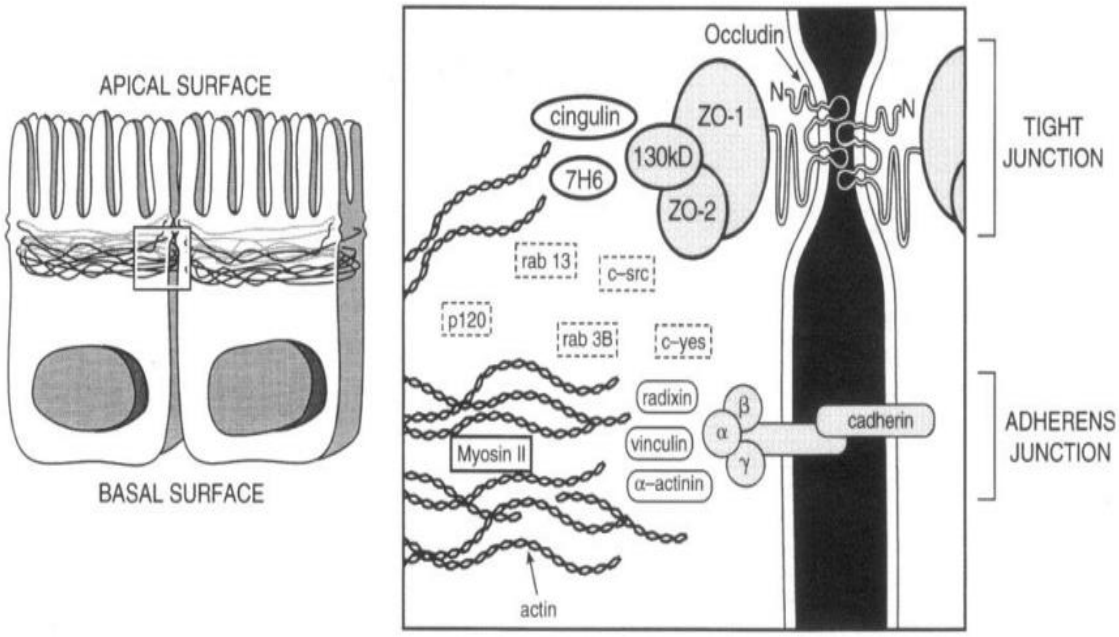

Figure 7-1: Hypothetical Model of Tight Junction and Adherens Junction Between Epithelial Cells. The tight junction is formed by contact of the transmembrane protein occludin with occludin from the neighboring cell. Occludin is bound to zonula occluden-1 (ZO-1) within the cytoplasm. ZO-1 forms a dimer with ZO-2, which binds an uncharacterized 130 kDa protein. The interactions of cingulin and 7H6 antigen are undefined. Adherens junctions are maintained by the transmembrane protein cadherin, which directly associates with cytoplasmic proteins α-, β-, and γ-catenin. Numerous regulatory signaling proteins are localized within the cytoplasm at the adherens junctional complex. Reprinted with permission from Anderson and Van Itallie.[1]

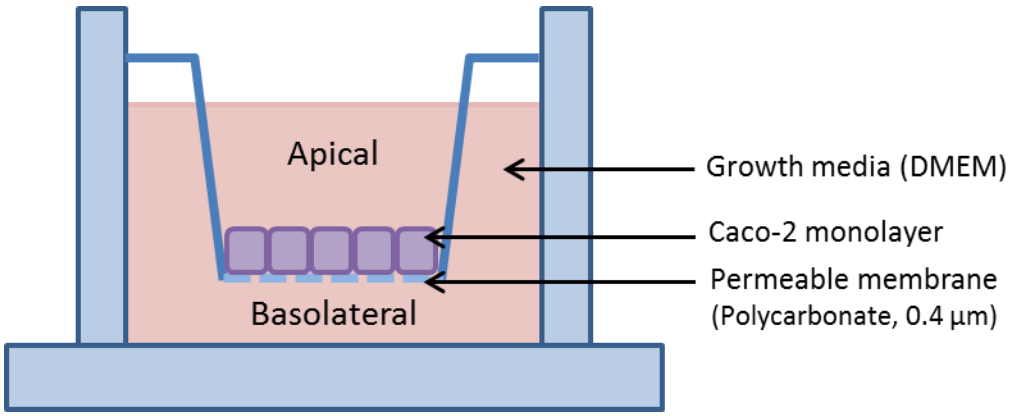

Figure 7-2: Schematic of Caco-2 Transwell Intestinal Absorption Model.

Table 7-1: Caco-2 *In Vitro* Permeability Study. Study comparing apparent permeability of unmodified and PEGylated salmon calcitonin in absence of and presence of 1:2 P(IA-co-NVP) hydrogel microparticles. All values are reported as average ± standard deviation.

Test Group	**Apparent Permeability, P_{app} (x 10^{-9} cm/s)**	**TEER, t = 0 h (Ω-cm^2)**	**TEER, t = 2 h (Ω-cm^2)**
sCT Only	2.71 ± 2.81	554 ± 18	760 ± 123
sCT-PEG Only	221 ± 216	566 ± 85	602 ± 230
sCT + Microparticles	3.60 ± 3.56	590 ± 68	794 ± 164
sCT-PEG + Microparticles	263 ± 189	479 ± 124	668 ± 168

7.4 REFERENCES

(1) Anderson, J. M.; Itallie, C. M. V. Tight Junctions and the Molecular Basis for Regulation of Paracellular Permeability. *Am. J. Physiol. - Gastrointest. Liver Physiol.* **1995**, *269*, G467–G475.

(2) Powell, D. W. Barrier Function of Epithelia. *Am. J. Physiol. - Gastrointest. Liver Physiol.* **1981**, *241*, G275–G288.

(3) Sambuy, Y.; De Angelis, I.; Ranaldi, G.; Scarino, M. L.; Stammati, A.; Zucco, F. The Caco-2 Cell Line as a Model of the Intestinal Barrier: Influence of Cell and Culture-Related Factors on Caco-2 Cell Functional Characteristics. *Cell Biol. Toxicol.* **2005**, *21*, 1–26.

(4) Pinto, M.; Robine-Leon, S.; Appay, M.-D.; Kedinger, M.; Triadou, N.; Dussaulx, E.; Lacroix, B.; Simon-Assmann, P.; Haffen, K.; Fogh, J.; *et al.* Enterocyte-like Differentiation and Polarization of the Human Colon Carcinoma Cell Line Caco-2 in Culture. *Biol. Cell* **1983**, *47*, 323–330.

(5) Hidalgo, I. J.; Raub, T. J.; Borchardt, R. T. Characterization of the Human Colon Carcinoma Cell Line (Caco-2) as a Model System for Intestinal Epithelial Permeability. *Gastroenterology* **1989**, *96*, 736–749.

(6) Artursson, P.; Karlsson, J. Correlation between Oral Drug Absorption in Humans and Apparent Drug Permeability Coefficients in Human Intestinal Epithelial (Caco-2) Cells. *Biochem. Biophys. Res. Commun.* **1991**, *175*, 880–885.

(7) Yee, S. In Vitro Permeability Across Caco-2 Cells (Colonic) Can Predict In Vivo (Small Intestinal) Absorption in Man—Fact or Myth. *Pharm. Res.* **1997**, *14*, 763–766.

(8) Shah, P.; Jogani, V.; Bagchi, T.; Misra, A. Role of Caco-2 Cell Monolayers in Prediction of Intestinal Drug Absorption. *Biotechnol. Prog.* **2006**, *22*, 186–198.

(9) Yamashita, S.; Furubayashi, T.; Kataoka, M.; Sakane, T.; Sezaki, H.; Tokuda, H. Optimized Conditions for Prediction of Intestinal Drug Permeability Using Caco-2 Cells. *Eur. J. Pharm. Sci.* **2000**, *10*, 195–204.

(10) Artursson, P.; Palm, K.; Luthman, K. Caco-2 Monolayers in Experimental and Theoretical Predictions of Drug Transport. *Adv. Drug Deliv. Rev.* **2012**, *64, Supplement*, 280–289.

(11) Artursson, P. Cell Cultures as Models for Drug Absorption across the Intestinal Mucosa. *Crit. Rev. Ther. Drug Carrier Syst.* **1991**, *8*, 305–330.

(12) Lennernäs, H.; Palm, K.; Fagerholm, U.; Artursson, P. Comparison between Active and Passive Drug Transport in Human Intestinal Epithelial (caco-2) Cells in Vitro and Human Jejunum in Vivo. *Int. J. Pharm.* **1996**, *127*, 103–107.

(13) Dantzig, A. H.; Bergin, L. Uptake of the Cephalosporin, Cephalexin, by a Dipeptide Transport Carrier in the Human Intestinal Cell Line, Caco-2. *Biochim. Biophys. Acta BBA - Biomembr.* **1990**, *1027*, 211–217.

(14) Kavimandan, N. J.; Losi, E.; Peppas, N. A. Novel Delivery System Based on Complexation Hydrogels as Delivery Vehicles for Insulin–transferrin Conjugates. *Biomaterials* **2006**, *27*, 3846–3854.

(15) Wood, K. M.; Stone, G. M.; Peppas, N. A. The Effect of Complexation Hydrogels on Insulin Transport in Intestinal Epithelial Cell Models. *Acta Biomater.* **2010**, *6*, 48–56.
(16) Youn, Y. S.; Jung, J. Y.; Oh, S. H.; Yoo, S. D.; Lee, K. C. Improved Intestinal Delivery of Salmon Calcitonin by Lys18-Amine Specific PEGylation: Stability, Permeability, Pharmacokinetic Behavior and in Vivo Hypocalcemic Efficacy. *J. Controlled Release* **2006**, *114*, 334–342.
(17) Kavimandan, N. J.; Peppas, N. A. Confocal Microscopic Analysis of Transport Mechanisms of Insulin across the Cell Monolayer. *Int. J. Pharm.* **2008**, *354*, 143–148.
(18) Ichikawa, H.; Peppas, N. A. Novel Complexation Hydrogels for Oral Peptide Delivery: In Vitro Evaluation of Their Cytocompatibility and Insulin-Transport Enhancing Effects Using Caco-2 Cell Monolayers. *J. Biomed. Mater. Res. A* **2003**, *67A*, 609–617.
(19) Foss, A. C.; Peppas, N. A. Investigation of the Cytotoxicity and Insulin Transport of Acrylic-Based Copolymer Protein Delivery Systems in Contact with Caco-2 Cultures. *Eur. J. Pharm. Biopharm.* **2004**, *57*, 447–455.
(20) López, J. E.; Peppas, N. A. Cellular Evaluation of Insulin Transmucosal Delivery. *J. Biomater. Sci. Polym. Ed.* **2004**, *15*, 385–396.
(21) Torres-Lugo, M.; García, M.; Record, R.; Peppas, N. A. pH-Sensitive Hydrogels as Gastrointestinal Tract Absorption Enhancers: Transport Mechanisms of Salmon Calcitonin and Other Model Molecules Using the Caco-2 Cell Model. *Biotechnol. Prog.* **2002**, *18*, 612–616.
(22) Carr, D. A.; Peppas, N. A. Assessment of Poly(methacrylic Acid-Co-N-Vinyl Pyrrolidone) as a Carrier for the Oral Delivery of Therapeutic Proteins Using Caco-2 and HT29-MTX Cell Lines. *J. Biomed. Mater. Res. A* **2010**, *92A*, 504–512.
(23) Matter, K.; Balda, M. S. Signalling to and from Tight Junctions. *Nat. Rev. Mol. Cell Biol.* **2003**, *4*, 225–237.
(24) Steed, E.; Balda, M. S.; Matter, K. Dynamics and Functions of Tight Junctions. *Trends Cell Biol.* **2010**, *20*, 142–149.
(25) Balda, M. S.; Matter, K. Tight Junctions. *J. Cell Sci.* **1998**, *111*, 541–547.

Chapter 8: Aptamer Selection for Enhancing Intestinal Absorption of Therapeutic Proteins

8.1 INTRODUCTION

As discussed extensively in Chapter 7, the intestinal absorption of protein therapeutics into the bloodstream is the most significant remaining obstacle to effective oral delivery. Typical protein absorption lies in the range of 0-5%, severely limiting the bioavailability of protein therapeutics even with complete release of protein in the small intestine.[1,2] As shown in Chapter 7, the presence of PEG can enhance apparent permeability observed in Caco-2 models by orders of magnitude, raising the expected absorption of salmon calcitonin into a more functional range of 20-75%. However, paracellular transport through the tight junctions is a size-selective process,[3–5] meaning that absorption of larger molecules such as antibodies would remain too insignificant for oral delivery to be financially feasible as a therapeutic delivery option. Therefore, improvements are needed to enhance intestinal absorption to overcome this barrier to clinical treatment options.

Studies with insulin and salmon calcitonin have suggested that the primary method of transport of these proteins across the small intestine is via the paracellular route.[6,7] Transport across the epithelium through the paracellular route is driven by diffusion through the tight junctions. Diffusive processes operate on a relatively slow timescale compared to active transport within the body. Therefore, even with the use of (potentially dangerous) permeation enhancers, the rate of intestinal absorption will be

limited by diffusion kinetics. Utilizing one of the many cellular mechanisms for achieving active, transcellular transport of proteins across the epithelium could greatly enhance both the rate and overall magnitude of intestinal absorption.

An increase in intestinal absorption has previously been demonstrated by conjugation of transferrin to a therapeutic protein.[8–11] Transferrin is an 80 kDa protein that is responsible for regulating the level of iron in the bloodstream. Each transferrin molecule can bind up to two iron (III) ions and undergoes receptor-mediated endocytosis upon binding to a transferrin receptor present on a cell surface. Active cellular transport occurs at a rate that is almost always greater than the rate of diffusive paracellular transport, especially for large molecules that are otherwise prevented from passing through the tight junctions by size exclusion.[12] Therefore, conjugation of a protein therapeutic to transferrin can effectively bypass the barrier of the small intestinal epithelium by hijacking a pathway already present in the body through evolution. In a Caco-2 transport study using an insulin-transferrin conjugate, the apparent permeability of the conjugate proved to be 15x greater than that of the unmodified insulin, despite the significantly increased size of the conjugate.[8]

Although this method presents one means of increasing the achievable bioavailability of orally delivered proteins, the size of the transferrin molecule presents some drawbacks. Primarily, the increased size of the conjugate compared to the unmodified therapeutic will inhibit the protein loading and release capability using the P(IA-co-NVP) hydrogels. As shown in Chapter 5, increased size has a significant impact on the delivery capability of a particular hydrogel formulation because the rate of

diffusion is reduced for a larger solute and the mesh size of the hydrogel must be large enough to accommodate. The negative impact of conjugation with transferrin on delivery can be mitigated by using lower crosslinking density, but the diffusional kinetics will remain slower.

Furthermore, conjugation of a large protein (transferrin) to a smaller protein (e.g., insulin, salmon calcitonin) can potentially inhibit the activity of the therapeutic protein due to steric hindrance.[13] However, this effect can be largely negated by wise choice of crosslinking chemistry: crosslinks made to degrade at some point after endocytosis, such as an acid labile crosslink triggered by the acidic pH shift to pH 5.5 inside the vesicle, can release the protein once active transport has been successfully initiated, leaving the original protein with full functionality.

Finally, it has been shown that transferrin receptors on cell surfaces can saturate, placing an upper limit on the transport rate of protein across the small intestine regardless of the apical dose.[14,15] Although this rate remains significantly faster than the rate of paracellular transport of proteins, there may be other receptors present in the epithelium that achieve a faster rate of delivery, enabling higher bioavailability and higher doses. Furthermore, should receptor saturation occur, having a smaller conjugate that can simultaneously undergo paracellular transport would also be desirable.

In this chapter, work towards developing a smaller, but nevertheless effective ligand for initiating active transcellular transport is presented. Monoclonal antibodies are the current gold standard for binding to target molecules or receptors, but are even larger than transferrin (~144 kDa vs. 80 kDa) and require significant time and skill to develop

and manufacture. Therefore, this work focuses on using aptamers, which are nucleic acid analogues of antibodies, as an auspicious substitute for an antibody.

As described in Chapter 2, aptamers have several advantages over antibodies that make them a strong candidate for this application. First and foremost, by virtue of being easily replicated and amplified *in vitro* through the polymerase chain reaction (PCR), aptamers can be quickly and inexpensively developed through evolutionary techniques that require no explicit knowledge about the target *a priori*. Unlike antibodies, which are typically painstakingly manufactured individually in sufficient quantities using recombinant DNA technology, aptamers can be amplified as a complete library, enabling one single reaction to replicate an enormous variety of sequences. Therefore, by using the SELEX protocol, as seen in Figure 8-1, a researcher can allow nature to determine both the optimal receptor and the optimal sequence to bind to it for maximizing transcellular absorption.[16,17]

Beyond the relatively straightforward discovery process, aptamers also exhibit high specificity and binding, often on the order exhibited by antibodies.[18,19] At the same time, the size of effective aptamers typically range from only 5 – 40 kDa in size, making them significantly smaller than transferrin or antibodies.[19] The reduced size is especially important from an oral delivery perspective, as it benefits the loading and release properties, the rate of diffusion, the probability of paracellular transport, and the activity of the therapeutic following conjugation.

On account of their relatively small size, selective binding capability, and facile discovery and amplification, aptamers were selected using Caco-2 models of the small

intestine in order to develop a suitable ligand for enabling transcellular uptake of protein therapeutics. This chapter describes the selection procedure used, the sequencing of the selected aptamers, and the absorption of the aptamers across the model epithelium.

8.2 MATERIALS AND METHODS

8.2.1 Modified Cellular SELEX Protocol

8.2.1.1 Initial Aptamer Library Preparation

A library of DNA sequences consisting of a twenty-nucleotide random sequence (N_{20}) flanked by forward promoter and reverse promoter sequences was used for the selection process (TriLink Biotechnologies, San Diego, CA). A T7-promoter forward primer was incorporated in the sequence at the 5' end by PCR amplification. Three volumes of CleanAmp PCR master mix (TriLink Biotechnologies) were mixed with one volume each of 20 μM T7-promoter forward primer, 20 μM reverse primer, and 10 μM N_{20}-library. The solution underwent PCR amplification in an Applied Biosystems 2720 thermocycler (Life Technologies, Carlsbad, CA), consisting of: heating at 95 °C for 5 min; 40 thermal cycles of 30 s at 95 °C, 30 s at 55 °C, and 30 s at 72 °C; and finally 10 min at 72 °C. The final reaction mixture was purified of unreacted components using a MinElute PCR purification kit (Qiagen, Valencia, CA). The resulting library, termed the "naïve library," was used as the starting point for selection cycles.

8.2.1.3 In Vitro *Transcription*

The amplified dsDNA library for each selection round was transcribed into 2'-fluorine-modified RNA using the DuraScribe T7 transcription kit (Epicentre, Madison, WI). In brief, 3 volumes of dsDNA, 3 volumes of nuclease-free water, and 2 volumes of each reagent (DuraScribe T7 reaction buffer, 50 mM ATP, 50 mM GTP, 50 mM 2'-F-dCTP, 50 mM 2'-F-dUTP, 100 mM dithiothreitol (DTT), and DuraScribe T7 enzyme mix) were combined and incubated for 4 h at 37 °C. After incubation, DNA was digested by adding 1 volume of DNase I and incubating for 15 min. The resulting RNA library was purified using a miRNeasy purification kit (Qiagen).

8.2.1.4 Cellular Selection

Cellular selection was performed using a Caco-2 Transwell model. Caco-2 cells were seeded and grown in 12-well Transwell plates, as described in section 7.2.2. After at least 21 days of culture in the Transwell plate, the culture media was removed from the transport wells and the wells were washed with Hank's Balanced Salt Solution (HBSS) (Life Technologies). The basolateral chamber was filled with 1.5 HBSS while the apical chamber received 0.5 mL HBSS with the RNA library added at a concentration of 5 μg/mL or greater, uniform across all wells. The wells were incubated for 1.5 h at 37 °C, after which the basolateral solution was collected for quantification and purification using a miRNeasy purification kit.

8.2.1.5 In Vitro *Reverse Transcription*

The selected RNA was reverse transcribed to complementary DNA using SuperScript III reverse transcriptase (Life Technologies). A mixture of 1 volume of 20 μM T7-promoter forward primer, 1 volume of 20 μM reverse primer, 10 volumes of purified RNA, and 1 volume of dNTP mixture (Life Technologies) was heated to 65 °C for 5 min and placed on ice for 1 min. Following this, 4 volumes of SuperScript First-Strand Buffer, 1 volume 0.1 M DTT, and 1 volume of SuperScript III reverse transcriptase were added. The reaction mixture was incubated at 55 °C for 1 h, followed by incubation at 70 °C for 15 min to stop the reaction. The resulting cDNA was purified using a MinElute PCR purification kit.

8.2.1.6 Nucleic Acid Quantification

Following each step in the selection process—PCR amplification, transcription, selection, or reverse transcription—the DNA or RNA was quantified using 2 μL of sample in a Nanodrop 1000 UV-Vis spectrophotometer (Thermo Fisher Scientific, Wilmington, DE). The amount of DNA or RNA was quantified by UV absorbance measurement at 260 nm. Purity was ensured using ratios of absorbances at different characteristic wavelengths, namely the 260/230 and 260/280 ratios.

8.2.1.7 Cycle Repetition

Following reverse transcription and purification, the resulting DNA library functioned as a new starting library for another selection round. The new library was

amplified using the PCR reaction described in section 8.2.1.1 and carried through the entire selection protocol 3 times. A flowchart summarizing the process is shown in Figure 8-2. The selection protocol was carried out in 4 parallel samples ($n = 4$).

8.2.2 Sequencing of Selected Aptamers

8.2.2.1 Sequencing Procedure

After the final selection step, the selected RNA sequences were reverse transcribed to dsDNA and PCR amplified for sequencing. Library preparation and sequencing was performed by the Genomic Sequencing and Analysis Facility at The University of Texas at Austin using standard Illumina library preparation kits and a 2 x 150 MiSeq sequencer (Illumina, San Diego, CA). Selected aptamer libraries and the naïve library were sequenced.

8.2.2.2 Data Analysis

Sequencing data were analyzed using Galaxy (usegalaxy.org).[20–22] The FastQ files containing sequence reads were analyzed using the following workflow. Data quality was ensured using the FastQC quality report tool.[23] Sequence reads containing the expected T7 primer were selected and trimmed to isolate the N_{20} random sequence. The data was converted from FastQ to tabular format,[24] to enable counting of the number of occurrences of each sequence. Finally, the data was sorted to identify the most numerous N_{20} sequence reads. This analysis was performed on the individual selected libraries, the naïve library, and the combined data from all selected aptamer libraries.

8.3 RESULTS AND DISCUSSION

8.3.1 Modified Cellular SELEX Protocol

The *in vitro* selection process was designed to enable the cellular selection of transcellular transport-initiating aptamers with minimal experimentation needed to determine optimal targets. Although many aptamer design studies have been performed, these have used isolated binding targets that are easily separable, such as by immobilization on magnetic beads to enable magnetic separation of bound aptamers from unbound nucleic acids.[25] Using isolated targets has been necessary largely due to the poor stability of nucleic acids in biological systems, thus necessitating a selection environment completely free of nucleases, but requires the researcher to know *a priori* what the desired target is.

By using nucleotides with 2'-fluorine modifications on the pyrimidines, the *in vivo* half-life can be greatly extended,[26] allowing selection to occur directly in a cellular environment without nuclease digestion destroying the aptamers. Similar selection protocols have previously been reported, demonstrating successful use of cellular aptamer selection.[27,28] Applying the systematic evolution protocol within the Caco-2 cellular model should therefore enable discovery of the optimal aptamer sequences for enhancing intestinal absorption, without requiring prior knowledge of the optimal transport receptors for the aptamer to bind. Therefore, the modifications incorporated into this protocol should enable a rapid, yet robust aptamer discovery process that mimics the full complexity of the system.

Furthermore, the use of high throughput sequencing rather than traditional Sanger sequencing greatly benefits the aptamer selection process. Traditionally, SELEX protocols require 10 or more rounds of selection followed by cloning of a small number of sequences to isolate and amplify individual sequences before Sanger sequencing can accurately identify the sequence. However, use of next-generation sequencing (NGS) enables tens of millions of unique sequences to be identified simultaneously, allowing the researcher to analyze the distribution of an entire library within a far faster time frame. As such, applying NGS to the traditional SELEX protocol allows for optimal aptamer sequences to be determined within a few selection rounds rather than 10 or more, greatly reducing the experimental time frame, reducing the chances of identifying sequences most present due to PCR amplification bias rather than optimal binding, and increasing the accuracy with which the library's sequence distribution can be determined.[25,29–38]

The protocol was successfully performed as described, with 4 aptamer libraries undergoing the selection protocol in parallel. Only 3 of the aptamer libraries successfully formed sequencing libraries upon sample preparation; all analysis was carried out using these 3 libraries.

8.3.2 Aptamer Sequencing

The aptamer libraries were successfully sequenced and analyzed as described in section 8.2.2. Table 8-1 shows the total number of sequence reads for each of the individual libraries studied. Each library had over 4 million sequence reads. However, with a 20 nucleotide random sequence, the potential number of sequences is 4^{20}

sequences, or approximately 1.1 trillion possibilities. Therefore, 4 million reads can only cover at most 3.6 x 10^{-4}% of all possible sequences, meaning the expected number of each sequence actually observed in the naïve library is only 1 because the odds of observing that sequence are so low. This is reflected in our samples, as the number of unique sequences is 0.93x as many as the total observed, indicating an average observed copy number of only 1.07. As such, sequences observed more than once in the native library are likely benefitting from PCR bias, where the PCR process amplifies a particular sequence to a greater degree than others due to one of numerous potential factors (e.g., preferable primer or enzyme binding). In an effort to control for PCR bias in the final aptamer libraries, the observed number of aptamers will be compared to the observed number of the same aptamer in the naïve library.

The top 10 most commonly observed N_{20} sequences in the combined aptamer library are shown in Table 8-2, along with the number of instances in each sample set. Although the selected aptamers are RNA molecules, sequencing requires complementary DNA. Therefore, the sequences shown in Table 8-2 are actually the DNA sequences (as observed in the MiSeq results) that will transcribe into the desired RNA aptamers.

As with the naïve library, the expected number of times a particular sequence would be observed in the combined aptamer sequencing data based purely on probability is 0.000015 times. However, despite sheer probability suggesting a particular sequence would not even be observed, the most frequently observed sequence was sequenced 100 times, indicating a significant degree of selection pressure making this sequence so prevalent compared to random chance.

The selection pressure could be due to one of several factors, including improved Caco-2 permeability (as desired), PCR bias, or sequencing bias.[39,40] Unfortunately, sequencing bias cannot be easily controlled because it is inherent to the identification method at the current time. PCR bias is also inherent to the selection process, but can be partially controlled for by comparing the relative number of sequence reads between the selected and naïve libraries. Interestingly, all of the 6 most commonly observed sequences in the aptamer library (and 8 of the top 10) were also observed in the naïve library. Given the low probability of observing a specific sequence in the naïve library, it is likely that these sequences benefitted from either PCR or sequencing bias to make them all appear in the naïve library sequences, most at more than one read.

Nevertheless, the degree to which these sequences are overexpressed is quite significant. After dividing the number of sequences observed in the selected libraries by the count in the naïve library and accounting for the difference in number of total reads, the degree to which these sequences were upregulated was determined. This ratio of the number of observed reads in the aptamer libraries to the number of expected reads based on the naïve library is defined as the "selection ratio." The 6 sequences with the highest selection ratios are shown in Table 8-3, along with the 4 remaining sequences from the 10 most prevalent (Table 8-2) that either were not in the top 6 sequences or did not appear in the naïve library sequence reads.

After correcting for the prevalence in the naïve library, several sequences emerge as potential ligands for further study, such as the sequence GAGTCGTATTACCTGTTCAG with a selection ratio indicating 10-fold upregulation

over the course of the selection protocol. Furthermore, the two sequences that were not observed in the naïve library reads that were in the top 10 most prevalent sequences—ACGTATTACCTGAAAGATCG and GTTGTATTACCTGAAAGATC—are especially interesting. The fact that they were not observed in the naïve library could indicate that they are becoming more prevalent in the sample due entirely to the selection process rather than PCR or sequencing bias, which would have likely shown in the naïve library. Finally, the most prevalent sequence in the aptamer libraries, AGTATTACCTGAAAGATCGG, remains in the top 5 sequences with the highest selection ratio, indicating strong selection preference, despite potential PCR bias. These few sequences are worth studying individually to see if they do in fact aid in intestinal absorption, to what extent, and by what mechanism they achieve selective absorption.

8.3.3 Caco-2 Intestinal Absorption

The nucleic acids were quantified before and after selection in the Caco-2 Transwell model to determine the percent absorption across the cellular monolayer. The percent recovery after each selection round is shown in Figure 8-3. It is interesting to note that each subsequent step in the selection process shows a greater percentage of the aptamer library applied to the apical chamber being absorbed across the Caco-2 monolayer into the basolateral chamber. Furthermore, the increase in absorption is statistically significant ($p < 0.05$) for each subsequent selection round. This trend provides further support for the fundamental hypothesis that the selection process is

driving the aptamer library toward a distribution of sequences that are more adept at transport across the intestinal epithelium by eliminating poorly absorbed sequences.

Given this data, the selection and sequencing processes were quite successful. An initial library containing 1.1 trillion potential sequences was narrowed down to 5-10 sequences that appear to be strong candidates for enabling high bioavailability across the intestinal epithelium. The selection protocol required a minimal number of selection steps and little *a priori* knowledge of the optimal binding targets, yet demonstrated significant improvements in transport across a Caco-2 monolayer over subsequent selection rounds.

Further studies would be needed to fully characterize the identified RNA aptamers. Caco-2 studies using isolated sequences, both with free protein therapeutic and with protein-aptamer conjugates, could better determine if and to what extent these aptamers increase protein absorption, as well as the mechanism for the enhancement. Nevertheless, this work has successfully identified several promising candidate sequences for further study that could provide a relatively low molecular weight (6.6 - 21.3 kDa, depending on if primers are necessary for activity) alternative to transferrin that enables similar or improved levels of protein absorption across the intestinal epithelium.

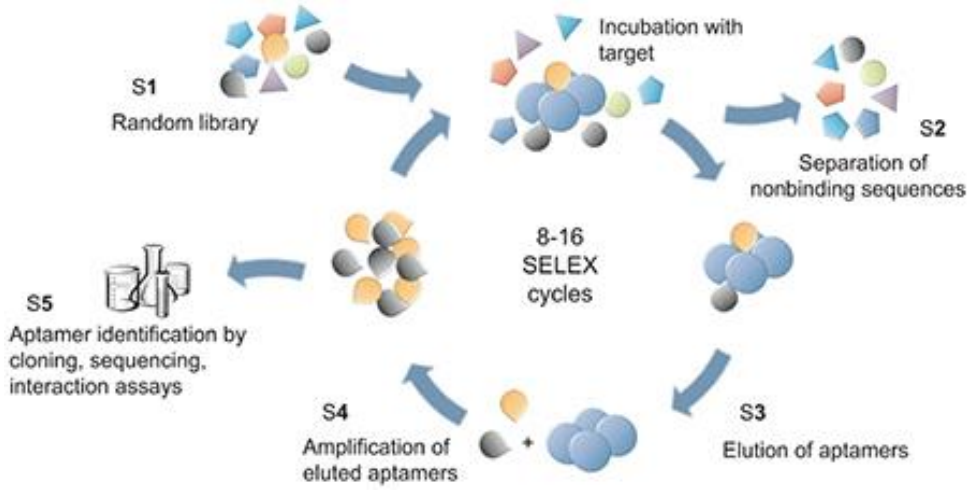

Figure 8-1: Steps of a Typical SELEX Aptamer Selection Protocol. A random library of DNA or RNA molecules (S1) is incubated with a target molecule, and bound complexes are separated from unbound sequences (S2). Bound aptamers are eluted (S3) and amplified by PCR (S4), forming a new library for further evolutionary selection. Following multiple selection cycles, the optimal aptamer sequence(s) are determined by cloning and Sanger sequencing. Reprinted with permission from Blind and Blank, *Mol. Ther. Nucleic Acids*, 2015.[25]

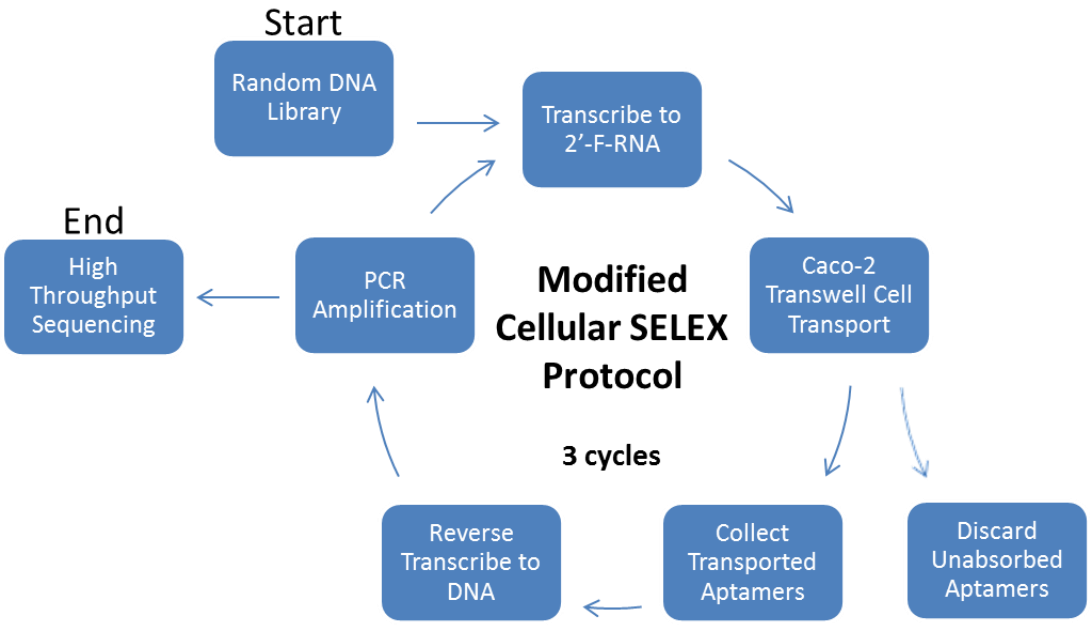

Figure 8-2: Modified Cellular SELEX Protocol. A random library of DNA molecules is transcribed to 2'-fluorine-modified RNA. RNA is incubated in the apical chamber of a Transwell plate with Caco-2 monolayer for 1.5 h and transported sequences are isolated from unabsorbed sequences. The absorbed aptamers are reverse transcribed to DNA and amplified by PCR, forming a new library for further evolutionary selection. Following only 3 selection cycles, the optimal aptamer sequences are determined using high throughput sequencing.

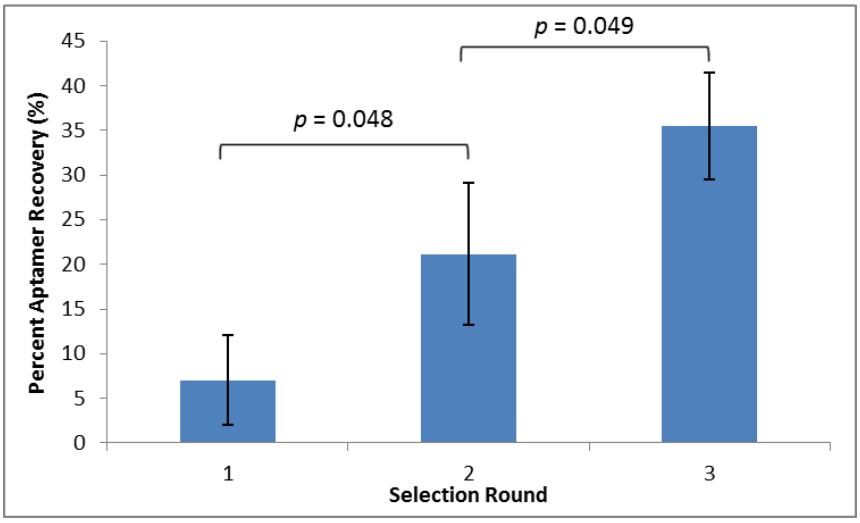

Figure 8-3: Aptamer Absorption in Caco-2 Transwell Model. Percent aptamer absorption was determined after each selection step for $n = 4$ parallel selection libraries using UV-Vis spectrometry. Reported as average ± standard deviation.

Table 8-1: Overview of MiSeq High Throughput Aptamer Sequencing Results.

Library	**Total Sequence Reads (Millions)**	**Total Identified Aptamer Sequences (Millions)**	**Unique Aptamer Sequences (Millions)**
Naïve Library	4.98	1.46	1.37
Aptamer, #1	6.47	2.70	2.52
Aptamer, #2	4.29	1.79	1.67
Aptamer, #3	5.80	2.46	2.26

Table 8-2: Top 10 Most Commonly Sequenced N_{20} Aptamer Sequences. Sequences are named using the DNA sequence read on the MiSeq platform; the actual aptamer sequence is the RNA transcript of the listed sequence. Number of sequence reads are listed as the total occurrences across all three sequenced aptamer libraries, the occurrences within individual libraries, and the occurrences in the naïve DNA library.

DNA N_{20} Sequence	**Number of Sequences Observed**				
	Total, All Aptamers	**Aptamer, #1**	**Aptamer, #2**	**Aptamer, #3**	**Naïve Library**
AGTATTACCTGAAAGATCGG	100	65	14	21	5
TGACTAGTACATGACCACTT	80	36	17	27	12
GTATTACCTGAAAGATCGGA	64	42	10	12	2
TGTATTACCTGAAAGATCGG	59	39	10	10	2
AGATCGGAAGAGCGTCGTGT	37	33	3	1	5
GAGTCGTATTACCTGTTCAG	35	9	9	17	1
ACGTATTACCTGAAAGATCG	33	16	6	11	0
CTCGTATGCCGTCTTCTGCT	32	7	12	13	9
GTTGTATTACCTGAAAGATC	26	15	5	6	0
TCGTATTACCTGAATTCAGG	26	5	6	15	5

Table 8-3: Selection Ratios of Sequenced Aptamers. Sequences are named using the DNA sequence read on the MiSeq platform; the actual aptamer sequence is the RNA transcript of the listed sequence. Selection ratio is defined as number of occurrences of aptamer in selected libraries divided by the number of occurrences expected based on the number of occurrences in the naïve library. Selection ratio rank is numerical rank of sequence by selection ratio as compared to all observed sequences with a defined selection ratio.

DNA N_{20} Sequence	**Number of Sequences Observed**			
	Total, All Aptamers	**Naïve Library**	**Selection Ratio**	**Selection Ratio Rank**
GAGTCGTATTACCTGTTCAG	35	1	10.53	1
GTATTACCTGAAAGATCGGA	64	2	9.62	2
TGTATTACCTGAAAGATCGG	59	2	8.87	3
GAGTCGTATTACCTGAATTC	24	1	7.22	4
AGTATTACCTGAAAGATCGG	100	5	6.01	5
GCGTATTACCTGAAAGATCG	19	1	5.71	6
AGATCGGAAGAGCGTCGTGT	37	5	2.23	22
TGACTAGTACATGACCACTT	80	12	2.00	27
TCGTATTACCTGAATTCAGG	26	5	1.56	37
CTCGTATGCCGTCTTCTGCT	32	9	1.07	55
ACGTATTACCTGAAAGATCG	33	0	Undefined	N/A
GTTGTATTACCTGAAAGATC	26	0	Undefined	N/A

8.4 REFERENCES

(1) Artursson, P.; Karlsson, J. Correlation between Oral Drug Absorption in Humans and Apparent Drug Permeability Coefficients in Human Intestinal Epithelial (Caco-2) Cells. *Biochem. Biophys. Res. Commun.* **1991**, *175*, 880–885.

(2) Yee, S. In Vitro Permeability Across Caco-2 Cells (Colonic) Can Predict In Vivo (Small Intestinal) Absorption in Man—Fact or Myth. *Pharm. Res.* **1997**, *14*, 763–766.

(3) Balda, M. S.; Matter, K. Tight Junctions. *J. Cell Sci.* **1998**, *111*, 541–547.

(4) Matter, K.; Balda, M. S. Signalling to and from Tight Junctions. *Nat. Rev. Mol. Cell Biol.* **2003**, *4*, 225–237.

(5) Steed, E.; Balda, M. S.; Matter, K. Dynamics and Functions of Tight Junctions. *Trends Cell Biol.* **2010**, *20*, 142–149.

(6) Torres-Lugo, M.; García, M.; Record, R.; Peppas, N. A. pH-Sensitive Hydrogels as Gastrointestinal Tract Absorption Enhancers: Transport Mechanisms of Salmon Calcitonin and Other Model Molecules Using the Caco-2 Cell Model. *Biotechnol. Prog.* **2002**, *18*, 612–616.

(7) Kavimandan, N. J.; Peppas, N. A. Confocal Microscopic Analysis of Transport Mechanisms of Insulin across the Cell Monolayer. *Int. J. Pharm.* **2008**, *354*, 143–148.

(8) Kavimandan, N. J.; Losi, E.; Peppas, N. A. Novel Delivery System Based on Complexation Hydrogels as Delivery Vehicles for Insulin–transferrin Conjugates. *Biomaterials* **2006**, *27*, 3846–3854.

(9) Bai, Y.; Ann, D. K.; Shen, W.-C. Recombinant Granulocyte Colony-Stimulating Factor-Transferrin Fusion Protein as an Oral Myelopoietic Agent. *Proc. Natl. Acad. Sci. U. S. A.* **2005**, *102*, 7292–7296.

(10) Shah, D.; Shen, W. Transcellular Delivery of an Insulin-Transferrin Conjugate in Enterocyte-like Caco-2 Cells. *J. Pharm. Sci.* **1996**, *85*, 1306–1311.

(11) Xia, C. Q.; Wang, J.; Shen, W.-C. Hypoglycemic Effect of Insulin-Transferrin Conjugate in Streptozotocin-Induced Diabetic Rats. *J. Pharmacol. Exp. Ther.* **2000**, *295*, 594–600.

(12) Alberts, B.; Johnson, A.; Lewis, J.; Raff, M.; Roberts, K.; Walter, P. Carrier Proteins and Active Membrane Transport. **2002**.

(13) Wu, C.-S.; Lee, C.-C.; Wu, C.-T.; Yang, Y.-S.; Ko, F.-H. Size-Modulated Catalytic Activity of Enzyme–nanoparticle Conjugates: A Combined Kinetic and Theoretical Study. *Chem. Commun.* **2011**, *47*, 7446–7448.

(14) Brewer, E.; Lowman, A. Characterization of Drug Delivery Systems Utilizing Receptor-Mediated Transport. *Bioeng. Conf. NEBEC 201238th Annu. Northeast* **2012**, 105–106.

(15) Brewer, E.; Lowman, A. M. Assessing the Transport of Receptor-Mediated Drug-Delivery Devices across Cellular Monolayers. *J. Biomater. Sci. Polym. Ed.* **2014**, *25*, 455–473.

(16) Tuerk, C.; Gold, L. Systematic Evolution of Ligands by Exponential Enrichment: RNA Ligands to Bacteriophage T4 DNA Polymerase. *Science* **1990**, *249*, 505–510.
(17) Ellington, A. D.; Szostak, J. W. In Vitro Selection of RNA Molecules That Bind Specific Ligands. *Nature* **1990**, *346*, 818–822.
(18) Jayasena, S. D. Aptamers: An Emerging Class of Molecules That Rival Antibodies in Diagnostics. *Clin. Chem.* **1999**, *45*, 1628–1650.
(19) Nimjee, S. M.; Rusconi, C. P.; Sullenger, B. A. Aptamers: An Emerging Class of Therapeutics. *Annu. Rev. Med.* **2005**, *56*, 555–583.
(20) Blankenberg, D.; Von Kuster, G.; Coraor, N.; Ananda, G.; Lazarus, R.; Mangan, M.; Nekrutenko, A.; Taylor, J. Galaxy: A Web-Based Genome Analysis Tool for Experimentalists. In *Current Protocols in Molecular Biology*; John Wiley & Sons, Inc., 2010; pp. 1–21.
(21) Giardine, B.; Riemer, C.; Hardison, R. C.; Burhans, R.; Elnitski, L.; Shah, P.; Zhang, Y.; Blankenberg, D.; Albert, I.; Taylor, J.; *et al.* Galaxy: A Platform for Interactive Large-Scale Genome Analysis. *Genome Res.* **2005**, *15*, 1451–1455.
(22) Goecks, J.; Nekrutenko, A.; Taylor, J.; The Galaxy Team. Galaxy: A Comprehensive Approach for Supporting Accessible, Reproducible, and Transparent Computational Research in the Life Sciences. *Genome Biol.* **2010**, *11*, R86.
(23) Andrews, S. *FastQC A Quality Control Tool for High Throughput Sequence Data*; 2015.
(24) Blankenberg, D.; Gordon, A.; Kuster, G. V.; Coraor, N.; Taylor, J.; Nekrutenko, A.; The Galaxy Team. Manipulation of FASTQ Data with Galaxy. *Bioinformatics* **2010**, *26*, 1783–1785.
(25) Blind, M.; Blank, M. Aptamer Selection Technology and Recent Advances. *Mol. Ther. — Nucleic Acids* **2015**, *4*, e223.
(26) Ulrich, H.; Martins, A. H. B.; Pesquero, J. B. RNA and DNA Aptamers in Cytomics Analysis. *Cytometry A* **2004**, *59A*, 220–231.
(27) Cerchia, L.; Ducongé, F.; Pestourie, C.; Boulay, J.; Aissouni, Y.; Gombert, K.; Tavitian, B.; de Franciscis, V.; Libri, D. Neutralizing Aptamers from Whole-Cell SELEX Inhibit the RET Receptor Tyrosine Kinase. *PLoS Biol* **2005**, *3*, e123.
(28) Thiel, K. W.; Hernandez, L. I.; Dassie, J. P.; Thiel, W. H.; Liu, X.; Stockdale, K. R.; Rothman, A. M.; Hernandez, F. J.; McNamara, J. O.; Giangrande, P. H. Delivery of Chemo-Sensitizing siRNAs to HER2+-Breast Cancer Cells Using RNA Aptamers. *Nucleic Acids Res.* **2012**, *40*, 6319–6337.
(29) Berezhnoy, A.; Stewart, C. A.; Mcnamara Ii, J. O.; Thiel, W.; Giangrande, P.; Trinchieri, G.; Gilboa, E. Isolation and Optimization of Murine IL-10 Receptor Blocking Oligonucleotide Aptamers Using High-Throughput Sequencing. *Mol. Ther.* **2012**, *20*, 1242–1250.
(30) Cho, M.; Xiao, Y.; Nie, J.; Stewart, R.; Csordas, A. T.; Oh, S. S.; Thomson, J. A.; Soh, H. T. Quantitative Selection of DNA Aptamers through Microfluidic Selection and High-Throughput Sequencing. *Proc. Natl. Acad. Sci.* **2010**, *107*, 15373–15378.

(31) Hoon, S.; Zhou, B.; Janda, K. D.; Brenner, S.; Scolnick, J. Aptamer Selection by High-Throughput Sequencing and Informatic Analysis. *BioTechniques* **2011**, *51*, 413–416.
(32) Schütze, T.; Wilhelm, B.; Greiner, N.; Braun, H.; Peter, F.; Mörl, M.; Erdmann, V. A.; Lehrach, H.; Konthur, Z.; Menger, M.; *et al.* Probing the SELEX Process with Next-Generation Sequencing. *PLoS ONE* **2011**, *6*, e29604.
(33) Bayrac, A. T.; Sefah, K.; Parekh, P.; Bayrac, C.; Gulbakan, B.; Oktem, H. A.; Tan, W. In Vitro Selection of DNA Aptamers to Glioblastoma Multiforme. *ACS Chem. Neurosci.* **2011**, *2*, 175–181.
(34) Cho, M.; Oh, S. S.; Nie, J.; Stewart, R.; Eisenstein, M.; Chambers, J.; Marth, J. D.; Walker, F.; Thomson, J. A.; Soh, H. T. Quantitative Selection and Parallel Characterization of Aptamers. *Proc. Natl. Acad. Sci.* **2013**, *110*, 18460–18465.
(35) Ditzler, M. A.; Lange, M. J.; Bose, D.; Bottoms, C. A.; Virkler, K. F.; Sawyer, A. W.; Whatley, A. S.; Spollen, W.; Givan, S. A.; Burke, D. H. High-Throughput Sequence Analysis Reveals Structural Diversity and Improved Potency among RNA Inhibitors of HIV Reverse Transcriptase. *Nucleic Acids Res.* **2013**, *41*, 1873–1884.
(36) Jolma, A.; Kivioja, T.; Toivonen, J.; Cheng, L.; Wei, G.; Enge, M.; Taipale, M.; Vaquerizas, J. M.; Yan, J.; Sillanpää, M. J.; *et al.* Multiplexed Massively Parallel SELEX for Characterization of Human Transcription Factor Binding Specificities. *Genome Res.* **2010**, *20*, 861–873.
(37) Kupakuwana, G. V.; Crill, J. E., II; McPike, M. P.; Borer, P. N. Acyclic Identification of Aptamers for Human Alpha-Thrombin Using Over-Represented Libraries and Deep Sequencing. *PLoS ONE* **2011**, *6*, e19395.
(38) Zimmermann, B.; Bilusic, I.; Lorenz, C.; Schroeder, R. Genomic SELEX: A Discovery Tool for Genomic Aptamers. *Methods* **2010**, *52*, 125–132.
(39) Ross, M. G.; Russ, C.; Costello, M.; Hollinger, A.; Lennon, N. J.; Hegarty, R.; Nusbaum, C.; Jaffe, D. B. Characterizing and Measuring Bias in Sequence Data. *Genome Biol.* **2013**, *14*, R51.
(40) Chen, Y.-C.; Liu, T.; Yu, C.-H.; Chiang, T.-Y.; Hwang, C.-C. Effects of GC Bias in Next-Generation-Sequencing Data on De Novo Genome Assembly. *PLoS ONE* **2013**, *8*, e62856.

Chapter 9: *In Vivo* Evaluation of Oral Protein Delivery Systems

9.1 INTRODUCTION

Significant improvement in high pI protein delivery capability has been demonstrated by using P(IA-co-NVP) hydrogels with a low ionic strength loading solution with high protein concentration. However, these improvements have been demonstrated in idealized, *in vitro* conditions. Because of the comparative complexity of the body, a system that appears to work well for delivering proteins *in vitro* may not actually work well in an *in vivo* setting.

Numerous factors may affect the results seen in the *in vitro* tests: the stomach and intestine have numerous proteins present that could inhibit therapeutic release due to adsorption or electrostatic interactions; the enzymes present in the small intestine could severely limit bioavailability by digesting the released drug; or, the level of absorption of proteins across the intestinal epithelium could differ significantly from what was observed in Caco-2 cultures.

An excellent preclinical method of testing the efficacy of a drug delivery system is to use *in vivo* animal models. An animal model provides the complex environments that the delivery vehicles will experience in a human, including enzymes, bacteria, intestinal mucosa, etc., that could cause large deviations from *in vitro* results. As a result, *in vivo* results are often an unstated necessity before a medical product can begin clinical trials.

In vivo testing of pH-responsive hydrogel microparticles for oral protein delivery has previously been performed in rats using P(MAA-g-EG) hydrogel particles with encapsulated insulin.[1–6] These studies indicated dose-dependent hypoglycemic effects upon administration of insulin-loaded hydrogel particles, with relative bioavailability ranging from 4.2 – 9.5% compared to subcutaneous injection of insulin. All of these studies utilized a closed-loop rat model, wherein drug-loaded hydrogel microparticles were surgically inserted into a sutured section of the rat's small intestine and blood samples were acquired to determine plasma concentrations of insulin and glucose. The closed-loop model for testing intestinal drug perfusion was first described by Doluisio et al. in 1969,[7] and has been used as one of the standard models of the small intestine ever since.[8–15] Correlations to determine absorption rate constants and effective permeability coefficients are available for use with this model, enabling comparison of results between experiments.

9.2 MATERIALS AND METHODS

9.2.1 Drug Loading

Two pH-responsive hydrogel formulations were used in this study. The formulations made with molar monomer ratios of 1:2 P(IA-co-NVP) and 45:45:10 P(IA-co-NVP-co-MMA) demonstrated the highest levels of salmon calcitonin delivery in the *in vitro* testing discussed in Chapter 5 and were therefore used in this experiment. Salmon calcitonin (Selleck Chemicals, Houston, TX) was dissolved in 1.5 mM PBS (0.01x) at a concentration of 0.5 mg/mL. Purified and dried hydrogel microparticles,

sieved to 90-150 μm in size, were added to this solution at a concentration of 2.5 mg/mL. The solution's pH was adjusted to pH 7.2, and the suspension was agitated on a rotary mixer for 24 h. The solution was then acidified to pH 2.5 using 1 N HCl to collapse microparticles. Microparticles were isolated by centrifugation and washed 2 times with 0.01 N HCl (0.2 mL/mg hydrogel) via agitation followed by centrifugation. Protein loading levels were determined by analysis of loading and wash supernatants using a MicroBCA assay (Thermo Scientific Pierce, Rockford, IL).

Doses to be administered to the rats were pre-weighed and stored at 4 °C overnight prior to surgery. Rats receiving P(IA-co-NVP) or P(IA-co-NVP-co-MMA) hydrogel microparticle-delivered salmon calcitonin received doses of 12000 IU/kg with respect to the total encapsulated protein. Rats in the control group received subcutaneous injections of salmon calcitonin dissolved in sterile PBS buffer at doses of 600 IU/kg.

9.2.2 Closed-loop Intestinal Rat Model[2]

Adult, male, Sprague-Dawley rats (Charles River Laboratories, Wilmington, MA) with weights ranging from 328 g to 381 g were studied. Twelve rats were used (n = 4/group) for the study. All rats had jugular catheters for blood draws during the studies. Rats were acclimatized to the research environment for at least 3 days with free access to water and solid food. The rats were then placed on an all-liquid diet of TestDiet LD101 (TestDiet, St. Louis, MO) for 2 days and fasted overnight immediately prior to surgery. The rats were induced and maintained under anesthesia throughout the duration of the

[2] The surgical procedures described in this section were performed by Stephanie Steichen, Lindsey Sharpe, David Spencer, and Sarena Horava. The author monitored anesthesia and assisted with blood draws.

experiment using isoflurane. To maintain body temperature, the rats were placed in a supine position with body drapes on heated-water heating pads maintained at 37 °C.

A closed-loop intestinal perfusion model was used in this study. Experiments were performed in compliance with protocols approved by the Institutional Animal Care and Use Committee at The University of Texas at Austin. An initial blood draw of 150 μL was obtained via the jugular catheter to determine baseline calcitonin levels. An abdominal mid-line incision was then made in each rat, and a 10 cm length of the ileum was isolated and clamped at both ends using silk sutures.

Hydrogel microparticles with encapsulated salmon calcitonin (dosage and trial cohorts are described in section 9.2.1) were dispersed in 0.5 mL PBS (or 0.5 mL PBS for the subcutaneous control group) and injected into the closed-loop intestinal segment by syringe. Rats in the subcutaneous control group received an injection of 0.5 mL PBS into the ileal loop as well as 0.1 mL of salmon calcitonin dissolved in PBS by subcutaneous injection under the animals' neck scruff. Blood samples (150 μL) were withdrawn from the jugular catheter at times of 5, 10, 15, 30, 60, 120, and 180 min following hydrogel administration and replaced with 150 μL of sterile PBS to maintain circulatory volume. Blood samples were immediately centrifuged at 2000 RCF for 15 min to isolate serum and frozen until analyzed by ELISA.

9.2.3 Blood Serum Analysis

Blood serum was isolated by centrifugation and analyzed for salmon calcitonin concentration using a salmon calcitonin ELISA kit (Phoenix Pharmaceuticals, Inc., Burlingame, CA). All samples were assayed in duplicate.

Relative bioavailability was determined using the area under the curve (AUC) for the entire 3 h experiment as compared to the subcutaneous injection control group. AUC was calculated for each rat using numeric integration by the trapezoid rule with concentrations as determined by ELISA. Average AUC and standard deviation were determined for each group, and relative bioavailability of each group was determined using Equation 9-1,

$$F_{rel} = 100\% \cdot \frac{AUC_{hg} \cdot D_{sc}}{AUC_{sc} \cdot D_{hg}} \qquad \text{Equation 9-1}$$

where F_{rel} is the relative bioavailability as compared to subcutaneous injection [%], AUC_{hg} is the AUC calculated for a particular group receiving hydrogel administered sCT [ng-min/mL], AUC_{sc} is the AUC calculated for the group receiving subcutaneous injection, D_{sc} is the subcutaneous dosage administered [IU/kg], and D_{hg} is the dosage administered to the particular group by hydrogel administration. Data is presented as average ± standard deviation. Comparison across groups was performed by analysis of variance (ANOVA), and significant differences were verified with a Student's, unpaired, 2-tailed, heteroscedastic *t*-test.

9.3 RESULTS AND DISCUSSION

A summary of rat weights prior to surgery and the administered doses is provided in Table 9-1. All rats weighed between 328 and 381 g, and no rats displayed significant weight loss prior to surgery. One of the rats to be included in the P(IA-co-NVP-co-MMA) group had a faulty catheter that did not allow for blood draws, and was not included in the data analysis. All other surgeries were successful.

The dosage of salmon calcitonin administered to the control rats (600 IU/kg) was lower than that administered to the rats receiving hydrogel administration (12000 IU/kg). The study was designed with the expectation that relative protein bioavailability would be similar to that observed in previous *in vivo* studies using insulin, around 5%.[1–6] To accommodate the reduced bioavailability observed with oral delivery compared to subcutaneous injection (owing to incomplete release and poor intestinal absorption), a 20x multiple was built into the hydrogel doses so that expected serum protein concentrations would remain within the detectable range of the ELISA kit (0.3 – 100 ng/mL). This correction factor does not prevent accurate determination of relative bioavailability, as it is easily corrected by linear scaling, as seen in the calculation of relative bioavailability (F_{rel}) in Equation 9-1.

Calcitonin was successfully encapsulated in both of the hydrogel formulations. The MicroBCA revealed a high loading level for both groups: 193.8 μg sCT/mg hydrogel in the P(IA-co-NVP) microparticles, and 112.8 μg sCT/mg hydrogel in the P(IA-co-NVP-co-MMA) microparticles. The loading procedure was performed in a relatively large batch compared with the much smaller 1.5 mL batches used in the

loading and release experiments described in Chapter 5. As a result, the pH of the loading solution was more precisely controlled, as larger amounts of acid or base were required to make small changes in the solution pH, which allowed for the improvements in the loading procedure described in Chapter 5 to be fully utilized for maximum effect. In addition, the high loading levels achieved using the same procedure in a larger batch show that the process is scalable and could easily be scaled up to full industrial production.

Following the *in vivo* experiment, blood serum was analyzed by ELISA for salmon calcitonin concentration. The blood serum sCT concentrations for the individual rats (graphed by group) are shown in Figure 9-1 (P(IA-co-NVP)), Figure 9-2 (P(IA-co-NVP-co-MMA)), and Figure 9-3 (subcutaneous injection). Although there are noticeable differences between rats within the study groups, certain trends can be identified. The subcutaneous control group shows an early peak in sCT concentration in serum that rapidly declines back to the base level. This result is expected since the drug is directly injected with little diffusion required to enter the bloodstream, therefore quickly entering circulation in essentially one large dose and declining quickly due to rapid clearance by the reticuloendothelial system. In contrast, the two groups that were administered sCT by hydrogel microparticles in the intestine demonstrated a slower, but sustained increase in sCT concentration over time as compared to the rapid peak seen with the subcutaneous group. Again, this result is expected. The hydrogel administration pathway requires diffusive release from the hydrogel particles and transport across the intestinal epithelium before the protein reaches the bloodstream, which results in a slight lag time before the

concentration increases. Fortunately, this lag time appears to be quite short, with 6 of 7 rats experiencing a 91% increase in plasma sCT levels within 15 min. Furthermore, the hydrogel microparticles act as a drug delivery depot demonstrating sustained release, as protein molecules must travel longer diffusive distances the closer they are to the center of the microparticle, resulting in proteins being released at different times over the course of the experiment, rather than in one single, bolus dose.

The combined results are shown in Figure 9-4 and Table 9-2. Due to the wide variations within test groups, the ANOVA analysis identified only one time point at which statistically significant differences ($p < 0.05$) between groups occurred. Student's *t*-test confirmed that at 15 min after drug administration, the group receiving subcutaneous administration of sCT had significantly higher sCT concentration in serum than both groups receiving sCT encapsulated in P(IA-co-NVP) ($p = 0.022$) and P(IA-co-NVP-co-MMA) ($p = 0.015$). At this early time point, the subcutaneous administration method yields higher sCT concentration due to the more rapid transport into the blood, resulting in an early, large peak in concentration that finds its maximum value at $t = 15$ min. At later times after drug administration, the drug begins to make it into the bloodstream after diffusing out of the microparticles as well, resulting in the hydrogel-administered groups achieving similar sCT levels for the rest of the experiment.

The calculated average AUC for each group is given in Table 9-2. Although the subcutaneous group showed higher sCT serum concentration at early time points, the hydrogels achieved similar concentration levels within 30 min and for the remainder of the experiment. As such, the AUCs are very similar between all groups. The ANOVA

analysis confirms that there is no statistically significant difference among the study groups ($p = 0.89$); pairwise *t*-tests corroborated this result ($p > 0.40$). This result indicates that the developed systems can provide a more convenient alternative to injection-based delivery of protein therapeutics.

The relative bioavailability of sCT delivered by the hydrogels compared to subcutaneous injection is also shown in Table 9-2. Although all groups received similar total amounts of sCT in the bloodstream with similar serum levels at nearly all time points, the relative bioavailability of sCT as administered by the hydrogels remains low at 4.98 ± 3.23% for P(IA-co-NVP) administration and 4.23 ± 1.21% for P(IA-co-NVP-co-MMA) administration. These bioavailabilities are unfortunately low, indicating that the majority of salmon calcitonin administered to the rats is lost due to a combination of enzymatic degradation in the small intestine, incomplete release of protein from the microparticles, and incomplete absorption across the intestinal epithelium. As a result, use of these systems in humans without further improvement would result in increased cost due to the need for larger doses of protein. While such cost will be offset to some degree by eliminating the need for syringes and needles, easing manufacturing requirements, and obviating the need for healthcare professionals to administer the drugs, it is unlikely that such improvements will match the cost of producing 20x as much protein. Thus, for the delivery systems studied in this experiment, financially feasible oral delivery may only be possible for therapeutic proteins that are inexpensive to produce.

Nevertheless, the results of this experiment are still positive. The experiment shows that oral delivery of protein therapeutics exhibiting high isoelectric points is fundamentally feasible with the pH-responsive delivery systems developed herein. Furthermore, the bioavailability observed for salmon calcitonin in this experiment is of the same order of magnitude as that observed for insulin using P(MAA-g-EG) microparticles in previous *in vivo* experiments (4.2 - 9.5%),[1–6] indicating that the improvements made in the pH-responsive material properties and the protein loading procedure described in Chapter 5 have largely overcome the challenges associated with the loading and release of the protein from the hydrogel. If the electrostatic interactions that prevented sufficient protein release in previous studies[16] still dominated over diffusive release of the protein, the bioavailability would be much lower than that observed for a low isoelectric point protein of similar size that demonstrated high levels of protein release in *in vitro* tests. Fortunately, that is not the case.

The results therefore indicate that the remaining obstacle to oral delivery of therapeutic proteins is likely intestinal absorption. From studies of intestinal permeability, proteins are considered to be poorly absorbed compounds with only 0-20% absorption.[17,18] Chemicals with reported Caco-2 permeabilities similar to that of salmon calcitonin (1.5 x 10^{-7}/cm^2)[19] such as 1-deamino-8-D-arginine-vasopressin (1.3 x 10^{-7}/cm^2) or doxorubicin (1.6 x 10-7/cm^2) show 1% and 5% absorption, respectively; therefore, the total absorption is expected to be within this range.[17,18] The observed bioavailability being at the high end of the expected absorption range (4-5%) therefore indicates that the intestinal absorption accounts for the majority of the low bioavailability. With

subsequent improvements enhancing intestinal absorption, such as aptamer-targeted active transport or PEGylation as described in Chapters 7 and 8, this bioavailability can be dramatically enhanced to levels that would enable cost-effective delivery of protein therapeutics via the highly preferred oral route.

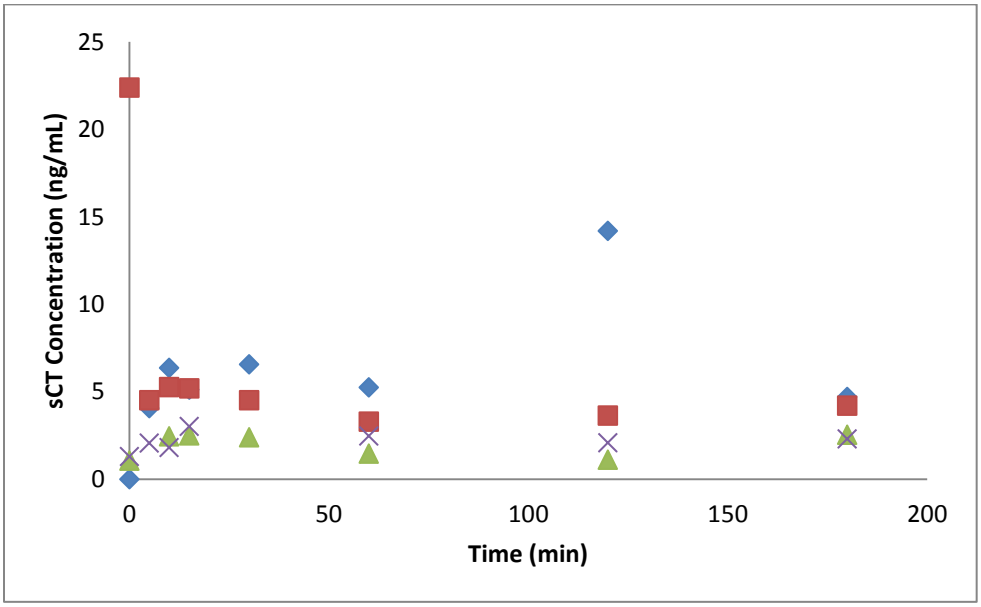

Figure 9-1: Closed-Loop Study—Blood Serum Concentration of Salmon Calcitonin in Rats Receiving Salmon Calcitonin Encapsulated in 1:2 P(IA-co-NVP) Microparticles. Each data series represents a different test subject.

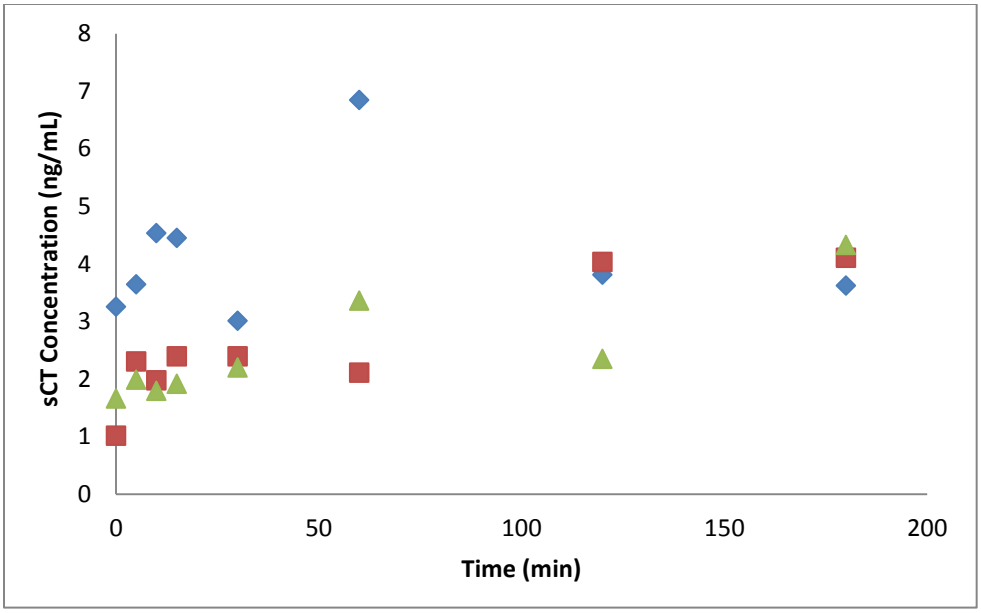

Figure 9-2: Closed-Loop Study—Blood Serum Concentration of Salmon Calcitonin in Rats Receiving Salmon Calcitonin Encapsulated in 45:45:10 P(IA-co-NVP-co-MMA) Microparticles. Each data series represents a different test subject.

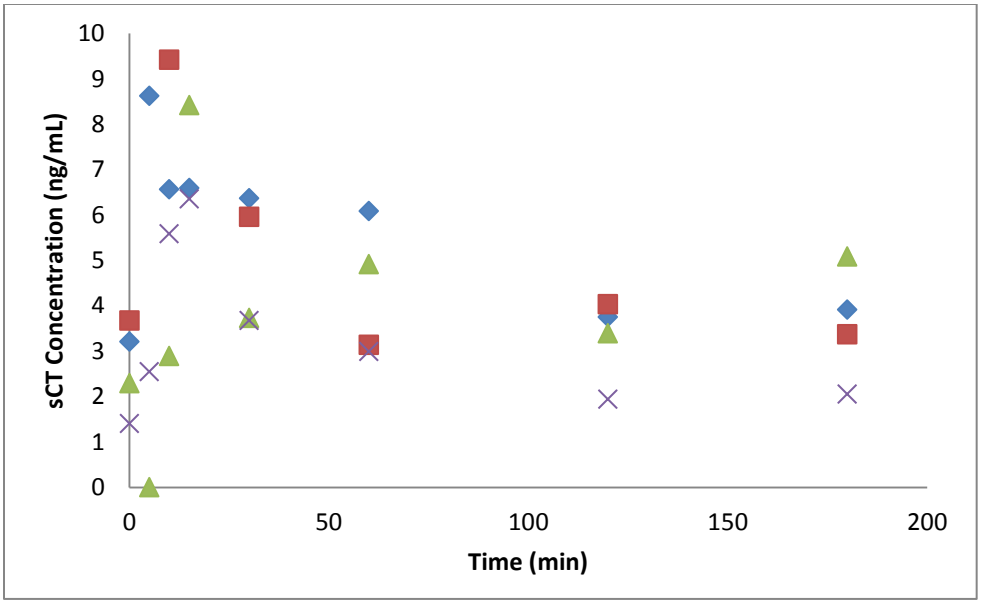

Figure 9-3: Closed-Loop Study—Blood Serum Concentration of Salmon Calcitonin in Rats Receiving Salmon Calcitonin by Subcutaneous Injection. Each data series represents a different test subject.

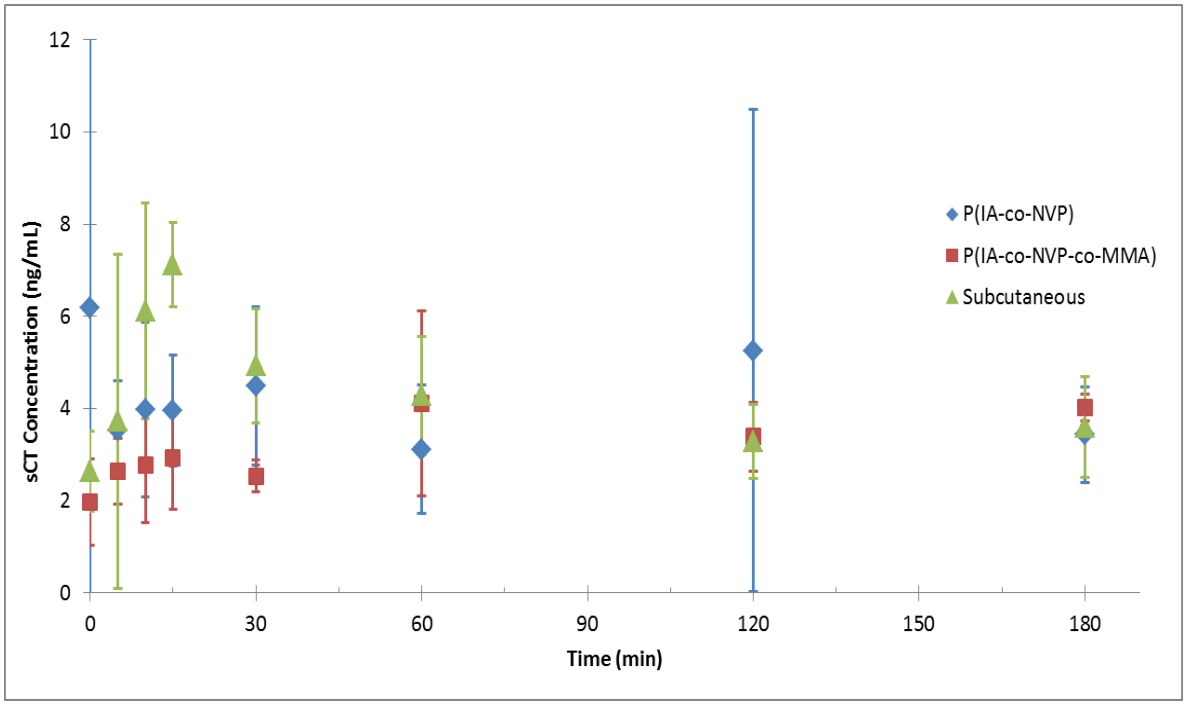

Figure 9-4: Closed-Loop Study Combined Data. Each data series represents a different test group, receiving salmon calcitonin by: 1:2 P(IA-co-NVP) microparticles; 45:45:10 microparticles; or subcutaneous injection. Reported as average ± standard deviation.

Table 9-1: Animal Dosing Summary. Rat weights were recorded 12 h prior to surgery. Salmon calcitonin loading levels were determined by MicroBCA assay.

Rat Test Group, Identifier	Weight, Before Surgery (g)	Dose Level (IU/kg)	sCT Loading Level (μg/mg hydrogel)	Dose Administered (mg hydrogel)
P(IA-co-NVP), #1	328	12000	193.8	3.38
P(IA-co-NVP), #2	363			3.75
P(IA-co-NVP), #3	349			3.60
P(IA-co-NVP), #4	363			3.75
P(IA-co-NVP-co-MMA), #1	352	12000	112.8	6.24
P(IA-co-NVP-co-MMA), #2*	333			5.90
P(IA-co-NVP-co-MMA), #3	371			6.58
P(IA-co-NVP-co-MMA), #4	381			6.76
Subcutaneous, #1	330	600	N/A	33.0 μg sCT
Subcutaneous, #2	332			33.2 μg sCT
Subcutaneous, #3	337			33.7 μg sCT
Subcutaneous, #4	370			37.0 μg sCT

*Rat had non-functioning catheter and was not used in studies.

Table 9-2: *In Vivo* Study Combined Bioavailability Results. All values are reported as average ± standard deviation. Relative bioavailability is normalized to the subcutaneous absorption as 100% relative bioavailability. AUC was determined by numerical integration of individual rats' serum sCT concentration profiles.

Test Group	**Total sCT Absorbed, AUC (ng-min/mL)**	**Relative Bioavailability, F_{rel} (%)**
P(IA-co-NVP)	740 ± 456	4.98 ± 3.23
P(IA-co-NVP-co-MMA)	628 ± 128	4.23 ± 1.21
Subcutaneous	743 ± 149	100 ± 28.3

9.4 REFERENCES

(1) Morishita, M.; Takayama, K.; Nagai, T.; Lowman, A. M.; Peppas, N. A. Application of a pH-Responsive Polymer to an Insulin Oral Dosage Form. *Yakuzaigaku* **1997**, *57*, 96–97.

(2) A. M. Lowman; Nicholas A. Peppas; M. Morishita; T. Nagai. Novel Bioadhesive Complexation Networks for Oral Protein Drug Delivery. In *Tailored Polymeric Materials for Controlled Delivery Systems*; ACS Symposium Series; American Chemical Society, 1998; Vol. 709, pp. 156–164.

(3) Lowman, A. M.; Morishita, M.; Kajita, M.; Nagai, T.; Peppas, N. A. Oral Delivery of Insulin Using pH-Responsive Complexation Gels. *J. Pharm. Sci.* **1999**, *88*, 933–937.

(4) Nakamura, K.; Murray, R. J.; Joseph, J. I.; Peppas, N. A.; Morishita, M.; Lowman, A. M. Oral Insulin Delivery Using P(MAA-G-EG) Hydrogels: Effects of Network Morphology on Insulin Delivery Characteristics. *J. Controlled Release* **2004**, *95*, 589–599.

(5) Morishita, M.; Goto, T.; Nakamura, K.; Lowman, A. M.; Takayama, K.; Peppas, N. A. Novel Oral Insulin Delivery Systems Based on Complexation Polymer Hydrogels: Single and Multiple Administration Studies in Type 1 and 2 Diabetic Rats. *J. Controlled Release* **2006**, *110*, 587–594.

(6) Tuesca, A.; Nakamura, K.; Morishita, M.; Joseph, J.; Peppas, N.; Lowman, A. Complexation Hydrogels for Oral Insulin Delivery: Effects of Polymer Dosing on in Vivo Efficacy. *J. Pharm. Sci.* **2008**, *97*, 2607–2618.

(7) Doluisio, J. T.; Billups, N. F.; Dittert, L. W.; Sugita, E. T.; Swintosky, J. V. Drug Absorption I: An in Situ Rat Gut Technique Yielding Realistic Absorption Rates. *J. Pharm. Sci.* **1969**, *58*, 1196–1200.

(8) Griffin, B.; O'Driscoll, C. Models of the Small Intestine. In *Drug Absorption Studies: In Situ, In Vitro and In Silico Models*; Ehrhardt, C.; Kim, K.-J., Eds.; Biotechnology: Pharmaceutical Aspects; Springer Science & Business Media, 2007; Vol. 7, p. 720.

(9) Chetty, U.; Gilmour, H. M.; Taylor, T. V. Experimental Acute Pancreatitis in the Rat--a New Model. *Gut* **1980**, *21*, 115–117.

(10) Murray, M. J.; Barbose, J. J.; Cobb, C. F. Serum D(-)-Lactate Levels as a Predictor of Acute Intestinal Ischemia in a Rat Model. *J. Surg. Res.* **1993**, *54*, 507–509.

(11) Aldemir, M.; Kökoğlu, Ö. F.; Geyik, M. F.; Büyükbayram, H. Effects of Octreotide Acetate and Saccharomyces Boulardii on Bacterial Translocation in an Experimental Intestinal Loop Obstruction Model of Rats. *Tohoku J. Exp. Med.* **2002**, *198*, 1–9.

(12) Thiagarajah, J. R.; Broadbent, T.; Hsieh, E.; Verkman, A. S. Prevention of Toxin-Induced Intestinal Ion and Fluid Secretion by a Small-Molecule CFTR Inhibitor. *Gastroenterology* **2004**, *126*, 511–519.

(13) Tozaki, H.; Fujita, T.; Odoriba, T.; Terabe, A.; Okabe, S.; Muranishi, S.; Yamamoto, A. Validation of a Pharmacokinetic Model of Colon-Specific Drug

Delivery and the Therapeutic Effects of Chitosan Capsules Containing 5-Aminosalicylic Acid on 2,4,6-Trinitrobenzenesulphonic Acid-Induced Colitis in Rats. *J. Pharm. Pharmacol.* **1999**, *51*, 1107–1112.

(14) Yamamoto, A.; Taniguchi, T.; Rikyuu, K.; Tsuji, T.; Fujita, T.; Murakami, M.; Muranishi, S. Effects of Various Protease Inhibitors on the Intestinal Absorption and Degradation of Insulin in Rats. *Pharm. Res.* **1994**, *11*, 1496–1500.

(15) Pron, B.; Boumaila, C.; Jaubert, F.; Sarnacki, S.; Monnet, J.-P.; Berche, P.; Gaillard, J.-L. Comprehensive Study of the Intestinal Stage of Listeriosis in a Rat Ligated Ileal Loop System. *Infect. Immun.* **1998**, *66*, 747–755.

(16) Carr, D. A.; Gómez-Burgaz, M.; Boudes, M. C.; Peppas, N. A. Complexation Hydrogels for the Oral Delivery of Growth Hormone and Salmon Calcitonin. *Ind. Eng. Chem. Res.* **2010**, *49*, 11991–11995.

(17) Artursson, P.; Karlsson, J. Correlation between Oral Drug Absorption in Humans and Apparent Drug Permeability Coefficients in Human Intestinal Epithelial (Caco-2) Cells. *Biochem. Biophys. Res. Commun.* **1991**, *175*, 880–885.

(18) Yee, S. In Vitro Permeability Across Caco-2 Cells (Colonic) Can Predict In Vivo (Small Intestinal) Absorption in Man—Fact or Myth. *Pharm. Res.* **1997**, *14*, 763–766.

(19) Youn, Y. S.; Jung, J. Y.; Oh, S. H.; Yoo, S. D.; Lee, K. C. Improved Intestinal Delivery of Salmon Calcitonin by Lys18-Amine Specific PEGylation: Stability, Permeability, Pharmacokinetic Behavior and in Vivo Hypocalcemic Efficacy. *J. Controlled Release* **2006**, *114*, 334–342.

Chapter 10: Conclusions

Therapeutic proteins are currently administered predominantly by injection, which significantly reduces patient quality of life due to the associated fear and pain, causing occasional and dangerous non-compliance with treatment. The oral route would significantly improve patient quality of life by providing a more convenient administration pathway, but is difficult to use due to the proteolytic environment of the gastrointestinal tract and poor absorption across the epithelial cell lining of the small intestine.

The overarching goal of this research was to overcome the multiple obstacles preventing the effective delivery of therapeutic proteins, particularly those expressing a high isoelectric point. Many improvements toward this goal were accomplished using a combinatorial approach of redesign of hydrogels, optimization of hydrogel and drug loading parameters, bioconjugation strategies, and discovery of RNA aptamers as ligands to provide transcellular transport capability to enhance protein absorption across the small intestine.

Hydrogels using itaconic acid as the pH-responsive unit rather than methacrylic acid, namely P(IA-co-NVP), P(IA-g-EG), and P(IA-co-NVP-co-MMA), were synthesized and evaluated. Characterization of the hydrogels showed that the hydrogels were well tolerated by Caco-2 cells, showing no significant cytotoxicity or impact on cell proliferation even at high concentrations of 5 mg/mL. Furthermore, itaconic acid-based hydrogels demonstrated significantly enhanced swelling properties at neutral pH

compared to the previously studied P(MAA-co-NVP) hydrogel. All itaconic acid-based hydrogels tested demonstrated greater equilibrium swelling ratios—up to a 69% improvement—and vastly greater dynamic swelling ratios in time-limited experiments—up to a 10-fold improvement—as compared to P(MAA-co-NVP), indicating a faster response and greater swelling, both of which should assist in protein delivery. Thermogravimetric analysis of hydrogels also showed that itaconic acid and methacrylic acid based hydrogels were very thermally stable up to temperatures well beyond what will be experienced in end use.

Calculation of the average mesh sizes within these hydrogels using the best available models indicated very small mesh size at acidic pH, ranging from 0.4 – 1.3 nm, which is sufficiently small to prevent protein transport into or out of the mesh, providing strong protection of the encapsulated proteins. At neutral pH, the mesh size was much larger, ranging from 3.7 to 28.0 nm—large enough for efficient diffusional release of most proteins. Calculated mesh sizes in itaconic acid gels (7.1 – 28.0 nm) were significantly greater than the calculated mesh size in P(MAA-co-NVP) (3.7 nm), indicating improved molecular scale morphology for enhanced delivery.

In *in vitro* loading and release studies, itaconic acid-based hydrogels also performed significantly better than methacrylic acid-based gels. The P(IA-co-NVP) hydrogel formulation prepared using a 1:2 molar ratio of itaconic acid to N-vinylpyrrolidone exhibited the greatest delivery levels of salmon calcitonin, achieving up to 12.4 μg sCT/mg hydrogel drug release within 3 h at neutral conditions—2.7 times more than P(MAA-g-EG) and 16.8 times more than P(MAA-co-NVP) achieved. Charge

localization within the polymer backbone is believed to account for the improved delivery.

The ionic strength of the loading solution was optimized for high isoelectric point exhibiting proteins. Use of a low ionic strength solution for protein imbibition into the hydrogel yielded vast improvements in drug delivery potential of salmon calcitonin. In one trial, 1:2 P(IA-co-NVP) microparticles loaded with sCT in a 1.50 mM PBS buffer loaded and released 83x more sCT per mass of hydrogel than microparticles loaded in a 150 mM PBS buffer. The vast improvement in protein delivery results from increased hydrogel swelling and more favorable electrostatic interactions between the polymer and therapeutic in a low ionic strength medium.

The particle size of the microparticles was found to have little effect on drug delivery within the size ranges studied. Microparticles ranging from 45-75 μm in size exhibited significantly greater percent release of encapsulated sCT compared to microparticles 90-150 μm in size. However, the overall delivery potential was not significantly different between the two hydrogel size ranges. Size effects may manifest at the smaller nano-scale, but were not observed at the micro-scale.

Crosslinking density within the hydrogels was found to significantly affect oral protein delivery capability, and proved to offer a facile method for tuning the hydrogels to accommodate different protein sizes. The small 3.4 kDa protein salmon calcitonin experienced the greatest delivery capability using hydrogels with 5 mol% crosslinker in the monomer feed. On the other hand, the much larger monoclonal antibody, Rituxan (rituximab), experienced the greatest delivery levels using hydrogels with only 1 mol%

crosslinker in the monomer feed. Crosslinking density provides a straightforward method of tuning the mesh size of the hydrogels without altering any of the more fundamental properties of the hydrogel affecting biocompatibility or pK_a. Larger proteins will benefit from low crosslinking density, yielding larger mesh sizes for increased diffusion out of the hydrogel, while smaller proteins benefit from higher crosslinking density, yielding better protection from proteolytic enzymes in the stomach.

Hydrogels formed using enzymatically degradable peptide crosslinks exhibited high specificity for degradation in the small intestine and high delivery capability. P(IA-co-NVP) hydrogels with the MMRRRKK peptide crosslinker exhibited lower loading levels of salmon calcitonin than P(IA-co-NVP) hydrogels with the non-degradable TEGDMA crosslinker, but exhibited complete release of encapsulated protein upon degradation, giving greater overall delivery capability. As such, these systems hold great promise for increasing the bioavailability of orally delivered proteins, although the relatively high cost of the peptide crosslinker may make such systems economically unviable.

PEGylation of therapeutic proteins is a common technique for enhancing solubility and half-life *in vivo*. To study the effect of PEGylation on oral protein delivery, salmon calcitonin was PEGylated and used in *in vitro* loading and release studies. The presence of PEG did not significantly affect the loading level of sCT into 1:2 P(IA-co-NVP) microparticles, but reduced the overall delivery level of the protein by 40.6%. Nevertheless, depending on the protein, the improvements in half-life from PEGylation could more than offset the loss in protein release, which would result in a

more effective therapeutic. Furthermore, the increased size resulting from PEGylation could be readily accommodated by tuning the crosslinking density.

PEGylation also proved to enhance the absorption of salmon calcitonin across a Caco-2 Transwell model of the intestinal epithelium. Unmodified sCT exhibited apparent permeability on the order of 10^{-9} cm/s while sCT-PEG conjugates exhibited apparent permeability on the order of 10^{-7} cm/s—a two order of magnitude improvement that could offer intestinal absorption levels as high as 75%. Microparticles of P(IA-co-NVP) demonstrated insignificant effect on the intestinal absorption. These results indicate that PEG exhibits some interaction with the tight junctions that significantly enhances protein absorption, thus strongly promoting the use of PEG as a conjugate, hydrogel monomer, or co-delivered excipient to help overcome the significant barrier of small intestinal absorption. Some previous studies showed an improvement in perfusion in the presence of P(MAA-g-EG) microparticles, but attributed the improvement to Ca^{2+} binding by the anionic hydrogels. These results demonstrate that the PEG is responsible for the improvement through some interaction with the cells, while Ca^{2+} chelation by the hydrogels plays a minor or negligible role.

Limited absorption of proteins across the intestinal epithelium greatly impedes the ability to achieve high bioavailability by the oral route. PEG proved to enhance the transport across the intestinal epithelium, but there may be more optimal molecules available. A modified SELEX protocol was developed and used in order to systematically reveal aptamer sequences that could significantly promote intestinal perfusion. The modified protocol utilized a Caco-2 Transwell model of the small

intestine as a selection step rather than isolated target molecules, necessitating the use of 2'-fluorine modified nucleotides to resist degradation by nucleases in the cellular environment. Using this model, optimal aptamers for enhancing intestinal absorption could be selected without knowing *a priori* the ideal transport receptors to target.

The aptamer library demonstrated significant improvements in percent absorption of RNA from selection round to selection round ($p < 0.05$), indicating preferential selection of aptamers achieving high transport across the epithelium. High throughput sequencing using an Illumina MiSeq revealed numerous sequences that were significantly upregulated. RNA transcripts of the N_{20} DNA sequences GAGTCGTATTACCTGTTCAG, GTATTACCTGAAAGATCGGA, AGTATTACCTGAAAGATCGG, ACGTATTACCTGAAAGATCG, and GTTGTATTACCTGAAAGATC are especially promising, as these sequences' transcripts achieved selection ratios of up to 10.53 (i.e., 10.53x the number of expected sequences were actually observed). Further studies of these sequences' RNA transcripts are necessary to fully test their intestinal transport enhancement capability. Nevertheless, this experiment was successful as a discovery process by taking a library of 1.1 trillion possible candidate molecules and rapidly identifying a select 5-10 sequences that appear to exhibit enhanced intestinal transport ability.

Finally, two of the hydrogels studied in this work were tested using *in vivo* closed-loop intestinal perfusion studies in rats. The 1:2 P(IA-co-NVP) and P(IA-co-NVP-co-MMA) hydrogels were loaded with salmon calcitonin in a low ionic strength buffer and injected into the small intestine of rats to compare to subcutaneous injection.

The hydrogels demonstrated 4.98% and 4.23% relative bioavailability as compared to the subcutaneous control. These results demonstrate the ability of the hydrogels to achieve therapeutically relevant delivery levels via the oral route despite the complex challenges presented by the gastrointestinal environment. However, the low absorption across the small intestine also highlights the need for methods to overcome the final barrier of absorption across the small intestinal epithelium.

Using the improved design and procedure changes evaluated in this work, hydrogels can be readily tailored to accommodate the oral delivery of a wide variety of high isoelectric point-exhibiting therapeutic proteins. High bioavailability can now be achieved up to the final barrier of crossing the small intestine, and progress toward overcoming this barrier has been made in this work through use of PEG conjugates and discovery of potential aptamers for enhancing protein absorption. Once these strategies are fully explored, it is not unreasonable to believe that the oral delivery of therapeutic proteins will become a reality, leading to a more convenient and less invasive method of treatment for hundreds of millions of patients suffering debilitating diseases worldwide.

Appendix: Dissemination of Research

A.1 PUBLICATIONS

1. **Koetting, M. C.**; Peppas, N. A. pH-Responsive Poly(itaconic Acid-Co-N-Vinylpyrrolidone) Hydrogels with Reduced Ionic Strength Loading Solutions Offer Improved Oral Delivery Potential for High Isoelectric Point-Exhibiting Therapeutic Proteins. *Int. J. Pharm.* **2014**, *471*, 83–91.
2. **Koetting, M. C.**; Peters, J. T.; Steichen, S. D.; Peppas, N. A. Stimulus-Responsive Hydrogels: Theory, Modern Advances, and Applications. *Mater. Sci. Eng. R Rep.* Accepted, In press.

A.2 PATENT

1. **Koetting, M. C.**; Peppas, N. A. Polymers for Delivery of Therapeutic Proteins. Patent pending.

A.3 PRESENTATIONS

1. **Koetting, M. C.**; Guido, J.; Zhang, A.; Peppas, N. A. *Improved Oral Delivery of High Isoelectric Point Therapeutic Proteins using P(IA-co-NVP) Hydrogels*. 2015 BMES Cellular and Molecular Bioengineering Conference, St. Thomas, USVI, **2015** (Poster).
2. **Koetting, M. C.**; Zhang, A.; Peppas, N. A. *pH-Sensitive P(IA-co-NVP) Hydrogels As Oral Delivery Vehicles for High Isoelectric Point-Exhibiting*

Therapeutic Proteins. 2014 AIChE Annual Meeting, Atlanta, GA, **2014** (Oral presentation).

3. **Koetting, M. C.**; Zhang, A.; Peppas, N. A. *pH-Responsive P(IA-co-NVP) Hydrogels for the Oral Delivery of High Isoelectric Point Proteins*. BMES 2014 Annual Meeting, San Antonio, TX, **2014** (Poster).
4. **Koetting, M. C.**; Zhang, A.; Peppas, N. A. *pH-Responsive P(IA-co-NVP) Hydrogels as Vehicles for the Oral Delivery of High Isoelectric Point-Exhibiting Therapeutic Proteins*. Biomaterials Day, College Station, TX, **2014** (Poster).
5. **Koetting, M. C.**; Peppas, N. A. *Stimuli-Responsive Hydrogels for the Oral Delivery of High Isoelectric Point-Exhibiting Therapeutic Proteins*. ACS 2014 National Meeting and Exposition, Dallas, TX, **2014** (Oral presentation).
6. **Koetting, M. C.**; Peppas, N. A. *Improved Release of Salmon Calcitonin from pH-Responsive Hydrogels*. 2013 AAPS Annual Meeting and Exposition, San Antonio, TX, **2013** (Poster).
7. **Koetting, M. C.**; Peppas, N. A. *Oral Delivery of Therapeutic Proteins Exhibiting High Isoelectric Points in pH-Responsive Hydrogels.* AIChE Annual Meeting, San Francisco, CA, **2013** (Oral presentation).
8. **Koetting, M. C.**; Peppas, N. A. *pH-Responsive Hydrogels for Improved Bioavailability of Therapeutic Proteins by Oral Administration.* Biomaterials Day, Austin, TX, **2013** (Poster).

9. **Koetting, M. C.**; Peppas, N. A. *pH-responsive Hydrogels for Oral Delivery of Therapeutic Proteins*. Biomaterials Day, Houston, TX, **2012** (Poster).
10. **Koetting, M. C.**; Peppas, N. A. *pH-responsive Hydrogels for Oral Delivery of Therapeutic Proteins*. 2012 AIChE Annual Meeting, Pittsburgh, PA, **2012** (Oral presentation).
11. Carrillo-Conde, B; **Koetting, M. C.**; Steichen, S. D. *Complexation Hydrogels as Oral Delivery Vehicles of Therapeutic Proteins: Evaluation of Protein Release and Bioactivity*. Society for Biomaterials Fall Symposium, New Orleans, LA, **2012** (Oral, non-presenting contributor).

Bibliography

Listed in order of appearance in entire text. (Citation numbers here may not match in-text citation numbers, which are listed accurately at the end of each chapter.)

(1) Mullard, A. 2012 FDA Drug Approvals. *Nat. Rev. Drug Discov.* **2013**, *12*, 87–90.
(2) *FY 2011 Innovative Drug Approvals*; U.S. Food and Drug Administration, 2012; pp. 1–28.
(3) Dimitrov, D. S. Therapeutic Proteins. In; Voynov, V.; Caravella, J. A., Eds.; Methods in Molecular Biology; Humana Press, 2012.
(4) RNCOS. *Global Protein Therapeutics Market Outlook 2018*; 2014; p. 140.
(5) *Global Protein Therapeutics Market Analysis*; RNCOS, 2011; pp. 1–180.
(6) Drugs.com. Top 100 Drugs for Q4 2013 by Sales - U.S. Pharmaceutical Statistics http://www.drugs.com/stats/top100/sales.
(7) Leader, B.; Baca, Q. J.; Golan, D. E. Protein Therapeutics: A Summary and Pharmacological Classification. *Nat. Rev. Drug Discov.* **2008**, *7*, 21–39.
(8) Hiller, A. Fast Growth Foreseen for Protein Therapeutics. *Genet. Eng. Biotechnol. News* **2009**, *29*, 1–2.
(9) Peyrot, M.; Rubin, R. R.; Kruger, D. F.; Travis, L. B. Correlates of Insulin Injection Omission. *Diabetes Care* **2010**, *33*, 240–245.
(10) Fasano, A. Innovative Strategies for the Oral Delivery of Drugs and Peptides. *Trends Biotechnol.* **1998**, *16*, 152–157.
(11) Morishita, M.; Peppas, N. A. Is the Oral Route Possible for Peptide and Protein Drug Delivery? *Drug Discov. Today* **2006**, *11*, 905–910.
(12) Renukuntla, J.; Vadlapudi, A. D.; Patel, A.; Boddu, S. H. S.; Mitra, A. K. Approaches for Enhancing Oral Bioavailability of Peptides and Proteins. *Int. J. Pharm.* **2013**, *447*, 75–93.
(13) Gupta, S.; Jain, A.; Chakraborty, M.; Sahni, J. K.; Ali, J.; Dang, S. Oral Delivery of Therapeutic Proteins and Peptides: A Review on Recent Developments. *Drug Deliv.* **2013**, *20*, 237–246.
(14) Mojaverian, P.; Vlasses, P. H.; Kellner, P. E.; Jr, M. L. R. Effects of Gender, Posture, and Age on Gastric Residence Time of an Indigestible Solid: Pharmaceutical Considerations. *Pharm. Res.* **1988**, *5*, 639–644.
(15) Dunn, B. M. Overview of Pepsin-like Aspartic Peptidases. In *Current Protocols in Protein Science*; John Wiley & Sons, Inc., 2001.
(16) Cox, M.; Nelson, D. R.; Lehninger, A. L. *Lehninger Principles of Biochemistry*; 5th ed.; W. H. Freeman: San Francisco, 2008.
(17) Fink, A. L.; Calciano, L. J.; Goto, Y.; Kurotsu, T.; Palleros, D. R. Classification of Acid Denaturation of Proteins: Intermediates and Unfolded States. *Biochemistry (Mosc.)* **1994**, *33*, 12504–12511.

(18) Dressman, J. B.; Berardi, R. R.; Dermentzoglou, L. C.; Russell, T. L.; Schmaltz, S. P.; Barnett, J. L.; Jarvenpaa, K. M. Upper Gastrointestinal (GI) pH in Young, Healthy Men and Women. *Pharm. Res.* **1990**, *7*, 756–761.
(19) Rodriguez, J.; Gupta, N.; Smith, R. D.; Pevzner, P. A. Does Trypsin Cut Before Proline? *J. Proteome Res.* **2007**, *7*, 300–305.
(20) Appel, W. Chymotrypsin: Molecular and Catalytic Properties. *Clin. Biochem.* **1986**, *19*, 317–322.
(21) Kavimandan, N. J.; Losi, E.; Peppas, N. A. Novel Delivery System Based on Complexation Hydrogels as Delivery Vehicles for Insulin–transferrin Conjugates. *Biomaterials* **2006**, *27*, 3846–3854.
(22) Jones, E. A.; Waldmann, T. A. The Mechanism of Intestinal Uptake and Transcellular Transport of IgG in the Neonatal Rat. *J. Clin. Invest.* **1972**, *51*, 2916–2927.
(23) Kavimandan, N. J.; Peppas, N. A. Confocal Microscopic Analysis of Transport Mechanisms of Insulin across the Cell Monolayer. *Int. J. Pharm.* **2008**, *354*, 143–148.
(24) Artursson, P.; Karlsson, J. Correlation between Oral Drug Absorption in Humans and Apparent Drug Permeability Coefficients in Human Intestinal Epithelial (Caco-2) Cells. *Biochem. Biophys. Res. Commun.* **1991**, *175*, 880–885.
(25) Yee, S. In Vitro Permeability Across Caco-2 Cells (Colonic) Can Predict In Vivo (Small Intestinal) Absorption in Man—Fact or Myth. *Pharm. Res.* **1997**, *14*, 763–766.
(26) Lowman, A. M.; Morishita, M.; Kajita, M.; Nagai, T.; Peppas, N. A. Oral Delivery of Insulin Using pH-Responsive Complexation Gels. *J. Pharm. Sci.* **1999**, *88*, 933–937.
(27) Carr, D. A.; Gómez-Burgaz, M.; Boudes, M. C.; Peppas, N. A. Complexation Hydrogels for the Oral Delivery of Growth Hormone and Salmon Calcitonin. *Ind. Eng. Chem. Res.* **2010**, *49*, 11991–11995.
(28) Carr, D. A.; Peppas, N. A. Assessment of Poly(methacrylic Acid-Co-N-Vinyl Pyrrolidone) as a Carrier for the Oral Delivery of Therapeutic Proteins Using Caco-2 and HT29-MTX Cell Lines. *J. Biomed. Mater. Res. A* **2010**, *92A*, 504–512.
(29) Foss, A. C.; Peppas, N. A. Investigation of the Cytotoxicity and Insulin Transport of Acrylic-Based Copolymer Protein Delivery Systems in Contact with Caco-2 Cultures. *Eur. J. Pharm. Biopharm.* **2004**, *57*, 447–455.
(30) Kamei, N.; Morishita, M.; Chiba, H.; Kavimandan, N. J.; Peppas, N. A.; Takayama, K. Complexation Hydrogels for Intestinal Delivery of Interferon B and Calcitonin. *J. Controlled Release* **2009**, *134*, 98–102.
(31) Brannon-Peppas, L.; Peppas, N. A. Equilibrium Swelling Behavior of Dilute Ionic Hydrogels in Electrolytic Solutions. *J. Controlled Release* **1991**, *16*, 319–329.

(32) López, J. E.; Peppas, N. A. Effect of Poly (Ethylene Glycol) Molecular Weight and Microparticle Size on Oral Insulin Delivery from P(MAA-g-EG) Microparticles. *Drug Dev. Ind. Pharm.* **2004**, *30*, 497–504.
(33) Morishita, M.; Goto, T.; Takayama, K.; Peppas, N. A. Oral Insulin Delivery Systems Based on Complexation Polymer Hydrogels. *J. Drug Deliv. Sci. Technol.* **2006**, *16*, 19–24.
(34) Tuesca, A.; Nakamura, K.; Morishita, M.; Joseph, J.; Peppas, N.; Lowman, A. Complexation Hydrogels for Oral Insulin Delivery: Effects of Polymer Dosing on in Vivo Efficacy. *J. Pharm. Sci.* **2008**, *97*, 2607–2618.
(35) Knox, C.; Law, V.; Jewison, T.; Liu, P.; Ly, S.; Frolkis, A.; Pon, A.; Banco, K.; Mak, C.; Neveu, V.; *et al.* DrugBank 3.0: A Comprehensive Resource for "Omics" Research on Drugs. *Nucleic Acids Res.* **2011**, *39*, D1035–D1041.
(36) Wu, S.; Wan, P.; Li, J.; Li, D.; Zhu, Y.; He, F. Multi-Modality of pI Distribution in Whole Proteome. *Proteomics* **2006**, *6*, 449–455.
(37) Torres-Lugo, M.; Peppas, N. A. Molecular Design and in Vitro Studies of Novel pH-Sensitive Hydrogels for the Oral Delivery of Calcitonin. *Macromolecules* **1999**, *32*, 6646–6651.
(38) Dressman, J. B.; Krämer, J. *Pharmaceutical Dissolution Testing*; Taylor & Francis: Boca Raton, FL, 2005.
(39) Roberts, M. J.; Bentley, M. D.; Harris, J. M. Chemistry for Peptide and Protein PEGylation. *Adv. Drug Deliv. Rev.* **2012**, *64, Supplement*, 116–127.
(40) Veronese, F. M. Peptide and Protein PEGylation: A Review of Problems and Solutions. *Biomaterials* **2001**, *22*, 405–417.
(41) Veronese, F. M.; Pasut, G. PEGylation, Successful Approach to Drug Delivery. *Drug Discov. Today* **2005**, *10*, 1451–1458.
(42) Jevševar, S.; Kunstelj, M.; Porekar, V. G. PEGylation of Therapeutic Proteins. *Biotechnol. J.* **2010**, *5*, 113–128.
(43) Harris, J. M.; Chess, R. B. Effect of Pegylation on Pharmaceuticals. *Nat. Rev. Drug Discov.* **2003**, *2*, 214–221.
(44) Harris, D. J. M.; Martin, N. E.; Modi, M. Pegylation. *Clin. Pharmacokinet.* **2012**, *40*, 539–551.
(45) Owens III, D. E.; Peppas, N. A. Opsonization, Biodistribution, and Pharmacokinetics of Polymeric Nanoparticles. *Int. J. Pharm.* **2006**, *307*, 93–102.
(46) Aggarwal, P.; Hall, J. B.; McLeland, C. B.; Dobrovolskaia, M. A.; McNeil, S. E. Nanoparticle Interaction with Plasma Proteins as It Relates to Particle Biodistribution, Biocompatibility and Therapeutic Efficacy. *Adv. Drug Deliv. Rev.* **2009**, *61*, 428–437.
(47) Youn, Y. S.; Jung, J. Y.; Oh, S. H.; Yoo, S. D.; Lee, K. C. Improved Intestinal Delivery of Salmon Calcitonin by Lys18-Amine Specific PEGylation: Stability, Permeability, Pharmacokinetic Behavior and in Vivo Hypocalcemic Efficacy. *J. Controlled Release* **2006**, *114*, 334–342.
(48) Gorochovceva, N.; Makuška, R. Synthesis and Study of Water-Soluble Chitosan-O-Poly(ethylene Glycol) Graft Copolymers. *Eur. Polym. J.* **2004**, *40*, 685–691.

(49) Toncheva, V.; Wolfert, M. A.; Dash, P. R.; Oupicky, D.; Ulbrich, K.; Seymour, L. W.; Schacht, E. H. Novel Vectors for Gene Delivery Formed by Self-Assembly of DNA with Poly(l-Lysine) Grafted with Hydrophilic Polymers. *Biochim. Biophys. Acta BBA - Gen. Subj.* **1998**, *1380*, 354–368.
(50) Nguyen, H.-K.; Lemieux, P.; Vinogradov, S. V.; Gebhart, C. L.; Guérin, N.; Paradis, G.; Bronich, T. K.; Alakhov, V. Y.; Kabanov, A. V. Evaluation of Polyether-Polyethyleneimine Graft Copolymers as Gene Transfer Agents. *Gene Ther.* **2000**, *7*, 126–138.
(51) Abuchowski, A.; McCoy, J. R.; Palczuk, N. C.; Es, T. van; Davis, F. F. Effect of Covalent Attachment of Polyethylene Glycol on Immunogenicity and Circulating Life of Bovine Liver Catalase. *J. Biol. Chem.* **1977**, *252*, 3582–3586.
(52) Staros, J. V.; Wright, R. W.; Swingle, D. M. Enhancement by N-Hydroxysulfosuccinimide of Water-Soluble Carbodiimide-Mediated Coupling Reactions. *Anal. Biochem.* **1986**, *156*, 220–222.
(53) Grabarek, Z.; Gergely, J. Zero-Length Crosslinking Procedure with the Use of Active Esters. *Anal. Biochem.* **1990**, *185*, 131–135.
(54) Sehgal, D.; Vijay, I. K. A Method for the High Efficiency of Water-Soluble Carbodiimide-Mediated Amidation. *Anal. Biochem.* **1994**, *218*, 87–91.
(55) Nakajima, N.; Ikada, Y. Mechanism of Amide Formation by Carbodiimide for Bioconjugation in Aqueous Media. *Bioconjug. Chem.* **1995**, *6*, 123–130.
(56) Pierce Protein Biology Products. Carbodiimide Crosslinker Chemistry http://www.piercenet.com/method/carbodiimide-crosslinker-chemistry (accessed Jan 22, 2015).
(57) Hermanson, G. T. *Bioconjugate Techniques*; Academic press, 2013.
(58) King, J. L.; Jukes, T. H. Non-Darwinian Evolution. *Science* **1969**, *164*, 788–798.
(59) Arkov, A. L.; Korolev, S. V.; Kisselev, L. L. Termination of Translation in Bacteria May Be Modulated via Specific Interaction between Peptide Chain Release Factor 2 and the Last Peptidyl-tRNASer/Phe. *Nucleic Acids Res.* **1993**, *21*, 2891–2897.
(60) Alff-Steinberger, C.; Epstein, R. Codon Preference in the Terminal Region of E. Coli Genes and Evolution of Stop Codon Usage. *J. Theor. Biol.* **1994**, *168*, 461–463.
(61) Arkov, A. L.; Korolev, S. V.; Kisslev, L. L. 5′ Contexts of Escherichia Coli and Human Termination Codons Are Similar. *Nucleic Acids Res.* **1995**, *23*, 4712–4716.
(62) Berezovsky, I. N.; Kilosanidze, G. T.; Tumanyan, V. G.; Kisselev, L. L. Amino Acid Composition of Protein Termini Are Biased in Different Manners. *Protein Eng.* **1999**, *12*, 23–30.
(63) DePristo, M. A.; Zilversmit, M. M.; Hartl, D. L. On the Abundance, Amino Acid Composition, and Evolutionary Dynamics of Low-Complexity Regions in Proteins. *Gene* **2006**, *378*, 19–30.

(64) Fahey, R. C.; Hunt, J. S.; Windham, G. C. On the Cysteine and Cystine Content of Proteins. Differences between Intracellular and Extracellular Proteins. *J. Mol. Evol.* **1977**, *10*, 155–160.
(65) Pierce Protein Biology Products. Protein Crosslinking Applications http://www.piercenet.com/method/crosslinking-applications#proteindna (accessed Jan 22, 2015).
(66) Ghosh, S. S.; Kao, P. M.; McCue, A. W.; Chappelle, H. L. Use of Maleimide-Thiol Coupling Chemistry for Efficient Syntheses of Oligonucleotide-Enzyme Conjugate Hybridization Probes. *Bioconjug. Chem.* **1990**, *1*, 71–76.
(67) Brinkley, M. A Brief Survey of Methods for Preparing Protein Conjugates with Dyes, Haptens and Crosslinking Reagents. *Bioconjug. Chem.* **1992**, *3*, 2–13.
(68) Smyth, D. G.; Blumenfeld, O. O.; Konigsberg, W. Reactions of N-Ethylmaleimide with Peptides and Amino Acids. *Biochem. J.* **1964**, *91*, 589–595.
(69) Gorin, G.; Martic, P. A.; Doughty, G. Kinetics of the Reaction of N-Ethylmaleimide with Cysteine and Some Congeners. *Arch. Biochem. Biophys.* **1966**, *115*, 593–597.
(70) Heitz, J. R.; Anderson, C. D.; Anderson, B. M. Inactivation of Yeast Alcohol Dehydrogenase by N-Alkylmaleimides. *Arch. Biochem. Biophys.* **1968**, *127*, 627–636.
(71) Partis, M. D.; Griffiths, D. G.; Roberts, G. C.; Beechey, R. B. Cross-Linking of Protein by Ω-Maleimido Alkanoyl N-Hydroxysuccinimido Esters. *J. Protein Chem.* **1983**, *2*, 263–277.
(72) Brewer, C. F.; Riehm, J. P. Evidence for Possible Nonspecific Reactions between N-Ethylmaleimide and Proteins. *Anal. Biochem.* **1967**, *18*, 248–255.
(73) Hogg, P. J. Disulfide Bonds as Switches for Protein Function. *Trends Biochem. Sci.* **2003**, *28*, 210–214.
(74) Gorman, J. J.; Corino, G. L.; Mitchell, S. J. Fluorescent Labeling of Cysteinyl Residues. *Eur. J. Biochem.* **1987**, *168*, 169–179.
(75) Jones, M. W.; Strickland, R. A.; Schumacher, F. F.; Caddick, S.; Baker, J. R.; Gibson, M. I.; Haddleton, D. M. Polymeric Dibromomaleimides As Extremely Efficient Disulfide Bridging Bioconjugation and Pegylation Agents. *J. Am. Chem. Soc.* **2012**, *134*, 1847–1852.
(76) Smith, M. E. B.; Schumacher, F. F.; Ryan, C. P.; Tedaldi, L. M.; Papaioannou, D.; Waksman, G.; Caddick, S.; Baker, J. R. Protein Modification, Bioconjugation, and Disulfide Bridging Using Bromomaleimides. *J. Am. Chem. Soc.* **2010**, *132*, 1960–1965.
(77) Tedaldi, L. M.; Smith, M. E. B.; Nathani, R. I.; Baker, J. R. Bromomaleimides: New Reagents for the Selective and Reversible Modification of Cysteine. *Chem. Commun.* **2009**, 6583–6585.
(78) Jayasena, S. D. Aptamers: An Emerging Class of Molecules That Rival Antibodies in Diagnostics. *Clin. Chem.* **1999**, *45*, 1628–1650.
(79) Nimjee, S. M.; Rusconi, C. P.; Sullenger, B. A. Aptamers: An Emerging Class of Therapeutics. *Annu. Rev. Med.* **2005**, *56*, 555–583.

(80) Tuerk, C.; Gold, L. Systematic Evolution of Ligands by Exponential Enrichment: RNA Ligands to Bacteriophage T4 DNA Polymerase. *Science* **1990**, *249*, 505–510.
(81) Ellington, A. D.; Szostak, J. W. In Vitro Selection of RNA Molecules That Bind Specific Ligands. *Nature* **1990**, *346*, 818–822.
(82) Klug, S. J.; Famulok, M. All You Wanted to Know about SELEX. *Mol. Biol. Rep.* **1994**, *20*, 97–107.
(83) Stoltenburg, R.; Reinemann, C.; Strehlitz, B. SELEX—A (r)evolutionary Method to Generate High-Affinity Nucleic Acid Ligands. *Biomol. Eng.* **2007**, *24*, 381–403.
(84) Shamah, S. M.; Healy, J. M.; Cload, S. T. Complex Target SELEX. *Acc. Chem. Res.* **2008**, *41*, 130–138.
(85) Ulrich, H.; Martins, A. H. B.; Pesquero, J. B. RNA and DNA Aptamers in Cytomics Analysis. *Cytometry A* **2004**, *59A*, 220–231.
(86) Lin, Y.; Qiu, Q.; Gill, S. C.; Jayasena, S. D. Modified RNA Sequence Pools for in Vitro Selection. *Nucleic Acids Res.* **1994**, *22*, 5229–5234.
(87) Pagratis, N. C.; Bell, C.; Chang, Y.-F.; Jennings, S.; Fitzwater, T.; Jellinek, D.; Dang, C. Potent 2′-Amino-, and 2′-Fluoro-2′- Deoxyribonucleotide RNA Inhibitors of Keratinocyte Growth Factor. *Nat. Biotechnol.* **1997**, *15*, 68–73.
(88) Eulberg, D.; Klussmann, S. Spiegelmers: Biostable Aptamers. *ChemBioChem* **2003**, *4*, 979–983.
(89) Klußmann, S.; Nolte, A.; Bald, R.; Erdmann, V. A.; Fürste, J. P. Mirror-Image RNA That Binds D-Adenosine. *Nat. Biotechnol.* **1996**, *14*, 1112–1115.
(90) Nolte, A.; Klußmann, S.; Bald, R.; Erdmann, V. A.; Fürste, J. P. Mirror-Design of L-Oligonucleotide Ligands Binding to L-Arginine. *Nat. Biotechnol.* **1996**, *14*, 1116–1119.
(91) Wieland, M.; Benz, A.; Klauser, B.; Hartig, J. S. Artificial Ribozyme Switches Containing Natural Riboswitch Aptamer Domains. *Angew. Chem.* **2009**, *121*, 2753–2756.
(92) Lamm, M. E. Current Concepts in Mucosal Immunity. IV. How Epithelial Transport of IgA Antibodies Relates to Host Defense. *Am. J. Physiol. - Gastrointest. Liver Physiol.* **1998**, *274*, G614–G617.
(93) Brewer, E.; Lowman, A. Characterization of Drug Delivery Systems Utilizing Receptor-Mediated Transport. *Bioeng. Conf. NEBEC 201238th Annu. Northeast* **2012**, 105–106.
(94) Fisher, O. Z.; Peppas, N. A. Quantifying Tight Junction Disruption Caused by Biomimetic pH-Sensitive Hydrogel Drug Carriers. *J. Drug Deliv. Sci. Technol.* **2008**, *18*, 47–50.
(95) Madsen, F.; Peppas, N. A. Complexation Graft Copolymer Networks: Swelling Properties, Calcium Binding and Proteolytic Enzyme Inhibition. *Biomaterials* **1999**, *20*, 1701–1708.
(96) Ichikawa, H.; Peppas, N. A. Novel Complexation Hydrogels for Oral Peptide Delivery: In Vitro Evaluation of Their Cytocompatibility and Insulin-Transport

Enhancing Effects Using Caco-2 Cell Monolayers. *J. Biomed. Mater. Res. A* **2003**, *67A*, 609–617.
(97) Blanchette, J.; Kavimandan, N.; Peppas, N. A. Principles of Transmucosal Delivery of Therapeutic Agents. *Biomed. Pharmacother.* **2004**, *58*, 142–151.
(98) Koetting, M. C.; Peppas, N. A. pH-Responsive Poly(itaconic Acid-Co-N-Vinylpyrrolidone) Hydrogels with Reduced Ionic Strength Loading Solutions Offer Improved Oral Delivery Potential for High Isoelectric Point-Exhibiting Therapeutic Proteins. *Int. J. Pharm.* **2014**, *471*, 83–91.
(99) Peppas, N. A.; Bures, P.; Leobandung, W.; Ichikawa, H. Hydrogels in Pharmaceutical Formulations. *Eur. J. Pharm. Biopharm.* **2000**, *50*, 27–46.
(100) Yong Qiu; Kinam Park. Environment-Sensitive Hydrogels for Drug Delivery. *Adv. Drug Deliv. Rev.* **2001**, *53*, 321–339.
(101) Allan S Hoffman. Stimuli-Responsive Polymers: Biomedical Applications and Challenges for Clinical Translation. *Adv. Mater.* **2013**, *65*, 10–16.
(102) Horbett, T. A.; Ratner, B. D.; Kost, J.; Singh, M. A Bioresponsive Membrane for Insulin Delivery. In *Recent Advances in Drug Delivery Systems*; Anderson, J. M.; Kim, S. W., Eds.; Springer US, 1984; pp. 209–220.
(103) Horbett, T. A.; Kost, J.; Ratner, B. D. Swelling Behavior of Glucose Sensitive Membranes. In *Polymers as Biomaterials*; Shalaby, S. W.; Hoffman, A. S.; Ratner, B. D.; Horbett, T. A., Eds.; Springer US, 1984; pp. 193–207.
(104) Albin, G.; Horbett, T. A.; Ratner, B. D. Glucose Sensitive Membranes for Controlled Delivery of Insulin: Insulin Transport Studies. *J. Controlled Release* **1985**, *2*, 153–164.
(105) Betancourt, T.; Pardo, J.; Soo, K.; Peppas, N. A. Characterization of pH-Responsive Hydrogels of Poly(itaconic Acid-G-Ethylene Glycol) Prepared by UV-Initiated Free Radical Polymerization as Biomaterials for Oral Delivery of Bioactive Agents. *J. Biomed. Mater. Res. A* **2010**, *93A*, 175–188.
(106) Carr, D. A.; Peppas, N. A. Molecular Structure of Physiologically-Responsive Hydrogels Controls Diffusive Behavior. *Macromol. Biosci.* **2009**, *9*, 497–505.
(107) Knipe, J. M.; Chen, F.; Peppas, N. A. Enzymatic Biodegradation of Hydrogels for Protein Delivery Targeted to the Small Intestine. *Biomacromolecules* **2015**, *16*, 962–972.

(108) Peppas, N. A.; Merrill, E. W. Poly(vinyl Alcohol) Hydrogels: Reinforcement of Radiation-Crosslinked Networks by Crystallization. *J. Polym. Sci. Polym. Chem. Ed.* **1976**, *14*, 441–457.

(109) Brannon-Peppas, L.; Peppas, N. A. Equilibrium Swelling Behavior of pH-Sensitive Hydrogels. *Chem. Eng. Sci.* **1991**, *46*, 715–722.

(110) Şen, M.; Güven, O. Prediction of Swelling Behaviour of Hydrogels Containing Diprotic Acid Moieties. *Polymer* **1998**, *39*, 1165–1172.

(111) Orwoll, R. A.; Arnold, P. A. Polymer–Solvent Interaction Parameter X. In *Physical Properties of Polymers Handbook*; Mark, J. E., Ed.; Springer New York, 2007; pp. 233–257.

(112) Şen, M.; Yakar, A.; Güven, O. Determination of Average Molecular Weight between Cross-Links (Mc) from Swelling Behaviours of Diprotic Acid-Containing Hydrogels. *Polymer* **1999**, *40*, 2969–2974.

(113) Silberberg, A.; Eliassaf, J.; Katchalsky, A. Temperature-Dependence of Light Scattering and Intrinsic Viscosity of Hydrogen Bonding Polymers. *J. Polym. Sci.* **1957**, *23*, 259–284.

(114) Brock Thomas, J.; Tingsanchali, J. H.; Rosales, A. M.; Creecy, C. M.; McGinity, J. W.; Peppas, N. A. Dynamics of Poly(ethylene Glycol)-Tethered, pH Responsive Networks. *Polymer* **2007**, *48*, 5042–5048.

(115) Marvel, C. S.; Shepherd, T. H. Polymerization Reactions of Itaconic Acid and Some of Its Derivatives. *J. Org. Chem.* **1959**, *24*, 599–605.

(116) Tate, B. E. Polymerization of Itaconic Acid and Derivatives. *Fortschritte Hochpolym.-Forsch.* **1967**, *5*, 214–232.

(117) Şen, M.; Yakar, A. Controlled Release of Antifungal Drug Terbinafine Hydrochloride from poly(N-Vinyl 2-Pyrrolidone/itaconic Acid) Hydrogels. *Int. J. Pharm.* **2001**, *228*, 33–41.

(118) Nakamura, K.; Murray, R. J.; Joseph, J. I.; Peppas, N. A.; Morishita, M.; Lowman, A. M. Oral Insulin Delivery Using P(MAA-G-EG) Hydrogels: Effects of Network Morphology on Insulin Delivery Characteristics. *J. Controlled Release* **2004**, *95*, 589–599.

(119) Foss, A. C.; Goto, T.; Morishita, M.; Peppas, N. A. Development of Acrylic-Based Copolymers for Oral Insulin Delivery. *Eur. J. Pharm. Biopharm.* **2004**, *57*, 163–169.

(120) Carr, D. A. *Molecular Design of Biomaterial Systems for the Oral Delivery of Therapeutic Proteins*; ProQuest, 2008.

(121) Peppas, N. A.; Wood, K. M.; Thomas, J. B. Membranes in Controlled Release. In *Membranes for the Life Sciences*; Peinemann, K.-V.; Nunes, S. P., Eds.; Wiley-VCH Verlag GmbH & Co. KGaA, 2007; pp. 175–190.

(122) Erman, B.; Mark, J. E. *Structures and Properties of Rubberlike Networks*; Topic in polymer science; Oxford University Press: Oxford, 1997.

(123) Giussani, L.; Fois, E.; Gianotti, E.; Tabacchi, G.; Gamba, A.; Coluccia, S. On the Compatibility Criteria for Protein Encapsulation inside Mesoporous Materials. *ChemPhysChem* **2010**, *11*, 1757–1762.
(124) Reth, M. Matching Cellular Dimensions with Molecular Sizes. *Nat. Immunol.* **2013**, *14*, 765–767.
(125) Sambuy, Y.; De Angelis, I.; Ranaldi, G.; Scarino, M. L.; Stammati, A.; Zucco, F. The Caco-2 Cell Line as a Model of the Intestinal Barrier: Influence of Cell and Culture-Related Factors on Caco-2 Cell Functional Characteristics. *Cell Biol. Toxicol.* **2005**, *21*, 1–26.
(126) Pinto, M.; Robine-Leon, S.; Appay, M.-D.; Kedinger, M.; Triadou, N.; Dussaulx, E.; Lacroix, B.; Simon-Assmann, P.; Haffen, K.; Fogh, J.; *et al.* Enterocyte-like Differentiation and Polarization of the Human Colon Carcinoma Cell Line Caco-2 in Culture. *Biol. Cell* **1983**, *47*, 323–330.
(127) Hidalgo, I. J.; Raub, T. J.; Borchardt, R. T. Characterization of the Human Colon Carcinoma Cell Line (Caco-2) as a Model System for Intestinal Epithelial Permeability. *Gastroenterology* **1989**, *96*, 736–749.
(128) Ho, B.-C.; Lee, Y.-D.; Chin, W.-K. Thermal Degradation of Polymethacrylic Acid. *J. Polym. Sci. Part Polym. Chem.* **1992**, *30*, 2389–2397.
(129) Schild, H. G. Thermal Degradation of Poly(methacrylic Acid): Further Studies Applying TGA/FTIR. *J. Polym. Sci. Part Polym. Chem.* **1993**, *31*, 2403–2405.
(130) Lowman, A. M. The Dynamics of Complexation Graft Copolymers: Structural Analysis, NMR Spectroscopy, and Their Implications for Biomedical Applications. *Theses Diss. Available ProQuest* **1997**, 1–316.
(131) Feldstein, M. M. Adhesive Hydrogels: Structure, Properties, and Applications (a Review). *Polym. Sci. Ser. Chem. Phys.* **2004**, *46*, 1165–1191.
(132) Liu, S.; Fang, Y.; Hu, D.; Gao, G.; Ma, J. Complexation between Poly(methacrylic Acid) and Poly(vinylpyrrolidone). *J. Appl. Polym. Sci.* **2001**, *82*, 620–627.
(133) Bekturov, E. A.; Bimendina, L. A. Interpolymer Complexes. In *Speciality Polymers*; Advances in Polymer Science; Springer Berlin Heidelberg, 1981; pp. 99–147.
(134) Wood, K. M.; Stone, Gregory M.; Peppas, N. A. Wheat Germ Agglutinin Functionalized Complexation Hydrogels for Oral Insulin Delivery. *Biomacromolecules* **2008**, *9*, 1293–1298.
(135) Wood, K. M.; Stone, Gregory M.; Peppas, N. A. In Vitro Investigation of Oral Insulin Delivery Systems Using Lectin Functionalized Complexation Hydrogels. *Adv. Med. Eng. Drug Deliv. Syst. Ther. Syst.* **2006**, 75–83.
(136) Schoener, C. A.; Hutson, H. N.; Peppas, N. A. pH-Responsive Hydrogels with Dispersed Hydrophobic Nanoparticles for the Oral Delivery of Chemotherapeutics. *J. Biomed. Mater. Res. A* **2013**, *101A*, 2229–2236.
(137) Schoener, C. A.; Hutson, H. N.; Peppas, N. A. Amphiphilic Interpenetrating Polymer Networks for the Oral Delivery of Chemotherapeutics. *AIChE J.* **2013**, *59*, 1472–1478.

(138) Schoener, C. A.; Peppas, N. A. pH-Responsive Hydrogels Containing PMMA Nanoparticles: An Analysis of Controlled Release of a Chemotherapeutic Conjugate and Transport Properties. *J. Biomater. Sci. Polym. Ed.* **2013**, *24*, 1027–1040.
(139) Fink, A. L. Protein Aggregation: Folding Aggregates, Inclusion Bodies and Amyloid. *Fold. Des.* **1998**, *3*, R9–R23.
(140) Shire, S. J.; Shahrokh, Z.; Liu, J. Challenges in the Development of High Protein Concentration Formulations. *J. Pharm. Sci.* **2004**, *93*, 1390–1402.
(141) Thayer, A. M. Making Peptides at Large Scale. *Chem. Eng. News* **2011**, *89*, 21–25.
(142) Artursson, P. Cell Cultures as Models for Drug Absorption across the Intestinal Mucosa. *Crit. Rev. Ther. Drug Carrier Syst.* **1990**, *8*, 305–330.
(143) Artursson, P.; Karlsson, J. Correlation between Oral Drug Absorption in Humans and Apparent Drug Permeability Coefficients in Human Intestinal Epithelial (Caco-2) Cells. *Biochem. Biophys. Res. Commun.* **1991**, *175*, 880–885.
(144) Lennernäs, H. Regional Intestinal Drug Permeation: Biopharmaceutics and Drug Development. *Eur. J. Pharm. Sci.* **2014**, *57*, 333–341.
(145) Lennernäs, H.; Palm, K.; Fagerholm, U.; Artursson, P. Comparison between Active and Passive Drug Transport in Human Intestinal Epithelial (caco-2) Cells in Vitro and Human Jejunum in Vivo. *Int. J. Pharm.* **1996**, *127*, 103–107.
(146) Dantzig, A. H.; Bergin, L. Uptake of the Cephalosporin, Cephalexin, by a Dipeptide Transport Carrier in the Human Intestinal Cell Line, Caco-2. *Biochim. Biophys. Acta BBA - Biomembr.* **1990**, *1027*, 211–217.
(147) World Health Organization. Multisource (generic) Products and Interchangeability: Training Workshop on Dissolution, Pharmaceutical Product Interchangeability and Biopharmaceutical Classification System, 2007.
(148) Israelachvili, J. The Different Faces of Poly(ethylene Glycol). *Proc. Natl. Acad. Sci.* **1997**, *94*, 8378–8379.
(149) Roberts, M. J.; Bentley, M. D.; Harris, J. M. Chemistry for Peptide and Protein PEGylation. *Adv. Drug Deliv. Rev.* **2002**, *54*, 459–476.
(150) Sheth, S. R.; Leckband, D. Measurements of Attractive Forces between Proteins and End-Grafted Poly(ethylene Glycol) Chains. *Proc. Natl. Acad. Sci.* **1997**, *94*, 8399–8404.
(151) Youn, Y. S.; Kwon, M. J.; Na, D. H.; Chae, S. Y.; Lee, S.; Lee, K. C. Improved Intrapulmonary Delivery of Site-Specific PEGylated Salmon Calcitonin: Optimization by PEG Size Selection. *J. Controlled Release* **2008**, *125*, 68–75.
(152) Lee, K. C.; Moon, S. C.; Park, M. O.; Lee, J. T.; Na, D. H.; Yoo, S. D.; Lee, H. S.; DeLuca, P. P. Isolation, Characterization, and Stability of Positional Isomers of Mono-PEGylated Salmon Calcitonins. *Pharm. Res.* **1999**, *16*, 813–818.
(153) Hermanson, G. T. Chapter 3 - Zero-Length Crosslinkers. In *Bioconjugate Techniques (Second Edition)*; Hermanson, G. T., Ed.; Academic Press: New York, 2008; pp. 213–233.

(154) Wu, C.-S.; Lee, C.-C.; Wu, C.-T.; Yang, Y.-S.; Ko, F.-H. Size-Modulated Catalytic Activity of Enzyme–nanoparticle Conjugates: A Combined Kinetic and Theoretical Study. *Chem. Commun.* **2011**, *47*, 7446–7448.
(155) Anderson, J. M.; Itallie, C. M. V. Tight Junctions and the Molecular Basis for Regulation of Paracellular Permeability. *Am. J. Physiol. - Gastrointest. Liver Physiol.* **1995**, *269*, G467–G475.
(156) Powell, D. W. Barrier Function of Epithelia. *Am. J. Physiol. - Gastrointest. Liver Physiol.* **1981**, *241*, G275–G288.
(157) Shah, P.; Jogani, V.; Bagchi, T.; Misra, A. Role of Caco-2 Cell Monolayers in Prediction of Intestinal Drug Absorption. *Biotechnol. Prog.* **2006**, *22*, 186–198.
(158) Yamashita, S.; Furubayashi, T.; Kataoka, M.; Sakane, T.; Sezaki, H.; Tokuda, H. Optimized Conditions for Prediction of Intestinal Drug Permeability Using Caco-2 Cells. *Eur. J. Pharm. Sci.* **2000**, *10*, 195–204.
(159) Artursson, P.; Palm, K.; Luthman, K. Caco-2 Monolayers in Experimental and Theoretical Predictions of Drug Transport. *Adv. Drug Deliv. Rev.* **2012**, *64, Supplement*, 280–289.
(160) Artursson, P. Cell Cultures as Models for Drug Absorption across the Intestinal Mucosa. *Crit. Rev. Ther. Drug Carrier Syst.* **1991**, *8*, 305–330.
(161) Lennernäs, H.; Palm, K.; Fagerholm, U.; Artursson, P. Comparison between Active and Passive Drug Transport in Human Intestinal Epithelial (caco-2) Cells in Vitro and Human Jejunum in Vivo. *Int. J. Pharm.* **1996**, *127*, 103–107.
(162) Dantzig, A. H.; Bergin, L. Uptake of the Cephalosporin, Cephalexin, by a Dipeptide Transport Carrier in the Human Intestinal Cell Line, Caco-2. *Biochim. Biophys. Acta BBA - Biomembr.* **1990**, *1027*, 211–217.
(163) Wood, K. M.; Stone, G. M.; Peppas, N. A. The Effect of Complexation Hydrogels on Insulin Transport in Intestinal Epithelial Cell Models. *Acta Biomater.* **2010**, *6*, 48–56.
(164) López, J. E.; Peppas, N. A. Cellular Evaluation of Insulin Transmucosal Delivery. *J. Biomater. Sci. Polym. Ed.* **2004**, *15*, 385–396.
(165) Torres-Lugo, M.; García, M.; Record, R.; Peppas, N. A. pH-Sensitive Hydrogels as Gastrointestinal Tract Absorption Enhancers: Transport Mechanisms of Salmon Calcitonin and Other Model Molecules Using the Caco-2 Cell Model. *Biotechnol. Prog.* **2002**, *18*, 612–616.
(166) Matter, K.; Balda, M. S. Signalling to and from Tight Junctions. *Nat. Rev. Mol. Cell Biol.* **2003**, *4*, 225–237.
(167) Steed, E.; Balda, M. S.; Matter, K. Dynamics and Functions of Tight Junctions. *Trends Cell Biol.* **2010**, *20*, 142–149.
(168) Balda, M. S.; Matter, K. Tight Junctions. *J. Cell Sci.* **1998**, *111*, 541–547.
(169) Bai, Y.; Ann, D. K.; Shen, W.-C. Recombinant Granulocyte Colony-Stimulating Factor-Transferrin Fusion Protein as an Oral Myelopoietic Agent. *Proc. Natl. Acad. Sci. U. S. A.* **2005**, *102*, 7292–7296.
(170) Shah, D.; Shen, W. Transcellular Delivery of an Insulin-Transferrin Conjugate in Enterocyte-like Caco-2 Cells. *J. Pharm. Sci.* **1996**, *85*, 1306–1311.

(171) Xia, C. Q.; Wang, J.; Shen, W.-C. Hypoglycemic Effect of Insulin-Transferrin Conjugate in Streptozotocin-Induced Diabetic Rats. *J. Pharmacol. Exp. Ther.* **2000**, *295*, 594–600.
(172) Alberts, B.; Johnson, A.; Lewis, J.; Raff, M.; Roberts, K.; Walter, P. Carrier Proteins and Active Membrane Transport. **2002**.
(173) Brewer, E.; Lowman, A. M. Assessing the Transport of Receptor-Mediated Drug-Delivery Devices across Cellular Monolayers. *J. Biomater. Sci. Polym. Ed.* **2014**, *25*, 455–473.
(174) Blankenberg, D.; Von Kuster, G.; Coraor, N.; Ananda, G.; Lazarus, R.; Mangan, M.; Nekrutenko, A.; Taylor, J. Galaxy: A Web-Based Genome Analysis Tool for Experimentalists. In *Current Protocols in Molecular Biology*; John Wiley & Sons, Inc., 2010; pp. 1–21.
(175) Giardine, B.; Riemer, C.; Hardison, R. C.; Burhans, R.; Elnitski, L.; Shah, P.; Zhang, Y.; Blankenberg, D.; Albert, I.; Taylor, J.; *et al.* Galaxy: A Platform for Interactive Large-Scale Genome Analysis. *Genome Res.* **2005**, *15*, 1451–1455.
(176) Goecks, J.; Nekrutenko, A.; Taylor, J.; The Galaxy Team. Galaxy: A Comprehensive Approach for Supporting Accessible, Reproducible, and Transparent Computational Research in the Life Sciences. *Genome Biol.* **2010**, *11*, R86.
(177) Andrews, S. *FastQC A Quality Control Tool for High Throughput Sequence Data*; 2015.
(178) Blankenberg, D.; Gordon, A.; Kuster, G. V.; Coraor, N.; Taylor, J.; Nekrutenko, A.; The Galaxy Team. Manipulation of FASTQ Data with Galaxy. *Bioinformatics* **2010**, *26*, 1783–1785.
(179) Blind, M.; Blank, M. Aptamer Selection Technology and Recent Advances. *Mol. Ther. — Nucleic Acids* **2015**, *4*, e223.
(180) Cerchia, L.; Ducongé, F.; Pestourie, C.; Boulay, J.; Aissouni, Y.; Gombert, K.; Tavitian, B.; de Franciscis, V.; Libri, D. Neutralizing Aptamers from Whole-Cell SELEX Inhibit the RET Receptor Tyrosine Kinase. *PLoS Biol* **2005**, *3*, e123.
(181) Thiel, K. W.; Hernandez, L. I.; Dassie, J. P.; Thiel, W. H.; Liu, X.; Stockdale, K. R.; Rothman, A. M.; Hernandez, F. J.; McNamara, J. O.; Giangrande, P. H. Delivery of Chemo-Sensitizing siRNAs to HER2+-Breast Cancer Cells Using RNA Aptamers. *Nucleic Acids Res.* **2012**, *40*, 6319–6337.
(182) Berezhnoy, A.; Stewart, C. A.; Mcnamara Ii, J. O.; Thiel, W.; Giangrande, P.; Trinchieri, G.; Gilboa, E. Isolation and Optimization of Murine IL-10 Receptor Blocking Oligonucleotide Aptamers Using High-Throughput Sequencing. *Mol. Ther.* **2012**, *20*, 1242–1250.
(183) Cho, M.; Xiao, Y.; Nie, J.; Stewart, R.; Csordas, A. T.; Oh, S. S.; Thomson, J. A.; Soh, H. T. Quantitative Selection of DNA Aptamers through Microfluidic Selection and High-Throughput Sequencing. *Proc. Natl. Acad. Sci.* **2010**, *107*, 15373–15378.

(184) Hoon, S.; Zhou, B.; Janda, K. D.; Brenner, S.; Scolnick, J. Aptamer Selection by High-Throughput Sequencing and Informatic Analysis. *BioTechniques* **2011**, *51*, 413–416.
(185) Schütze, T.; Wilhelm, B.; Greiner, N.; Braun, H.; Peter, F.; Mörl, M.; Erdmann, V. A.; Lehrach, H.; Konthur, Z.; Menger, M.; *et al.* Probing the SELEX Process with Next-Generation Sequencing. *PLoS ONE* **2011**, *6*, e29604.
(186) Bayrac, A. T.; Sefah, K.; Parekh, P.; Bayrac, C.; Gulbakan, B.; Oktem, H. A.; Tan, W. In Vitro Selection of DNA Aptamers to Glioblastoma Multiforme. *ACS Chem. Neurosci.* **2011**, *2*, 175–181.
(187) Cho, M.; Oh, S. S.; Nie, J.; Stewart, R.; Eisenstein, M.; Chambers, J.; Marth, J. D.; Walker, F.; Thomson, J. A.; Soh, H. T. Quantitative Selection and Parallel Characterization of Aptamers. *Proc. Natl. Acad. Sci.* **2013**, *110*, 18460–18465.
(188) Ditzler, M. A.; Lange, M. J.; Bose, D.; Bottoms, C. A.; Virkler, K. F.; Sawyer, A. W.; Whatley, A. S.; Spollen, W.; Givan, S. A.; Burke, D. H. High-Throughput Sequence Analysis Reveals Structural Diversity and Improved Potency among RNA Inhibitors of HIV Reverse Transcriptase. *Nucleic Acids Res.* **2013**, *41*, 1873–1884.
(189) Jolma, A.; Kivioja, T.; Toivonen, J.; Cheng, L.; Wei, G.; Enge, M.; Taipale, M.; Vaquerizas, J. M.; Yan, J.; Sillanpää, M. J.; *et al.* Multiplexed Massively Parallel SELEX for Characterization of Human Transcription Factor Binding Specificities. *Genome Res.* **2010**, *20*, 861–873.
(190) Kupakuwana, G. V.; Crill, J. E., II; McPike, M. P.; Borer, P. N. Acyclic Identification of Aptamers for Human Alpha-Thrombin Using Over-Represented Libraries and Deep Sequencing. *PLoS ONE* **2011**, *6*, e19395.
(191) Zimmermann, B.; Bilusic, I.; Lorenz, C.; Schroeder, R. Genomic SELEX: A Discovery Tool for Genomic Aptamers. *Methods* **2010**, *52*, 125–132.
(192) Ross, M. G.; Russ, C.; Costello, M.; Hollinger, A.; Lennon, N. J.; Hegarty, R.; Nusbaum, C.; Jaffe, D. B. Characterizing and Measuring Bias in Sequence Data. *Genome Biol.* **2013**, *14*, R51.
(193) Chen, Y.-C.; Liu, T.; Yu, C.-H.; Chiang, T.-Y.; Hwang, C.-C. Effects of GC Bias in Next-Generation-Sequencing Data on De Novo Genome Assembly. *PLoS ONE* **2013**, *8*, e62856.
(194) Morishita, M.; Takayama, K.; Nagai, T.; Lowman, A. M.; Peppas, N. A. Application of a pH-Responsive Polymer to an Insulin Oral Dosage Form. *Yakuzaigaku* **1997**, *57*, 96–97.
(195) A. M. Lowman; Nicholas A. Peppas; M. Morishita; T. Nagai. Novel Bioadhesive Complexation Networks for Oral Protein Drug Delivery. In *Tailored Polymeric Materials for Controlled Delivery Systems*; ACS Symposium Series; American Chemical Society, 1998; Vol. 709, pp. 156–164.
(196) Morishita, M.; Goto, T.; Nakamura, K.; Lowman, A. M.; Takayama, K.; Peppas, N. A. Novel Oral Insulin Delivery Systems Based on Complexation Polymer Hydrogels: Single and Multiple Administration Studies in Type 1 and 2 Diabetic Rats. *J. Controlled Release* **2006**, *110*, 587–594.

(197) Doluisio, J. T.; Billups, N. F.; Dittert, L. W.; Sugita, E. T.; Swintosky, J. V. Drug Absorption I: An in Situ Rat Gut Technique Yielding Realistic Absorption Rates. *J. Pharm. Sci.* **1969**, *58*, 1196–1200.
(198) Griffin, B.; O'Driscoll, C. Models of the Small Intestine. In *Drug Absorption Studies: In Situ, In Vitro and In Silico Models*; Ehrhardt, C.; Kim, K.-J., Eds.; Biotechnology: Pharmaceutical Aspects; Springer Science & Business Media, 2007; Vol. 7, p. 720.
(199) Chetty, U.; Gilmour, H. M.; Taylor, T. V. Experimental Acute Pancreatitis in the Rat--a New Model. *Gut* **1980**, *21*, 115–117.
(200) Murray, M. J.; Barbose, J. J.; Cobb, C. F. Serum D(-)-Lactate Levels as a Predictor of Acute Intestinal Ischemia in a Rat Model. *J. Surg. Res.* **1993**, *54*, 507–509.
(201) Aldemir, M.; Kökoğlu, Ö. F.; Geyik, M. F.; Büyükbayram, H. Effects of Octreotide Acetate and Saccharomyces Boulardii on Bacterial Translocation in an Experimental Intestinal Loop Obstruction Model of Rats. *Tohoku J. Exp. Med.* **2002**, *198*, 1–9.
(202) Thiagarajah, J. R.; Broadbent, T.; Hsieh, E.; Verkman, A. S. Prevention of Toxin-Induced Intestinal Ion and Fluid Secretion by a Small-Molecule CFTR Inhibitor. *Gastroenterology* **2004**, *126*, 511–519.
(203) Tozaki, H.; Fujita, T.; Odoriba, T.; Terabe, A.; Okabe, S.; Muranishi, S.; Yamamoto, A. Validation of a Pharmacokinetic Model of Colon-Specific Drug Delivery and the Therapeutic Effects of Chitosan Capsules Containing 5-Aminosalicylic Acid on 2,4,6-Trinitrobenzenesulphonic Acid-Induced Colitis in Rats. *J. Pharm. Pharmacol.* **1999**, *51*, 1107–1112.
(204) Yamamoto, A.; Taniguchi, T.; Rikyuu, K.; Tsuji, T.; Fujita, T.; Murakami, M.; Muranishi, S. Effects of Various Protease Inhibitors on the Intestinal Absorption and Degradation of Insulin in Rats. *Pharm. Res.* **1994**, *11*, 1496–1500.
(205) Pron, B.; Boumaila, C.; Jaubert, F.; Sarnacki, S.; Monnet, J.-P.; Berche, P.; Gaillard, J.-L. Comprehensive Study of the Intestinal Stage of Listeriosis in a Rat Ligated Ileal Loop System. *Infect. Immun.* **1998**, *66*, 747–755.

Vita

Michael Clinton Koetting was born in Lubbock, TX. He received a Bachelor of Science degree in Chemical Engineering from Texas A&M University in May 2011, graduating with *summa cum laude* honors. As an undergraduate, Michael completed industrial internships as a process engineer with MEMC in Pasadena, TX, and Eastman Chemical Company in Longview, TX. Michael then attended graduate school at The University of Texas at Austin, pursuing research under Dr. Nicholas Peppas in the field of drug delivery, with focus on enabling the oral delivery of therapeutic proteins. He received his Master of Science degree in Chemical Engineering in August 2013, and completed his Ph.D. research in April 2015.

Permanent email: mkoetting@utexas.edu

This dissertation was typed by the author.